Secondary metabolites governing staphylococcal survival in the nasal microbiome

Dissertation

der Mathematisch-Naturwissenschaftlichen Fakultät

der Eberhard Karls Universität Tübingen

zur Erlangung des Grades eines

Doktors der Naturwissenschaften

(Dr. rer. nat.)

vorgelegt von

Benjamin Orlando Torres Salazar

aus Hamburg

Tübingen

2021

Table of contents

Abstract

Staphylococcus species are amongst the ubiquitous members of the human microbiome and generally populate human epithelial surfaces such as the skin and nose. The nare microbiomes of ~30% of the human population include the frequently multidrug-resistant facultative pathogen *Staphylococcus aureus*, which can cause a broad range of often severe infections. Although *S. aureus* nasal colonization is linked to an enhanced risk of endogenous *S. aureus* infections, the reasons for why only a subset of the human population is colonized have remained largely unknown. Increasing evidence points to important roles of bacterial secondary metabolites, in particular antimicrobial compounds, in shaping microbiome composition and dynamics, and, hence, in pathogen exclusion. Here, we report a novel antimicrobial compound produced by the human nasal isolate *Staphylococcus epidermidis* IVK83, epifadin, describe how mutualistic nasal bacteria promote nasal colonization by *S. lugdunensis*, the producer of the recently published microbiome-derived antimicrobial lugdunin, and elucidate the mechanisms of lugdunin secretion and producer immunity.

Epifadin is the first example of a staphylococcal bacteriocin produced by both, non-ribosomal peptide synthetases (NRPS) and polyketide synthases (PKS). It is active against a broad spectrum of major nasal microbiome members and enables *S. epidermidis* to outcompete *S. aureus in vitro* and *in vivo*. Interestingly, epifadin exhibits a very short half-life, thereby presumably preventing collateral damage of mutualistic bacteria. The unprecedented molecular architecture and instability render epifadin a novel and unusual antimicrobial.

We demonstrate that lugdunin secretion and self-resistance are mediated by two ABC transporters, which are encoded within the lugdunin locus. They display distinct but overlapping functions and are both required for full level lugdunin resistance.

Furthermore, we show that nasal carriage of *S. lugdunensis* is linked to a significantly decreased *S. aureus* colonization rate in healthy volunteers, as previously observed in hospitalized patients. A long-term analysis of *S. lugdunensis* carriers revealed that nasal colonization by *S. lugdunensis* is rather stable and mainly associated with microbiomes dominated by other *Staphylococcus* and/or by *Corynebacterium* species. Some of these bacteria promote *S. lugdunensis* growth via the production of iron-scavenging siderophores, indicating mutualistic interactions.

Our findings demonstrate the potential of secondary metabolites in modulating interbacterial interactions. Further investigations will help us understand their real impact in shaping microbiome composition.

Zusammenfassung

Staphylokokken gehören zu den weitverbreitetsten Vertretern des menschlichen Mikrobioms und besiedeln menschliche Epitheloberflächen wie die der Haut oder der Nase. Bei ca. 30% der menschlichen Bevölkerung ist zudem der häufig multiresistente Erreger *Staphylococcus aureus* in der Nase vorzufinden, der eine Vielzahl von oft schweren Infektionen verursachen kann. Eine nasale Besiedlung wird mit einem erhöhten Risiko für endogene *S. aureus*-Infektionen in Verbindung gebracht, die Gründe jedoch, warum nur ein Anteil der Bevölkerung mit *S. aureus* besiedelt ist, sind noch weitgehend unbekannt. Es gibt jedoch immer mehr Hinweise darauf, dass bakterielle Sekundärmetabolite, insbesondere antimikrobielle Substanzen, einen wesentlichen Einfluss auf die Zusammensetzung und Dynamik von Mikrobiomen haben, und somit auch zum Ausschluss von Pathogenen beitragen. In der vorliegenden Arbeit berichten wir über eine neuartige antimikrobielle Substanz, Epifadin, welche von dem humanen Nasenisolat *Staphylococcus epidermidis* IVK83 produziert wird, beschreiben, wie mutualistische nasale Bakterien die nasale Kolonisierung von *Staphylococcus lugdunensis* fördern - dem Produzenten der vor kurzem veröffentlichten, vom Mikrobiom abgeleiteten, antimikrobiellen Substanz Lugdunin - und klären die Mechanismen auf, welche die Sekretion von Lugdunin ermöglichen und dem Produzenten Immunität gegenüber Lugdunin verleihen.

Epifadin ist das erste Staphylokokken-Bakteriozin, welches von nicht-ribosomalen Peptidsynthetasen (NRPS) und Polyketidsynthasen (PKS) produziert wird. Es weist ein breites Hemmspektrum gegenüber vielen mikrobiellen Konkurrenten auf und ermöglicht es *S. epidermidis*, *S. aureus* sowohl *in vitro* als auch *in vivo* zu verdrängen. Interessanterweise besitzt Epifadin eine kurze Halbwertszeit, die vermutlich Kollateralschäden am Wirt oder an mutualistischen Bakterien verhindert. Die neuartige molekulare Architektur und die Instabilität machen Epifadin zu einer neuen und ungewöhnlichen antimikrobiellen Substanz.

Wir zeigen zudem, dass die Sekretion von und die Resistenz gegenüber Lugdunin von zwei ABC-Transportern vermittelt werden, welche im Lugdunin-Lokus kodiert sind. Die Transporter haben unterschiedliche, aber überlappende Funktionen und sind beide für eine vollständige Lugdunin-Resistenz erforderlich. Des Weiteren zeigen wir, dass eine nasale Besiedlung mit *S. lugdunensis* bei gesunden Probanden mit einer deutlich verringerten *S. aureus*-Kolonisierungsrate verbunden ist, wie es zuvor bereits bei hospitalisierten Patienten beobachtet werden konnte. Eine Langzeitanalyse von *S. lugdunensis*-Trägern ergab, dass die

nasale Besiedlung von *S. lugdunensis* relativ stabil ist und hauptsächlich mit Mikrobiomen assoziiert ist, die von *Staphylococcus*- und/oder *Corynebacterium*-Spezies dominiert werden. Einige dieser Bakterien fördern das Wachstum von *S. lugdunensis* durch die Produktion von Eisen-komplexierenden Siderophoren, was auf mutualistische Interaktionen hindeutet.

Unsere Ergebnisse zeigen, welches Potenzial Sekundärmetabolite auf die Modulierung von interbakteriellen Interaktionen haben können. Weitere Untersuchungen werden uns dabei helfen, ihren tatsächlichen Einfluss auf die Zusammensetzung des Mikrobioms zu verstehen.

Chapter 1 – General introduction

Secondary metabolites governing microbiome interaction of staphylococcal pathogens and commensals

Benjamin O. Torres Salazar[a,b,c], Simon Heilbronner[a,b,c], Andreas Peschel[a,b,c], Bernhard Krismer[a,b,c]

[a] Department of Infection Biology, Interfaculty Institute of Microbiology and Infection Medicine, University of Tübingen, Tübingen, Germany; [b] Cluster of Excellence EXC 2124 Controlling Microbes to Fight Infections; [c] German Center for Infection Research (DZIF), partner site Tübingen

Corresponding Author:

Bernhard Krismer, Andreas Peschel

Department of Infection Biology

Interfaculty Institute of Microbiology and Infection Medicine

Auf der Morgenstelle 28

Tübingen, Baden-Württemberg, 72076, Germany

Tel: +49 (07071) 29 74640 or 75935

E-mail: b.krismer@uni-tuebingen.de, andreas.peschel@uni-tuebingen.de

Abstract

Various *Staphylococcus* species colonize skin and upper airways of warm-blooded animals. They compete successfully with many other microorganisms under the hostile and nutrient-poor conditions of these habitats using mechanisms that we are only beginning to appreciate. Small-molecule mediators, whose biosynthesis requires complex enzymatic cascades, so-called secondary metabolites, have emerged as crucial components of staphylococcal microbiome interactions. Such mediators belong to a large variety of compound classes and several of them have attractive properties for future drug development. They include, for instance, bacteriocins such as lanthipeptides, thiopeptides, and fibupeptides that inhibit bacterial competitor species; signaling molecules such as thiolactone peptides that induce or inhibit sensory cascades in other bacteria; or metallophores such as staphyloferrins and staphylopine that scavenge scant transition metal ions. For some secondary metabolites such as the aureusimines, the exact function remains to be elucidated. How secondary metabolites shape the fitness of *Staphylococcus* species in the complex context of other microbial and host defense factors remains a challenging field of future research. A detailed understanding will help to harness staphylococcal secondary metabolites for excluding the pathogenic species *Staphylococcus aureus* from the nasal microbiomes of at-risk patients and it will be instrumental for the development of advanced anti-infective interventions.

Introduction

The genus *Staphylococcus* comprises dozens of species that are frequent colonizers of epithelial surfaces such as the skin or nasal cavities of humans and animals [1, 2]. The most prominent and most extensively investigated species is the coagulase-positive *Staphylococcus aureus*, an opportunistic human pathogen that can switch from a commensal to a pathogenic lifestyle, thereby causing a variety of infections [3]. In contrast, the vast majority of staphylococci belongs to coagulase-negative *Staphylococcus* (CoNS) species including for instance the species *Staphylococcus epidermidis* and *Staphylococcus hominis,* which are considered to be mostly commensals and less harmful than *S. aureus*, although they occasionally also cause infections [4]. With their high prevalence on skin and the epithelia of the nose, staphylococci are regarded as key members of the human microbiome [2].

Compared to the microbiome of the gastrointestinal tract, the microbiomes of the human skin and nose has only moderate biodiversity with a considerable overlap in occurring species. The nose, for example, is home to members of the genera *Cutibacterium*, *Corynebacterium*, *Moraxella*, and *Dolosigranulum* forming communities with staphylococci [5, 6]. They are considered to support the first line of host defense because some commensals can inhibit

colonization and infection by more pathogenic species such as *S. aureus* [2]. We have only begun to understand by which mechanisms these beneficial species can confer pathogen colonization resistance. The composition of bacterial communities is influenced by host-bacteria interactions (reviewed in more detail elsewhere [7-9]) and by interbacterial interactions. Such bacterial interactions involve the exchange of nutrients and molecules that induce or inhibit specific functions in target bacteria, so called secondary metabolites. The latter are highly diverse organic compounds that are often not essential for bacterial primary metabolism but may provide beneficial traits to the producing bacteria [10]. Secondary metabolites exert a wide range of bioactivities, which can be beneficial, detrimental, or even fatal for close-by bacterial community members. The production of such secondary metabolites can be an important strategy for bacteria to ensure their own survival and affect that of other bacteria.

Owing to recent advances in genome-wide sequencing techniques, we begin to understand the role of staphylococci within bacterial skin and nasal communities and to unravel the nature of their interactions. Many of these attempts were focused on *S. aureus* and its interaction with the human microbiome, to find new strategies for interfering with *S. aureus* colonization (to establish colonization resistance) [8, 11]. Three types of secondary metabolites have been found to be particularly important. The first includes bacteriocins, antimicrobial compounds that inhibit the growth of other bacteria [12]. Bacteriocins strongly impact the competition of bacteria for colonization sites and/or nutrients [5]. Bacteriocins have been defined as ribosomally synthesized peptides [13]. However, to cover all known antimicrobial compounds, the term bacteriocin is used in a broader sense to include all antimicrobial substances used by staphylococci in microbiome competition, independent of their biosynthetic pathway.

Several previous studies have demonstrated that nasal and skin staphylococcal species frequently produce antimicrobial compounds that are active against other inhabitants of the same niche, suggesting, that their production may be advantageous for the producers' establishment and survival on the human epithelia [14, 15]. Nakatsuji et al. observed that *S. aureus* occurrence on skin of atopic dermatitis patients is significantly reduced in the presence of staphylococcal commensals that produce bacteriocins of the lantibiotics type [16, 17]. Of note, also non-staphylococcal species such as *Cutibacterium acnes* produce antimicrobials that inhibit staphylococci including *S. epidermidis* [18, 19].

The second type covers molecules that interfere with bacterial signaling pathways, in particular the staphylococcal accessory gene regulator (*agr*), a quorum sensing system. This system is present in all staphylococci. It uses thiolactone/lactone containing autoinducing peptides (AIPs) for cell density-dependent signaling [20]. They exist as members of different structural subgroups and several studies have demonstrated that AIPs can cross-inhibit signaling of

staphylococci belonging to other subgroups, a phenomenon referred to as quorum quenching [8, 21, 22].

Metallophores have almost exclusively been investigated for their importance during infections, but they may play an important role for bacterial interactions in the microbiome. These low-molecular weight molecules are produced by bacteria during limited availability of essential transition metal ions, such as iron or zinc, in order to scavenge them from the environment and to deliver them back to the cells [23]. The human nasal epithelium represents an environment with limited availability of essential metals such as iron [5] suggesting that metallophores may be also involved in staphylococcal persistence in human microbiomes.

As diverse as bacterial interactions are, as manifold are the substance classes and biosynthetic pathways of bacterial interactions shaping secondary compounds, ranging from ribosomally synthesized and post-translationally modified peptides (RiPPs) to non-ribosomally synthesized peptides (NRPs) and non-peptide molecules. In this review we outline the different classes of the hitherto identified community-active secondary compounds produced by staphylococcal species, with emphasis on the biosynthetic pathways. Secondary metabolites from the group of unmodified peptides (class-II bacteriocins) and the small-peptide family of phenol-soluble modulins are not covered by this review, despite their presumably huge impact on the microbiome.

Ribosomally synthesized and post-translationally modified peptides (RiPPs):

The term "RiPPs" was first introduced in a review published by a discussion group under the leadership of Wilfred van der Donk as a recommendation to summarize the plethora of peptides that are ribosomally synthesized and get subsequently modified by enzymes that are encoded in diverse biosynthetic gene clusters (BGCs) [13, 24]. RiPPs are relatively small molecules with a size below 10 kDa, representing a superfamily of natural products with diverse structural features and biological functions [13].

The peptide backbones of RiPPs are encoded by structural genes leading to precursor peptides with lengths of 20-110 amino acids. The precursor peptide is composed of different segments, of which the so-called core peptide will eventually be transformed into the mature bioactive product [13]. Most precursor peptides of RiPPs possess a leader peptide attached to the core peptide at the N-terminus, which will be removed upon RiPP maturation [25]. In some cases, the leader peptide is attached to the C-terminus of the core peptide and can contain recognition sequences, which are important during maturation of the peptide for excision and cyclization [13].

During RiPP biosynthesis, the leader peptide is used for recognition of the unprocessed precursor peptide by post-translational modification (PTM) enzymes and by export proteins [25]. Those enzymes gradually modify the unmodified core peptide (UCP) to yield the modified core peptide (MCP) [13]. Post-translational modifications of RiPPs can be highly diverse and include, for instance, dehydration, phosphorylation, cyclization and oxidation reactions. Further downstream of the modification process, the leader peptide is finally removed from the MCP by proteolytic cleavage, resulting in the release of the mature bioactive RiPP [13].

In staphylococci, the currently known RiPPs are bacteriocins or signaling molecules, belonging to the classes of lanthipeptides, sactipeptides, thiopeptides, or thiolactones, which will be discussed in this section (see also Table 1).

Lanthipeptides.

Lanthipeptides are RiPPs containing the unusual amino acids lanthionine (Lan) or 3-methyllanthionine (MeLan) and, sometimes, the dehydrated amino acids didehydroalanine (Dha) or didehydrobutyrine (Dhb) [26, 27]. Lan and 3-MeLan result from the condensation of a Dha or Dhb with a Cys leading to a thioether linkage that connects their β-carbons [27]. They are typically formed by PTM enzymes with dehydratase and cyclase activities from Ser or Thr, which are in the first step dehydrated to Dha or Dhb, respectively, and, in a second step, linked to the thiol group of intramolecular Cys residues resulting in Lan or MeLan formation, respectively [27].

Lanthipeptides with antimicrobial activity are called lantibiotics and, according to Knerr and van der Donk [28], can be further divided into class I-IV lantibiotics, depending on the enzymes involved in post-translational modification of the lantibiotic. In class-I lantibiotics, two separate enzymes mediate dehydration and cyclization, the dehydratase LanB and the cyclase LanC, respectively, while in class-II (LanM), class-III (LanKC) and class-IV (LanL) only one enzyme accomplishes lanthionine formation [28].

The target sites of lantibiotics are typically surface structures of Gram-positive bacteria such as lipid I and II, which are precursors for peptidoglycan biosynthesis [29-31], as well as lipid III and IV, precursors for wall teichoic acid biosynthesis [32]. For epidermin/gallidermin, two of the lantibiotics produced by staphylococci, it has been demonstrated that upon binding to lipid II, the incorporation of lipid II via the trans-peptidase/trans-glycosylase into the growing peptidoglycan network is blocked, thus resulting in the death of target bacterial cells [33]. Furthermore, pore formation with a consequent dissipation of the membrane potential is associated with killing. However, this seems to depend on the thickness of the membrane of the target cell and the length of lantibiotics [31, 34].

In general, the generic locus symbol *lan* is used to designate the entire group of lantibiotic gene clusters, which have, depending on the lantibiotic, more specific genotypic denotations, e.g. *nuk* for nukacin ISK-1 or *gdm* for gallidermin [13]. Further, the gene clusters typically contain genes encoding the precursor peptide (*lanA*), PTM enzymes (*lanB*, *lanC*, *lanM*, *lanL* etc.), an exporter (*lanT*), and extracellular protease (*lanP*) for the transport of the MCP and proteolytic cleavage of the leader peptide, and proteins for immunity (*lanI*, *lanH*, *lanFEG*) that protect the producer from its own product [35, 36]. In some staphylococcal class-I lantibiotics, additional PTM enzymes such as LanD [37, 38] and LanO [39] have been identified that are associated with additional post-translational modifications, e.g. for epidermin or epilancin 15X, respectively.

Epidermin and its natural derivative gallidermin are among the best described staphylococcal class-I lantibiotics and were originally discovered in *S. epidermidis* Tü3298 and *S. gallinarum* Tü3928, respectively [40, 41]. The biosynthesis of epidermin and gallidermin is nearly identical, and the core peptides only differ by one amino acid (Leu6Ile in gallidermin) [41]. Both BGCs consist of 11 genes and are, in the case of epidermin, organized as a *epiGEFHTABCDQP* locus, with *epiQ* [42] and *epiD* [37, 38] encoding for a regulator and an additional PTM enzyme, respectively.

The ribosomally synthesized precursor peptide contains the 22-aa core peptide that will become the mature lanthipeptide. The formation of lanthionine and methyllanthionine is mediated via EpiB and EpiC, resulting in the generation of three thioether ring structures in the epidermin core peptide segment (Fig. 1) [33]. One special structural feature of epidermin and gallidermin is the fourth thioether ring at the C-terminus, a S-((Z)-2-aminovinyl)-D-Cys (AviCys) residue, generated by the PTM enzyme EpiD/GdmD, a flavoprotein that binds the coenzyme flavin mononucleotide (FMN) [33, 43, 44]. The resulting MCP is then secreted via the ABC transporter EpiHT in a sec-independent way and is extracellularly cleaved by the leader peptidase EpiP to form the mature and active gallidermin [33, 45].

Over the years, further staphylococcal class-I lantibiotics have been identified that are variants of or closely related to epidermin: 1V,6L-epidermin from *S. epidermidis* V1 and V301 [46], staphylococcin T (identical to gallidermin) from *Staphylococcus cohnii* T [47], staphylococcin Au-26/Bsa/aureodermin [48-50] and BacCH91 [51] from *S. aureus*, and agneticin 3682 (formerly hyicin 3682) isolated from *Staphylococcus agnetis* (formerly *Staphylococcus hyicus*) [52, 53].

Another member of staphylococcal class-I lantibiotics is epilancin 15X, originating from *S. epidermidi*s 15X154 and encoded by the BGC *elxOTAPBCI* [39, 54]. A special feature of epilancin 15X is an N-terminal lactate residue (Fig. 1). Upon biosynthesis of the precursor

Table 1. Bacteriocins identified from Staphylococcus species

Bacteriocin		Producer	Susceptible bacteria & mode of action	References
Lantibiotics	Agneticin 3682	*S. agnetis* 3682	Firmicutes: *S. aureus, Bacillus spp., Listeria spp., Lactobacillus spp., Lactococcus lactis, Leuconostoc mesenteroides* Actinobacteria: *M. luteus, Corynebacterium fimi, Kocuria rhizophila, Geobacillus stearothermophilus*	[52; 53]
	BacCH91	*S. aureus* CH-91	Firmicutes: *Staphylococcus spp.*	[51]
	Epidermin	*S. epidermidis* Tü3298	Firmicutes: *Staphylococcus spp., Streptococcus spp., Corynebacterium spp., Bacillus spp., Listeria spp., Lactobacillus spp., Lactococcus lactis, Leuconostoc mesenteroides, Peptostreptococcus anaerobicus, Geobacillus stearothermophilus* Actinobacteria: *Micrococcus luteus, Cutibacterium acnes, Kocuria rhizophila* Interaction with lipid I/II (peptidoglycan biosynthesis) and lipid III/IV (wall teichoic acid biosynthesis); membrane pore formation	[30; 32; 33; 41; 52]
	Gallidermin	*S. gallinarum* Tü3928	Firmicutes: *Staphylococcus spp., Streptococcus spp., Peptostreptococcus anaerobicus* Actinobacteria: *Micrococcus luteus, Cutibacterium acnes, Kocuria rhizophila, Corynebacterium xerosis* Interaction with lipid I/II (peptidoglycan biosynthesis) and lipid III/IV (wall teichoic acid biosynthesis); membrane pore formation	[30; 32; 33; 41]
	Epilancin K7	*S. epidermidis* K7	Firmicutes: *S. simulans, Streptococcus agalactiae*	[55; 146]
	Epilancin 15x	*S. epidermidis* 15X154	Firmicutes: *S. aureus, Streptococcus spp., Enterococcus spp.*	[39; 54]
	Epicidin 280	*S. epidermidis* BN280	Firmicutes: *Staphylococcus spp., S. agalactiae* Actinobacteria: *M. luteus*	[57; 146]
	Pep5	*S. epidermidis* 5	Firmicutes: *Staphylococcus spp.* Actinobacteria: *Micrococcus spp.* Membrane pore formation	[57; 136; 147; 148]
	Nisin J	*S. capitis* APC 2923	Firmicutes: *Staphylococcus spp., Enterococcus spp., L. monocytogenes, Lactobacillus delbrueckii, L. lactis* Actinobacteria: *C. acnes, C. xerosis*	[64]
	Nukacin ISK-1	*S. warneri* ISK1	Firmicutes: *Staphylococcus spp., Streptococcus bovis, Bacillus subtilis, Lactobacillus spp., Lactococcus lactis, Pediococcus pentosaceus, Enterococcus faecalis* Actinobacteria: *Micrococcus luteus* Interaction with lipid II (peptidoglycan biosynthesis)	[65; 149; 150; 151]
	Nukacin IVK45	*S. epidermidis* IVK45	Firmicutes: *(S. aureus ∆dltA), S. pyogenes, Dolosigranulum pigrum,* Actinobacteria: *C. accolens, Micrococcus luteus* Gammaproteobacteria: *Moraxella catarrhalis*	[14]
	Nukacin KQU-131	*S. hominis* KQU-13	Firmicutes: *Bacillus sp., Lactic acid bacteria (LAB)* Actinobacteria: *Micrococcus sp.*	[71]
	Warnericin RB4	*S. warneri* RB4	Firmicutes: *Alicyclobacillus acidoterrestris, Alicyclobacillus acidocaldarius,* Actinobacteria: *Micrococcus luteus*	[73]
	Staphylococcin C55	*S. aureus* C55	Firmicutes: *S. aureus* Actinobacteria: *M. luteus*	[74]
Sactibiotics	Hyicin 4244	*S. hyicus* 4244	Firmicutes: *Staphylococcus spp., Enterococcus spp., Lactobacillus spp., Listeria spp., L. lactis,* Actinobacteria: *M. luteus*	[82]
Thiopeptides	Micoroccin P1	*S. equorum* WS 2733/ *S. hominis* S34-1	Firmicutes: *Staphylococcus spp., Enterococcus spp., Listeria spp., Lactobacillus sp., Bacillus cereus, Clostridium perfringens* Actinobacteria: *Corynebacterium sp., Micrococcus sp., Brevibacterium sp., Arthrobacter sp., Microbacterium sp.* Interaction with complex formed between L11 binding domain of 50S ribosomal subunit and 23S ribosomal RNA, thereby inhibiting peptide chain elongation	[91; 152]
Fibupeptides	Lugdunin	*S. lugdunensis* IVK28	Firmicutes: *S. aureus, E. faecium, E. faecalis, L. monocytogenes, S. pneumoniae,* Actinobacteria: *C. acnes* Protonophore-like mode of action, causing proton leakage in membranes(, independent of proteinaceous membrane molecules)	[112; 113]

peptide and Lan/MeLan formation, the leader peptide is proteolytically removed by ElxP, a presumed intracellular protease that leaves the 31-aa core peptide with an N-terminal Dha [39]. Due to instability, the Dha undergoes spontaneous hydrolysis to form a pyruvate residue, which is then reduced by the NADPH-dependent PTM enzyme ElxO, resulting in an N-terminal lactate residue [39]. The mature peptide is most likely secreted by ElxT, a putative ABC exporter [39]. Like epilancin 15X, its natural derivative epilancin K7 also possesses an N-terminal lactate residue [55, 56]. However, to date, no LanO has been identified that could be responsible for this modification step in epilancin K7 [39, 57]. Nevertheless, an *elxO* homolog could be found in the BGC *eciOIAPBC* of epicidin 280, a lantibiotic derived from *S. epidermidis* BN280 (Fig. 1) [57]. Here, the *elxO* homolog *eciO* encodes a PTM enzyme EciO with putative oxidoreductase function. Most likely EciO catalyzes the conversion of the N-terminal pyruvate to a lactate residue, however, experimental evidence for this is currently lacking [57, 58].

Closely related to epicidin 280 is Pep5, originally identified in *S. epidermidis* 5, which harbors the Pep 5 BGC *pepTIAPBC* [59-61]. The BGC of Pep5 is organized in the same order as epicidin 280 BGC and the encoding proteins contain high levels of amino acid similarity [57, 62]. The precursor peptides of the two bacteriocins share 58.9% amino acid identity and both are synthesized with a 26-aa leader peptide. However, the Pep5 core peptide consist of 34 aa, while that of epicidin 280 consists of only 30 aa [62]. The mature peptide harbors an N-terminal oxobutyryl residue, which is formed by spontaneous deamination of the N-terminal Dhb (Fig. 1) [46, 60, 63]. In contrast to epicidin 280, the Pep5 BGC lacks a *lanO* gene and only the two PMT enzymes PepB/C are used to modify the Pep5 core peptide [61]. Thus, Pep5 represents a class-I lantibiotic without any further enzymatic modification besides the formation of Lan/MeLan and Dha/Dhb. Apart from Pep5, there have been other lantibiotics isolated from staphylococci modified only by LanB and LanC, such as nisin J from *Staphylococcus capitis* [64].

A typical example for staphylococcal class-II lantibiotics is nukacin ISK-1, a 27-aa lantibiotic, originally isolated from *Staphylococcus warneri* ISK1, harboring the nukacin ISK-1 BGC *nukAMTFEGH* [65-67]. In contrast to the class-I lantibiotics described above, the formation of Lan and MeLan in nukacin ISK-1 is mediated by the single bi-functional enzyme LanM (NukM) [68, 69]. Whereas the C-terminal cyclase domain of LanM modification enzymes shares homologies to LanC enzymes, the N-terminal dehydratase domain of LanM bears no sequence similarities to LanB enzymes [28]. These differences are also reflected by the distinct modes of dehydration of Ser and Thr, as dehydration mediated by LanM occurs via phosphorylation instead of glutamylation via LanB (reviewed in more detail elsewhere [58]). As for staphylococcal class-I lantibiotics, the leader peptide of NukA is removed after NukM catalyzed Lan/MeLan formation, and the mature core peptide is released. However, both, the cleavage
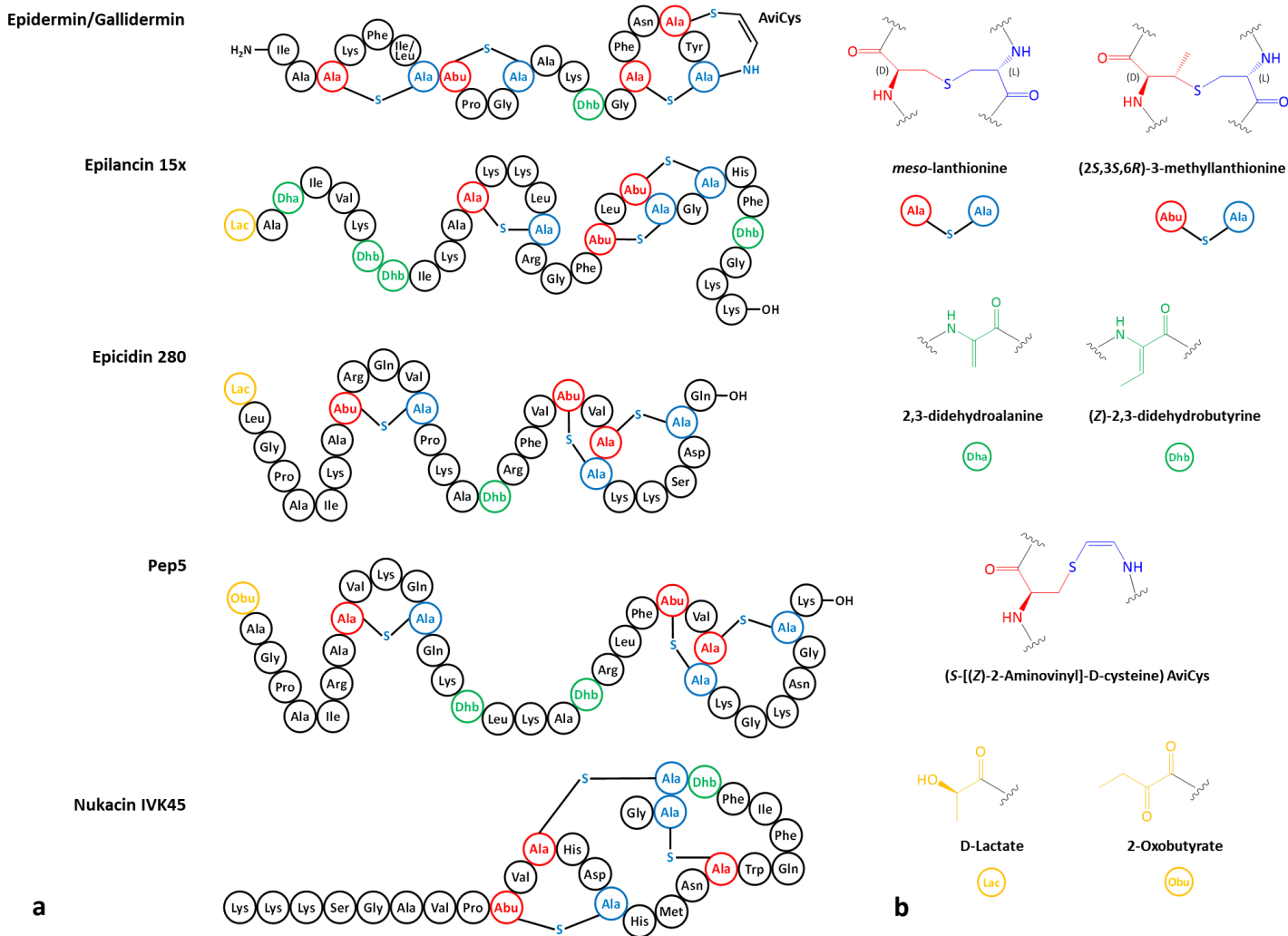
Fig. 1. a, Amino acid sequence and ring topologies/structures of staphylococcal lanthipeptides. Red: Alanine (Ala) and aminobutyric acid (Abu) derived from serine and threonine; blue: Ala derived from cysteine; green: 2,3-didehydroalanine (Dha) and (Z)-2,3-didehydrobutyrine (Dhb) derived from serine and threonine; yellow: D-lactate and 2-oxobutyrate derived from N-terminal Dha or Dhb. **b,** Chemical structures of lanthipeptide characteristic unnatural amino acids lanthionine, methyllanthionine, dehydroalanine and dehydrobutyrine and further chemical modifications.

of the MCP and the export of the resultant nukacin ISK-1 is mediated by only one enzyme, NukT, an ABC transporter maturation and secretion (AMS) protein [70], which includes a peptidase domain.

Apart from *S. warneri* ISK-1, nukacin variants could be isolated from other staphylococcal species. Janek and colleagues identified the first *S. epidermidis*-derived nukacin-like bacteriocin produced by the human nasal isolate *S. epidermidis* IVK45, termed nukacin IVK45 (Fig. 1) [14]. The gene cluster of nukacin IVK45 shares high similarities to that of nukacin ISK-1 and nukacin KQU-131, another variant produced by *S. hominis* from fermented fish [14, 71]. The mature nukacin IVK45 differs from the other two nukacins by five and by six amino acids, respectively, and the leader peptide by another five amino acids [14]. Further examples of staphylococcal nukacin-like bacteriocins are nukacin 3299 (formerly designated simulancin 3299), a peptide produced by *Staphylococcus simulans* shown to be identical to nukacin ISK-1 [72], or warnericin RB4, a nukacin variant produced by *S. warneri* [73].

A rather exotic class-II lantibiotic is staphylococcin C55, a two-component lantibiotic produced by *S. aureus* C55 [74]. Its BGC harbors two structural genes *sacαA* und *sacβA*, encoding C55α and C55β, respectively, the two *lanM* genes *sacM*1 and *sacM*2, an AMS protein encoding gene *sacT,* and a gene coding for an additional modification enzyme, SacJ, a zinc and NADPH-dependent LanJ$_A$-type dehydrogenase [58, 75]. The function of LanJ was first characterized for the biosynthesis of lacticin 3147 from *Lactococcus lactis* DPC3147, where it is thought to be responsible for the introduction of the amino acid D-Ala into the peptides [76]. In general, this modification step occurs after Dha formation by LanM, followed by a diastereoselective hydrogenation of Dha mediated by LanJ, resulting in the formation of D-Ala, thereby rendering Dha a substrate not only for Lan formation by LanM but also for D-Ala formation by LanJ [76]. The cleavage and transport of the two MCPs is most likely mediated by SacT, in the same way as LtnT in the lacticin 3147 biosynthesis process [75, 76]. Interestingly, even though faint antimicrobial activity could be observed for the single peptides C55α and C55β, a combination of them at equimolar ratio is required to obtain full antimicrobial activity of staphylococcin C55 [74]. The genetic determinants of staphylococcin C55 could also be identified in *S. aureus* strain U0007 [77].

Most recently, the BGC for another putative two-component lantibiotic was discovered in *S. hominis* APC 3824, exhibiting similarities to the BGC of haloduracin, a lantibiotic produced by *Bacillus halodurans* C-125 [78].

Sactipeptides

Sactipeptides are a class of RiPPs containing intramolecular thioether linkages between the thiol group of Cys and the α-carbon of an acceptor amino acid [13]. Such „sulfur-to-α-carbon" condensations are generally mediated by radical S-adenosylmethionine (SAM) enzymes harboring [4Fe-4S] clusters [79]. The general mechanism of thioether bond formation by the radical SAM enzyme has been described in more detail for subtilosin A, a sactipeptide derived from *Bacillus subtilis* [79].

Sactipeptides with antimicrobial properties are called sactibiotics [13]. Only a few studies have elucidated the mode of action of sactibiotics. Most sactipeptides have relatively high hydrophobic properties and tend to form hairpin structures due to their sulfur-to-α-carbon linkages. Their hydrophobic residues are pointing to the outside, enabling an interaction with the membrane of the targeted organism, possibly resulting in some kind of membrane damage [80].

Among staphylococci, only one sactibiotic has been described in more detail so far, hyicin 4244, which is produced by *Staphylococcus hycius*, whose final structure has yet to be elucidated [81, 82]. Its BGC is located on the chromosome and consists of eight genes (*hyiSABCDEFG*) with an organization resembling that of subtilosin A. The structural gene *hycS* encodes a 43-aa precursor peptide with high identity (71%) to the precursor peptide of subtilosin A (SboA). It harbors three thioether donor Cys residues (Cys12, Cys15, Cys21) and acceptor amino acids (Phe30, Phe39 and Thr36). The mature hyicin 4244 is assumed to be 35-aa long and probably also undergoes macrocyclization to form a circular bacteriocin related to subtilosin A [81].

The proteins encoded by the hyicin 4244 BGC also display high similarities (from 42% to 70%) to the proteins of subtilosin A. Hence, they have most likely the same functions. In brief, HycA is the radical SAM enzyme that presumably introduces thioether linkages in HycS, analogous to AlbA for subtilosin A, while HycE and HycF are predicted to be cytoplasmic proteases that are involved in the removal of the leader peptide and macrocyclization to generate the mature hyicin. Further genes encode the putative immunity factors *hycB*, *hycC,* and *hycD,* whereas the latter two are presumably also involved in the transport of the mature peptide [81].

Recently, four putative distinct sactipeptides were identified in *S. epidermidis* genomes, displaying only little sequence similarity to known sactibiotics (<20.6%) [78]. Although the producers showed antimicrobial activitiy against various bacteria, those sactibiotics were mostly investigated on a genetic level and further research is required to confirm that the antimicrobial activity was caused by to these putative sactibiotics.

Thiopeptides

Thiopeptides, or thiazolyl peptides, represent one of the most extensively modified RiPP class [83, 84]. They typically comprise a characteristic six-membered, nitrogenous heterocycle located at the center of the peptide, which functions as a scaffold for at least one peptide macrocycle and a tail. Both are featured by azole rings (oxazole, thiazole, or thiazoline) and dehydroamino acids (Dha/Dhb), which are derived from multistep modifications of Ser, Thr, and Cys [83, 85].

Thiopeptides can be classified into five series (a-e) according to their structure, depending on the substitution pattern and oxidation state of the nitrogenous heterocycle [83]. They often exhibit antimicrobial activities against Gram-positive bacteria, and their modes of action are usually linked to the inhibition of protein biosynthesis. On one hand, this process can occur by binding to the GTPase-associated region of the ribosome/L11 complex, thereby hindering elongation factors to bind, which results in ribosome stalling [85-87]. On the other hand, the peptide can bind to the elongation factor TU (EF-Tu), which prevents the formation of the EF-Tu·aminoacyl-tRNA complex [88, 89].
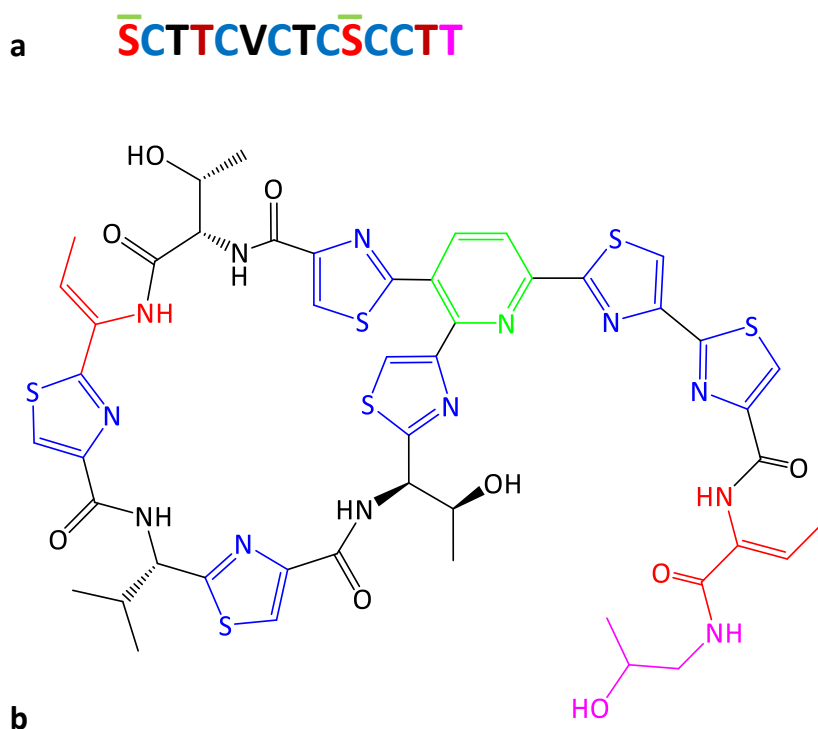

Fig. 2. **a,** Amino acid sequence of micrococcin P1. Color code indicates posttranslational modifications. Red: dehydration; blue: thiazole formation; pink: dehydrogenation; green line: cyclization and pyridine formation. **b,** Chemical structure of micrococcin P1.

The first and yet only thiopeptide identified in the genus *Staphylococcus* is micrococcin P1 (MP1), originally isolated 1948 from *Micrococcus* sp. and since then found twice, in *Staphylococcus equorum* WS 2733 and in *S. hominis* (Fig. 2) [90-92]. As for the latter, the BGC for MP1 is located on a plasmid and shows high similarities to the MP1 BGC found in *Macrococcus caseolyticus* (formerly falsely classified as *S. epidermidis*) [92-94]. Using *Bacillus subtilis* for heterologous gene expression, eight PTM enzymes encoded by the *tclIJKLMNPS* BGC have been shown to be sufficient to produce MP1 [94]. The structural gene *tclE* encodes a 49-aa MP1 precursor peptide of which the 14-aa at the C-terminus represent the core peptide with a high content of Ser, Thr, and Cys, which eventually is transformed into mature MP1 with two Dhb residues, six thiazole rings, and one central pyridine ring (Fig. 2) .

Bewley et al. proposed a biosynthetic pathway for MP1 based on homology comparisons with other well-studied thiopeptides (thiocillin and thiomuracin) and supportive experimental data [95]. In brief: During MP1 biosynthesis, the formation of thiazole rings is catalyzed by TclI (precursor peptide recognition), TclJ (a thiazole/oxazole-modified microcin family cyclodehydratase) and TclN (FMN-binding McbC-type dehydrogenase) in an ATP- and FMN-dependent manner [95]. The alcohol residue at the C-terminal tail of MP1 is generated by the two predicted short-chain dehydrogenases TclP and TclS, with TclP responsible for the formation of a ketone residue that is later reduced by TclS to an alcohol. The two enzymes TclK and TclL catalyze the dehydration of Ser and Thr to Dha and Dhb, respectively, and the multifunctional TclM catalyzes the formation of the central pyridine ring, the peptide macrocyclization and leader peptide elimination. Further genes, not associated with MP1 PTM but encoded within the same cluster, are *tclQ*, *tclU,* and *orf18*, encoding a MP1-insensitive ribosomal protein L11 homolog conferring immunity, a putative transcriptional regulator, and a putative protein of unknown function, respectively [94].

Thiolactones/thiolactone-containing peptides

Thiolactones are heterocyclic rings of different sizes that contain a sulfur atom adjacent to a carbonyl group. In virtually all *Staphylococcus* species, thiolactones are structural elements of autoinducing peptides (AIPs) that are involved in the accessory gene regulation (*agr*) quorum sensing (QS) system, allowing population density/environment-dependent gene regulation through cell-cell communication [20, 22, 96]. In brief, the *agr* locus consists of two transcriptional units, RNAII and RNAIII, of which the RNAII locus contains the four genes *agrB*, *agrC*, *agrD,* and *agrA* involved in QS [20]. AgrC and AgrA represent a two-component signal transduction system. AgrC is the transmembrane histidine kinase sensor that gets auto-phosphorylated upon AIP binding [97]. Subsequently, it transfers the phosphate group to the

associated response regulator AgrA, which then activates the P2/P3 promotor regions of RNAII/RNAIII, respectively, resulting in an auto-feedback regulation of *agrBDCA* and transcription/translation of RNAIII that regulates expression of *agr* target genes [98-100].

It was shown in *S. aureus*, that the two genes *agrD* and *agrB* mediate the biosynthesis of AIPs [96]. The gene *agrD* encodes a precursor peptide consisting of a core peptide that is flanked by an N-terminal amphipathic helical region and a C-terminal highly negatively charged recognition sequence/region [101]. AgrD is processed by AgrB, a membrane protein with endopeptidase activity, and an additional protease that is thought to be SpsB, the general signal peptidase associated with Sec and Tat secretion system [102], via the following (proposed) pathway [101]: Upon translation, the precursor peptide localizes to the inner leaflet of the cell membrane via the N-terminal amphipathic helix structure [103]. In the next step, AgrB removes the C-terminal recognition sequence of the precursor peptide, which is followed by formation of the thiolactone ring between a Cys of the core peptide and its C-terminus [101]. By means of a yet unknown mechanism, the AIP precursor is translocated to the outer cytoplasmic membrane leaflet, either by AgrB or another protein, where the N-terminal amphipathic helix is subsequently removed, presumably by the peptidase SpsB, which results in the release of the mature AIP [104].
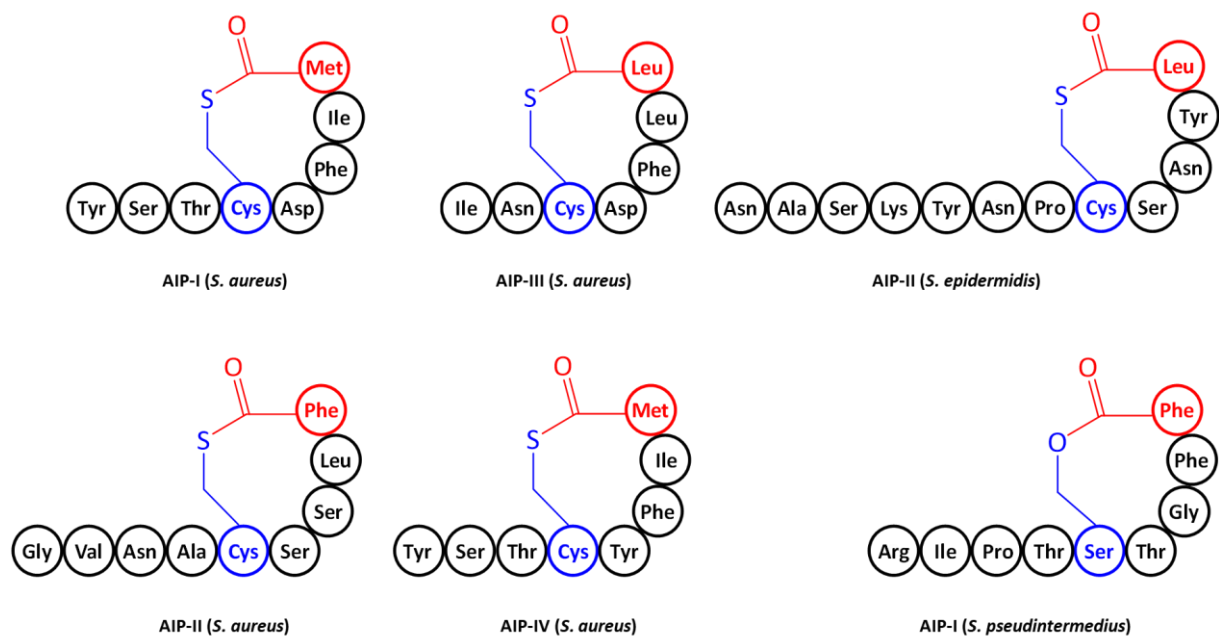

Fig. 3. Amino acid sequence and ring topologies/structures of (staphylococcal) autoinducing peptides. Thiolacte and lactone rings formed between amino acids are indicated in blue (Cys/Ser) and red (AA).

Table 2. Amino acids sequences of autoinducing peptides (AIPs) produced by *Staphylococcus* species.

Species	Sequence	Inhibited Agr	Source
S. argenteus	YSTCDFIM (identical to *S. aureus* AIP-I)		[137]
S. aureus	YSTCDFIM (AIP-I)	*S. aureus* Agr-II/III, *S. simulans* Agr-III	[21; 96; 138]
	GVNACSSLF (AIP-II)	*S. aureus* Agr-I/III/IV	[21]
	INCDFLL (AIP-III)	*S. aureus* Agr-I/II/IV	[21]
	YSTCYFIM (AIP-IV)	*S. aureus* Agr-II/III, *S. simulans* Agr-III, *S. epidermidis* Agr-I	[138; 139; 140]
S. caprae	YSTCSYYF	*S. aureus* Agr-I/II/II/IV	[106]
S. chromogenes	SINPCTGFF		[137]
S. epidermidis	DSVCASYF (AIP-I)	*S. epidermidis* Agr-II/III, *S. aureus* Agr-I/II/III	[105; 140; 141]
	NASKYNPCSNYL (AIP-II)	*S. epidermidis* Agr-I, *S. aureus* Agr-I	[141; 142]
	NAAKYNPCASYL (AIP-III)	*S. epidermidis* Agr-I, *S. aureus* Agr-I	[141; 142]
S. haemolyticus	SFTPCTTYF		[137]
S. hominis	TYSTCYGYF		[137]
	SYNVCGGYF	*S. aureus* Agr-I	[142]
S. hyicus	KINPCTVFF		[137]
S. lugdunensis	DICNAYF	*S. aureus* Agr-I/II/III	[21; 140]
	DMCNGYF (AIP-II)		[137]
S. pseudintermedius	RIPTSTGFF (AIP-I)		[143]
S. saprophyticus	INPCFGYT		[137; 144]
S. schleiferi	KYPFCIGYF	*S. aureus* Agr-I/II/III/IV	[137; 145]
S. schweitzeri	YSTCYFIM (identical to *S. aureus* AIP-IV)		[137]
S. simulans	KYNPCLGFL (AIP-I)		[137]
	KYYPCWGYF (AIP-II)	*S. simulans* Agr-I *S. aureus* Agr-I/II/III/IV	[138]
	KYNPCWGYF (AIP-III)	*S. simulans* Agr-I, *S. aureus* Agr-I/II/III	[138]
S. vitulinus	VIRGCTAFL		[137]
S. warneri	YSPCTNFF		[137]

19

Although the *agr* QS system is present in all staphylococci, the length and amino acid compositions of AIP precursors/mature AIPs are highly diverse between different staphylococcal species and, intriguingly, also between different clonal groups of a given species [20]. In *S. aureus*, for instance, four *agr* types with four different AIPs (AIP I-IV) are known that show cross-inhibition towards strains possessing other *agr* types, a phenomenon called "quorum quenching", that also occurs on the interspecies level [21, 105, 106]. The amino acid sequences of AIPs produced by staphylococci are summarized in Table 2, including also the AIP variant of *S. pseudintermedius*, where the thiolactone is replaced by a lactone, and Figure 3 shows representative AIP structures.

NRPs (non-ribosomal peptides)

Non-ribosomal peptides are secondary metabolites found in bacteria, and fungi with manifold biological activities [107]. In contrast to RiPPs described above, NRPs are produced by non-ribosomal peptide synthetases (NRPSs), a family of large multimodular mega-enzymes; thus, NRPSs constitute RNA- and ribosome-independent machineries for peptide biosynthesis.

NRPSs are typically organized in multiple, distinct modules comprising catalytic domains that are responsible for the coordinated incorporation of a single amino acid or related building block into a polypeptide product. Those modules can either be encoded by a single gene to form a single, large NRPS protein with multiple modules, or by multiple genes encoding individual NRPS proteins that interact sequentially with each other to form a multienzyme complex [107, 108]. A minimal module, usually found as the first module initiating peptide synthesis, consists of an adenylation (A) and a peptidyl carrier protein (PCP) domain, while modules further downstream generally also contain an additional condensation (C) domain. NRP biosynthesis comprises several biochemical steps that are described at greater detail elsewhere [107, 108].

In brief: The A domain is responsible for the selection of the amino acid to be incorporated into the NRPS product and is therefore often referred to as the "gate keeper" of NRPSs [108, 109]. During NRP synthesis, the A domain activates the amino acid in an ATP-dependent manner to form an amino acyl adenylate that is loaded onto a PCP. The C-domain is then responsible for the elongation/extension of the NRP as it catalyzes the peptide bond formation between the two amino acyl adenylates tethered to PCPs of adjacent modules [107, 110]. This new peptide serves again as a substrate for the further downstream located C-domains, continuing the elongation process. At the end of the elongation process, release of the nascent peptide from the last PCP is usually catalyzed by a thioesterase (TE) domain but can occasionally also

be catalyzed by a reductase domain (R) [107, 111]. In case of the latter, the hitherto identified NRPs from staphylococci are released via an NADPH-dependent reductase.

Fibupeptides

Fibupeptides are a recently discovered class of NRPs defined as macrocyclic peptides containing a thiazolidine moiety [112]. This class is represented by lugdunin, currently the first and only member of natural fibupeptides (Fig. 4a) [113]. Lugdunin has protonophore activity combined with antibiotic properties. It is produced by *Staphylococcus lugdunensis*, a commensal of the human nose and skin microbiomes that inhibits the growth of *S. aureus* (among other bacteria) by causing the breakdown of energy supply. Furthermore, it could be shown that the risk of nasal carriage of *S. aureus* was approx. 6-fold reduced when human individuals were colonized by lugdunin-producing *S. lugdunensis*, which was also confirmed in animal models, indicating a microbiome-shaping role of lugdunin-producing *S. lugdunensis* that may contribute to human resilience against *S. aureus* carriage [113].

The lugdunin BGC is located on the chromosome and contains the genes responsible for lugdunin biosynthesis; the four genes *lugA-D*, encoding the NRPS modules, and the genes *lugT* and *lugZ*, encoding a thioesterase involved in repair/recovery of stalled PCP domains and a 4'-phosphopantetheinyl transferase, respectively. It further contains genes involved in lugdunin transport and immunity (*lugI-H*) or, presumably, regulation (*lugJ*, *lugR*) [113, 114].

The four NRPS modules of LugA-D contain five adenylation domains for Cys, Val, Trp, Leu, Val and also three epimerization domains, which catalyze the conversion of L-amino acids to D-amino acids. The biosynthesis is initiated by LugD and continues with LugA-C, with LugC contributing three Val, resulting in the formation of a linear hepta-peptide consisting of L-Cys, D-Val, L-Trp, D-Leu, L-Val, D-Val, and L-Val, tethered to the last PCP of LugC. The C-terminal reductase of LugC releases the peptide from the last PCP, leading to aldehyde formation at the C-terminal L-Val that is subsequently nucleophilically attacked by the N-terminal amine of L-Cys to form a macrocyclic imine. A second nucleophilic attack of the thiol group of Cys to the imine finally generates the five-membered thiazolidine heterocycle, the hallmark of fibupeptides [113].

Pyrazinones

Pyrazinones are 6-membered, nitrogenous heterocycles that are constituents of aureusimines, non-ribosomally synthesized, cyclic dipeptides produced by some *Staphylococcus* species Aureusimines were discovered almost simultaneously by the two groups of Fischbach [115]
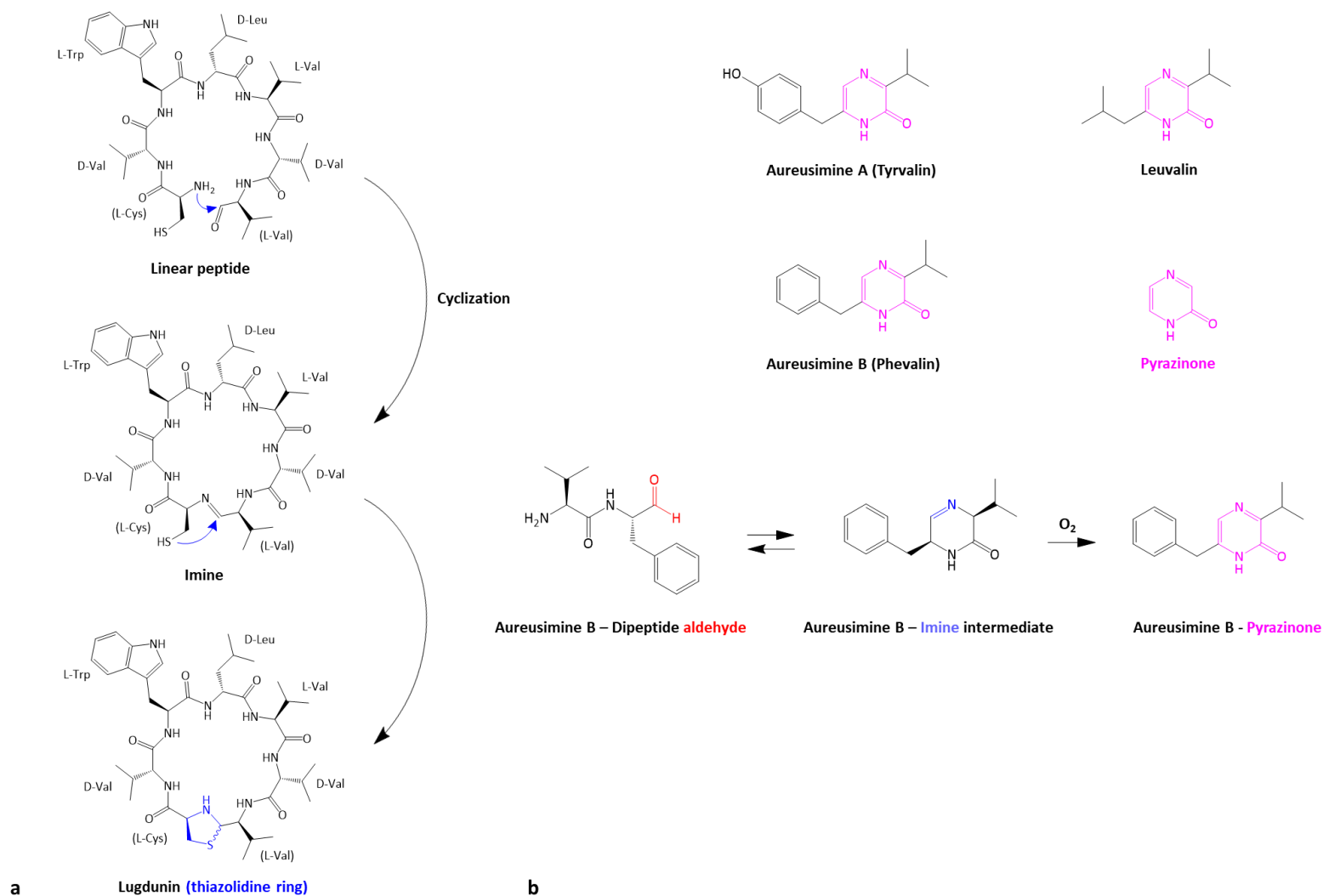
Fig. 4. Community active NRPS products of staphylococci. **a,** Chemical structure of the fibupeptide lugdunin and its conversion from a linear peptide, over an imine intermediate to the final lugdunin product. Thiazolidine ring is indicated in blue. **b,** Chemical structures of aureusimines and their conversion from a dipeptide aldehyde (red), over an imine intermediate (blue) to a pyrazinone product (pink), on the example of aureusimine B**.**

and Magarvey [116] in *S. aureus*, and their BGCs were shown to be conserved in several staphylococcal species including *S. aureus*, *S. epidermidis*, *S. lugdunensis,* and *S. capitis* [115].

The BGC of aureusimine is located on the chromosome and consists of genes coding for the 4'-phosphopantetheinyl transferase AusB and the single, dimodular NRPS protein AusA, whose first A domain has a preference for incorporation of Val and the second A domain for the aromatic amino acids Tyr or Phe and the aliphatic amino acid Leu [116, 117]. Biosynthesis leads to a dipeptide consisting of L-Val and either L-Tyr, L-Phe, or L-Leu that is released from the last PCP via the C-terminal reductase. The resulting aldehyde at L-Tyr/L-Phe/L-Leu subsequently undergoes cyclization with the amine of the N-terminal L-Val to form an intermediate imine that again spontaneously oxidizes to the final pyrazinone product, aureusimine A (tyrvalin), aureusimine B (phevalin) or leuvalin, respectively (Figure 4b) [115, 116].

The biological roles of aureusimines have been investigated by several groups, which initially thought that these compounds are involved in virulence factor regulation, which, however, was later attributed to a mutation in the *saeS* gene, a known regulator of virulence factors [116, 118]. Nevertheless, aureusimines may play a role in *S. aureus* virulence. The group of Fraunholz [119] has shown that aureusimines are involved in phenol soluble modulin (PSM)-mediated phagosomal escape of internalized *S. aureus* in a currently unknown way and therefore contribute to an important survival strategy. More recently, a study based on the investigation of NRPS BGCs of the human gut microbiome suggested that peptide aldehydes, such as the aureusimine B aldehyde, are also potent inhibitors of cathepsins, a cysteine protease family involved in Toll-like receptor 9 activation in macrophages and dendritic cells and in antigen processing and presentation [108, 120]. Interestingly, the linear dipeptide aldehyde seems to be the bioactive form rather than the cyclic pyrazinone peptide. The gut represents an anaerobic environment, where the linear dipeptide and the cyclic imine exist in equilibrium [120]. Only in the presence of oxygen, the irreversible conversion from the cyclic imine to the pyrazinone occurs, suggesting that the pyrazinone variant may be the unfavorable form of aureusimines. If aureusimines are also inhibitors of host cysteine proteases and whether this potential activity contributes to the prevention of PSM degradation or of antigen processing remains to be explored.

Polycarboxylate Siderophores

(Poly-)carboxylates are one of the four known classes of siderophores, low-molecular weight molecules with ferric iron-chelating properties. They were classified based on the chemical

moieties with which they coordinate Fe(III), as described in more detail elsewhere [23]. Siderophores are produced by bacteria under iron-limited conditions to secure proliferation by scavenging iron ions from the environment. In staphylococci, staphyloferrin A and B have been documented, which belong to the (poly)carboxylate class of siderophores (Fig. 5a) [121, 122]. While many siderophores are produced by NRPS systems, staphyloferrin A and B are produced via NRPS-independent siderophore (NIS) synthetases.

NIS enzymes catalyze the condensation of citric acid or derivatives with amines or alcohols, and are characterized by a conserved N-terminal iron uptake chelate (Iuc) domain and a C-terminal domain associated with iron transport or metabolism [123].

Only two and three NIS enzymes are required for synthesis of staphyloferrin A and B, respectively [123, 124]. These enzymes are encoded by the genes *sfaB*/*sfaD* for staphyloferrin A [125, 126] and *sbnE*/*sbnC*/*sbnF* for staphyloferrin B [127, 128], which are found adjacent to genes coding for proteins involved in siderophore export and uptake. While the gene locus for staphyloferrin B seems to be limited to only a few staphylococcal species such as *S. aureus*, *S. pseudintermedius or S. hyicus*, the genes of staphyloferrin A seem to be present in almost all staphylococcal species. Only some species such as *S. lugdunensis* lack of *sfaA* and *sfaD* suggesting that these species do not produce their own siderophores. Nevertheless, *S. lugdunensis* encodes the uptake systems for both, staphyloferrinA and staphyloferrin B allowing to sequester siderophores from other microbiome member species [129].

Staphyloferrin A is composed of two citric acid moieties that are linked to a D-ornithine [121] (Fig. 5a). The biosynthesis of staphyloferrin A can be divided into two steps and is initiated by SfaD that connects a citrate with a D-ornithine to generate a citryl-D-ornithine intermediate in an ATP and Mg^{2+}-dependent manner. In the second step, SfaB adds another citrate to the intermediate, resulting in the formation of staphyloferrin A.

Staphyloferrin B consists of L-2,3-diaminopropionic acid (L-Dap), citrate, 1,2-diaminoethane, and α-ketoglutarate and is synthesized by the SbnCEF NIS and the PLP-decarboxylase SbnH [122, 128]. Here, SbnE connects a citrate with L-Dap to form a citryl-diaminopropionic acid intermediate, which is decarboxylated by SbnH to a citryl-diaminethane. SbnF then adds another L-Dap to the intermediate and SbnC completes staphyloferrin B biosynthesis by adding α-ketoglutarate to the decarboxylated Dap residue [123, 128].
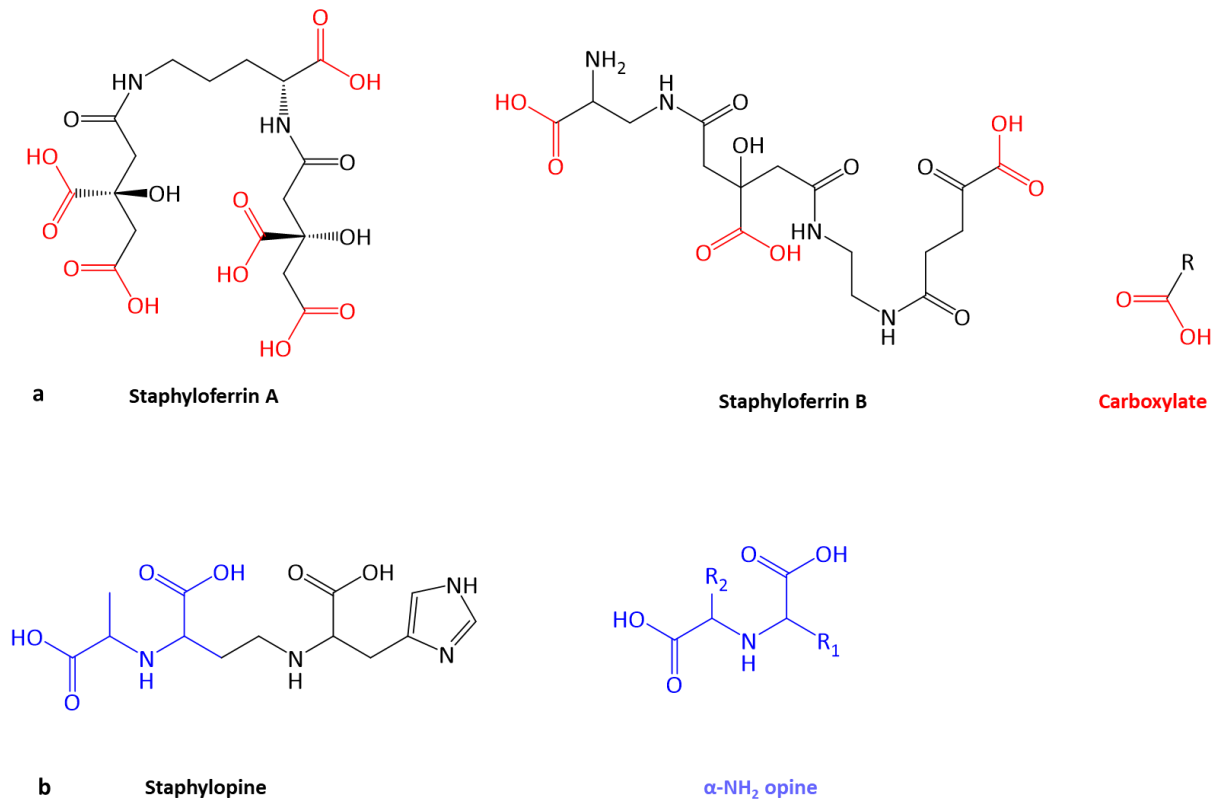
a Staphyloferrin A

Staphyloferrin B

Carboxylate

b Staphylopine

α-NH₂ opine

Fig. 5. Metallophores produced by staphylococci. **a,** Chemical structures of the two siderophores staphyloferrin A and B. Carboxylates are depicted and indicated in red. **b,** Chemical structure of staphylopine. The opine scaffold is depicted and indicated in blue.

Opines (metallophore)

Opines are nitrogenous compounds with diverse biological roles that consist of a variety of α-keto acid and amino acid substrates. The synthesis of opines is usually mediated by opine dehydrogenases that catalyze the condensation of the amino group of an amino acid with an α-keto acid and a subsequent NAD(P)H dependent reduction [130]. Recently, a novel opine compound produced by *S. aureus* has been identified that was termed staphylopine (Fig. 5 B) [131].

Staphylopine is a broad-spectrum metallophore with a nicotianamine-like entity responsible for its metal-chelating properties, showing binding affinities for nickel, copper, cobalt, iron, and zinc. It is produced under zinc-limited conditions and has been shown to play an important role in zinc acquisition, virulence, and fitness of *S. aureus* [131-134].

The BGC of staphylopine consists of the three genes, *cntKLM*, that are encoded adjacent to genes involved in staphylopine export, *cntE*, and recognition and import, *cntABCDF* [131]. The staphylopine biosynthesis is initiated by the His racemase *cntK* that provides a D-His, which is connected by the nicotianamine synthase CntL to SAM, generating a D-His-nicotianamine (D-

HisNA) intermediate. In the last step, the opine dehydrogenase CtnM adds a pyruvate to D-HisNA, followed by a NADPH-dependent reduction, resulting in the mature staphylopine molecule [130, 131].

Conclusion

Bacterial communities of the human microbiome comprise a multitude of bacterial species and we are only just starting to decipher the mechanisms shaping their compositions. In this context, aside from host-bacteria interactions, specific secondary metabolites may play an important role in bacteria-bacteria interactions [8]. On many occasions, staphylococci have demonstrated to be a rich source of versatile bioactive compounds, including metallophores, bacteriocins, and signaling-interfering AIPs, which are produced by a large repertoire of biosynthetic pathways.

However, whereas a lot of these compounds have been thoroughly studied with respect to their bioactive properties *in vitro*, their ecological relevance for bacterial interactions *in vivo* remains widely elusive. This fact is due to at least two main reasons. Firstly, research on staphylococci has focused largely on infections, caused by *S. aureus* and only a few other species [135], while the commensal lifestyle has been addressed only by a few studies. Secondly, interactions within bacterial communities are complex, require sophisticated model systems, and are difficult to study with standard laboratory methodology. Members of bacterial communities on human body surfaces have to deal with cocktails of different secondary metabolites produced by many different host and bacterial cells. Therefore, it is often challenging to pinpoint the impact of individual compounds or their producers on community composition and dynamic. New model systems simulating complex bacterial communities under realistic conditions that allow the dynamic monitoring of fitness traits of individual bacterial clones need to be developed.

Despite of these difficulties, the interest in the field of functional microbiome science is continuously increasing owing to recent advances in techniques, such as next-generation sequencing, metagenome analyses, metabolomics, and suitable *in vivo* models, [8]. A better understanding of the biological roles of specific secondary metabolites in bacterial interactions, however, requires further advances in these techniques. Such developments will not only facilitate to elucidate the role of novel compounds, but also to examine compounds that have been identified in the past but have not been investigated in terms of their significance for bacterial interactions yet.

Furthermore, staphylococci and their potent bioactive compounds may become of interest for translational medicine. Bacteriocins, in particular, seem to be prevalent among staphylococci

and recent studies have shown that staphylococci are a reservoir of new bacteriocins of different and often novel substance classes [14, 16, 78]. Thus, either isolated bacteriocins or the bacteriocin producer strains may become useful alternatives or complementary agents for clinically used antibiotics for infection treatment or as probiotics for pathogen decolonization strategies. In addition, QS-inhibitory AIP variants may become attractive anti-virulence drugs, since they interfere with the staphylococcal *agr* systems that regulate virulence-associated genes and, hence, may prevent infections or attenuate their severity.

Statements

Acknowledgments

Conflict of Interest Statement

Eberhard Karls University Tübingen holds a patent (EP3072899B1) covering the compound lugdunin, derivatives thereof, and the bacterial infection prevention by lugdunin producing bacteria. The patent has also been filed in the USA (US2018/0155397A1).

Funding Sources

Author Contributions

All authors contributed to the preparation of this document and their contributions according to the authorship criteria are as follows. B.O.T.S.: drafting the work and preparation of figures. S.H., A.P. and B.K.: substantial contributions to the conception and design of the work and revising the work critically for important intellectual content. All authors gave final approval of the version to be published.

References

1.   Grice EA, Segre JA. The skin microbiome. Nature reviews Microbiology. 2011;9(4):244-53. doi: 10.1038/nrmicro2537. PubMed PMID: 21407241.

2.   Coates R, Moran J, Horsburgh MJ. Staphylococci: colonizers and pathogens of human skin. Future Microbiol. 2014;9(1):75-91. Epub 2013/12/18. doi: 10.2217/fmb.13.145. PubMed PMID: 24328382.

3.   Lee AS, de Lencastre H, Garau J, Kluytmans J, Malhotra-Kumar S, Peschel A, et al. Methicillin-resistant Staphylococcus aureus. Nat Rev Dis Primers. 2018;4:18033. Epub 2018/06/01. doi: 10.1038/nrdp.2018.33. PubMed PMID: 29849094.

4.   Becker K, Heilmann C, Peters G. Coagulase-Negative Staphylococci. Clinical Microbiology Reviews. 2014;27(4):870. doi: 10.1128/CMR.00109-13.

5.   Krismer B, Weidenmaier C, Zipperer A, Peschel A. The commensal lifestyle of Staphylococcus aureus and its interactions with the nasal microbiota. Nature Reviews Microbiology. 2017;15(11):675-87. doi: 10.1038/nrmicro.2017.104.

6.   Rawls M, Ellis AK. The microbiome of the nose. Ann Allergy Asthma Immunol. 2019;122(1):17-24. Epub 2018/12/24. doi: 10.1016/j.anai.2018.05.009. PubMed PMID: 30579432.

7.   Flowers L, Grice EA. The Skin Microbiota: Balancing Risk and Reward. Cell Host & Microbe. 2020;28(2):190-200. doi: https://doi.org/10.1016/j.chom.2020.06.017.

8.   Otto M. Staphylococci in the human microbiome: the role of host and interbacterial interactions. Current Opinion in Microbiology. 2020;53:71-7. doi: https://doi.org/10.1016/j.mib.2020.03.003.

9.   Parlet CP, Brown MM, Horswill AR. Commensal Staphylococci Influence Staphylococcus aureus Skin Colonization and Disease. Trends Microbiol. 2019;27(6):497-507. Epub 2019/03/09. doi: 10.1016/j.tim.2019.01.008. PubMed PMID: 30846311; PubMed Central PMCID: PMCPMC7176043.

10.   Braga RM, Dourado MN, Araújo WL. Microbial interactions: ecology in a molecular perspective. Braz J Microbiol. 2016;47 Suppl 1(Suppl 1):86-98. Epub 2016/11/09. doi: 10.1016/j.bjm.2016.10.005. PubMed PMID: 27825606; PubMed Central PMCID: PMCPMC5156507.

11.   Botelho-Nevers E, Gagnaire J, Verhoeven PO, Cazorla C, Grattard F, Pozzetto B, et al. Decolonization of Staphylococcus aureus carriage. Médecine et Maladies Infectieuses. 2017;47(5):305-10. doi: https://doi.org/10.1016/j.medmal.2016.10.005.

12.   Cotter PD, Hill C, Ross RP. Bacteriocins: developing innate immunity for food. Nature Reviews Microbiology. 2005;3(10):777-88. doi: 10.1038/nrmicro1273.

13.   Arnison PG, Bibb MJ, Bierbaum G, Bowers AA, Bugni TS, Bulaj G, et al. Ribosomally synthesized and post-translationally modified peptide natural products: overview and recommendations for a universal nomenclature. Nat Prod Rep.

2013;30(1):108-60. Epub 2012/11/21. doi: 10.1039/c2np20085f. PubMed PMID: 23165928; PubMed Central PMCID: PMCPMC3954855.

14.   Janek D, Zipperer A, Kulik A, Krismer B, Peschel A. High Frequency and Diversity of Antimicrobial Activities Produced by Nasal Staphylococcus Strains against Bacterial Competitors. PLoS Pathog. 2016;12(8):e1005812. doi: 10.1371/journal.ppat.1005812. PubMed PMID: 27490492; PubMed Central PMCID: PMCPMC4973975.

15.   O'Sullivan JN, Rea MC, O'Connor PM, Hill C, Ross RP. Human skin microbiota is a rich source of bacteriocin-producing staphylococci that kill human pathogens. FEMS Microbiology Ecology. 2018;95(2). doi: 10.1093/femsec/fiy241.

16.   Nakatsuji T, Chen TH, Narala S, Chun KA, Two AM, Yun T, et al. Antimicrobials from human skin commensal bacteria protect against Staphylococcus aureus and are deficient in atopic dermatitis. Sci Transl Med. 2017;9(378):eaah4680. doi: 10.1126/scitranslmed.aah4680. PubMed PMID: 28228596.

17.   Nakatsuji T, Hata TR, Tong Y, Cheng JY, Shafiq F, Butcher AM, et al. Development of a human skin commensal microbe for bacteriotherapy of atopic dermatitis and use in a phase 1 randomized clinical trial. Nature medicine. 2021. doi: 10.1038/s41591-021-01256-2. PubMed PMID: 33619370.

18.   Christensen GJ, Scholz CF, Enghild J, Rohde H, Kilian M, Thürmer A, et al. Antagonism between Staphylococcus epidermidis and Propionibacterium acnes and its genomic basis. BMC Genomics. 2016;17:152. Epub 2016/03/01. doi: 10.1186/s12864-016-2489-5. PubMed PMID: 26924200; PubMed Central PMCID: PMCPMC4770681.

19.   Claesen J, Spagnolo JB, Ramos SF, Kurita KL, Byrd AL, Aksenov AA, et al. A Cutibacterium acnes antibiotic modulates human skin microbiota composition in hair follicles. Sci Transl Med. 2020;12(570). Epub 2020/11/20. doi: 10.1126/scitranslmed.aay5445. PubMed PMID: 33208503.

20.   Le KY, Otto M. Quorum-sensing regulation in staphylococci—an overview. Frontiers in Microbiology. 2015;6(1174). doi: 10.3389/fmicb.2015.01174.

21.   Ji G, Beavis R, Novick RP. Bacterial interference caused by autoinducing peptide variants. Science. 1997;276(5321):2027-30. Epub 1997/06/27. doi: 10.1126/science.276.5321.2027. PubMed PMID: 9197262.

22.   Thoendel M, Kavanaugh JS, Flack CE, Horswill AR. Peptide signaling in the staphylococci. Chem Rev. 2011;111(1):117-51. Epub 2010/12/23. doi: 10.1021/cr100370n. PubMed PMID: 21174435; PubMed Central PMCID: PMCPMC3086461.

23.   Kramer J, Özkaya Ö, Kümmerli R. Bacterial siderophores in community and host interactions. Nature Reviews Microbiology. 2020;18(3):152-63. doi: 10.1038/s41579-019-0284-4.

24.   Montalban-Lopez M, Scott TA, Ramesh S, Rahman IR, van Heel AJ, Viel JH, et al. New developments in RiPP discovery, enzymology and engineering. Nat Prod Rep.

2021;38(1):130-239. doi: 10.1039/d0np00027b. PubMed PMID: 32935693; PubMed Central PMCID: PMCPMC7864896.

25.   Oman TJ, van der Donk WA. Follow the leader: the use of leader peptides to guide natural product biosynthesis. Nat Chem Biol. 2010;6(1):9-18. Epub 2009/12/18. doi: 10.1038/nchembio.286. PubMed PMID: 20016494; PubMed Central PMCID: PMCPMC3799897.

26.   Schnell N, Entian K-D, Schneider U, Götz F, Zähner H, Kellner R, et al. Prepeptide sequence of epidermin, a ribosomally synthesized antibiotic with four sulphide-rings. Nature. 1988;333(6170):276-8. doi: 10.1038/333276a0.

27.   Guder A, Wiedemann I, Sahl H-G. Posttranslationally modified bacteriocins—the lantibiotics. Peptide Science. 2000;55(1):62-73. doi: https://doi.org/10.1002/1097-0282(2000)55:1<62::AID-BIP60>3.0.CO;2-Y.

28.   Knerr PJ, van der Donk WA. Discovery, Biosynthesis, and Engineering of Lantipeptides. Annual Review of Biochemistry. 2012;81(1):479-505. doi: 10.1146/annurev-biochem-060110-113521.

29.   Reisinger P, Seidel H, Tschesche H, Hammes WP. The effect of nisin on murein synthesis. Archives of Microbiology. 1980;127(3):187-93. doi: 10.1007/BF00427192.

30.   Brötz H, Bierbaum G, Leopold K, Reynolds PE, Sahl H-G. The Lantibiotic Mersacidin Inhibits Peptidoglycan Synthesis by Targeting Lipid II. Antimicrobial Agents and Chemotherapy. 1998;42(1):154. doi: 10.1128/AAC.42.1.154.

31.   Breukink E, Wiedemann I, Kraaij Cv, Kuipers OP, Sahl HG, de Kruijff B. Use of the Cell Wall Precursor Lipid II by a Pore-Forming Peptide Antibiotic. Science. 1999;286(5448):2361. doi: 10.1126/science.286.5448.2361.

32.   Müller A, Ulm H, Reder-Christ K, Sahl HG, Schneider T. Interaction of type A lantibiotics with undecaprenol-bound cell envelope precursors. Microb Drug Resist. 2012;18(3):261-70. Epub 2012/03/22. doi: 10.1089/mdr.2011.0242. PubMed PMID: 22432708.

33.   Götz F, Perconti S, Popella P, Werner R, Schlag M. Epidermin and gallidermin: Staphylococcal lantibiotics. International Journal of Medical Microbiology. 2014;304(1):63-71. doi: https://doi.org/10.1016/j.ijmm.2013.08.012.

34.   Bonelli RR, Schneider T, Sahl HG, Wiedemann I. Insights into in vivo activities of lantibiotics from gallidermin and epidermin mode-of-action studies. Antimicrob Agents Chemother. 2006;50(4):1449-57. Epub 2006/03/30. doi: 10.1128/aac.50.4.1449-1457.2006. PubMed PMID: 16569864; PubMed Central PMCID: PMCPMC1426925.

35.   Siezen RJ, Kuipers OP, de Vos WM. Comparison of lantibiotic gene clusters and encoded proteins. Antonie Van Leeuwenhoek. 1996;69(2):171-84. Epub 1996/02/01. doi: 10.1007/bf00399422. PubMed PMID: 8775977.

36. Bierbaum G, Sahl HG. Lantibiotics: Mode of Action, Biosynthesis and Bioengineering. Current Pharmaceutical Biotechnology. 2009;10(1):2-18. doi: http://dx.doi.org/10.2174/138920109787048616.

37. Schnell N, Engelke G, Augustin J, Rosenstein R, Ungermann V, Götz F, et al. Analysis of genes involved in the biosynthesis of lantibiotic epidermin. Eur J Biochem. 1992;204(1):57-68. Epub 1992/02/15. doi: 10.1111/j.1432-1033.1992.tb16605.x. PubMed PMID: 1740156.

38. Kupke T, Kempter C, Gnau V, Jung G, Götz F. Mass spectroscopic analysis of a novel enzymatic reaction. Oxidative decarboxylation of the lantibiotic precursor peptide EpiA catalyzed by the flavoprotein EpiD. J Biol Chem. 1994;269(8):5653-9. Epub 1994/02/25. PubMed PMID: 8119901.

39. Velásquez Juan E, Zhang X, van der Donk Wilfred A. Biosynthesis of the Antimicrobial Peptide Epilancin 15X and Its N-Terminal Lactate. Chemistry & Biology. 2011;18(7):857-67. doi: https://doi.org/10.1016/j.chembiol.2011.05.007.

40. Allgaier H JG, Werner R, Schneider U, Zähner H Strukturaufklärung von Epidermin, einem ribosomal synthetisierten, heterodet tetracyclischen Polypeptid-Antibioticum. Angewandte Chemie (International ed in English). 1985. doi: 10.1002/ange.19850971214.

41. Kellner R, Jung G, Hörner T, Zähner H, Schnell N, Entian KD, et al. Gallidermin: a new lanthionine-containing polypeptide antibiotic. Eur J Biochem. 1988;177(1):53-9. Epub 1988/10/15. doi: 10.1111/j.1432-1033.1988.tb14344.x. PubMed PMID: 3181159.

42. Peschel A, Augustin J, Kupke T, Stevanovic S, Götz F. Regulation of epidermin biosynthetic genes by EpiQ. Molecular Microbiology. 1993;9(1):31-9. doi: https://doi.org/10.1111/j.1365-2958.1993.tb01666.x.

43. Kupke T, Stevanović S, Sahl HG, Götz F. Purification and characterization of EpiD, a flavoprotein involved in the biosynthesis of the lantibiotic epidermin. Journal of Bacteriology. 1992;174(16):5354-61. doi: 10.1128/jb.174.16.5354-5361.1992.

44. Kupke T, Götz F. The enethiolate anion reaction products of EpiD. Pka value of the enethiol side chain is lower than that of the thiol side chain of peptides. J Biol Chem. 1997;272(8):4759-62. Epub 1997/02/21. doi: 10.1074/jbc.272.8.4759. PubMed PMID: 9030529.

45. Geissler S, Götz F, Kupke T. Serine protease EpiP from Staphylococcus epidermidis catalyzes the processing of the epidermin precursor peptide. Journal of Bacteriology. 1996;178(1):284-8. doi: 10.1128/jb.178.1.284-288.1996.

46. Bierbaum G, Götz F, Peschel A, Kupke T, van de Kamp M, Sahl H-G. The biosynthesis of the lantibiotics epidermin, gallidermin, Pep5 and epilancin K7. Antonie van Leeuwenhoek. 1996;69(2):119-27. doi: 10.1007/BF00399417.

47. Furmanek B, Kaczorowski T, Bugalski R, Bielawski K, Bohdanowicz J, Podhajska AJ. Identification, characterization and purification of the lantibiotic staphylococcin T, a natural gallidermin variant. J Appl Microbiol. 1999;87(6):856-66. Epub 2000/02/09. doi: 10.1046/j.1365-2672.1999.00937.x. PubMed PMID: 10664909.

48.   Scott JC, Sahl HG, Carne A, Tagg JR. Lantibiotic-mediated anti-lactobacillus activity of a vaginal Staphylococcus aureus isolate. FEMS Microbiol Lett. 1992;72(1):97-102. Epub 1992/05/15. doi: 10.1016/0378-1097(92)90496-b. PubMed PMID: 1612423.

49.   Daly KM, Upton M, Sandiford SK, Draper LA, Wescombe PA, Jack RW, et al. Production of the Bsa Lantibiotic by Community-Acquired Staphylococcus aureus Strains. Journal of Bacteriology. 2010;192(4):1131-42. doi: 10.1128/jb.01375-09.

50.   Joo HS, Cheung GY, Otto M. Antimicrobial activity of community-associated methicillin-resistant Staphylococcus aureus is caused by phenol-soluble modulin derivatives. J Biol Chem. 2011;286(11):8933-40. Epub 2011/02/01. doi: 10.1074/jbc.M111.221382. PubMed PMID: 21278255; PubMed Central PMCID: PMCPMC3059065.

51.   Wladyka B, Wielebska K, Wloka M, Bochenska O, Dubin G, Dubin A, et al. Isolation, biochemical characterization, and cloning of a bacteriocin from the poultry-associated Staphylococcus aureus strain CH-91. Applied Microbiology and Biotechnology. 2013;97(16):7229-39. doi: 10.1007/s00253-012-4578-y.

52.   Fagundes PC, Ceotto H, Potter A, Vasconcelos de Paiva Brito MA, Brede D, Nes IF, et al. Hyicin 3682, a bioactive peptide produced by Staphylococcus hyicus 3682 with potential applications for food preservation. Res Microbiol. 2011;162(10):1052-9. Epub 2011/10/25. doi: 10.1016/j.resmic.2011.10.002. PubMed PMID: 22019494.

53.   Fagundes PC, Francisco MS, Sousa Santos IN, Marques-Bastos SLS, Paz JAS, Albano RM, et al. Draft genome sequence of Staphylococcus agnetis 3682, the producing strain of the broad-spectrum lantibiotic agneticin 3682. Journal of Global Antimicrobial Resistance. 2019;19:50-2. doi: https://doi.org/10.1016/j.jgar.2019.08.014.

54.   Ekkelenkamp MB, Hanssen M, Danny Hsu S-T, de Jong A, Milatovic D, Verhoef J, et al. Isolation and structural characterization of epilancin 15X, a novel lantibiotic from a clinical strain of Staphylococcus epidermidis. FEBS Letters. 2005;579(9):1917-22. doi: 10.1016/j.febslet.2005.01.083.

55.   van de Kamp M, Horstink LM, Van Den Hooven HW, Konings RNH, Hilbers CW, Frey A, et al. Sequence Analysis by NMR Spectroscopy of the Peptide Lantibiotic Epilancin K7 from Staphylococcus epidermidis K7. European Journal of Biochemistry. 1995;227(3):757-71. doi: https://doi.org/10.1111/j.1432-1033.1995.0757p.x.

56.   van de Kamp M, van den Hooven HW, Konings RN, Bierbaum G, Sahl HG, Kuipers OP, et al. Elucidation of the primary structure of the lantibiotic epilancin K7 from Staphylococcus epidermidis K7. Cloning and characterisation of the epilancin-K7-encoding gene and NMR analysis of mature epilancin K7. Eur J Biochem. 1995;230(2):587-600. Epub 1995/06/01. doi: 10.1111/j.1432-1033.1995.tb20600.x. PubMed PMID: 7607233.

57.   Heidrich C, Pag U, Josten M, Metzger J, Jack RW, Bierbaum G, et al. Isolation, Characterization, and Heterologous Expression of the Novel Lantibiotic Epicidin 280

and Analysis of Its Biosynthetic Gene Cluster. Applied and Environmental Microbiology. 1998;64(9):3140. doi: 10.1128/AEM.64.9.3140-3146.1998.

58.   Repka LM, Chekan JR, Nair SK, van der Donk WA. Mechanistic Understanding of Lanthipeptide Biosynthetic Enzymes. Chem Rev. 2017;117(8):5457-520. Epub 2017/01/31. doi: 10.1021/acs.chemrev.6b00591. PubMed PMID: 28135077; PubMed Central PMCID: PMCPMC5408752.

59.   Ersfeld-Dressen H, Sahl HG, Brandis H. Plasmid involvement in production of and immunity to the staphylococcin-like peptide Pep 5. J Gen Microbiol. 1984;130(11):3029-35. Epub 1984/11/01. doi: 10.1099/00221287-130-11-3029. PubMed PMID: 6527128.

60.   Weil HP, Beck-Sickinger AG, Metzger J, Stevanovic S, Jung G, Josten M, et al. Biosynthesis of the lantibiotic Pep5. Isolation and characterization of a prepeptide containing dehydroamino acids. Eur J Biochem. 1990;194(1):217-23. Epub 1990/11/26. doi: 10.1111/j.1432-1033.1990.tb19446.x. PubMed PMID: 2253617.

61.   Meyer C, Bierbaum G, Heidrich C, Reis M, Süling J, Iglesias-Wind MI, et al. Nucleotide sequence of the lantibiotic Pep5 biosynthetic gene cluster and functional analysis of PepP and PepC. Evidence for a role of PepC in thioether formation. Eur J Biochem. 1995;232(2):478-89. Epub 1995/09/01. doi: 10.1111/j.1432-1033.1995.tb20834.x. PubMed PMID: 7556197.

62.   Bastos MC, Ceotto H, Coelho ML, Nascimento JS. Staphylococcal antimicrobial peptides: relevant properties and potential biotechnological applications. Curr Pharm Biotechnol. 2009;10(1):38-61. Epub 2009/01/20. doi: 10.2174/138920109787048580. PubMed PMID: 19149589.

63.   Kellner R, Jung G, Josten M, Kaletta C, Entian K-D, Sahl H-G. Pep5: Structure Elucidation of a Large Lantibiotic. Angewandte Chemie International Edition in English. 1989;28(5):616-9. doi: 10.1002/anie.198906161.

64.   O'Sullivan JN, O'Connor PM, Rea MC, O'Sullivan O, Walsh CJ, Healy B, et al. Nisin J, a Novel Natural Nisin Variant, Is Produced by Staphylococcus capitis Sourced from the Human Skin Microbiota. J Bacteriol. 2020;202(3). Epub 2019/11/20. doi: 10.1128/jb.00639-19. PubMed PMID: 31740495; PubMed Central PMCID: PMCPMC6964739.

65.   Kimura H, Matsusaki H, Sashihara T, Sonomoto K, Ishizaki A. Purification and Partial Identification of Bacteriocin ISK-1, a New Lantibiotic Produced by Pediococcus sp. ISK-1. Biosci Biotechnol Biochem. 1998;62(12):2341-5. Epub 1998/01/01. doi: 10.1271/bbb.62.2341. PubMed PMID: 27392396.

66.   Kimura H, Sashihara T, Matsusaki H, Sonomoto K, Ishizaki A. Novel bacteriocin of Pediococcus sp. ISK-1 isolated from well-aged bed of fermented rice bran. Ann N Y Acad Sci. 1998;864:345-8. Epub 1999/02/03. doi: 10.1111/j.1749-6632.1998.tb10336.x. PubMed PMID: 9928112.

67.   Sashihara T, Kimura H, Higuchi T, Adachi A, Matsusaki H, Sonomoto K, et al. A Novel Lantibiotic, Nukacin ISK-1, of Staphylococcus warneri ISK-1: Cloning of the

Structural Gene and Identification of the Structure. Bioscience, Biotechnology, and Biochemistry. 2000;64(11):2420-8. doi: 10.1271/bbb.64.2420.

68.   Aso Y, Sashihara T, Nagao J, Kanemasa Y, Koga H, Hashimoto T, et al. Characterization of a gene cluster of Staphylococcus warneri ISK-1 encoding the biosynthesis of and immunity to the lantibiotic, nukacin ISK-1. Biosci Biotechnol Biochem. 2004;68(8):1663-71. Epub 2004/08/24. doi: 10.1271/bbb.68.1663. PubMed PMID: 15322349.

69.   Shimafuji C, Noguchi M, Nishie M, Nagao J, Shioya K, Zendo T, et al. In vitro catalytic activity of N-terminal and C-terminal domains in NukM, the post-translational modification enzyme of nukacin ISK-1. J Biosci Bioeng. 2015;120(6):624-9. Epub 2015/05/15. doi: 10.1016/j.jbiosc.2015.03.020. PubMed PMID: 25971839.

70.   Nishie M, Shioya K, Nagao J-i, Jikuya H, Sonomoto K. ATP-dependent leader peptide cleavage by NukT, a bifunctional ABC transporter, during lantibiotic biosynthesis. Journal of Bioscience and Bioengineering. 2009;108(6):460-4. doi: https://doi.org/10.1016/j.jbiosc.2009.06.002.

71.   Wilaipun P, Zendo T, Okuda K, Nakayama J, Sonomoto K. Identification of the nukacin KQU-131, a new type-A(II) lantibiotic produced by Staphylococcus hominis KQU-131 isolated from Thai fermented fish product (Pla-ra). Biosci Biotechnol Biochem. 2008;72(8):2232-5. Epub 2008/08/08. doi: 10.1271/bbb.80239. PubMed PMID: 18685189.

72.   Ceotto H, Holo H, da Costa KFS, Nascimento JdS, Salehian Z, Nes IF, et al. Nukacin 3299, a lantibiotic produced by Staphylococcus simulans 3299 identical to nukacin ISK-1. Veterinary Microbiology. 2010;146(1):124-31. doi: https://doi.org/10.1016/j.vetmic.2010.04.032.

73.   Minamikawa M, Kawai Y, Inoue N, Yamazaki K. Purification and Characterization of Warnericin RB4, Anti-Alicyclobacillus Bacteriocin, Produced by Staphylococcus warneri RB4. Current Microbiology. 2005;51(1):22-6. doi: 10.1007/s00284-005-4456-2.

74.   Navaratna MA, Sahl HG, Tagg JR. Two-component anti-Staphylococcus aureus lantibiotic activity produced by Staphylococcus aureus C55. Applied and environmental microbiology. 1998;64(12):4803-8. PubMed PMID: 9835565.

75.   O'Connor EB, Cotter PD, O'Connor P, O'Sullivan O, Tagg JR, Ross RP, et al. Relatedness between the two-component lantibiotics lacticin 3147 and staphylococcin C55 based on structure, genetics and biological activity. BMC Microbiology. 2007;7(1):24. doi: 10.1186/1471-2180-7-24.

76.   Cotter PD, O'Connor PM, Draper LA, Lawton EM, Deegan LH, Hill C, et al. Posttranslational conversion of L-serines to D-alanines is vital for optimal production and activity of the lantibiotic lacticin 3147. Proc Natl Acad Sci U S A. 2005;102(51):18584-9. Epub 2005/12/08. doi: 10.1073/pnas.0509371102. PubMed PMID: 16339304.

77.   Crupper SS, Gies AJ, Iandolo JJ. Purification and characterization of staphylococcin BacR1, a broad-spectrum bacteriocin. Appl Environ Microbiol.

1997;63(11):4185-90. Epub 1997/11/15. PubMed PMID: 9361402; PubMed Central PMCID: PMCPMC168735.

78.   Angelopoulou A, Warda AK, O'Connor PM, Stockdale SR, Shkoporov AN, Field D, et al. Diverse Bacteriocins Produced by Strains From the Human Milk Microbiota. Frontiers in Microbiology. 2020;11(788). doi: 10.3389/fmicb.2020.00788.

79.   Flühe L, Knappe TA, Gattner MJ, Schäfer A, Burghaus O, Linne U, et al. The radical SAM enzyme AlbA catalyzes thioether bond formation in subtilosin A. Nat Chem Biol. 2012;8(4):350-7. Epub 2012/03/01. doi: 10.1038/nchembio.798. PubMed PMID: 22366720.

80.   Mathur H, Fallico V, O'Connor PM, Rea MC, Cotter PD, Hill C, et al. Insights into the Mode of Action of the Sactibiotic Thuricin CD. Frontiers in microbiology. 2017;8:696-. doi: 10.3389/fmicb.2017.00696. PubMed PMID: 28473822.

81.   Duarte AFdS, Ceotto-Vigoder H, Barrias ES, Souto-Padrón TCBS, Nes IF, Bastos MdCdF. Hyicin 4244, the first sactibiotic described in staphylococci, exhibits an anti-staphylococcal biofilm activity. International Journal of Antimicrobial Agents. 2018;51(3):349-56. doi: https://doi.org/10.1016/j.ijantimicag.2017.06.025.

82.   Duarte AFdS, Ceotto H, Coelho MLV, Brito MAVdP, Bastos MdCdF. Identification of new staphylococcins with potential application as food biopreservatives. Food Control. 2013;32(1):313-21. doi: https://doi.org/10.1016/j.foodcont.2012.12.008.

83.   Bagley MC, Dale JW, Merritt EA, Xiong X. Thiopeptide Antibiotics. Chemical Reviews. 2005;105(2):685-714. doi: 10.1021/cr0300441.

84.   Wieland Brown LC, Acker MG, Clardy J, Walsh CT, Fischbach MA. Thirteen posttranslational modifications convert a 14-residue peptide into the antibiotic thiocillin. Proc Natl Acad Sci U S A. 2009;106(8):2549-53. Epub 2009/02/05. doi: 10.1073/pnas.0900008106. PubMed PMID: 19196969.

85.   Just-Baringo X, Albericio F, Álvarez M. Thiopeptide antibiotics: retrospective and recent advances. Mar Drugs. 2014;12(1):317-51. Epub 2014/01/22. doi: 10.3390/md12010317. PubMed PMID: 24445304; PubMed Central PMCID: PMCPMC3917276.

86.   Harms JM, Wilson DN, Schluenzen F, Connell SR, Stachelhaus T, Zaborowska Z, et al. Translational regulation via L11: molecular switches on the ribosome turned on and off by thiostrepton and micrococcin. Mol Cell. 2008;30(1):26-38. Epub 2008/04/15. doi: 10.1016/j.molcel.2008.01.009. PubMed PMID: 18406324.

87.   Walter JD, Hunter M, Cobb M, Traeger G, Spiegel PC. Thiostrepton inhibits stable 70S ribosome binding and ribosome-dependent GTPase activation of elongation factor G and elongation factor 4. Nucleic Acids Res. 2012;40(1):360-70. Epub 2011/09/09. doi: 10.1093/nar/gkr623. PubMed PMID: 21908407.

88.   Heffron SE, Jurnak F. Structure of an EF-Tu complex with a thiazolyl peptide antibiotic determined at 2.35 A resolution: atomic basis for GE2270A inhibition of EF-

Tu. Biochemistry. 2000;39(1):37-45. Epub 2000/01/08. doi: 10.1021/bi9913597. PubMed PMID: 10625477.

89.   Parmeggiani A, Krab IM, Okamura S, Nielsen RC, Nyborg J, Nissen P. Structural basis of the action of pulvomycin and GE2270 A on elongation factor Tu. Biochemistry. 2006;45(22):6846-57. Epub 2006/06/01. doi: 10.1021/bi0525122. PubMed PMID: 16734421.

90.   Su TL. Micrococcin, an antibacterial substance formed by a strain of Micrococcus. Br J Exp Pathol. 1948;29(5):473-81. Epub 1948/10/01. PubMed PMID: 18123292; PubMed Central PMCID: PMCPMC2073138.

91.   Carnio MC, Höltzel A, Rudolf M, Henle T, Jung G, Scherer S. The macrocyclic peptide antibiotic micrococcin P(1) is secreted by the food-borne bacterium Staphylococcus equorum WS 2733 and inhibits Listeria monocytogenes on soft cheese. Applied and environmental microbiology. 2000;66(6):2378-84. doi: 10.1128/aem.66.6.2378-2384.2000. PubMed PMID: 10831414.

92.   Liu Y, Liu Y, Du Z, Zhang L, Chen J, Shen Z, et al. Skin microbiota analysis-inspired development of novel anti-infectives. Microbiome. 2020;8(1):85-. doi: 10.1186/s40168-020-00866-1. PubMed PMID: 32503672.

93.   Bennallack PR, Burt SR, Heder MJ, Robison RA, Griffitts JS. Characterization of a novel plasmid-borne thiopeptide gene cluster in Staphylococcus epidermidis strain 115. J Bacteriol. 2014;196(24):4344-50. Epub 2014/10/15. doi: 10.1128/jb.02243-14. PubMed PMID: 25313391; PubMed Central PMCID: PMCPMC4248843.

94.   Bennallack PR, Bewley KD, Burlingame MA, Robison RA, Miller SM, Griffitts JS. Reconstitution and Minimization of a Micrococcin Biosynthetic Pathway in Bacillus subtilis. J Bacteriol. 2016;198(18):2431-8. Epub 2016/07/07. doi: 10.1128/jb.00396-16. PubMed PMID: 27381911; PubMed Central PMCID: PMCPMC4999933.

95.   Bewley KD, Bennallack PR, Burlingame MA, Robison RA, Griffitts JS, Miller SM. Capture of micrococcin biosynthetic intermediates reveals C-terminal processing as an obligatory step for in vivo maturation. Proc Natl Acad Sci U S A. 2016;113(44):12450-5. Epub 2016/11/03. doi: 10.1073/pnas.1612161113. PubMed PMID: 27791142; PubMed Central PMCID: PMCPMC5098666.

96.   Ji G, Beavis RC, Novick RP. Cell density control of staphylococcal virulence mediated by an octapeptide pheromone. Proceedings of the National Academy of Sciences. 1995;92(26):12055-9. doi: 10.1073/pnas.92.26.12055.

97.   Lina G, Jarraud S, Ji G, Greenland T, Pedraza A, Etienne J, et al. Transmembrane topology and histidine protein kinase activity of AgrC, the agr signal receptor in Staphylococcus aureus. Molecular Microbiology. 1998;28(3):655-62. doi: 10.1046/j.1365-2958.1998.00830.x.

98.   Novick RP, Projan SJ, Kornblum J, Ross HF, Ji G, Kreiswirth B, et al. The agr P2 operon: an autocatalytic sensory transduction system in Staphylococcus aureus. Mol Gen Genet. 1995;248(4):446-58. Epub 1995/08/30. doi: 10.1007/bf02191645. PubMed PMID: 7565609.

99.   Koenig RL, Ray JL, Maleki SJ, Smeltzer MS, Hurlburt BK. Staphylococcus aureus AgrA binding to the RNAIII-agr regulatory region. J Bacteriol. 2004;186(22):7549-55. Epub 2004/11/02. doi: 10.1128/jb.186.22.7549-7555.2004. PubMed PMID: 15516566; PubMed Central PMCID: PMCPMC524880.

100.   Queck SY, Jameson-Lee M, Villaruz AE, Bach T-HL, Khan BA, Sturdevant DE, et al. RNAIII-Independent Target Gene Control by the agr Quorum-Sensing System: Insight into the Evolution of Virulence Regulation in Staphylococcus aureus. Molecular Cell. 2008;32(1):150-8. doi: https://doi.org/10.1016/j.molcel.2008.08.005.

101.   Thoendel M, Horswill AR. Identification of Staphylococcus aureus AgrD residues required for autoinducing peptide biosynthesis. J Biol Chem. 2009;284(33):21828-38. Epub 2009/06/13. doi: 10.1074/jbc.M109.031757. PubMed PMID: 19520867; PubMed Central PMCID: PMCPMC2756194.

102.   Hazenbos WL, Skippington E, Tan M-W. Staphylococcus aureus type I signal peptidase: essential or not essential, that's the question. Microb Cell. 2017;4(4):108-11. doi: 10.15698/mic2017.04.566. PubMed PMID: 28435837.

103.   Zhang L, Lin J, Ji G. Membrane anchoring of the AgrD N-terminal amphipathic region is required for its processing to produce a quorum-sensing pheromone in Staphylococcus aureus. J Biol Chem. 2004;279(19):19448-56. Epub 2004/03/06. doi: 10.1074/jbc.M311349200. PubMed PMID: 15001569.

104.   Kavanaugh JS, Thoendel M, Horswill AR. A role for type I signal peptidase in Staphylococcus aureus quorum sensing. Mol Microbiol. 2007;65(3):780-98. Epub 2007/07/05. doi: 10.1111/j.1365-2958.2007.05830.x. PubMed PMID: 17608791.

105.   Otto M, Süßmuth R, Vuong C, Jung G, Götz F. Inhibition of virulence factor expression in Staphylococcus aureus by the Staphylococcus epidermidis agr pheromone and derivatives. FEBS Letters. 1999;450(3):257-62. doi: https://doi.org/10.1016/S0014-5793(99)00514-1.

106.   Paharik AE, Parlet CP, Chung N, Todd DA, Rodriguez EI, Van Dyke MJ, et al. Coagulase-Negative Staphylococcal Strain Prevents Staphylococcus aureus Colonization and Skin Infection by Blocking Quorum Sensing. Cell Host & Microbe. 2017;22(6):746-56.e5. doi: https://doi.org/10.1016/j.chom.2017.11.001.

107.   Finking R, Marahiel MA. Biosynthesis of nonribosomal peptides1. Annu Rev Microbiol. 2004;58:453-88. Epub 2004/10/19. doi: 10.1146/annurev.micro.58.030603.123615. PubMed PMID: 15487945.

108.   Gulick AM. Nonribosomal peptide synthetase biosynthetic clusters of ESKAPE pathogens. Natural product reports. 2017;34(8):981-1009. doi: 10.1039/c7np00029d. PubMed PMID: 28642945.

109.   Stachelhaus T, Mootz HD, Marahiel MA. The specificity-conferring code of adenylation domains in nonribosomal peptide synthetases. Chemistry & Biology. 1999;6(8):493-505. doi: https://doi.org/10.1016/S1074-5521(99)80082-9.

110.   Stachelhaus T, Mootz HD, Bergendahl V, Marahiel MA. Peptide bond formation in nonribosomal peptide biosynthesis. Catalytic role of the condensation domain. J Biol

Chem. 1998;273(35):22773-81. Epub 1998/08/26. doi: 10.1074/jbc.273.35.22773. PubMed PMID: 9712910.

111. Du L, Lou L. PKS and NRPS release mechanisms. Nat Prod Rep. 2010;27(2):255-78. Epub 2010/01/30. doi: 10.1039/b912037h. PubMed PMID: 20111804.

112. Schilling NA, Berscheid A, Schumacher J, Saur JS, Konnerth MC, Wirtz SN, et al. Synthetic Lugdunin Analogues Reveal Essential Structural Motifs for Antimicrobial Action and Proton Translocation Capability. Angewandte Chemie International Edition. 2019;58(27):9234-8. doi: 10.1002/anie.201901589.

113. Zipperer A, Konnerth MC, Laux C, Berscheid A, Janek D, Weidenmaier C, et al. Human commensals producing a novel antibiotic impair pathogen colonization. Nature. 2016;535(7613):511-6. doi: 10.1038/nature18634.

114. Krauss S, Zipperer A, Wirtz S, Saur J, Konnerth MC, Heilbronner S, et al. Secretion of and self-resistance to the novel fibupeptide antimicrobial lugdunin by distinct ABC transporters in Staphylococcus lugdunensis. Antimicrob Agents Chemother. 2020. Epub 2020/10/28. doi: 10.1128/aac.01734-20. PubMed PMID: 33106269.

115. Zimmermann M, Fischbach MA. A Family of Pyrazinone Natural Products from a Conserved Nonribosomal Peptide Synthetase in Staphylococcus aureus. Chemistry & Biology. 2010;17(9):925-30. doi: https://doi.org/10.1016/j.chembiol.2010.08.006.

116. Wyatt MA, Wang W, Roux CM, Beasley FC, Heinrichs DE, Dunman PM, et al. Staphylococcus aureus nonribosomal peptide secondary metabolites regulate virulence. Science. 2010;329(5989):294-6. Epub 2010/06/05. doi: 10.1126/science.1188888. PubMed PMID: 20522739.

117. Wilson DJ, Shi C, Teitelbaum AM, Gulick AM, Aldrich CC. Characterization of AusA: a dimodular nonribosomal peptide synthetase responsible for the production of aureusimine pyrazinones. Biochemistry. 2013;52(5):926-37. Epub 2013/01/23. doi: 10.1021/bi301330q. PubMed PMID: 23302043.

118. Sun F, Cho H, Jeong DW, Li C, He C, Bae T. Aureusimines in Staphylococcus aureus are not involved in virulence. PLoS One. 2010;5(12):e15703. Epub 2011/01/07. doi: 10.1371/journal.pone.0015703. PubMed PMID: 21209955; PubMed Central PMCID: PMCPMC3012096.

119. Blättner S, Das S, Paprotka K, Eilers U, Krischke M, Kretschmer D, et al. Staphylococcus aureus Exploits a Non-ribosomal Cyclic Dipeptide to Modulate Survival within Epithelial Cells and Phagocytes. PLoS Pathog. 2016;12(9):e1005857. Epub 2016/09/16. doi: 10.1371/journal.ppat.1005857. PubMed PMID: 27632173; PubMed Central PMCID: PMCPMC5025175.

120. Guo C-J, Chang F-Y, Wyche TP, Backus KM, Acker TM, Funabashi M, et al. Discovery of Reactive Microbiota-Derived Metabolites that Inhibit Host Proteases. Cell. 2017;168(3):517-26.e18. Epub 2017/01/19. doi: 10.1016/j.cell.2016.12.021. PubMed PMID: 28111075.

121. Konetschny-Rapp S, Jung G, Meiwes J, Zähner H. Staphyloferrin A: a structurally new siderophore from staphylococci. Eur J Biochem. 1990;191(1):65-74. Epub 1990/07/20. doi: 10.1111/j.1432-1033.1990.tb19094.x. PubMed PMID: 2379505.

122. Drechsel H, Freund S, Nicholson G, Haag H, Jung O, Zähner H, et al. Purification and chemical characterization of staphyloferrin B, a hydrophilic siderophore from staphylococci. Biometals. 1993;6(3):185-92. Epub 1993/01/01. doi: 10.1007/bf00205858. PubMed PMID: 8400765.

123. Carroll CS, Moore MM. Ironing out siderophore biosynthesis: a review of non-ribosomal peptide synthetase (NRPS)-independent siderophore synthetases. Crit Rev Biochem Mol Biol. 2018;53(4):356-81. Epub 2018/06/05. doi: 10.1080/10409238.2018.1476449. PubMed PMID: 29863423.

124. Oves-Costales D, Kadi N, Challis GL. The long-overlooked enzymology of a nonribosomal peptide synthetase-independent pathway for virulence-conferring siderophore biosynthesis. Chem Commun (Camb). 2009;(43):6530-41. Epub 2009/10/30. doi: 10.1039/b913092f. PubMed PMID: 19865642.

125. Cotton JL, Tao J, Balibar CJ. Identification and Characterization of the Staphylococcus aureus Gene Cluster Coding for Staphyloferrin A. Biochemistry. 2009;48(5):1025-35. doi: 10.1021/bi801844c.

126. Beasley FC, Vinés ED, Grigg JC, Zheng Q, Liu S, Lajoie GA, et al. Characterization of staphyloferrin A biosynthetic and transport mutants in Staphylococcus aureus. Mol Microbiol. 2009;72(4):947-63. Epub 2009/04/30. doi: 10.1111/j.1365-2958.2009.06698.x. PubMed PMID: 19400778.

127. Dale SE, Doherty-Kirby A, Lajoie G, Heinrichs DE. Role of siderophore biosynthesis in virulence of Staphylococcus aureus: identification and characterization of genes involved in production of a siderophore. Infect Immun. 2004;72(1):29-37. Epub 2003/12/23. doi: 10.1128/iai.72.1.29-37.2004. PubMed PMID: 14688077; PubMed Central PMCID: PMCPMC343950.

128. Cheung J, Beasley FC, Liu S, Lajoie GA, Heinrichs DE. Molecular characterization of staphyloferrin B biosynthesis in Staphylococcus aureus. Mol Microbiol. 2009;74(3):594-608. Epub 2009/09/25. doi: 10.1111/j.1365-2958.2009.06880.x. PubMed PMID: 19775248.

129. Brozyna JR, Sheldon JR, Heinrichs DE. Growth promotion of the opportunistic human pathogen, Staphylococcus lugdunensis, by heme, hemoglobin, and coculture with Staphylococcus aureus. Microbiologyopen. 2014;3(2):182-95. Epub 2014/02/07. doi: 10.1002/mbo3.162. PubMed PMID: 24515974.

130. McFarlane JS, Davis CL, Lamb AL. Staphylopine, pseudopaline, and yersinopine dehydrogenases: A structural and kinetic analysis of a new functional class of opine dehydrogenase. J Biol Chem. 2018;293(21):8009-19. Epub 2018/04/06. doi: 10.1074/jbc.RA118.002007. PubMed PMID: 29618515; PubMed Central PMCID: PMCPMC5971449.

131. Ghssein G, Brutesco C, Ouerdane L, Fojcik C, Izaute A, Wang S, et al. Biosynthesis of a broad-spectrum nicotianamine-like metallophore in Staphylococcus

aureus. Science. 2016;352(6289):1105-9. Epub 2016/05/28. doi: 10.1126/science.aaf1018. PubMed PMID: 27230378.

132. Ding Y, Fu Y, Lee JC, Hooper DC. Staphylococcus aureus NorD, a putative efflux pump coregulated with the Opp1 oligopeptide permease, contributes selectively to fitness in vivo. J Bacteriol. 2012;194(23):6586-93. Epub 2012/10/09. doi: 10.1128/jb.01414-12. PubMed PMID: 23042988; PubMed Central PMCID: PMCPMC3497520.

133. Remy L, Carrière M, Derré-Bobillot A, Martini C, Sanguinetti M, Borezée-Durant E. The Staphylococcus aureus Opp1 ABC transporter imports nickel and cobalt in zinc-depleted conditions and contributes to virulence. Molecular Microbiology. 2013;87(4):730-43. doi: 10.1111/mmi.12126.

134. Grim KP, San Francisco B, Radin JN, Brazel EB, Kelliher JL, Párraga Solórzano PK, et al. The Metallophore Staphylopine Enables Staphylococcus aureus To Compete with the Host for Zinc and Overcome Nutritional Immunity. mBio. 2017;8(5). Epub 2017/11/02. doi: 10.1128/mBio.01281-17. PubMed PMID: 29089427; PubMed Central PMCID: PMCPMC5666155.

135. Lowy FD. Staphylococcus aureus Infections. New England Journal of Medicine. 1998;339(8):520-32. doi: 10.1056/nejm199808203390806. PubMed PMID: 9709046.

136. Sahl HG, Brandis H. Production, purification and chemical properties of an antistaphylococcal agent produced by Staphylococcus epidermidis. J Gen Microbiol. 1981;127(2):377-84. Epub 1981/12/01. doi: 10.1099/00221287-127-2-377. PubMed PMID: 7343644.

137. Gless BH, Bojer MS, Peng P, Baldry M, Ingmer H, Olsen CA. Identification of autoinducing thiodepsipeptides from staphylococci enabled by native chemical ligation. Nature Chemistry. 2019;11(5):463-9. doi: 10.1038/s41557-019-0256-3.

138. Brown MM, Kwiecinski JM, Cruz LM, Shahbandi A, Todd DA, Cech NB, et al. Novel Peptide from Commensal Staphylococcus simulans Blocks Methicillin-Resistant Staphylococcus aureus Quorum Sensing and Protects Host Skin from Damage. Antimicrobial agents and chemotherapy. 2020;64(6):e00172-20. doi: 10.1128/AAC.00172-20. PubMed PMID: 32253213.

139. Jarraud S, Lyon GJ, Figueiredo AM, Lina G, Vandenesch F, Etienne J, et al. Exfoliatin-producing strains define a fourth agr specificity group in Staphylococcus aureus. Journal of bacteriology. 2000;182(22):6517-22. doi: 10.1128/jb.182.22.6517-6522.2000. PubMed PMID: 11053400.

140. Otto M. Staphylococcus aureus and Staphylococcus epidermidis peptide pheromones produced by the accessory gene regulator agr system. Peptides. 2001;22(10):1603-8. Epub 2001/10/06. doi: 10.1016/s0196-9781(01)00495-8. PubMed PMID: 11587788.

141. Olson ME, Todd DA, Schaeffer CR, Paharik AE, Van Dyke MJ, Büttner H, et al. Staphylococcus epidermidis agr quorum-sensing system: signal identification, cross talk, and importance in colonization. J Bacteriol. 2014;196(19):3482-93. Epub

2014/07/30. doi: 10.1128/jb.01882-14. PubMed PMID: 25070736; PubMed Central PMCID: PMCPMC4187671.

142. Williams MR, Costa SK, Zaramela LS, Khalil S, Todd DA, Winter HL, et al. Quorum sensing between bacterial species on the skin protects against epidermal injury in atopic dermatitis. Sci Transl Med. 2019;11(490). Epub 2019/05/03. doi: 10.1126/scitranslmed.aat8329. PubMed PMID: 31043573; PubMed Central PMCID: PMCPMC7106486.

143. Kalkum M, Lyon GJ, Chait BT. Detection of secreted peptides by using hypothesis-driven multistage mass spectrometry. Proc Natl Acad Sci U S A. 2003;100(5):2795-800. Epub 2003/02/18. doi: 10.1073/pnas.0436605100. PubMed PMID: 12591958.

144. Todd DA, Parlet CP, Crosby HA, Malone CL, Heilmann KP, Horswill AR, et al. Signal Biosynthesis Inhibition with Ambuic Acid as a Strategy To Target Antibiotic-Resistant Infections. Antimicrobial agents and chemotherapy. 2017;61(8):e00263-17. doi: 10.1128/AAC.00263-17. PubMed PMID: 28607020.

145. Canovas J, Baldry M, Bojer MS, Andersen PS, Gless BH, Grzeskowiak PK, et al. Cross-Talk between Staphylococcus aureus and Other Staphylococcal Species via the agr Quorum Sensing System. Frontiers in Microbiology. 2016;7(1733). doi: 10.3389/fmicb.2016.01733.

146. Varella Coelho ML, Santos Nascimento JD, Fagundes PC, Madureira DJ, Oliveira SS, Vasconcelos de Paiva Brito MA, et al. Activity of staphylococcal bacteriocins against Staphylococcus aureus and Streptococcus agalactiae involved in bovine mastitis. Res Microbiol. 2007;158(7):625-30. Epub 2007/08/28. doi: 10.1016/j.resmic.2007.07.002. PubMed PMID: 17719749.

147. Kordel M, Benz R, Sahl HG. Mode of action of the staphylococcinlike peptide Pep 5: voltage-dependent depolarization of bacterial and artificial membranes. J Bacteriol. 1988;170(1):84-8. Epub 1988/01/01. doi: 10.1128/jb.170.1.84-88.1988. PubMed PMID: 3335484; PubMed Central PMCID: PMCPMC210609.

148. Pag U, Heidrich C, Bierbaum G, Sahl HG. Molecular analysis of expression of the lantibiotic pep5 immunity phenotype. Appl Environ Microbiol. 1999;65(2):591-8. Epub 1999/01/30. doi: 10.1128/AEM.65.2.591-598.1999. PubMed PMID: 9925587; PubMed Central PMCID: PMCPMC91066.

149. Asaduzzaman SM, Nagao J, Iida H, Zendo T, Nakayama J, Sonomoto K. Nukacin ISK-1, a bacteriostatic lantibiotic. Antimicrob Agents Chemother. 2009;53(8):3595-8. Epub 2009/06/10. doi: 10.1128/AAC.01623-08. PubMed PMID: 19506061; PubMed Central PMCID: PMCPMC2715603.

150. Islam MR, Nishie M, Nagao J, Zendo T, Keller S, Nakayama J, et al. Ring A of nukacin ISK-1: a lipid II-binding motif for type-A(II) lantibiotic. J Am Chem Soc. 2012;134(8):3687-90. Epub 2012/02/15. doi: 10.1021/ja300007h. PubMed PMID: 22329487.

151. Roy U, Islam MR, Nagao J, Iida H, Mahin AA, Li M, et al. Bactericidal activity of nukacin ISK-1: an alternative mode of action. Biosci Biotechnol Biochem.

2014;78(7):1270-3. Epub 2014/09/18. doi: 10.1080/09168451.2014.918485. PubMed PMID: 25229869.

152.   Cundliffe E, Thompson J. Concerning the mode of action of micrococcin upon bacterial protein synthesis. Eur J Biochem. 1981;118(1):47-52. Epub 1981/08/01. doi: 10.1111/j.1432-1033.1981.tb05484.x. PubMed PMID: 6116602.

43

Chapter 2

Staphylococcus epidermidis* uses a fugacious mixed polypeptide/polyketide antimicrobial to outcompete *Staphylococcus aureus

Benjamin O. Torres Salazar[a,b,c], Nadine A. Schilling[b,d], Taulant Dema[b,d], Daniela Janek[a,b,c], Anne Berscheid[d,e], Sophia Krauss[a,b,c], Min Li[f], Mal Horsburgh[g], Tillmann Weber[h], Heike Brötz-Oesterhelt[b,d], Stephanie Grond[b,d*], Andreas Peschel[a,b,c*], Bernhard Krismer[a,b,c]

[a] Department of Infection Biology, Interfaculty Institute of Microbiology and Infection Medicine, University of Tübingen, Tübingen, Germany; [b] Cluster of Excellence EXC 2124 Controlling Microbes to Fight Infections; [c] German Center for Infection Research (DZIF), partner site Tübingen; [d] Institute of Organic Chemistry, University of Tübingen, Tübingen, Germany; [e] Department of Microbial Bioactive Compounds, Interfaculty Institute of Microbiology and Infection Medicine, University of Tübingen, Tübingen, Germany; [f] Department of Laboratory Medicine, Renji Hospital, School of Medicine, Shanghai Jiaotong University, Shanghai, China; [g] Department of Infection Biology and Microbiomes, University of Liverpool, Liverpool, UK; [h] The Novo Nordisk Foundation Center for Biosustainability, Technical University of Denmark, Kongens Lyngby, Denmark

* corresponding authors

Abstract

Staphylococcus epidermidis is a prevalent member of human nasal and skin microbiomes, whose fitness often relies on the production of bacteriocin-like antimicrobial molecules that inhibit bacterial competitors. We are only beginning to appreciate the diversity of such compounds and it has remained largely unclear how bacteria may limit negative side effects of bacteriocins against beneficial mutualists. We report here a new type of antimicrobial compound named epifadin produced by nasal *S. epidermidis* isolates. It encompasses two non-ribosomally synthesized units and a polyketide moiety in an unprecedented architecture. Epifadin is highly active against a wide range on unrelated microorganisms including the major pathogen *Staphylococcus aureus*. Surprisingly, epifadin is highly unstable under *in vivo*-like conditions such as ambient temperature, pH, and light exposure, presumably as a means to restrict its activity to the close vicinity of epifadin-producing *S. epidermidis* cells. Nevertheless, epifadin-producing *S. epidermidis* eliminated *S. aureus* effectively during co-cultivation in broth and in an experimental nasal colonization model indicating that epifadin-producing commensals could help to prevent nasal *S. aureus* carriage. Our study describes a new microbiome-derived antimicrobial compound class and suggests that limiting the half-life of an antimicrobial may be a valid way of balancing beneficial and detrimental activities against other bacteria.

Introduction

The microbiomes of human skin and upper airways play crucial roles for human health and predisposition to a variety of diseases. Microbiome compositions govern susceptibility to and severity of chronic diseases such as atopic dermatitis and acne, and such microbiomes can include facultative bacterial pathogens such as *Staphylococcus aureus*, which colonizes the anterior nares of ca. 30% of the human population [1-3]. Microbiome dynamics are likely to be shaped by antagonistic and mutualistic interactions between microbiome members but the elucidation of molecular mechanisms governing bacterial fitness has remained in its infancy.

Staphylococcus epidermidis is the most abundant and most consistently found member of human skin and nasal microbiomes [4, 5]. In contrast to *S. aureus*, which usually occurs as a single clone on a given human host, multiple different *S. epidermidis* strains can be found simultaneously in the same host niche [6]. The mechanisms underlying the ecological success of this species have remained largely unclear. *S. epidermidis* can modify its surface glycopolymers to alter its adhesive properties to different host surfaces [7] and it produces phenol-soluble modulin peptides, which modulate inflammatory reactions in skin and epithelia that seem to promote *S. epidermidis* persistence and may impair fitness of its major

competitors [8-10]. Moreover, *S. epidermidis* is known as a particularly frequent producer of bacteriocins, antibacterial peptides with highly variable structure and activity against potential target species [11-14]. Bacteriocins have traditionally been defined as ribosomally synthesized post-translationally modified peptides (RIPPs) but this term is increasingly used to generally encompass small-molecule antibacterial agents acting in their ecological niches, including also, for instance, non-ribosomally synthesized peptides (NRPs) [15].

Many of the bacteriocin biosynthetic gene clusters (BGCs) are located on plasmids or other mobile genetic elements, which facilitate their horizontal exchange with other *S. epidermidis* clones or other bacterial species, thereby entailing a high evolutionary dynamic of antibacterial BGC acquisition, diversification, or loss [16].

Bacteriocin production is often beneficial but can also cause collateral damage to the producer when other bacteria, which are necessary for the function of mutualistic networks, are also killed. Moreover, several bacteriocins can also damage host cells, which can lead to inflammation resulting in increased local antimicrobial defense [17, 18]. Bacteria have three potential ways to limit such bacteriocin-mediated collateral damage. They can use bacteriocins with extremely narrow and specific target range, such as most microcins, which would spare many important mutualists [19, 20]. Another strategy relies on contact-dependent bacteriocins such as effectors secreted by type-V-VII secretion systems, which rely on specific interbacterial adhesion mechanisms, sparing mutualistic bacteria that do not physically bind to the bacteriocin producer [21, 22]. Lastly, bacteria could produce bacteriocins with limited lifetime, which would preclude their accumulation at wider distance to the producing micro-colony. The latter strategy would not rely on a high selectivity of the compound for specific competitors, which may be difficult to achieve, but it would ensure that the producer inhibits only bacteria in close proximity but maintains long-distance interaction networks and maintains integrity of host cells. The latter strategy can only work if community density is rather low and individual bacteria are not constantly mixed, which is usually the case in skin and anterior nare habitats.

Here we report a novel bacteriocin-like antimicrobial produced by certain *S. epidermidis* strains that combines an unusually wide target range with a very short half-life thereby reflecting an unusual and previously unrecognized antimicrobial strategy. It is the first antimicrobial produced by a common member of the healthy human microbiota that combines moieties synthesized by non-ribosomal peptide synthetases (NRPS) and polyketide synthases (PKS) and it allows *S. epidermidis* to eliminate its competitor *S. aureus* from the same habitat, both *in vitro* and *in vivo*.

Results

S. epidermidis IVK83 produces a new type of mixed NRPS-/PKS-biosynthesized antimicrobial agent

We previously reported that more than 95% of _S. epidermidis_ isolates from the human nose produced antimicrobial molecules with activity against one or several other bacterial skin and nose microbiome members [11]. Whereas most inhibited only a limited number of test bacteria, isolate IVK83 was unique in its capacity to strongly inhibit most of the test strains, including representatives of Firmicutes, Actinobacteria, and γ-Proteobacteria. In order to identify the BGC responsible for synthesis of the antimicrobial compound, a transposon mutant library of IVK83 was established and screened for the lack of antimicrobial activity. A mutant was identified that failed to inhibit _S. aureus_ USA300 and other test strains. Whole genome sequencing (WGS) revealed that the transposon had integrated into an unknown BGC operon composed of ten putative genes, encompassing about 40 kb, which was located on a 55-kb plasmid (Fig. 1) that we named pIVK83. The gene cluster encoded an unusual set of a putative NRP synthase (NRPS) (EfiA), several PK synthases (PKS) (EfiB, EfiC, EfiD), a combined PKS/NRPS (EfiE), and an oxidoreductase (EfiO) encoded between _efiD_ and _efiE_, along with further genes required for NRP synthesis including a phosphopantetheinyl transferase (EfiP) and a thioesterase (EfiT). In addition, two genes encoded the components of a putative ABC transporter, EfiF, the ATP-binding, and EfiG, the membrane channel component (Fig. 1). The transposon had disrupted _efiA_, the first gene of the operon. To confirm the essential role of this BGC in the antimicrobial activity of IVK83, the _efiTP_ genes were deleted in the wild-type strain, which abrogated antibacterial activity. The activity was restored by complementation with a plasmid-encoded _efiTP_ copy thereby confirming that the BGC is required for the capacity of IVK83 to inhibit other bacteria (Fig. 1).

Screening of _S. epidermidis_ collections in our laboratories identified four additional isolates with identical antimicrobial activity and gene clusters, two more from Tübingen and each one from Shanghai (China) and Liverpool (United Kingdom). WGS of these strains revealed that they contained largely identical plasmids. The five strains belonged to four different multi-locus sequence types (STs), ST575 (IVK83, Tübingen), ST549 and ST615 (additional Tübingen strains), and ST73 (Shanghai and Liverpool). The plasmid and the _efiA-T_ BGC were absent from all _S. epidermidis_ genomes in publicly available genome sequence databases, indicating that the BGC is an infrequent accessory genetic element, which had probably been exchanged horizontally between the different clonal groups. Highly identical plasmids were also identified in two _Staphylococcus saccharolyticus_ genomes [23]. Since the plasmids encode a relaxase

of the newly described Mob$_L$ family, which is exclusively found in Firmicutes, mobilization via conjugation is most likely [24].
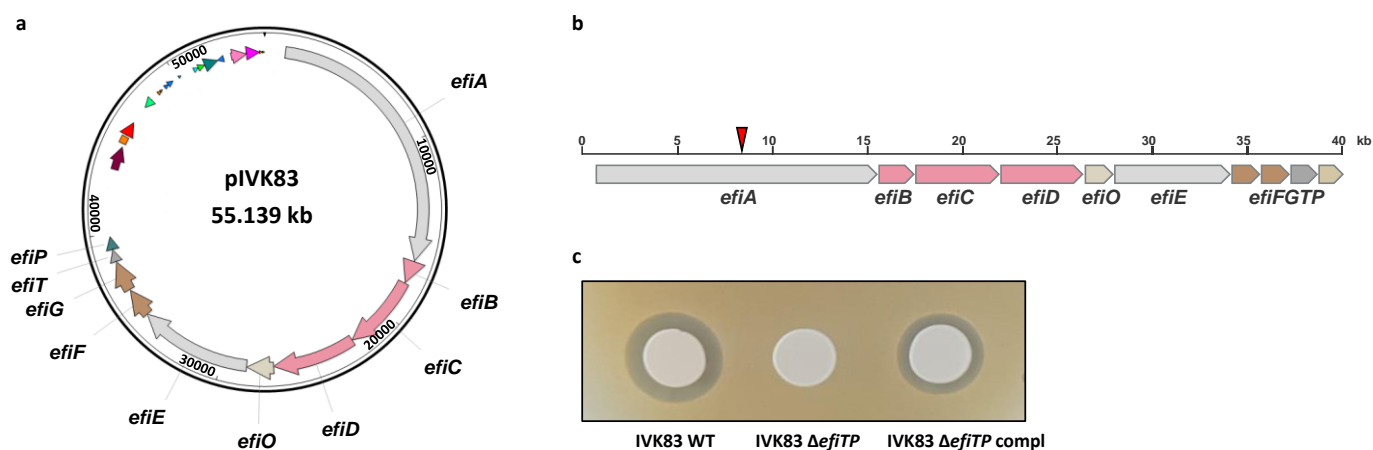

Figure 1. Biosynthetic gene cluster of epifadin. a, Plasmid map of pIVK83 (~55 kbp) harboring the epifadin operon (~40 kbp). **b,** The cluster consists of genes encoding a putative NRPS (*efiA*), three PKS (*efiB*, *efiC*, *efiD*), a hybrid PKS/NRPS (*efiE*), a putative/predicted NAD(P)/FAD-dependent oxidoreductase (*efiO*) located between *efiD* and *efiE*, a thioesterase (*efiT*), a phosphopantetheinyl transferase (*efiP*), and two ABC transporter genes (*efiF*, *efiG*). Red arrow indicates the insertion site of Tn917, generating an epifadin deficient mutant. **c,** Antimicrobial activity of IVK83 wild-type (WT), isogenic Δ*efiTP* mutant and complemented strain.

Epifadin is a new highly instable, drug-like antimicrobial agent

Culture filtrates of IVK83 contained antibacterial activity, which could be enriched by extraction with *n*-butanol or by precipitation by acidification (pH=2) with HCl and subsequent drying under vacuum. After following extraction with DMSO antibacterial activity was quite reproducibly observed. However, the compound had a very short half-life under standard laboratory conditions, which impeded further purification, e.g., via gel filtration, or further chromatography steps. Systematic variation of incubation conditions of the DMSO extract revealed rapid loss of antimicrobial activity, also by storage in aqueous solution, room temperature, any exposure to light, or any pH values above pH=5 (Fig. 2). However, stability of the antibacterial activity remained constant when the extract was maintained under acidic conditions, protected from oxygen and light, and stored with the oxidation inhibitor palmitoyl ascorbate (PA) at –80°C under argon atmosphere. When the DMSO extract was dissolved as an aqueous solution at pH 7, 37°C, and exposed to ambient laboratory illumination, the antimicrobial activity quickly faded and was completely lost after three hours (Fig. 2). Decomposition of the antibacterial agent occurred within two or even one hour when the pH was raised to eight or nine,

respectively. In contrast, other microbiome-derived bacteriocins and related antimicrobial peptides such as lugdunin from *Staphylococcus lugdunensis* [25], gallidermin from *Staphylococcus gallinarum* [26], and nisin A from *Lactococcus lactis* [27], did not lose activity under the same conditions for at least six hours.
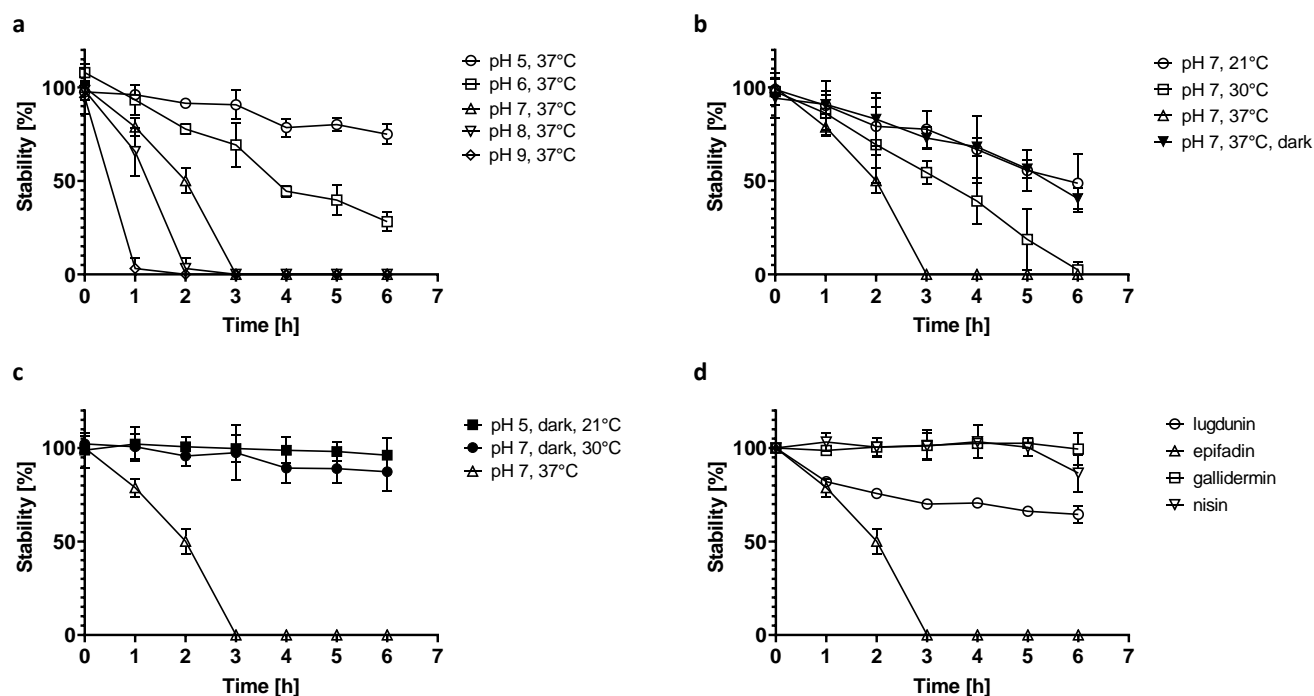
Figure 2. Instability of epifadin. DMSO extract of HCl-precipitate of IVK83 culture supernatants containing epifadin was added to TSB and incubated for 6 h under constant shaking at different conditions: **a**, different pH values with ambient laboratory light exposure; **b**, different temperatures with/without ambient laboratory light exposure and **c**, combinations of the conditions during the studies of a and b, in which the culture filtrate containing epifadin showed quite high stability. **d**, Stability of epifadin compared to other antibacterial agents under normal cultivation conditions (37°C, pH 7, ambient laboratory light exposure). Conditions at pH 7, 37°C and 0 h were used as reference and set to stability=100%.

HCl-precipitated and DMSO-PA-extracted preparations obtained from culture supernatants of the IVK83 wild-type or the *efiTP* mutant strain were lyophilized to dryness and used for chemical analysis by coupled reversed-phase high performance liquid chromatography (RP-HPLC) with ultra violet (UV)- and mass spectrometry (MS) detectors. No obvious difference between the wild-type and mutant strains was detected at the peptide-bond specific wavelength of 215 nm, although the presence of genes for NRPS pointed to multiple peptide bonds. Notably, wild-type and mutant differed in a major and in some adjacent, minor UV

signals detectable at 383 nm, indicating properties that are unusual for peptides, such as the presence of an expanded unsaturated system with double bonds (Fig. 3). Preparative HPLC purification revealed most of the antimicrobial activity in the major 383 nm peak fraction, while the adjacent fractions contained only a minor portion of the activity.

High-resolution MS of the main peak fraction suggested a quasi-molecular ion ([M+H]$^+$, $C_{51}H_{62}N_7O_{12}^+$, calculated m/z 964.4451, found 964.4472, 2.2 Δppm) suggesting an elementary composition for the antibacterial agent of $C_{51}H_{61}N_7O_{12}$ (Fig. 4). This formula was not found in data bases suggesting that IVK83 produces a novel compound. It was named epifadin (**1**) to reflect its origin from *S. epidermidis* and its rapidly fading activity at typical environmental conditions.
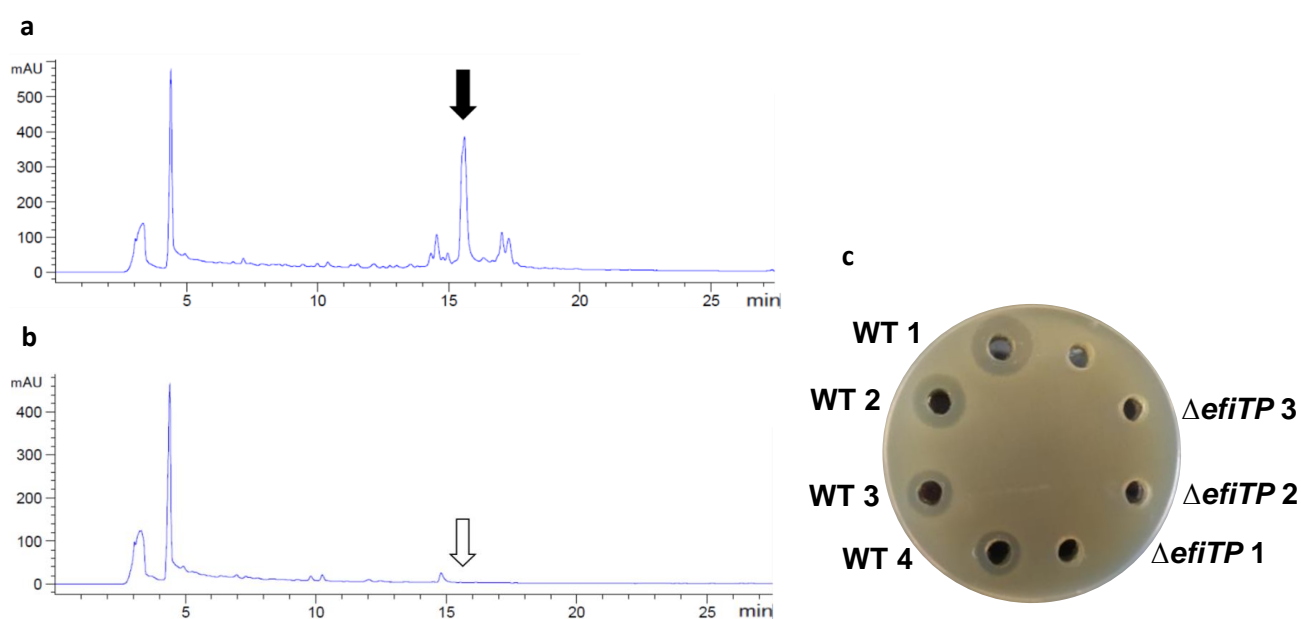
Figure 3. Detection and isolation of epifadin from DMSO extracts of HCl-precipitated culture supernatants. HPLC was performed with a solvent gradient of acetonitrile/H$_2$O with trifluoracetic acid. **a,b**, HPLC-UV chromatograms (λ=383 nm) of DMSO-PA extract of IVK83 wild type (a) and Δ*efiTP* mutant (b). A prominent peak (marked with a black arrow) of epifadin is only present in the wild-type sample with a retention time of ~15 min at 383 nm. **c**, The wild type fractions collected at 15.5 min displayed antimicrobial activity on TSA plates inoculated with *S. aureus*. Fraction at 14.5 min and all mutant fractions displayed no activity. WT: wild-type samples; Δ*efiTP*: Δ*efiTP* mutant samples; 1: 50 µL undiluted fractions collected at 15.5 min; 2: 50 µL 1:2 dilution of 1; 3: 50 µL 1:4 dilution of 1; 4: 50 µL undiluted fraction collected at 14.5 min.
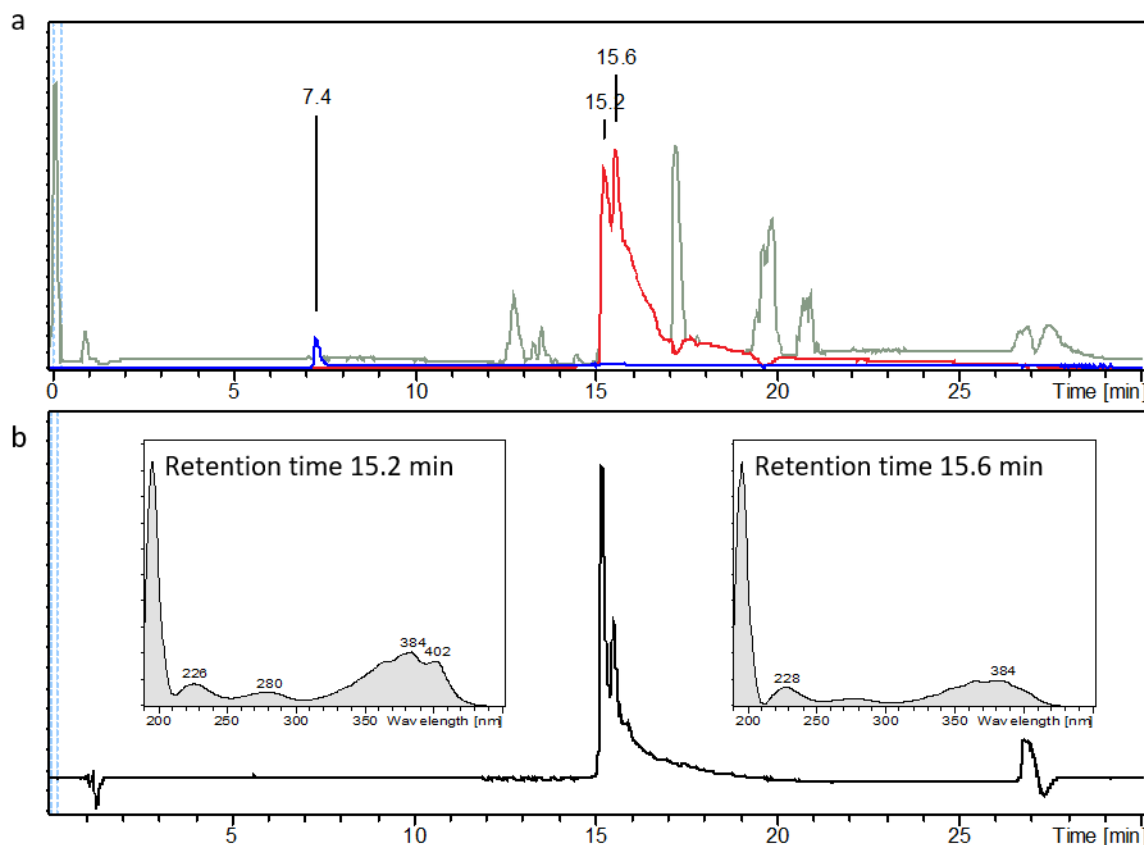
Figure 4. HPLC-UV-MS-chromatogram of epifadin (1) fraction. The epifadin enriched material was dissolved in a mixture of acetonitrile and water (1:1) with 0.05% trifluoroacetic acid, resulting in a concentration of 0.2 mg·mL^{-1} and analyzed by HPLC-ESI-TOF-high resolution MS. **a**, The extracted ion chromatogram (EIC) of epifadin (**1**, $C_{51}H_{61}N_7O_{12}$ = [M+H]$^+$, m/z 964.4451±0.005) is depicted in red (retention time 15.2 min and 15.6 min) and the base peak chromatogram (BPC) (gray). EIC of the peptide amide **2** ($C_{26}H_{32}N_6O_7$ = [M+H]$^+$, m/z 541.2405±0.005) is depicted in blue (retention time 7.4 min) accumulating by strong decomposition of **1** under environmental conditions. **b**, UV-chromatogram (λ= 383 nm) in black. UV-spectra of the active compound at 15.2 min and 15.6 min from 190 nm to 450 nm are shown (methanol as a solvent causes a strong absorbance at 200 nm). The absorbance of the specific regions is indicated (peptide bond 210-230 nm, Phe 280 nm, and polyene region 330-410 nm).

Epifadin is a complex natural product resulting from combined NRPS- and PKS-mediated biosynthesis

In order to elucidate putative structural features of epifadin (**1**) its BGC was analyzed with the antiSMASH 5.0 algorithm [28], which predicted a three-partite composition with an *N*-terminal NRP part followed by a PK moiety and a C-terminal single amino acid residue (Fig. 5).

Linear Peptide. The NRPS1 (EfiA) enzyme was predicted to start the biosynthesis with an aromatic amino acid. Since the first adenylation domain is followed by two condensation

domains the first amino acid is suggested to incorporate twice, and the second is converted to D-configuration by the second condensation domain with its epimerization domain (Fig. 5). The second adenylation domain of EfiA was predicted to incorporate aspartate, the third asparagine, which probably again is epimerized to D-asparagine. The following amino acid position did not yield a clear prediction. According to antiSMASH it could be a small or an aliphatic amino acid such as glycine, alanine, valine, leucine, isoleucine, or amino-butyric acid.
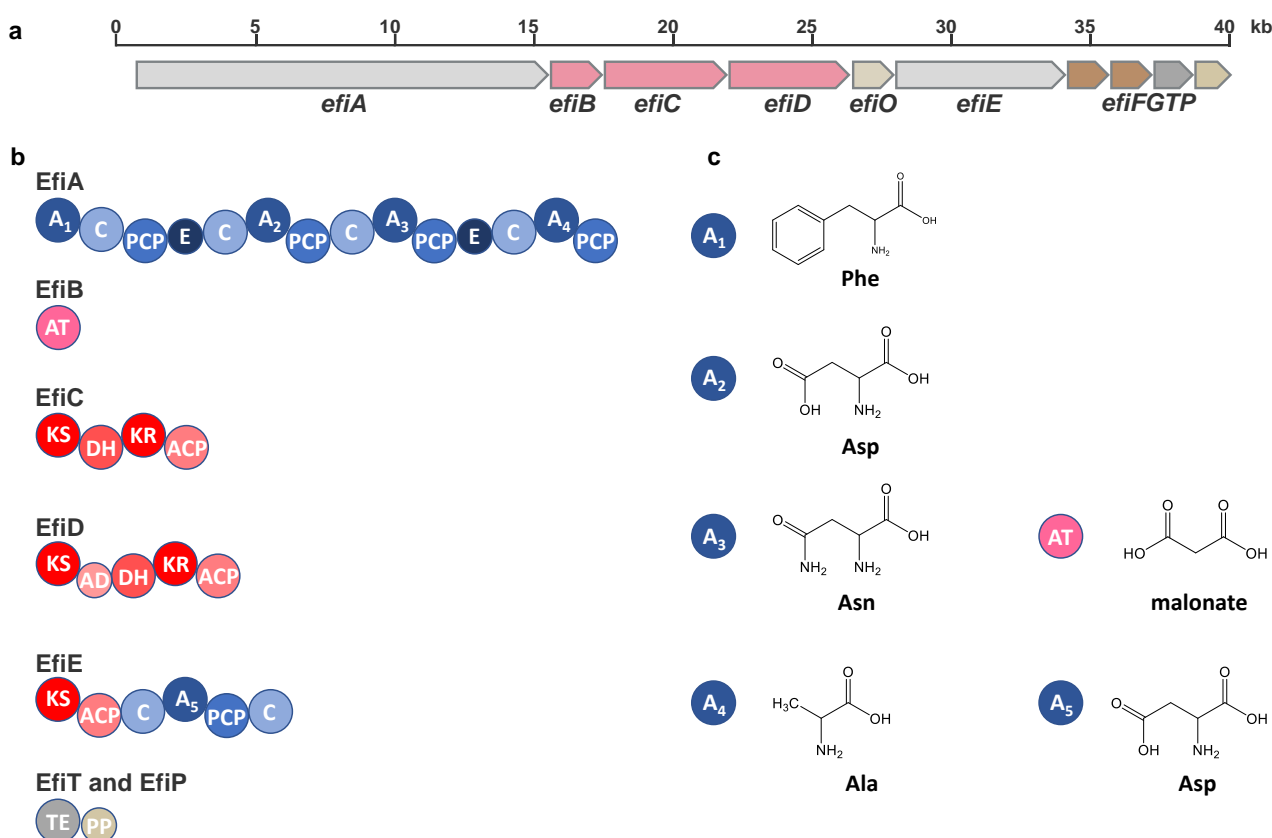
Figure 5. Gene, module, and domain organization of the epifadin NRPS/PKS gene cluster of IVK83. a, Biosynthetic gene cluster of epifadin (40 kb coding region). **b**, NRPS and PKS modules of EfiA, EfiB, EfiC, EfiD, EfiE, EfiT, and EfiP involved in epifadin biosynthesis. NRPS domains are depicted in bluish, PKS domains in reddish colors. Functional domains: A, adenylation; C, condensation; PCP, peptidyl carrier protein; E, epimerization; AT, acyltransferase; KS, ketosynthase; DH, dehydratase; KR, ketoreductase; ACP, acyl carrier protein; AD, Trans-AT docking; TE, thioesterase; PP, 4'-phosphopantetheinyl transferase. **c**, antiSMASH-predicted building blocks for adenylation domains A1 – A5 and the acyltransferase.

In order to obtain sufficient amount of the unstable compound for structural elucidation, epifadin was repeatedly purified from 100 L fermentation broth via acidic precipitation and DMSO-PA extraction immediately followed by preparative RP-HPLC in the dark, finally yielding 4 mg of the transiently intact compound, stored under argon at –80°C. Subsequently, samples

of purified epifadin (**1**) in DMSO-PA solution were applied immediately to antimicrobial activity assays. In addition, chemical analysis by coupled HPLC-UV-MS of the intact compound revealed a continuing degradation of epifadin after prolonged incubation for hours. A dominant decomposition product corresponding to the *N*-terminal NRP moiety is the peptide amide Phe-Phe-Asp-Asn-NH$_2$ (**2**, FFDN-NH$_2$) with the neutral sum formula C$_{26}$H$_{32}$N$_6$O$_7$ ([M+H]$^+$: C$_{26}$H$_{33}$N$_6$O$_7^+$, calculated m/z 541.2405, found 541.2422, Δppm 3.1) with a terminal amide group, presumably resulting from spontaneous distinct chemical decomposition of the enamide at the originally fifth amino acid. Tandem MS experiments (MS/MS) of intact epifadin yielded particular fragmentation patterns that supported this peptide sequence (Fig. 6, Fig. S1). The determined structure of the peptide amide **2** was confirmed by acetylation and esterification reactions with the natural product (Fig. S2). According to antiSMASH and the module organization of EfiA a L-D-L-D-amino acid configuration was predicted for peptide amide **2** (Fig. 5). L-Phe-D-Phe-L-Asp-D-Asn-NH$_2$ (FfDn-NH$_2$, **2**) was synthesized by chemical solid-phase synthesis employing the respective D-Asn rink-amide resin and purified to **2**. The retention time on a HPLC-RP-C$_{18}$ column as well as the MS/MS spectra were in accordance with the ones of the natural product **2** (Fig. S1 and S3). However, **2** was tested biologically inactive.
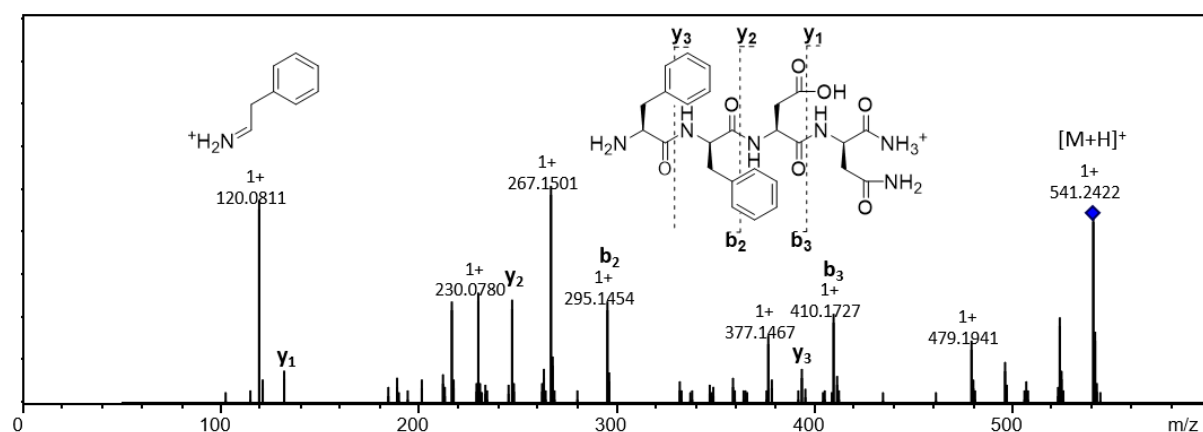
Figure 6. **MS/MS spectrum of the FFDN amide 2.**

Towards structure elucidation, a combination of ^{1}H-NMR and 2D-NMR experiments (e.g., ^{1}H-^{1}H-ROESY) fully assigned and confirmed the presence of four unmodified amino acids, the *N*-terminal L-Phe, followed by D-Phe, L-Asp, and D-Asn, consistent with the sequence deduced from MS (Fig. S1 and S5, Table S2). Additionally, NMR revealed the fifth amino acid to be a modified Ala (Fig. S7-8). This adjacent modified Ala residue lacks the C-terminal carbonyl group (C=O) as indicated by the NMR signals for a respective enamide moiety to resemble the -NH-C(CH$_3$)=CH-structure.

PKS polyene. The two-dimensional NMR experiments (Fig. S8) unambiguously emphasized the immediate linkage of the tetrapeptide to the polyene structure, with a tetraene starting at C_α of Ala, followed by a saturated methylene unit to extend an aliphatic bridge of epifadin (Fig. S7), which probably reflects the activities of predicted PKS-encoding genes *efiC, efiD* and *efiE*. Full structural elucidation of the PKS polyene by NMR assignment was not accomplished because of the instability of epifadin (**1**) during the time-consuming performance of two-dimensional NMR-spectra.

The epifadin BGC encodes three PKS enzymes (EfiB, EfiC, EfiD) and a combined PKS/NRPS enzyme (EfiE). EfiB represents a putative free-standing acyl carrier protein S-malonyltransferase suggesting that the PK moiety of epifadin is formed by malonyl residues (Fig. 5). The modules of EfiC and EfiD are probably responsible for the iterative condensation of the acetate extender units, which remain likely unsaturated because EfiC and EfiD contain ketosynthase (KS), peptidyl carrier protein (PCP), dehydratase (DH) and ketoreductase (KR) domains, of which the latter two generally catalyze double bond formation in polyketides. The PKS part of EfiE consists only of KS and acyl carrier protein (ACP) domains. The exact chemical structure of the PK part of epifadin could not fully be elucidated by only analytical methods as MS or NMR spectroscopy, because of the extraordinary instability of epifadin. The naturally occurring and ionization-induced fragments are unsaturated PKS moieties, which are difficult to detect by MS because they are often not prone to ionization. The unusual UV absorption maximum at 383 nm supports the presence of an unsaturated polyene PK moiety (Fig. 3 and 4). Similar, albeit not fully identical UV absorption properties are also found in the macrocyclic PK compound amphotericin B [29], which contains seven conjugated double bonds, the antifungal PK sugar macrocyclic agents nystatin A1 with four plus two conjugated double bonds or militarinone C with four conjugated double bonds representing a polyenoyl tetramic acid [30].

NRPS tail. The NRPS domain of EfiE was predicted by antiSMASH to link an Asp residue as sixth amino acid to the PK part of epifadin (**1**). Chemical HPLC-coupled high resolution MS (MS/MS) analyses of epifadin (**1**) point towards a modified Asp residue, more precisely a tetramic acid as structural feature of epifadin (**1**). MS analyses delivered a characteristic signal pattern for the hypothetical tetramic acid moiety, containing ions with well assigned fragment ions (e.g., $[M+H]^+$ $C_6H_8NO_4^+$, calculated m/z 158.0448, found 158.0454, Δ3.9 ppm; $[M+H]^+$ $C_6H_6NO_3^+$, calculated m/z 140.0342, found 140.0348, Δ4.1 ppm) (Fig. 7). The proposed, reasonable chemical fragmentation mechanisms support the structure (Fig. 7). Unfortunately, for such a heterocyclic tetramic acid part, the method of NMR gave only an incomplete set of signals, presumably as a result of pronounced tautomeric effects of the distinct charged tetramic acid tautomers. In addition, the genetic architecture of the BGC suggests that the

release of the final molecule (**1**) from the terminal NRP domain is probably catalyzed by cyclization to the tetramic acid via the terminal condensation domain part of EfiE (Fig. 5). A condensation with the Asp residue and the subsequent Dieckmann cyclization catalyzed by the C-terminal domain of EfiE could build the tetramic acid moiety, as already described for malonomycin [31] and fungal PKS-NRPS derived products such as cAATrp [32].
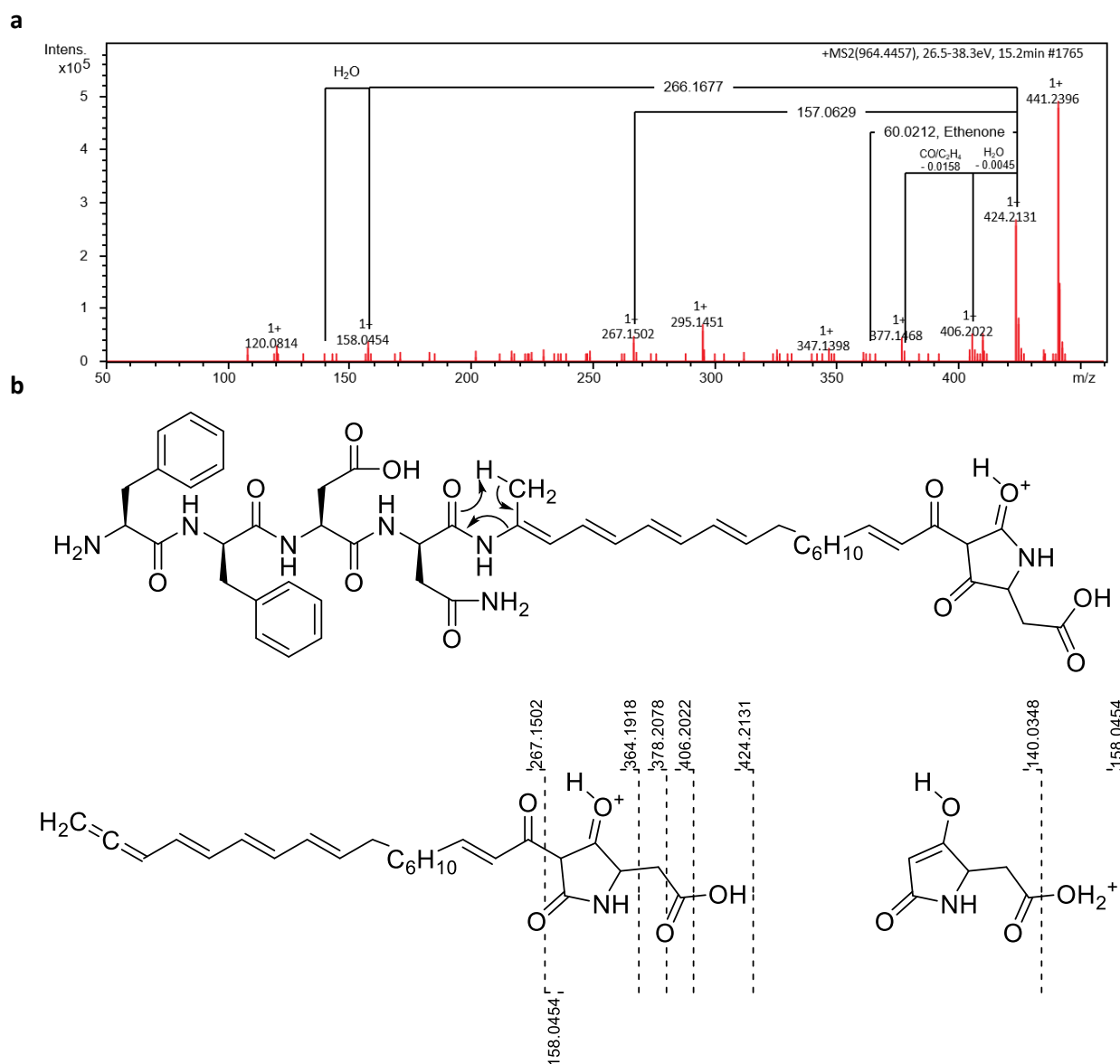
Figure 7. a, **MS/MS spectrum of the intact epifadin (HR-ESI(+) TOF mass spectrometry).** Fragmentation pattern of the PKS moiety from MS-data is shown in black. H_2O, water; CO, carbon monoxide. **b**, Deduced fragmentation pattern for the peptide amide 2 and the PKS/NRPS moiety. From a six-membered transition state a rearrangement results in a neutral loss of the peptide amide moiety. The newly formed allene (m/Z 424.2131) further fragments.

Final evidence for the full chemical architecture of the unusual, unprecedented peptide-polyene-tetramic acid structure such as in epifadin (**1**) requires acquisition and full assignment of all NMR signals, crystallography data, or chemical synthesis. So far, however, all attempts to isolate stable mg-amounts required to elucidate the complete structure of epifadin by NMR failed, most probably due to compound decomposition, even when completely shielded **1** from oxygen, light, and individual organic solvents during the final chromatographic and spectroscopic analyses with our currently available protocols. However, combining the available knowledge from 1) sequence data to predict enzyme functions of the BGC, 2) coupled HPLC-UV high-resolution MS analyses with sum formulae, fragmentation patterns, and UV spectrum, and 3) multidimensional NMR experiments with signals of most parts of the molecule (Fig. S7-S8) represent strong evidence for the given (**1**) epifadin structure (Fig. 8). A causal uncertainty exists only in the exact structure of the PK part merging into the tetramic acid. The BGC encodes the putative oxidoreductase EfiO, which might also play a role in the modification and maturation of epifadin.

Epifadin (**1**)
$C_{51}H_{61}N_7O_{12}$
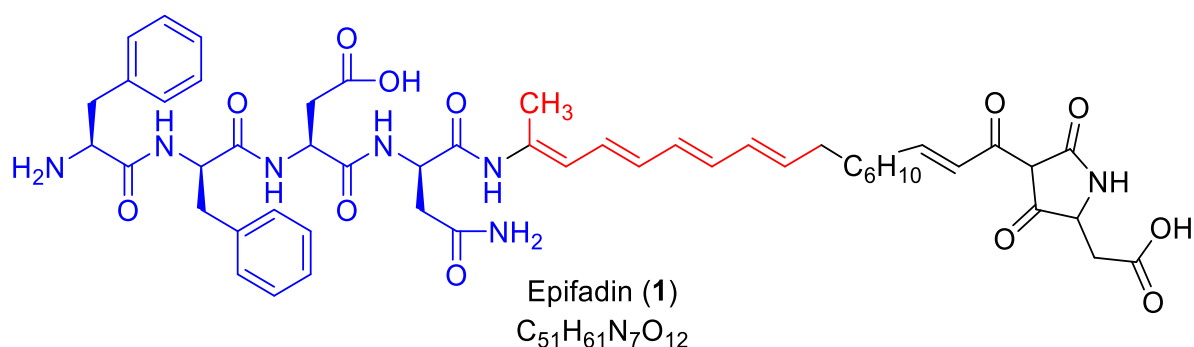
Figure 8. Molecular structure of epifadin (**1**). Blue moiety elucidated by NMR and MS, red moiety by NMR and suggested tetramic acid moiety by genetic-, single NMR- and MS data in accordance with detailed MS mechanistic considerations in black.

Epifadin is a potent, broad-spectrum, bactericidal antimicrobial

A larger panel of microorganisms from human nasal microbiomes was analyzed for susceptibility to epifadin (**1**) by monitoring inhibition zones around the epifadin producer IVK83, and in distinct assays with freshly purified epifadin compound, on lawns of test bacteria, which were cultivated in the dark to sustain the stability of epifadin. Most of the tested Firmicutes (several *Staphylococcus* species, *Streptococcus pyogenes*) and Actinobacteria (several *Corynebacterium* species, *Cutibacterium acnes*, *Micrococcus luteus*, *Kocuria* spec.) were

susceptible albeit with some variability between isolates of some of the species (Fig. 9). Notably, all tested *S. aureus* strains were susceptible to epifadin. In contrast, 9 of 16 tested nasal *S. epidermidis* isolates were resistant to epifadin. Most of the tested γ-Proteobacteria were resistant but *Raoultella ornithinolytica* was inhibited. Since amphotericin A, a natural derivative of amphotericin B, and nystatin A$_1$ [33] share structural similarities with epifadin in the polyene part and exhibit antifungal activity, *S. epidermidis* IVK83 was also tested against *Candida albicans* and *Saccharomyces cerevisiae*. Both fungal species were inhibited by *S. epidermidis* IVK83 (Fig. 9). Thus, epifadin has a very broad activity spectrum including Gram-positive and Gram-negative bacteria and yeast. However, strains of some bacterial species differ in susceptibility suggesting that specific strains may bear either resistance-conferring point mutations in target proteins or accessory resistance genes.

Species	Zone of inhibition
Bacillus cereus 1/3	yellow
Citrobacter freundii 2/2	grey
Citrobacter koseri 5/5	grey
Corynebacterium accolens 2/2	grey
Corynebacterium aurimucosum 1/1	grey
Corynebacterium pseudodiphteriticum 1/26	green
Corynebacterium pseudodiphteriticum 4/26	red
Corynebacterium pseudodiphteriticum 19/26	yellow
Cutibacterium acnes 3/3	yellow
Cutibacterium avidum 1/1	grey
Dermabacter hominis 1/1	grey
Dolosigranulum pigrum 1/1	grey
Enterococcus faecalis 8/8	grey
Enterococcus faecium 9/9	green
Escherichia coli 2/2	grey
Klebsiella oxytoca 2/2	grey
Klebsiella pneumoniae 3/3	grey
Kocuria spp 1/1	yellow
Micrococcus luteus 9/9	yellow
Raultella ornitholytica 1/2	yellow
Rotia mucilaginosa 1/1	yellow
Staphylococcus aureus 4/5	yellow
Staphylococcus aureus 1/5	green
Staphylococcus aureus ΔdltA	yellow
Staphylococcus capitis 2/2	grey
Staphylococcus caprae 2/2	grey
Staphylococcus carnosus 1/1	green
Staphylococcus epidermidis 4/16	yellow
Staphylococcus epidermidis 3/16	green
Staphylococcus epidermidis 9/16	grey
Staphylococcus hominis 3/3	yellow
Staphylococcus pettenkofferi 1/1	yellow
Staphylococcus sciuri 1/1	yellow
Staphylococcus warneri 2/2	yellow
Staphylococcus lugdunensis 1/2	green
Staphylococcus xylosus 1/1	yellow
Streptococcus pyogenes 1/1	yellow
Candida albicans 1/1	yellow
Saccharomyces cerevisiae 1/1	yellow

No inhibition
<1 mm
1-3 mm
3-5 mm

Figure 9. Antimicrobial activity spectrum of S. epidermidis IVK83 wild type. Zones of inhibition are depicted in different colors: grey, no inhibition; green, inhibition below 1 mm; yellow, inhibition between 1 mm and 3 mm; red, inhibition between 3 mm and 5 mm.

The availability of very limited amounts of freshly purified epifadin only allowed a more accurate determination of the minimal inhibitory concentration (MIC) for some of the test strains using a miniaturized agar diffusion assay. Epifadin turned out to be more active against *S. aureus* than vancomycin

and daptomycin with MIC values between 0.9 and 1.5 µg/mL (Table 1). Interestingly, among all the tested *Staphylococcus* species, epifadin was most active against *S. aureus* and had significantly higher MIC values between 3.7 and 8.6 µg/mL for susceptible strains of *S. epidermidis*, *Staphylococcus hominis*, *Staphylococcus sciuri*, and *Staphylococcus warneri*. Purified epifadin was bactericidal as exemplified for *S. aureus* - a tenfold MIC reduced the number of viable bacteria by three magnitudes in a four-hours incubation period (Fig. 10).

The antifungal activity of epifadin suggests that it targets a cellular mechanism that can also be essential in eukaryotic cells. However, epifadin impaired human HeLa cells only at ca. 20-fold MIC indicating that it might not have major cytotoxic potential for human cells (Fig. 10).

Table 1 Calculated minimal inhibitory concentration (MIC) of epifadin (1) against various bacteria. Assay was performed on TSA inoculated with the indicated bacterial strain. Experiment was performed once due to limited availability of pure epifadin.

Antibiotic	Strain	MIC in µg/mL	MIC in µM
Epifadin	*S. aureus* USA300 LAC	1.5	1.6
	S. aureus USA300 JE2	1.5	1.6
	S. aureus USA300 JE2 Δ*crtM*	1.5	1.6
	S. aureus Newman	1.5	1.6
	S. aureus RN4220	0.9	0.9
	S. aureus NCTC8325	0.9	0.9
	S. epidermidis IVK7	6.0	6.2
	S. hominis 9VPs_KB1	4.6	4.8
	S. hominis 89VPS_B7	8.6	8.9
	S. sciuri 50VAS_KB6	4.6	4.8
	S. warneri 1929	3.7	3.8
	S. warneri 1930	6.0	6.2
	M. luteus	7.4	7.7
	S. pyogenes	0.6	0.6
Vancomycin	*S. aureus* USA300 LAC	6.0	4.1
	S. aureus USA300 JE2	3.7	2.6
Daptomycin	*S. aureus* USA300 LAC	4.0	2.5
	S. aureus USA300 JE2	4.3	2.7

***S. epidermidis* uses epifadin to eliminate *S. aureus* during *in vitro* and *in vivo* co-cultivation.**

The particularly strong, bactericidal activity of epifadin (**1**) against *S. aureus* raised the question if epifadin can help *S. epidermidis* to outcompete *S. aureus*. Equal numbers of IVK83 wild type or epifadin-deficient mutant Δ*efiTP* were co-cultivated with *S. aureus* Newman, either on agar plate surfaces or in liquid broth, in the dark. *S. aureus* overgrew Δ*efiTP* under both conditions
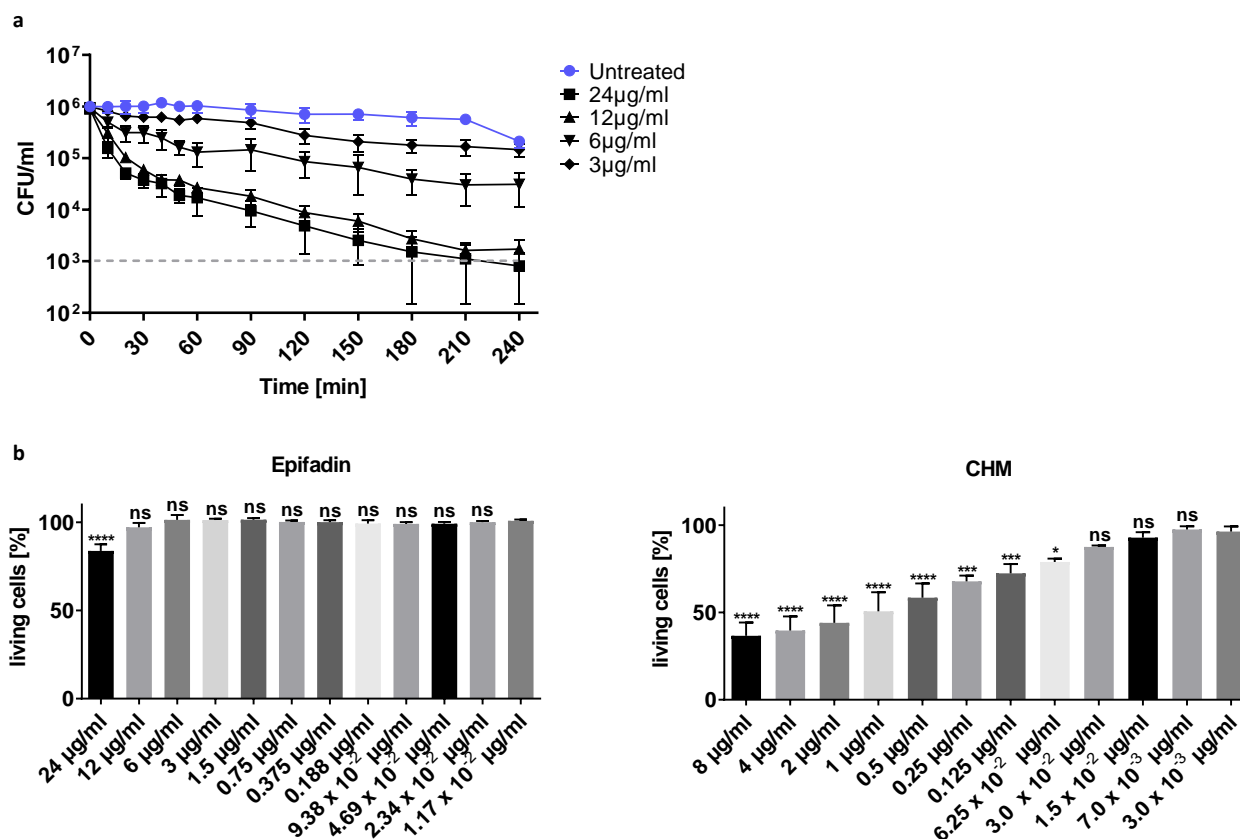
Figure 10. Epifadin is bactericidal for susceptible bacterial cells but does not inhibit mammalian cells. a, Time-dependent elimination of *S. aureus* by epifadin. Incubation of *S. aureus* USA300 LAC with epifadin concentrations of 24 µg/mL and 12 µg/mL led to a fast decline of CFUs reaching the detection limit of 1×10^3 CFU/mL after 210 min. Data represent means with SEM of three independent experiments. **b**, Cytotoxicity assay. HeLa cells incubated with epifadin do not show increased cell death compared to mock-treated cells even at high concentrations of 12 µg/mL. Cycloheximide (CHM) was included as a positive control. Only at concentration of 24 µg/mL, epifadin shows a significant cytotoxic effect, still leaving 84% of HeLa cells intact. Data points represent the mean ± SD of three independent experiments. Significant differences between lowest compound concentrations and higher concentrations were analyzed by one-way ANOVA ($*P < 0.05$; $**P < 0.01$; $***P < 0.001$; $****P < 0.0001$).

within 24 hours (Fig. 11, Fig. S6), which is in agreement with the previously documented capacity of *S. aureus* to grow faster or utilize nutrients better than *S. epidermidis* [34]. In contrast, the IVK83 wild type eradicated *S. aureus* completely within 24 hours, indicating that epifadin was effective enough under the used conditions to confer a significant fitness advantage over *S. aureus*. *S. aureus* had almost completely vanished after 24 hours, which is in agreement with the bactericidal activity of epifadin. Complementation of the mutant with a plasmid-encoded copy of *efiTP* restored the *S. aureus*-eradicating ability of IVK83 Δ*efiTP*,

thereby confirming that it is indeed epifadin that allowed *S. epidermidis* to outcompete *S. aureus* (Fig. 11, Fig. S6).

The ability of epifadin (**1**) to promote the competitive capacity of *S. epidermidis in vivo* was analyzed in the cotton rat-based model of nasal colonization. The IVK83 wild-type and Δ*efiTP* strains were similarly proficient in nasal colonization (Fig. 11). When either IVK83 wild type or *efiTP* mutant were instilled to the noses together with *S. aureus* Newman, the viable *S. aureus* counts were significantly lower after five days with the IVK83 wild-type compared to the Δ*efiTP*-colonized animals (Fig. 11), indicating that epifadin-producing *S. epidermidis* can effectively interfere with *S. aureus* nasal colonization.

Discussion

Recent metagenome- and cultivation-dependent screening approaches have revealed an increasing number of BGCs for complex natural products among bacteria from microbiomes [35, 36]. These included a number of NRP compounds such as lugdunin [25] and PK compounds such as wexrubicin [36]. We here report epifadin (**1**), the first example of an antibacterial molecule consisting of both, NRP and PK moieties produced by a common member of the human microbiome.

Such molecules have previously been associated with environmental and soil bacteria only. Our study further supports the notion that the antibacterial compounds produced by environmental and host-associated bacterial communities are based largely on the same chemical space [37].

Epifadin represents the founding member of a new class of mixed NRP/PK-containing compounds. Its antibacterial mechanism remains to be elucidated in the future. It is an amphiphilic, charged compound with unprecented alternation of the polar peptide, non-polar polyene, and, again, a polar and charged building block, that is unique. It remains to be clarified if and how epifadin may traverse the hydrophobic membrane bilayers to enter bacterial cells. The molecular target appears to be shared by bacterial and eukaryotic fungal cells. It also remains unclear why only fungal but not human HeLa cells were affected by epifadin. The extraordinary instability of epifadin may lead to higher impacts on cells that may take the compound up quickly, while slow uptake may lead to reduced activity due to the rapid loss of structure integrity and therefore diminished antimicrobial potential. The well-known *Bacillus* product bacillaene also became prominent due to its high instability and polyene-enamide NRPS-PKS structure [38]. How epifadin is taken up by target cells and how differences in uptake may contribute to susceptibility needs to be elucidated in the future. In several

Figure 11. Epifadin-producing *S. epidermidis* IVK83 restricts *S. aureus* growth *in vitro* and *in vivo* in cotton rats. a-c, in *vitro* competition assays on TSA. **a**, *S. aureus* growth is inhibited by IVK83 wild-type (WT) (grey or light blue bars, respectively) already after 24 h of incubation on TSA inoculated at ratios of ~50:50. **b**, In contrast, the mutant IVK83 Δ*efiTP* is overgrown by *S. aureus* over time when inoculated at a 50:50 ratio. **c**, Complementation restored the wild-type phenotype. Data points represent mean value ± SD of three independent experiments. Significant differences between starting condition and indicated time points were analyzed by one-way ANOVA (**$P < 0.01$; ***$P < 0.001$; ****$P < 0.0001$). **d**, Nasal colonization capability of IVK83 wild type and IVK83 Δ*efiTP* in cotton rats. Noses of cotton rats were instilled with 10^8 CFU/nose of either IVK83 wild type or mutant to determine their colonization efficiency. Per bacterial strain, five (for the mutant) or six (for the wild type) cotton rats were used and after 5 days of incubation the CFUs per nose were determined and plotted as individual dots. Horizontal lines represent the median of each group. **e**, Epifadin-producing IVK83 reduces *S. aureus* carriage in cotton rat noses. Ratios of *S. aureus* extracted from cotton rat noses (nine animals for the wild type and seven animals for the mutant group) were significantly lower when *S. aureus* was co-colonized with IVK83 wild type compared to the Δ*efiTP* mutant. Horizontal lines represent medians of each group. Significant differences were calculated by the Mann-Whitney test and are indicated (***$P = < 0.001$).

instances, the types of immunity (or self-protection) proteins encoded in a BGC can help to propose the mode of action of a new antibiotic. However, the epifadin BGC encodes only the two ABC transporter components EfiFG as potential resistance proteins, which may act as drug exporters and do not shed light on the antibacterial target.

The high instability remains a challenge for future structure elucidation studies. While the full epifadin molecule may remain refractory to NMR analysis, chemical synthesis of the most likely molecules and comparison of chromatographic, spectroscopic, and antimicrobial properties with native epifadin may lead to a final structure in the future. However, this will be a long-term endeavor because strategies for chemical synthesis of the complex and unstable enamide polyene tetramic acid **1** need to be developed. Such a proof of a propargyl tetramic acid natural product was recently exemplified [39]. Full structural assignment might finally arise from total chemical synthesis and prompt chemical analyses.

Previous approaches for the isolation of new microbiome-derived bacteriocins and related compounds have focused on stable compounds, which are rather easy to purify and to characterize. Short-lived antimicrobial compounds may have been overlooked in many of these studies and purification attempts may have remained unsuccessful; it is tempting to assume that epifadin is not the only short-lived antimicrobial produced in microbiomes. At first thought it may seem paradox and a waste of energy for a bacterium to produce an antimicrobial with such a short lifespan. However, limited stability may help to minimize collateral damage of bacterial mutualists and of host cells. Mounting evidence indicates that bacterial interactions in complex communities are not only shaped by antagonistic but also by multifactorial mutualistic interactions [40]. Bacterial life on mammalian skin and in the nares is challenging because nutrient supply is poor and many of the important cofactors and building blocks need to be synthesized [34, 41]. The collaborative degradation of complex host-derived polymers or assembly of critical building blocks seems to be more common in microbiomes than previously thought. All these constraints require that bacteria use antagonistic mechanisms with great care. Other strategies than using short-lived antimicrobials may be equally costly but even less effective. For instance, bacteriocins with very narrow target spectrum may work only in a community with very defined and stable composition and its transfer to other, even slightly different microbiomes may easily lead to loss of a competitive advantage. Likewise, contact-dependent bacteriocin delivery requires huge and complex secretion machineries, which are also very costly to synthesize and to maintain. A short-lived but broad-spectrum antimicrobial such as epifadin may be much more versatile and advantageous in microbiomes with limited density and spatial separation of individual bacterial microcolonies as on human skin and upper airways. It remains to be analyzed under which conditions epifadin is produced by *S.*

epidermidis. Our data suggest that it is constitutively expressed at different growth phases, which is supported by the absence of a putative regulatory gene in the BGC.

The epifadin BGC is located on a plasmid, which is probably readily transferred horizontally because it was found in different *S. epidermidis* clonal lineages and in *S. saccharolyticus* isolates [23]. The fact that we found epifadin to be produced by *S. epidermidis* isolates from three different geographical regions underscores its evolutionary success and fitness benefit. Furthermore, the plasmid seems to be highly stable, since the size and the BGC sequences were almost identical. Related gene clusters have also been found in *Lactococcus lactis* [42, 43] and *Streptococcus mutans* [44]. However, these two BGCs lack EfiO and the gene order is different from the epifadin BGC suggesting that the product is not identical to epifadin. The *L. lactis* epifadin-related BGC has recently been reported but the compound has not been characterized [42, 43]. A mutant with disrupted BGC was less tolerant to oxidative stress than the parental strain suggesting that the *L. lactis* compound may have the capacity to scavenge reactive oxygen species. We compared susceptibilities of the *S. epidermidis* IVK83 wild-type and *efiTP* mutant strains to oxidative stress but found no difference suggesting that epifadin is different from the *L. lactis* molecule in terms of structure and chemical properties.

Epifadin-producing *S. epidermidis* IVK83 had a strong capacity to eliminate the opportunistic pathogen *S. aureus* in experimental nasal colonization studies in a similar way as the recently reported *S. lugdunensis* strain IVK28 producing lugdunin [25]. Although epifadin is too instable in its native form to be considered as a new drug, epifadin-producing commensal bacteria could be used as probiotics that would eliminate *S. aureus* from the nares of at-risk patients. The search for fugacious bacteriocins should be extended to other microbes to identify more short-lived antimicrobials, which could hold promise for eradication of facultative pathogens in human microbiomes.

Materials and Methods

Bacterial strains and growth conditions. The bacterial strains used in this study are listed in Table S1. Tryptic soy broth (TSB) and tryptic soy agar (TSA) or basic medium (BM: 1% soy peptone, 0.5% yeast extract, 0.5% NaCl, 0.1% glucose and 0.1% K_2HPO_4, pH 7.2) and BM agar (BM with 1.5% agar) were used for bacteria cultivation. For Corynebacteria, 5% Sheep blood (Oxoid) were added. Cutibacteria were incubated under anaerobic conditions using an anaerobic jar and AnaeroGen™ (Thermo). When required, antibiotics were used at concentrations of 250 µg/mL for streptomycin, 10 µg/mL chloramphenicol, 100 µg/mL ampicillin or 2.5 µg/mL erythromycin. All media were prepared with water purified by a VEOLIA PureLab Chorus2 water purification system.

Antimicrobial spectrum of IVK83. The antimicrobial activity of *S. epidermidis* IVK83 was assessed by spotting *S. epidermidis* IVK83 on TSA agar plates containing lawns of bacterial test strains listed in Tab. 1. Therefore, the test strains were resuspended in 1 x phosphate-buffered saline (PBS, Gibco), adjusted to an OD_{600} of 0.5 and streaked out uniformly on TSA or TSA + blood plates with a cotton swab. *S. epidermidis* IVK83 grown on TSA was resuspended in 1 x PBS, adjusted to an OD_{600} of 1 and 10 µl spotted on the bacterial lawn. Plates were incubated for 24 h to 48 h at 37°C, anaerobic bacteria were grown under anaerobic conditions using an anaerobic jar and AnaeroGen™ (Thermo) and diameter of inhibition zones were measured.

Transposon mutagenesis for the identification of the epifadin gene cluster. Identification of the epifadin gene cluster was performed via transposon mutagenesis as described earlier [45]. In brief, *S. epidermidis* IVK83 was transformed with vector pTV1ts [46, 47] containing the transposon Tn917 with an erythromycin resistance gene (ermR). After growing in TSB supplemented with 10 µg/mL chloramphenicol at 30°C overnight, the culture was diluted (1:1000) in TSB containing 2.5 µg/mL erythromycin and cultivated at 42°C overnight. This step was repeated once more with 2.5 µg/mL erythromycin and once without erythromycin and the cells were subsequently plated on TSA containing 2.5 µg/mL erythromycin. Erythromycin-resistant but chloramphenicol-sensitive mutants, indicating *Tn*917 integration and loss of the plasmid, were screened for a loss of antimicrobial activity against *S. aureus*. The insertion sites were identified using isolated genomic DNA of non-inhibiting clones and primers Tn917 up and Ptn2 down, which were used to sequence upstream and downstream flanking regions of the transposon.

Construction of an epifadin production-deficient mutant and complementation. In order to generate a bacteriocin deficient mutant of *S. epidermidis* IVK83, the thermosensitive plasmid pBASE6 [48] and the primers listed in Table 1 were used. Therefore, DNA fragments up- and downstream of the genes *efiP* (phosphopantetheinyl-transferase) and *efiT* (thioesterase) were amplified by PCR using primers 83 KO Acc65I, 83 KO EcoRI and 83 KO BssHII and 83 KO SalI, respectively. After digestion of the upstream fragment with restriction enzymes EcoRI/Acc65I (Thermo) and the downstream fragment with BssHII/SalI (Thermo), the two fragments and the Acc65I-BssHII-digested erythromycin resistance cassette from plasmid pEC2 [49] were ligated into the EcoRI/SalI-digested vector pBASE6. After amplification of the generated plasmid pBASE6_KO83 in *E. coli* DC10B, IVK83 was transformed with the isolated plasmid where homologous recombination resulted in the bacteriocin deficient mutant IVK83 Δ*efiTP*.

For complementation, the genes $\Delta efiTP$ were amplified by PCR using primers 83 compl BamHI and 83 compl EcoRI. After digestion with BamHI/EcoRI (Thermo), the DNA fragment was ligated into BamHI/EcoRI digested pRB474 [50]. After transformation and amplification of the resulting vector pRB474-83compl *in E. coli* DC10B, the vector was transformed into the bacteriocin deficient IVK83 $\Delta efiTP$ and clones were screened for antimicrobial activity against *S. aureus*.

Purification of epifadin. All steps of the purification process were performed under reduced light exposure. From an overnight culture of IVK83 in TSB, fresh TSB was inoculated 1:1000 and incubated for 4 h at 37°C and constant shaking at 160 rpm to obtain bacteria in exponential growth phase. Subsequently, fresh TSB containing 5 g/l glucose was inoculated with an OD600 0.00125 of IVK83 and incubated for 44 h at 30°C and constant shaking at 160 rpm. Cultures were centrifuged and the supernatant adjusted to pH 2 using 37% HCl (Fisher Scientific) for 2 h at 4°C. The acidified supernatants were centrifuged at 8.000 x g for 15 min at 4°C, the clear supernatant was discarded, and the obtained precipitate was resuspended in small volumes of Milli-Q water and frozen at –80°C. The precipitate was lyophilized at –20°C and 1 mbar until water was completely removed. DMSO (Merck) supplemented with 0.05% palmitoyl ascorbate was added 20:1 (mL vol/g weight) to the precipitate to extract the active compound from the insoluble particles of the precipitate. After soft vortexing and centrifugation, the DMSO supernatant was transferred into a new vial. The extraction step of the precipitate was repeated once more. DMSO extractions were collected, lyophilized and the dry extract resuspended in a 1:2 mixture of system A (H_2O, 0.05% TFA) and system B (80% acetonitrile (Baker), 19.95% H_2O, 0,05% TFA). Subsequently, the solution was injected to a preparative, reversed-phase HPLC column (RP-HPLC-column Kromasil 100 C18.5 µm, 250x4 mm, Dr. Maisch GmbH) and HPLC was performed with a gradient from 50% system B to 100% system B in 30 min. The active compound displays a prominent absorption signal at ~383 nm, which is absent in the precipitate extract from the mutant. The product-containing fractions were collected at –77°C (dry ice isopropyl alcohol cooling bath) under an argon atmosphere, lyophilized, and stored at –80°C until further use.

Stability analysis of epifadin. The effect of different (abiotic) conditions on the bioactivity of epifadin was analyzed by agar diffusion assays against the sensitive indicator strain *S. aureus* USA300 LAC. Therefore, TSA was inoculated with an overnight culture of *S. aureus* to a final OD_{600} of 0.00125. After solidification of the agar, a cork borer was used to punch wells into the agar. TSB media with 50 mM sodium citrate (pH 5 and 6) or 50 mM Tris(hydroxymethyl)aminomethane (pH 8 and 9) were prepared. DMSO extraction of the epifadin containing precipitate (12 mg/mL) was performed in order to remove insoluble

particles. After centrifugation, the DMSO supernatant was added to the prepared TSB media to a final concentration equivalent of 750 µg/mL precipitate (37.5 µg in 50 µL). Media were incubated for six hours at 21°C, 30°C or 37°C with or without (laboratory) light exposure and constant shaking at 500 rpm in a thermomixer (Eppendorf). As control 70 µg/mL (3.5 µg in 50 µl) lugdunin, 24 µg/mL (1.2 µg in 50 µL) gallidermin and 100 µg/mL (5 µg in 50 µL) nisin were used. At different time points, 50 µl of each sample were pipetted into the wells of the agar plates. After incubation at 37°C overnight, zones of inhibition were photographed and analyzed with ImageJ software (version 1.8.0_112).

Analysis of epifadin by HPLC-ESI-TOF-HRMS. Mass spectra were recorded on a HPLC-UV-HR mass spectrometer (MaXis4G with Performance Upgrade kit with ESI-Interface, Bruker Daltonics). In order to obtain high resolution mass spectrometry (HR-MS) data, DMSO extracts were lyophilized, resuspended in the MeCN-water-mixture, and applied to a Dionex Ultimate 3000 HPLC system (Thermo Fisher Scientific), coupled to the MaXis 4G ESI-QTOF mass spectrometer (Bruker Daltonics). The ESI source was operated at a nebulizer pressure of 2.0 bar, and dry gas was set to 8.0 L·min^{-1} at 200°C. MS/MS spectra were recorded in auto MS/MS mode with collision energy stepping enabled. Sodium formiate was used as internal calibrant in each analysis. The routine gradient was 10% MilliQ-H$_2$O with 0.1% formic acid and 90% methanol with 0.06% formic acid to 100% methanol with 0.06% formic acid in 20 min with a flow rate of 0.3 mL/min on a Nucleoshell® EC RP-C$_{18}$ (150 x 2 mm, 2.7µm) from Macherey-Nagel.

Nuclear magnetic resonance spectroscopy. ^{1}H-NMR: *Bruker* AMX-600 (600 MHz), *Bruker* AvanceIII-700 (700 MHz). Chemical shifts are given as δ-values (ppm) relative to the solvent as internal standard. Coupling constants (*J*) are given in Hertz (Hz). Abbreviations for multiplicity description are as follows: s: singlet, d: duplet, dd: duplet of a duplet, m: multiplet. ^{13}C-NMR: *Bruker* AMX-600 (150.3 MHz), *Bruker* AvanceIII-700 (176.1 MHz). Chemical shifts are given as δ-values (ppm) relative to the solvent as internal standard. Homonuclear correlation experiment: ^{1}H-^{1}H-ROESY (Rotating Frame Overhauser Effect Spectroscopy).

Chemical solid-phase peptide synthesis of FfDn-NH$_2$. Fmoc-D-Asn(Trt) TG S RAM resin (loading: 0.23 mmol·g^{-1}, 150 mg, 34.5 µmol scale, Rapp Polymere) was swollen in DMF (2 mL) for 30 min. The Fmoc group was removed by treatment with a solution of 2% DBU/10% morpholine (v/v) in DMF (2 mL) for 3 min and additional 12 min. The resin-bound residue was submitted to iterative peptide assembly (Fmoc-SPPS) using 2% DBU/10% morpholine (v/v) in DMF (2 mL, 3 + 12 min) for Fmoc-deprotection and Fmoc-D/L-AA$_x$-OH (Fmoc-D-Asp(OtBu)-OH, Fmoc-D-Phe-OH and Fmoc-L-Phe-OH) (6 equiv.), HATU (6 equiv.), HOBt (6 equiv.) and

NMM (8 equiv.) in DMF (2 mL) for 45 min to couple each amino acid. After full assembly of linear peptide amide on the solid-support, the resin was washed with DMF (3 x 2 mL), DCM (3 x 2 mL), toluene (3 x 2 mL), IPA (3 x 2 mL), Et$_2$O (3 x 2 mL) and dried under reduced pressure for 3 h. The peptide was cleaved by treatment with TFA/TIPS/H$_2$O (95:5:5 v/v/v, 2 mL) for 3 x 1 h and one washing step with TFA (2 mL) for 10 min. The solvents were removed under reduced pressure, the residue was washed with Et$_2$O (3 x 2 mL) and centrifuged. The pale orange precipitate was lyophilized using *tert*-butanol/water (1:1 v/v, 10 mL).

Acetylation of 2 via chemical reaction with epifadin (1) extract. To 10 mg precipitate of IVK83 wild-type 200 µL 50 mM ammonium bicarbonate and 500 µL acetylation reagent (25 % acetic acid anhydride in pyridine) were added and stirred at room temperature for one hour. 100 µL of the reaction solution were taken, lyophilized and resolved in 50 µL LCMS-methanol for LCMS analytics.

Esterification of 2 with methanol via chemical reaction with epifadin (1) extract. To 10 mg precipitate of IVK83 wild-type 1 mL LCMS-MeOH and a droplet sulfuric acid were added and stirred at room temperature overnight. After centrifugation of the reaction solution 100 µL were taken for LCMS analytics.

Minimal Inhibitory Concentration (MIC) determination. Due to the low stability of epifadin under standard culture conditions and a low yield after purification, MIC determination via standardized laboratory approaches such as microdilution or agar dilution was not feasible. In order to approximately determine the MIC, TSA below 42°C were inoculated with different test strains with an OD$_{600}$ of 0.00125 and 17.5 mL were poured into petri dishes, resulting in agar layers of ~3.16 mm thickness. After solidification of the agar, a cork borer was used to punch wells with 4 mm diameter into the agar. 35 µl of DMSO containing different amounts of purified epifadin (2.4 µg, 1.2 µg, 0.6 µg, 0.3 µg, 0.15 µg and 0.075 µg) were pipetted into the wells and agar plates were incubated for 24 h at 37°C. Diameters of the zones of inhibition were measured and the volume containing the inhibitory epifadin concentration was calculated, using a modified formula for cylinder volume:

$$V_c = \pi \ x \ r^2 \ x \ h$$

V_c = cylinder volume

$$V_i = (\pi r_z^2 \ x \ h_a) - (\pi r_w^2 x h_a)$$

V_i = inhibited volume

r_z^2 = radius (diameter/2) zone of inhibition

r_w^2 = radius (diameter/2) of well

h_a = height of agar

The inhibited volume was then used to calculate the volume that was inhibited by 1 µg of epifadin, which was further used to approximately determine the MIC as follows:

If e.g., 2.4 µg of epifadin leads to an inhibited volume of 480 µl, in order to inhibit a volume of 1 mL, 5 µg epifadin is needed, which corresponds to a MIC of 5 µg/mL.

These calculations were conducted for the lowest amount of epifadin that led to a zone of inhibition to minimize the calculation error due to the gradient within the inhibition zone. The calculated concentration was used as an approximate MIC. As a control, the same assay was used to determine the MIC for vancomycin and daptomycin under these conditions.

Killing assay/minimal bactericidal concentration determination (MBC). Fresh TSB was inoculated 1:1000 with an overnight culture of *S. aureus* USA300 LAC and incubated for 4 h at 37°C and constant shaking at 160 rpm. Bacteria were centrifuged and washed once with 1 x PBS. Subsequently, cells were resuspended in 1 x PBS to an OD_{600} 0.00125 (1 x 10^6 CFU/mL) and different concentrations of purified epifadin were added. Bacteria were incubated for 4 h at 37°C and shaking (500 rpm, thermomixer). Every 30 min samples were taken, and serial dilutions were plated on TSA. After 24 h incubation at 37°C, CFUs were counted.

***In-vitro* competition assay.** *S. epidermidis* IVK83, *S. epidermidis* IVK83 Δ*efiTP, S. epidermidis* IVK83 Δ*efiTP* pRB474-83compl and a streptomycin-resistant *S. aureus* Newman were grown overnight in TSB at 37°C and constant shaking at 160 rpm. The strains were washed once with TSB and adjusted to 1 x 10^8 CFU/mL in TSB. For culture-based competition, 10 mL of *S. aureus* and 10 mL *S. epidermidis* were mixed in shaking flasks and incubated at 37°C and constant shaking at 160 rpm. After 24 h of incubation, fresh TSB was inoculated to an OD_{600} 0.5 with the previous culture (to ensure nutrition availability for antimicrobial production of IVK83) and incubated again at 37°C; this procedure was repeated after 48 h. Samples were taken at 0 h, 24 h, 48 h and 72 h and serial dilutions were plated on TSA and TSA supplemented with streptomycin for *S. aureus* Newman selection. After an overnight incubation at 37°C, CFUs were counted, and bacterial ratios were calculated.

For agar-based competition, overnight cultures of *S. aureus* and *S. epidermidis* were washed once with 1 x PBS and adjusted to 1 x 10^8 CFU/mL in 1 x PBS. 500 µL of *S. aureus* and 500 µl of *S. epidermidis* were mixed and 3 x 20 µL were spotted on TSA and incubated at 37°C. After 24 h incubation, bacterial cells were scraped from the three bacterial spots on agar plates, resuspended in 1 x PBS and adjusted to an OD_{600} 0.5 in 1 mL 1 x PBS, from which again 3 x 20µl were spotted on fresh TSA and incubated at 37°C; this procedure was repeated after 48 h. Samples of bacteria were taken at 0 h, 24 h, 48 h and 72 h, resuspended and serial dilutions were plated on TSA and TSA supplemented with streptomycin. After an overnight incubation at 37°C, CFUs were counted, and bacterial ratios were calculated.

Animal models and ethics statement. Animal experiments were performed in strict accordance with the German regulations of the "Gesellschaft für Versuchstierkunde/Society for Laboratory Animal Science" (GV-SOLAS) and the European Health Law of the Federation of Laboratory Animal Science Associations (FELASA) in accordance with German laws after approval (protocol IMIT1/15) by the local authorities (Regierungspräsidium Tübingen). The experiments were carried out at the Infection Biology Department of Tübingen and conformed to institutional animal care and use policies. Colonization and co-colonization experiments were performed with 8-12 weeks old cotton rats of both genders.

Colonization and co-colonization of cotton rat noses. For colonization of cotton rat noses, spontaneous streptomycin resistant *S. epidermidis* IVK83 and *S. epidermidis* IVK83 Δ*efiTP* mutants were generated by incubating and passaging those strains on TSA supplemented with 250 µg/mL streptomycin. For co-colonization, streptomycin-resistant *S. aureus* Newman was used. The cotton rat colonization model was described previously [51]. In previous experiments, Zipperer et al. have shown that an inoculum of 1 x 10^7 CFU/nose are required to obtain a stable colonization of 1 x 10^3 – 1 x 10^4 CFU/nose for *S. aureus* Newman, while other staphylococcal species like *S. lugdunensis* may require a higher inoculum [25]. Since the capability of *S. epidermidis* IVK83 and *S. epidermidis* IVK83 Δ*efiTP* to colonize cotton rat noses were unknown, firstly the inoculum required to obtain a stable colonization was determined. In brief, overnight cultures were washed twice in 1 x PBS and inocula were adjusted to 1 x 10^8 CFU/10 µl. Subsequently, cotton rats were anaesthetized with isoflurane and instilled intranasally with 1 x 10^8 CFU/nose. After 5 days, the cotton rats were euthanized, and the noses were removed and covered in 1 mL 1 x PBS. After heavy vortexing for 30 s, dilutions of the samples were plated on BM agar supplemented with 250 µg/mL streptomycin and incubated overnight at 37°C to obtain CFU/nose. We observed that an inoculum of 1 x 10^8 CFU/nose for both, IVK83 and IVK83 Δ*efiTP* is required to obtain slightly higher but comparable colonization level as *S. aureus* Newman with 1 x 10^7 CFU/nose. Based on this, co-colonization was performed with a tenfold increased inoculum for IVK83 and IVK83 Δ*efiTP*. For co-colonization, cotton rats were instilled intranasally with a mixture of 1 x 10^7 CFU/nose of *S. aureus* Newman and either 1 x 10^8 CFU/nose IVK83 or IVK83 Δ*efiTP.* After 5 days of incubation, bacteria were extracted from cotton rat noses as described above and the bacterial ratio was calculated; *S. aureus* (yellow) and *S. epidermidis* (white) were distinguished by color and colony size.

Cytotoxicity assay in HeLa cells. HeLa human cervical carcinoma cells were cultivated in RPMI cell culture medium (Thermofisher) supplemented with 10% fetal bovine serum (Thermofisher) at 37°C, 5% CO_2 and 95% relative humidity. A two-fold serial dilution of epifadin in RPMI was prepared in a microtiter plate and trypsinized HeLa cells to a final cell concentration of 1 x 10^4 per well were added. After 24 h incubation, 7-hydroxy-3H-phenoxazin-3-one-10-oxide (resazurin) was added to a final concentration of 200 µM and cells were again incubated for 24 h. Cell viability was evaluated by determining the reduction of resazurin to the fluorescent resorufin. Fluorescence was measured at an excitation wavelength of 560 nm and an emission wavelength of 600 nm (TECAN Infinite M200) in relation to an untreated control. As positive control, cycloheximide was used.

References

1.   Paller AS, Kong HH, Seed P, Naik S, Scharschmidt TC, Gallo RL, et al. The microbiome in patients with atopic dermatitis. J Allergy Clin Immunol. 2019;143(1):26-35. Epub 2018/11/27. doi: 10.1016/j.jaci.2018.11.015. PubMed PMID: 30476499; PubMed Central PMCID: PMCPMC7163929.

2.   Totté JE, van der Feltz WT, Hennekam M, van Belkum A, van Zuuren EJ, Pasmans SG. Prevalence and odds of Staphylococcus aureus carriage in atopic dermatitis: a systematic review and meta-analysis. Br J Dermatol. 2016;175(4):687-95. Epub 2016/03/20. doi: 10.1111/bjd.14566. PubMed PMID: 26994362.

3.   Lee YB, Byun EJ, Kim HS. Potential Role of the Microbiome in Acne: A Comprehensive Review. J Clin Med. 2019;8(7):987. doi: 10.3390/jcm8070987. PubMed PMID: 31284694.

4.   Kloos WE, Musselwhite MS. Distribution and persistence of Staphylococcus and Micrococcus species and other aerobic bacteria on human skin. Appl Microbiol. 1975;30(3):381-5. Epub 1975/09/01. PubMed PMID: 810086; PubMed Central PMCID: PMCPMC187193.

5.   Coates R, Moran J, Horsburgh MJ. Staphylococci: colonizers and pathogens of human skin. Future Microbiol. 2014;9(1):75-91. Epub 2013/12/18. doi: 10.2217/fmb.13.145. PubMed PMID: 24328382.

6.   Oh J, Byrd AL, Deming C, Conlan S, Kong HH, Segre JA. Biogeography and individuality shape function in the human skin metagenome. Nature. 2014;514(7520):59-64. Epub 2014/10/04. doi: 10.1038/nature13786. PubMed PMID: 25279917; PubMed Central PMCID: PMCPMC4185404.

7.   Du X, Larsen J, Li M, Walter A, Slavetinsky C, Both A, et al. Staphylococcus epidermidis clones express Staphylococcus aureus-type wall teichoic acid to shift from a commensal to pathogen lifestyle. Nature microbiology. 2021;6(6):757-68. Epub 2021/05/26. doi: 10.1038/s41564-021-00913-z. PubMed PMID: 34031577.

8.   Cogen AL, Yamasaki K, Muto J, Sanchez KM, Crotty Alexander L, Tanios J, et al. Staphylococcus epidermidis antimicrobial delta-toxin (phenol-soluble modulin-gamma) cooperates with host antimicrobial peptides to kill group A Streptococcus. PLoS One. 2010;5(1):e8557. Epub 2010/01/07. doi: 10.1371/journal.pone.0008557. PubMed PMID: 20052280; PubMed Central PMCID: PMCPMC2796718.

9.   Cogen AL, Yamasaki K, Sanchez KM, Dorschner RA, Lai Y, MacLeod DT, et al. Selective Antimicrobial Action Is Provided by Phenol-Soluble Modulins Derived from Staphylococcus epidermidis, a Normal Resident of the Skin. Journal of Investigative Dermatology. 2010;130(1):192-200. doi: https://doi.org/10.1038/jid.2009.243.

10.   Otto M. Phenol-soluble modulins. Int J Med Microbiol. 2014;304(2):164-9. Epub 2014/01/23. doi: 10.1016/j.ijmm.2013.11.019. PubMed PMID: 24447915; PubMed Central PMCID: PMCPMC4014003.

11.   Janek D, Zipperer A, Kulik A, Krismer B, Peschel A. High Frequency and Diversity of Antimicrobial Activities Produced by Nasal Staphylococcus Strains against Bacterial Competitors. PLoS Pathog. 2016;12(8):e1005812. doi: 10.1371/journal.ppat.1005812. PubMed PMID: 27490492; PubMed Central PMCID: PMCPMC4973975.

12.   O'Sullivan JN, Rea MC, O'Connor PM, Hill C, Ross RP. Human skin microbiota is a rich source of bacteriocin-producing staphylococci that kill human pathogens. FEMS Microbiology Ecology. 2018;95(2). doi: 10.1093/femsec/fiy241.

13.   Götz F, Perconti S, Popella P, Werner R, Schlag M. Epidermin and gallidermin: Staphylococcal lantibiotics. International Journal of Medical Microbiology. 2014;304(1):63-71. doi: https://doi.org/10.1016/j.ijmm.2013.08.012.

14.   Ekkelenkamp MB, Hanssen M, Danny Hsu S-T, de Jong A, Milatovic D, Verhoef J, et al. Isolation and structural characterization of epilancin 15X, a novel lantibiotic from a clinical strain of Staphylococcus epidermidis. FEBS Letters. 2005;579(9):1917-22. doi: 10.1016/j.febslet.2005.01.083.

15.   Heilbronner S, Krismer B, Brötz-Oesterhelt H, Peschel A. The microbiome-shaping roles of bacteriocins. Nat Rev Microbiol. 2021. Epub 2021/06/03. doi: 10.1038/s41579-021-00569-w. PubMed PMID: 34075213.

16.   Bastos MC, Ceotto H, Coelho ML, Nascimento JS. Staphylococcal antimicrobial peptides: relevant properties and potential biotechnological applications. Curr Pharm Biotechnol. 2009;10(1):38-61. Epub 2009/01/20. doi: 10.2174/138920109787048580. PubMed PMID: 19149589.

17.   Molloy EM, Cotter PD, Hill C, Mitchell DA, Ross RP. Streptolysin S-like virulence factors: the continuing sagA. Nature Reviews Microbiology. 2011;9(9):670-81. doi: 10.1038/nrmicro2624.

18.   Van Tyne D, Martin MJ, Gilmore MS. Structure, function, and biology of the Enterococcus faecalis cytolysin. Toxins (Basel). 2013;5(5):895-911. Epub 2013/05/01. doi: 10.3390/toxins5050895. PubMed PMID: 23628786; PubMed Central PMCID: PMCPMC3709268.

19.   Cascales E, Buchanan SK, Duché D, Kleanthous C, Lloubès R, Postle K, et al. Colicin biology. Microbiol Mol Biol Rev. 2007;71(1):158-229. doi: 10.1128/MMBR.00036-06. PubMed PMID: 17347522.

20.   Baquero F, Lanza VF, Baquero M-R, del Campo R, Bravo-Vázquez DA. Microcins in Enterobacteriaceae: Peptide Antimicrobials in the Eco-Active Intestinal Chemosphere. Front Microbiol. 2019;10(2261). doi: 10.3389/fmicb.2019.02261.

21.   Klein TA, Ahmad S, Whitney JC. Contact-Dependent Interbacterial Antagonism Mediated by Protein Secretion Machines. Trends Microbiol. 2020;28(5):387-400. Epub 2020/04/17. doi: 10.1016/j.tim.2020.01.003. PubMed PMID: 32298616.

22.   Cao Z, Casabona MG, Kneuper H, Chalmers JD, Palmer T. The type VII secretion system of Staphylococcus aureus secretes a nuclease toxin that targets competitor bacteria. Nat Microbiol. 2016;2:16183. Epub 2016/10/11. doi:

10.1038/nmicrobiol.2016.183. PubMed PMID: 27723728; PubMed Central PMCID: PMCPMC5325307.

23.   Brüggemann H, Poehlein A, Brzuszkiewicz E, Scavenius C, Enghild JJ, Al-Zeer MA, et al. Staphylococcus saccharolyticus Isolated From Blood Cultures and Prosthetic Joint Infections Exhibits Excessive Genome Decay. Front Microbiol. 2019;10(478). doi: 10.3389/fmicb.2019.00478.

24.   Ramachandran G, Miguel-Arribas A, Abia D, Singh PK, Crespo I, Gago-Córdoba C, et al. Discovery of a new family of relaxases in Firmicutes bacteria. PLoS Genet. 2017;13(2):e1006586. Epub 2017/02/17. doi: 10.1371/journal.pgen.1006586. PubMed PMID: 28207825; PubMed Central PMCID: PMCPMC5313138.

25.   Zipperer A, Konnerth MC, Laux C, Berscheid A, Janek D, Weidenmaier C, et al. Human commensals producing a novel antibiotic impair pathogen colonization. Nature. 2016;535(7613):511-6. doi: 10.1038/nature18634.

26.   Kellner R, Jung G, Hörner T, Zähner H, Schnell N, Entian KD, et al. Gallidermin: a new lanthionine-containing polypeptide antibiotic. Eur J Biochem. 1988;177(1):53-9. Epub 1988/10/15. doi: 10.1111/j.1432-1033.1988.tb14344.x. PubMed PMID: 3181159.

27.   Rogers LA, Whittier EO. LIMITING FACTORS IN THE LACTIC FERMENTATION. J Bacteriol. 1928;16(4):211-29. PubMed PMID: 16559334.

28.   Blin K, Shaw S, Steinke K, Villebro R, Ziemert N, Lee SY, et al. antiSMASH 5.0: updates to the secondary metabolite genome mining pipeline. Nucleic Acids Res. 2019;47(W1):W81-w7. Epub 2019/04/30. doi: 10.1093/nar/gkz310. PubMed PMID: 31032519; PubMed Central PMCID: PMCPMC6602434.

29.   Chang Y, Wang Y-H, Hu C-Q. Simultaneous determination of purity and potency of amphotericin B by HPLC. The Journal of Antibiotics. 2011;64(11):735-9. doi: 10.1038/ja.2011.83.

30.   Drescher C, Keller M, Potterat O, Hamburger M, Brückner R. Structure-Elucidating Total Synthesis of the (Polyenoyl)tetramic Acid Militarinone C§. Org Lett. 2020;22(7):2559-63. Epub 2020/03/20. doi: 10.1021/acs.orglett.0c00431. PubMed PMID: 32191484.

31.   Law BJC, Zhuo Y, Winn M, Francis D, Zhang Y, Samborskyy M, et al. A vitamin K-dependent carboxylase orthologue is involved in antibiotic biosynthesis. Nature Catalysis. 2018;1(12):977-84. doi: 10.1038/s41929-018-0178-2.

32.   Fujii I. Functional analysis of fungal polyketide biosynthesis genes. J Antibiot (Tokyo). 2010;63(5):207-18. Epub 2010/03/06. doi: 10.1038/ja.2010.17. PubMed PMID: 20203700.

33.   Cavassin FB, Baú-Carneiro JL, Vilas-Boas RR, Queiroz-Telles F. Sixty years of Amphotericin B: An Overview of the Main Antifungal Agent Used to Treat Invasive Fungal Infections. Infectious Diseases and Therapy. 2021;10(1):115-47. doi: 10.1007/s40121-020-00382-7.

34.   Krismer B, Liebeke M, Janek D, Nega M, Rautenberg M, Hornig G, et al. Nutrient limitation governs Staphylococcus aureus metabolism and niche adaptation in the human nose. PLoS Pathog. 2014;10(1):e1003862. doi: 10.1371/journal.ppat.1003862. PubMed PMID: 24453967; PubMed Central PMCID: PMCPMC3894218.

35.   Donia MS, Cimermancic P, Schulze CJ, Wieland Brown LC, Martin J, Mitreva M, et al. A systematic analysis of biosynthetic gene clusters in the human microbiome reveals a common family of antibiotics. Cell. 2014;158(6):1402-14. doi: 10.1016/j.cell.2014.08.032. PubMed PMID: 25215495.

36.   Sugimoto Y, Camacho FR, Wang S, Chankhamjon P, Odabas A, Biswas A, et al. A metagenomic strategy for harnessing the chemical repertoire of the human microbiome. Science. 2019;366(6471). Epub 2019/10/05. doi: 10.1126/science.aax9176. PubMed PMID: 31582523.

37.   Donia MS, Fischbach MA. HUMAN MICROBIOTA. Small molecules from the human microbiota. Science. 2015;349(6246):1254766. Epub 2015/07/25. doi: 10.1126/science.1254766. PubMed PMID: 26206939; PubMed Central PMCID: PMCPMC4641445.

38.   Moldenhauer J, Chen X-H, Borriss R, Piel J. Biosynthesis of the Antibiotic Bacillaene, the Product of a Giant Polyketide Synthase Complex of the trans-AT Family. Angewandte Chemie International Edition. 2007;46(43):8195-7. doi: https://doi.org/10.1002/anie.200703386.

39.   Myrtle JD, Beekman AM, Barrow RA. Ravynic acid, an antibiotic polyeneyne tetramic acid from Penicillium sp. elucidated through synthesis. Org Biomol Chem. 2016;14(35):8253-60. Epub 2016/08/16. doi: 10.1039/c6ob00938g. PubMed PMID: 27519121.

40.   Pacheco AR, Segrè D. A multidimensional perspective on microbial interactions. FEMS microbiology letters. 2019;366(11):fnz125. doi: 10.1093/femsle/fnz125. PubMed PMID: 31187139.

41.   Byrd AL, Belkaid Y, Segre JA. The human skin microbiome. Nature Reviews Microbiology. 2018;16(3):143-55. doi: 10.1038/nrmicro.2017.157.

42.   Golomb BL, Yu AO, Coates LC, Marco ML. The Lactococcus lactis KF147 nonribosomal peptide synthetase/polyketide synthase system confers resistance to oxidative stress during growth on plant leaf tissue lysate. Microbiologyopen. 2018;7(1):e00531. Epub 2017/09/18. doi: 10.1002/mbo3.531. PubMed PMID: 28921941.

43.   Khayatt BI, van Noort V, Siezen RJ. The Genome of the Plant-Associated Lactic Acid Bacterium Lactococcus lactis KF147 Harbors a Hybrid NRPS-PKS System Conserved in Strains of the Dental Cariogenic Streptococcus mutans. Curr Microbiol. 2020;77(1):136-45. Epub 2019/11/11. doi: 10.1007/s00284-019-01799-1. PubMed PMID: 31705391.

44.   Wu C, Cichewicz R, Li Y, Liu J, Roe B, Ferretti J, et al. Genomic island TnSmu2 of Streptococcus mutans harbors a nonribosomal peptide synthetase-polyketide synthase gene cluster responsible for the biosynthesis of pigments involved in oxygen

and H2O2 tolerance. Appl Environ Microbiol. 2010;76(17):5815-26. Epub 2010/07/20. doi: 10.1128/aem.03079-09. PubMed PMID: 20639370; PubMed Central PMCID: PMCPMC2935078.

45.   Neubauer H, Pantel I, Götz F. Molecular characterization of the nitrite-reducing system of Staphylococcus carnosus. J Bacteriol. 1999;181(5):1481-8. doi: 10.1128/JB.181.5.1481-1488.1999. PubMed PMID: 10049379.

46.   Gutierrez JA, Crowley PJ, Brown DP, Hillman JD, Youngman P, Bleiweis AS. Insertional mutagenesis and recovery of interrupted genes of Streptococcus mutans by using transposon Tn917: preliminary characterization of mutants displaying acid sensitivity and nutritional requirements. J Bacteriol. 1996;178(14):4166-75. Epub 1996/07/01. doi: 10.1128/jb.178.14.4166-4175.1996. PubMed PMID: 8763945; PubMed Central PMCID: PMCPMC178174.

47.   Youngman PJ, Perkins JB, Losick R. Genetic transposition and insertional mutagenesis in Bacillus subtilis with Streptococcus faecalis transposon Tn917. Proc Natl Acad Sci U S A. 1983;80(8):2305-9. Epub 1983/04/01. doi: 10.1073/pnas.80.8.2305. PubMed PMID: 6300908; PubMed Central PMCID: PMCPMC393808.

48.   Geiger T, Francois P, Liebeke M, Fraunholz M, Goerke C, Krismer B, et al. The stringent response of Staphylococcus aureus and its impact on survival after phagocytosis through the induction of intracellular PSMs expression. PLoS Pathog. 2012;8(11):e1003016. Epub 2012/12/05. doi: 10.1371/journal.ppat.1003016. PubMed PMID: 23209405; PubMed Central PMCID: PMCPMC3510239.

49.   Brückner R. Gene replacement in Staphylococcus carnosus and Staphylococcus xylosus. FEMS Microbiol Lett. 1997;151(1):1-8. Epub 1997/06/01. doi: 10.1111/j.1574-6968.1997.tb10387.x. PubMed PMID: 9198277.

50.   Bruckner R. A series of shuttle vectors for Bacillus subtilis and Escherichia coli. Gene. 1992;122(1):187-92. doi: 10.1016/0378-1119(92)90048-t. PubMed PMID: 1452028.

51.   Baur S, Rautenberg M, Faulstich M, Grau T, Severin Y, Unger C, et al. A nasal epithelial receptor for Staphylococcus aureus WTA governs adhesion to epithelial cells and modulates nasal colonization. PLoS Pathog. 2014;10(5):e1004089. Epub 2014/05/03. doi: 10.1371/journal.ppat.1004089. PubMed PMID: 24788600; PubMed Central PMCID: PMCPMC4006915.

52.   Kaspar U, Kriegeskorte A, Schubert T, Peters G, Rudack C, Pieper DH, et al. The culturome of the human nose habitats reveals individual bacterial fingerprint patterns. Environ Microbiol. 2016;18(7):2130-42. doi: 10.1111/1462-2920.12891. PubMed PMID: 25923378.

53.   Monk IR, Shah IM, Xu M, Tan MW, Foster TJ. Transforming the untransformable: application of direct transformation to manipulate genetically Staphylococcus aureus and Staphylococcus epidermidis. mBio. 2012;3(2). doi: 10.1128/mBio.00277-11. PubMed PMID: 22434850; PubMed Central PMCID: PMCPMC3312211.

54. Diep BA, Otto M. The role of virulence determinants in community-associated MRSA pathogenesis. Trends Microbiol. 2008;16(8):361-9. doi: 10.1016/j.tim.2008.05.002. PubMed PMID: 18585915; PubMed Central PMCID: PMCPMC2778837.

55. Tse H, Tsoi HW, Leung SP, Lau SK, Woo PC, Yuen KY. Complete genome sequence of Staphylococcus lugdunensis strain HKU09-01. J Bacteriol. 2010;192(5):1471-2. doi: 10.1128/JB.01627-09. PubMed PMID: 20047907; PubMed Central PMCID: PMCPMC2820864.

56. Duthie ES, Lorenz LL. Staphylococcal coagulase; mode of action and antigenicity. J Gen Microbiol. 1952;6(1-2):95-107. Epub 1952/02/01. doi: 10.1099/00221287-6-1-2-95. PubMed PMID: 14927856

57. Fey PD, Endres JL, Yajjala VK, Widhelm TJ, Boissy RJ, Bose JL, et al. A genetic resource for rapid and comprehensive phenotype screening of nonessential Staphylococcus aureus genes. mBio. 2013;4(1):e00537. doi: 10.1128/mBio.00537-12. PubMed PMID: 23404398.

58. Kreiswirth BN, Löfdahl S, Betley MJ, O'Reilly M, Schlievert PM, Bergdoll MS, et al. The toxic shock syndrome exotoxin structural gene is not detectably transmitted by a prophage. Nature. 1983;305(5936):709-12. doi: 10.1038/305709a0.

Supplemental Information

Supplementary Figures
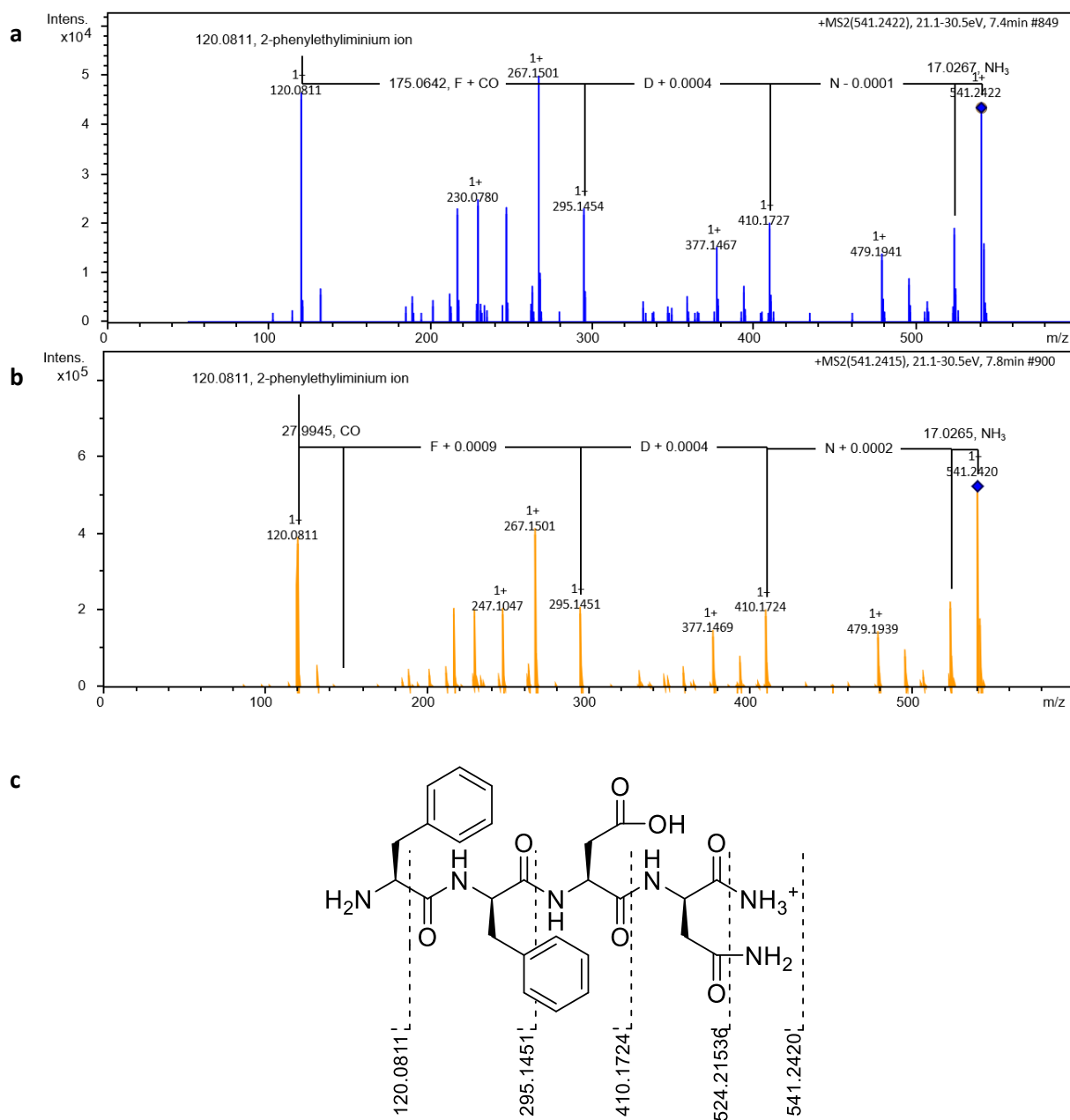
Figure S1. A comparison of the MS/MS spectra of synthetic and natural peptide amide 2. a, MS/MS spectrum of the natural peptide amide 2 after decomposition of epifadin **(1)**. **b**, MS/MS spectrum of the synthetic peptide amide 2. **c**, Fragmentation pattern of the synthetic and natural peptide amide 2. Fragmentation pattern for the peptide amide 2 is shown in black. F, phenylalanine; D, aspartate; N, asparagine; CO, carbon monoxide; NH_3, ammonia.

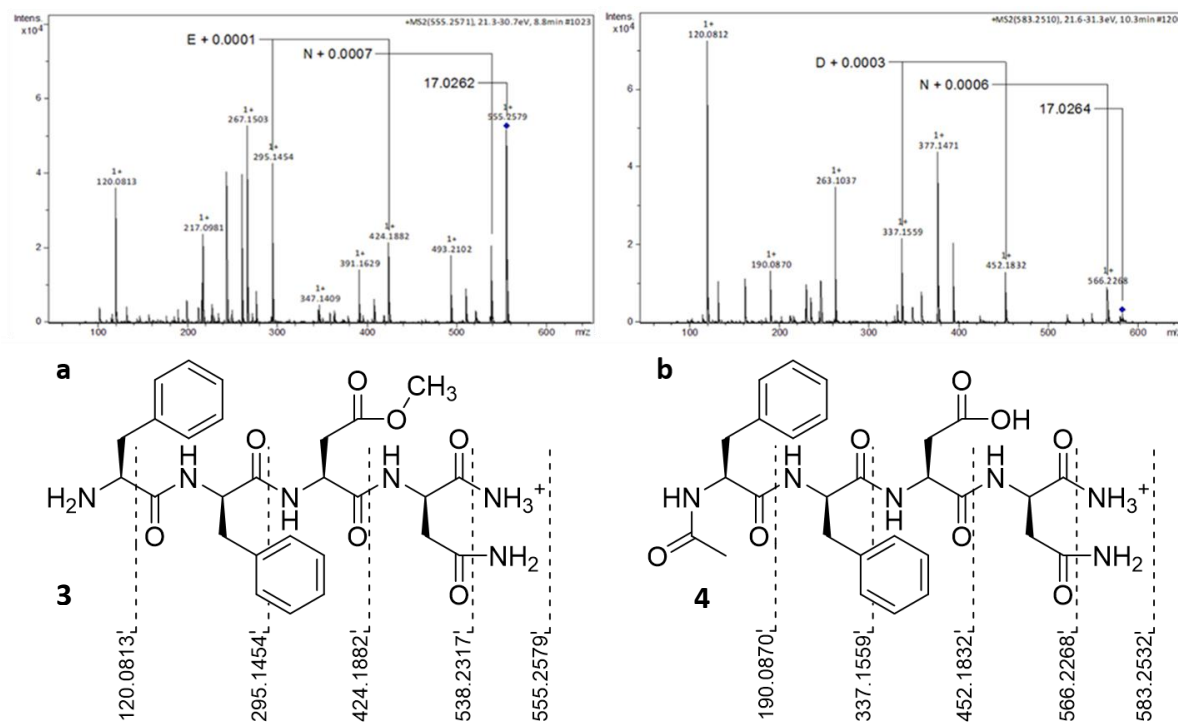**Figure S2. Structures of synthetic derivatives of peptide amide and MS/MS spectra** of **a,** methyl ester (**3**) of natural peptide amide and **b,** acetylated (**4**) natural peptide amide.
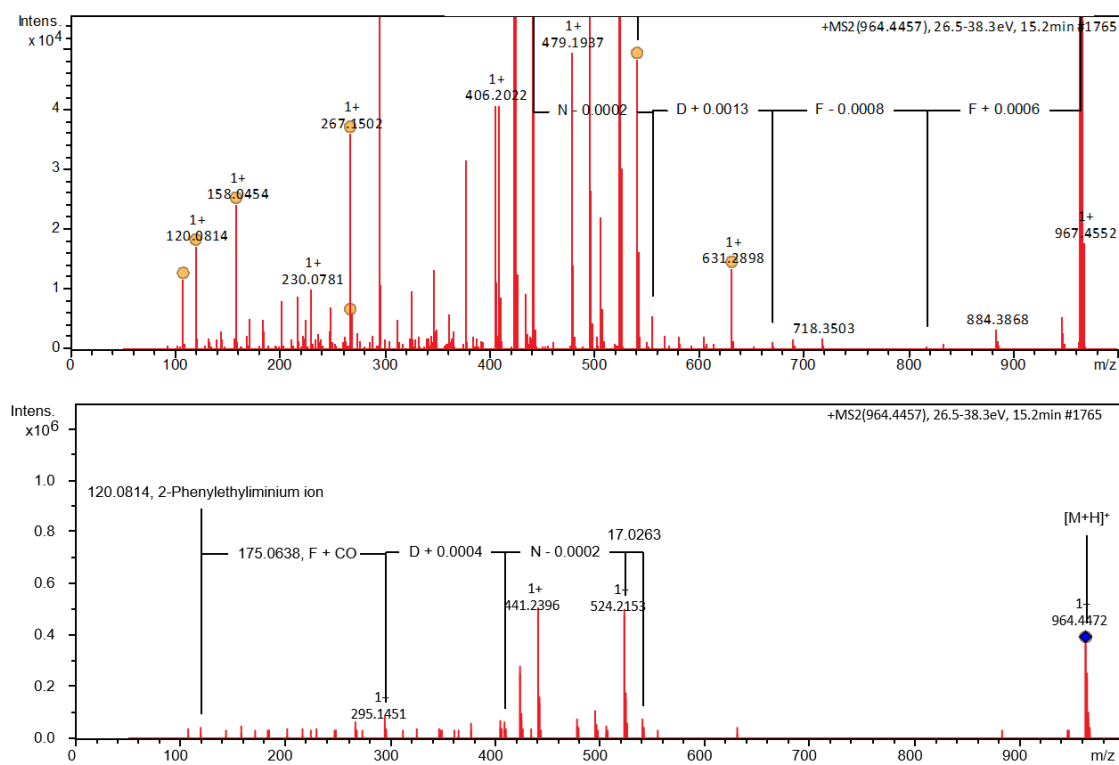
Figure S3. MS/MS spectra of epifadin (1) showing fragmentation products from ionization in mass spectrometry. The mass of 964 Da corresponds to the intact proton adduct (m/z 964.4) of **1**.

524 Da (m/z 524.2) corresponds to the proton adduct of the tetrapeptide EfiA product, and the mass of 441 Da /m/z 441.2) is assigned to the proton adduct of EfiBCDE product. Fragmentation pattern for the peptide moiety in epifadin is shown in black. [M+H]⁺, monoisotopic positively charged ion; F, phenylalanine; D, aspartate; N, asparagine; CO, carbon monoxide.
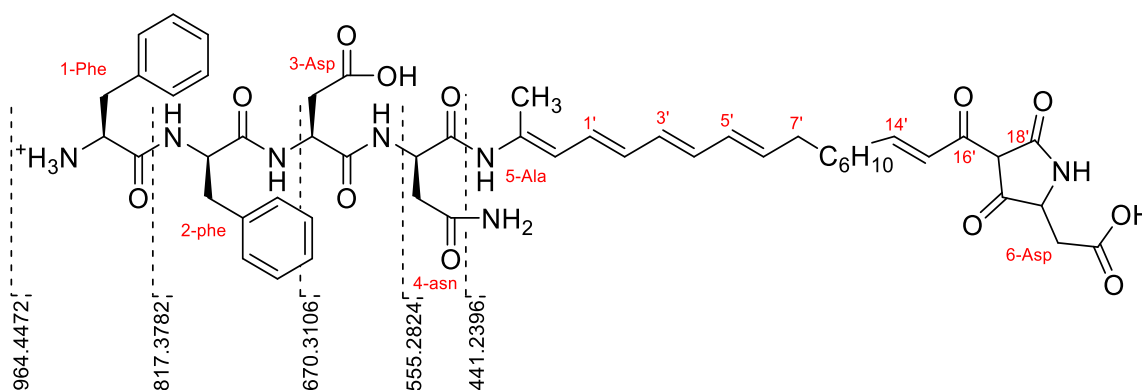
Figure S4. Deduced distinct fragmentation pattern for the peptide moiety of epifadin (1). The mass of 964 Da (m/z 964.4) corresponds to the intact proton adduct of epifadin (**1**). Numbering of amino acids and carbon atoms of PKS chain in red.
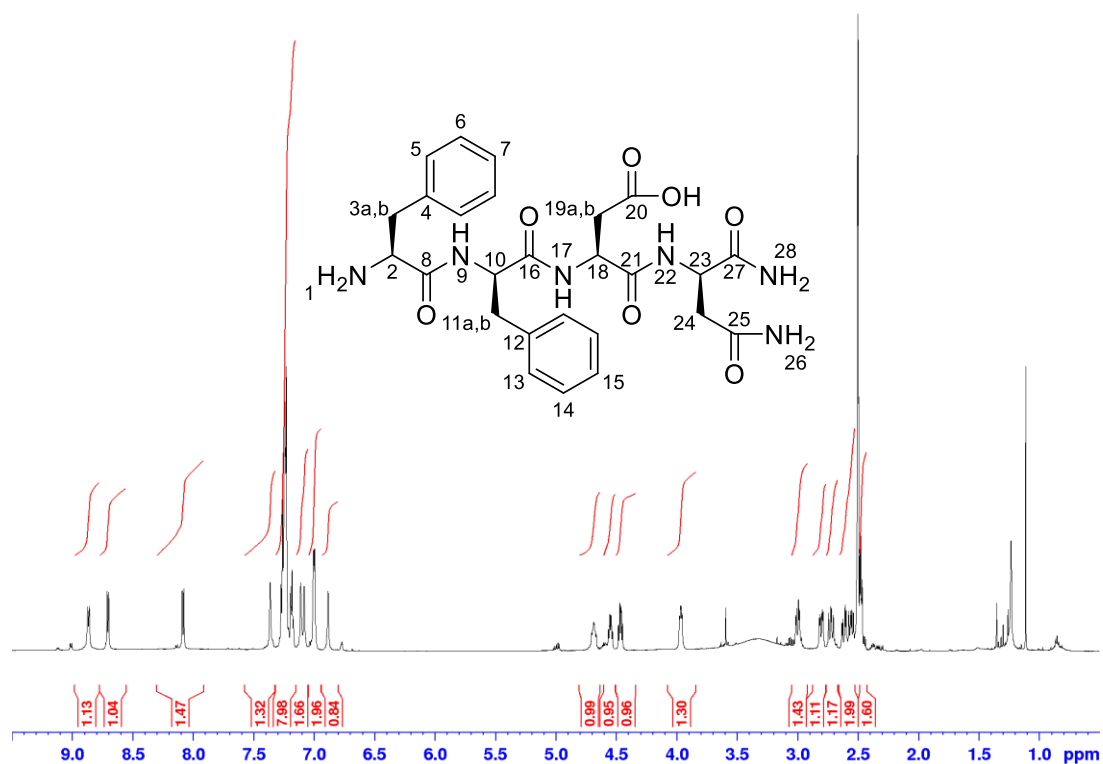
Figure S5. Proton NMR spectrum of the synthetic peptide amide 2 (DMSO-d₆, 600MHz, 303K) . The integrals of the proton signals are depicted in red. The blue scale shows the chemical shift *δ* in parts per million (ppm).
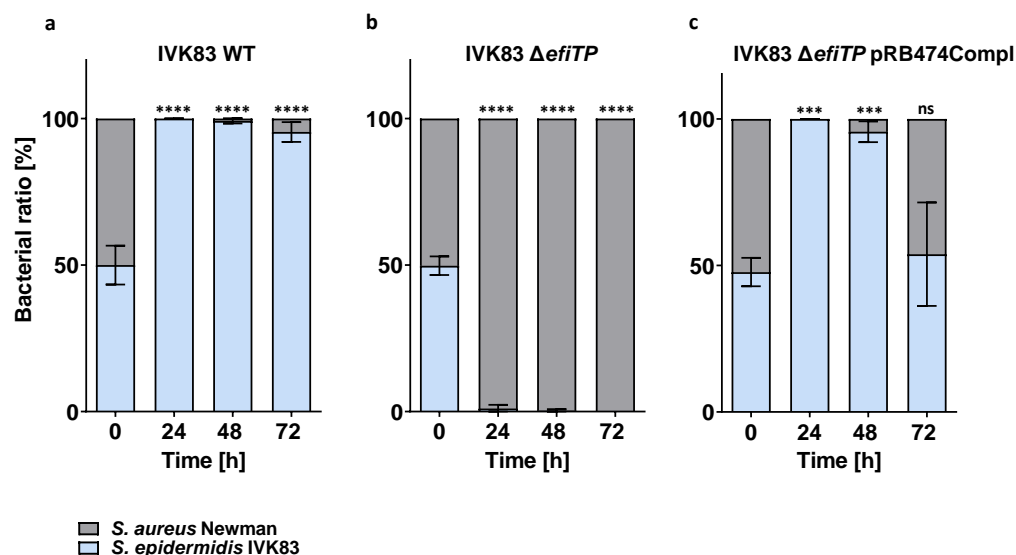
Figure S6. Epifadin-producing *S. epidermidis* IVK83 restricts *S. aureus* growth *in vitro*. a-c, in *vitro* competition assays in TSB. **a**, *S. aureus* growth is inhibited by IVK83 wild type (grey or light blue bars, respectively) already after 24 h of incubation in TSB inoculated at ratios of ~50:50. **b**, In contrast, the mutant IVK83 Δ*efiTP* is overgrown by *S. aureus* over time when inoculated at a 50:50 ratio. **c**, Complemented strain overgrew *S. aureus* for 48 h, after 72h, ratio of complemented strain and *S. aureus* were similar to starting conditions. Data points represent mean value ± SD of three independent experiments. Significant differences between the starting condition and the indicated time points were analyzed by one-way ANOVA (**P < 0.01; ***P < 0.001; ****P < 0.0001).
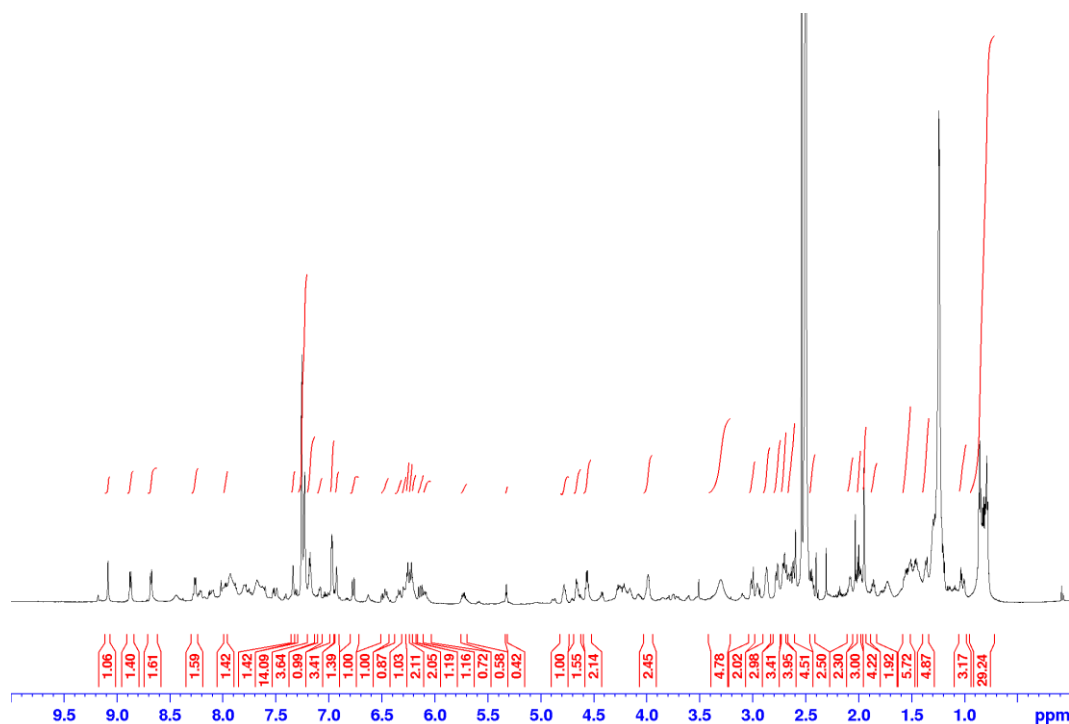
Figure S7. ^{1}H NMR spectrum (DMSO-d_6, 700 MHz, 303 K) of the purified epifadin (1). DMSO-d_6 signal at 2.50 ppm as reference. The integrals of the proton signals are depicted in red. The blue scale shows the chemical shift δ in parts per million (ppm).
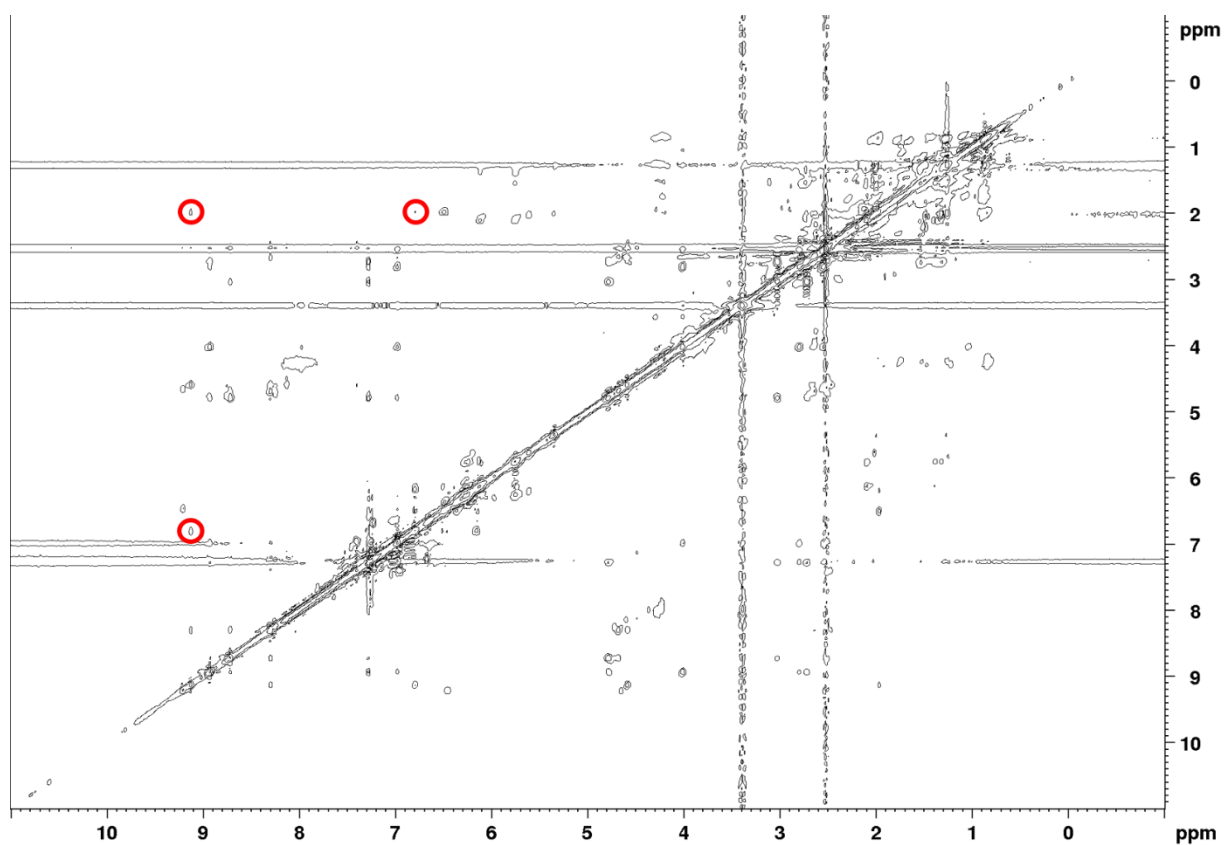
Figure S8. ^{1}H-^{1}H-ROESY NMR spectrum of the purified epifadin (1) in DMSO-d$_6$ (700 MHz, 303K) The red circles highlight coupling between the NH-proton and the protons of the methyl group of the Ala residue (9.14 ppm/1.95 ppm) and to the proton of methine group mentioned above (9.14 ppm/6.77 ppm). Also, the coupling of the protons of the methyl group from the Ala residue to the methine group is shown (6.77 ppm/1.95 ppm).

Supplementary Tables

Table S1 Bacterial strains, plasmids and oligonucleotides used in this study.

Bacterial species/strains	Description	Source or reference
Bacillus cereus	various human nasal isolates	Peschel strain collection
Citrobacter freundii	various human nasal isolates	Peschel strain collection
Citrobacter koseri	various human nasal isolates	Peschel strain collection
Corynebacterium aurimucosum		
10VPs_Sm8	human nasal isolate	[52]
Corynebacterium pseudodiphteriticum	various human nasal isolates	Peschel strain collection; [52]
Cutibacterium acnes	various human nasal isolates	Microbial diagnostics facility of University Hospital Tübingen; [52]
Dermabacter hominis	human nasal isolate	Peschel strain collection
Dolosigranulum pigrum		
9VAs_B4	human nasal isolate	[52]
Enterococcus faecium	various isolates	Tübingen diagnostic
Escherichia coli		
DH5α	K-12 derivative	New England BioLabs
DC10B	Δ*dcm* in the DH10B background	[53]
Klebsiella oxytoca	human nasal isolate	Peschel strain collection
Klebsiella pneumoniae	various human nasal isolates	Peschel strain collection
Kocuria sp.	various human nasal isolates	Peschel strain collection
Micrococcus luteus	various human nasal isolates	Peschel strain collection
Moraxella catarrhalis		
44VAs_Sm4	human nasal isolate	[52]
80VAs_B4	human nasal isolate	[52]
Moraxella nonliquefaciens	various human nasal isolates	Peschel strain collection
Photobacterium damselae		Medical Microbiology Department of Münster
Raultella ornitholytica	various human nasal isolates	Peschel strain collection
Staphylococcus aureus	various human nasal isolates	[11]
USA300 LAC	CA-MRSA isolate	[54]
Newman		[56]
Newman Δ*dltA*	Deletion of d-Alanyl carrier protein ligase	Peschel strain collection
Newman Strep[R]	Streptomycin resistent *S. aureus* Newman	[25]
USA300 LAC JE2	CA-MRSA isolate	[57]
USA300 LAC JE2 Δ*crtM*	4,4'-diapophytoene synthase mutant	Peschel strain collection
RN4220	mutation in *sau1 hsdR*	[58]

NCTC 8325		Culture Collections Public Health England, Porton Down, UK
Staphylococcus capitis		
10VAs_KB2	human nasal isolate	[52]
44UNs_B2	human nasal isolate	[52]
Staphylococcus caprae		
VA18305/14	human clinical isolate	Eppendorfklinikum, Hamburg
BK3880/14	human clinical isolate	Eppendorfklinikum, Hamburg
S*taphylococcus* carnosus		
TM300		
Staphylococcus epidermidis	various human nasal isolates	Peschel strain collection
IVK83	Human nasal isolate	This study
IVK83 Δ*efiTP*	Deletions of Δ*efiTP*	This study
IVK83 Δ*efiTP* pRB474-83compl	Complementation of Δ*efiTP*	This study
Staphylococcus hominis		
50MNs_Sa6	human nasal isolate	[52]
89VPs_B7	human nasal isolate	[52]
9VPs_KB1	human nasal isolate	[52]
Staphylococcus lugdunensis		
HKU09-01	human skin infection isolate	[55]
IVK28	human nasal isolate	[11]
Staphylococcus pettenkofferi		
210-70229632	human clinical isolate	Peschel strain collection
Staphylococcus sciuri		
50VAs_KB6	human nasal isolate	[52]
Staphylococcus warneri		
VA16066/14	human clinical isolate	Eppendorfklinikum, Hamburg
BK6091/14	human clinical isolate	Eppendorfklinikum, Hamburg
Staphylococcus xylosus		
C2a		Peschel strain collection
Streptococcus pyogenes		
BK2192		Peschel strain collection
Fungi		
Candida albicans	human clinical isolate	Medical microbiology
Saccharomyces cerevisiae		Dr. Oetker Trockenhefe

Plasmid	Description	Reference
pBASE6	thermosensitive vector for allelic exchange	[48]
pRB474	*E. coli/S. aureus* shuttle vector; constitutive active expression vector	[50]
pIVK83	plasmid containing the BGC for epifadin	This study
pTV1ts	plasmid containing Tn917 (ermR)	[47]

Oligonucleotides	Sequence (5'-3')	Purpose
83 KO Acc65I	AATGGTACCAAAATAATTTGCATTGTTT	generating upstream recombinant region for *efiTP* deletion
83 KO EcoRI	TAGAATTCATATCAGCTTAGTTATATATTA	generating upstream recombinant region for *efiTP* deletion
83 KO BssHI	AAGCGCGCATTCTTTCTTTCACATAATTTGC	generating downstream recombinant region for *efiTP* deletion
83 KO SalI	TAATGTCGACTAAAATTTCCAATTTCGG	generating downstream recombinant region for *efiTP* deletion
83 compl BamHI	AACTGGATCCAGGAAAAGAGGAAAACAATGC	generating *efiTP* genes for complementation with pRB474
83 compl EcoRI	AGAAGAATTCGTATAAATATCGGACTTATTATGTGC	generating *efiTP* genes for complementation with pRB474
Tn917 up	CTGCAATAACCGTTACCTGTTTGTGCC	Screening for Tn917 insertion site
Ptn2 down	GGCCTTGAAACATTGGTTTAGTGGG	Screening for Tn917 insertion site

Table S2 NMR signals of synthetic peptide amide FfDn-NH$_2$(2).

#	δ_H (mult., J)	δ_C	HMBC (H → #C)
1			
2	3.97 (m)	53.5	3, 4, 8
3a, 3b	2.56 (dd, 8.6, 14.2), 2.81(dd, 4.5, 14.2)	37.1	2, 4, 5, 8
4		134.9	
5	7.00 (d, 7.4)	129.4	3, 4, 5, 6, 7
6	7.23 (m)	128.4	4, 5, 7
7	7.23 (m)	127.0	4, 5, 6
8		168.3	
9	8.86 (d, 8.4)		8, 10, 11
10	4.69 (m)	54.0	11, 12, 16
11a, 11b	2.72 (dd, 10.0, 13.5), 3.00 (dd, 4.4, 14.2)	38.0	10, 12, 13, 16
12		137.3	
13	7.25 (m)	129.3	11, 12, 14, 15
14	7.26 (m)	128.1	12, 13, 15
15	7.18 (m)	126.5	12, 13, 14
16		170.8	
17	8.71 (d, 7.7)		16, 18, 19
18	4.55 (m)	49.6	16, 19, 20, 21
19a, 19b	2.62 (dd, 4.8, 16.7), 2.50 (overlapping with solvent)	36.4	18, 20, 21
20		171.7	
21		170.0	
22	8.09 (d, 8.2)		21, 23, 24
23	4.47 (m)	49.6	21, 24, 25, 27
24	2.48 (overlapping with solvent)	36.8	23, 25, 27
25		171.9	
26	6.88 (s), 7.36 (s)		24, 25
27		172.8	
28	7.08 (s), 7.11 (s)		23, 27
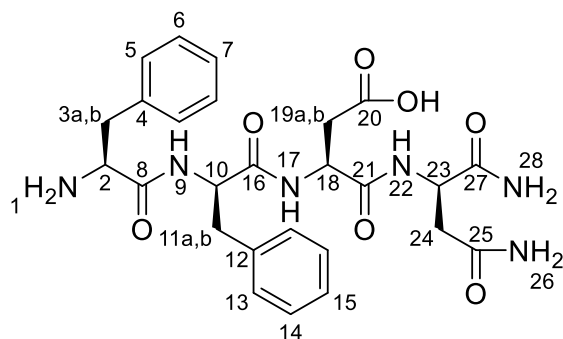
Chapter 3

Siderophore-producing commensals facilitate nasal colonization by the lugdunin-producing *Staphylococcus lugdunensis* to exclude the pathogen *Staphylococcus aureus*

Benjamin O. Torres Salazar[a,b,c], **Ralf Rosenstein**[a,b,c], **Claudia Sauer**[a,b,c], **Simon Heilbronner**[a,b,c], **Bernhard Krismer**[a,b,c] **and Andreas Peschel**[a,b,c]

[a] Department of Infection Biology, Interfaculty Institute of Microbiology and Infection Medicine, University of Tübingen, Tübingen, Germany; [b] Cluster of Excellence EXC 2124 Controlling Microbes to Fight Infections; [c] German Center for Infection Research (DZIF), partner site Tübingen

Abstract

Bacterial pathogens such as *Staphylococcus aureus* colonize body surfaces of part of the human population, which represents a critical risk factor for skin disorders and invasive infections. However, such pathogens do not belong to the human core microbiomes – beneficial 'commensal' bacteria can often prevent the persistence of certain pathogens – using molecular strategies that are only superficially understood. We recently reported that the commensal bacterium *Staphylococcus lugdunensis* produces the novel antibiotic lugdunin, which eradicates *S. aureus* from nasal microbiomes of hospitalized patients. However, it has remained unclear if *S. lugdunensis* may affect *S. aureus* carriage in the general population and how *S. lugdunensis* carriage could be promoted to enhance its *S. aureus*-eliminating capacity.

We could cultivate *S. lugdunensis* from the noses of 6.3% of healthy human volunteers. In addition, *S. lugdunensis* DNA could be identified in metagenomes of many culture-negative nasal samples indicating that cultivation success depends on a specific bacterial threshold density. *S. lugdunensis* carriers had a 5.2-fold lower propensity to be colonized by *S. aureus* indicating that lugdunin can eliminate *S. aureus* also in healthy humans. *S. lugdunensis*-positive microbiomes were dominated by either *Staphylococcus epidermidis*, *Corynebacterium* species, or *Dolosigranulum pigrum*. These and further bacterial commensals, whose abundance was positively associated with *S. lugdunensis*, promoted *S. lugdunensis* growth *in vitro*. Such mutualistic interactions depended on the production of iron-scavenging siderophores by supporting commensals, and on the capacity of *S. lugdunensis* to import siderophores.

These findings underscore the importance of microbiome homeostasis for eliminating pathogen colonization. Elucidating mechanisms that drive microbiome interactions will become crucial for microbiome-precision editing approaches.

Introduction

Host-associated microbiomes are shaped by mutualistic or antagonistic interactions among microbiome members [1, 2]. Some of these members depend on each other because they collaborate in the degradation and utilization of complex nutrient sources or the exchange of essential cofactors. These processes can be of mutual benefit for two partners or can support only one of them, which may exploit other bacterium's metabolic capacities. Interacting microorganisms can also antagonize each other directly by the release of antimicrobial bacteriocins, which inhibit major competitors to enhance the producer's fitness [3]. Such mutualistic and antagonistic mechanisms govern complex, often multi-dimensional interaction networks, which have remained largely unexplored.

Elucidating mechanisms that can promote the persistence of beneficial and impair that of harmful bacteria in microbiomes is of particular relevance for the prevention of infections caused by bacterial pathogens that use human microbiomes as their major reservoirs [4]. All of the notoriously antibiotic-resistant pathogens, vancomycin-resistant *Enterococcus faecalis* and *Enterococcus faecium*, methicillin-resistant *Staphylococcus aureus* (MRSA), and carbapenemase- or extended-spectrum betalactamase-producing *Klebsiella pneumoniae*, *Acinetobacter baumannii*, and *Escherichia coli*, can be found in the microbiomes of healthy humans or of at-risk patients [3, 4]. Carriage of such facultative antibiotic-resistant pathogens strongly increases the risk of invasive, difficult-to-treat infections. Microbiome composition has a dominant role in the capacity of pathogens to colonize, most probably as a consequence of antagonistic effects exerted by beneficial commensals [5]. However, current options for decolonization of pathogens are very limited, which demands the development of effective and specific pathogen eradication regimes, which should maintain microbiome integrity.

We recently reported that the production of bacteriocins is very frequent among commensal bacterial species of the human nasal microbiomes suggesting that such mechanisms should have a strong impact on microbiome composition and, potentially, the capacity to exclude specific pathogens [6]. Notably, many of these compounds did not or not only act against closely related species, which contradicts previous definitions of bacteriocins roles and indicates that bacteriocins are often produced to combat major competitors, irrespective of the relatedness of bacteriocin producer and target strain [3]. One of the antimicrobial molecules, the novel fibupeptide lugdunin, produced by the coagulase-negative *Staphylococcus* (CoNS) species *Staphylococcus lugdunensis*, was explored in detail [7]. Almost all of the nasal *S. lugdunensis* isolates contained the lugdunin-biosynthetic gene cluster. *S. lugdunensis* eradicated *S. aureus* in a lugdunin-dependent fashion, during cultivation in laboratory media and in animal models. Moreover, hospitalized patients carrying *S. lugdunensis* in their noses had a six-fold lower risk to be colonized by *S. aureus*. However, only 9.1% of the hospitalized patients were *S. lugdunensis* carriers, raising the question why only certain nasals microbiomes may permit the persistence of *S. lugdunensis* with its *S. aureus*-eradicating activity.

Here we describe that *S. lugdunensis* is equally rare in healthy humans as in hospitalized patients and promotes the elimination of *S. aureus* in both groups of humans. *S. lugdunensis* was positively associated with several other commensals, which were required for *S. lugdunensis* to thrive by providing essential iron-scavenging siderophores.

Results

1. *S. lugdunensis*-colonization reduces the risk of *S. aureus* carriage in healthy volunteers 5-fold

We wondered if our recent report on a strong negative correlation between nasal colonization by *S. lugdunensis* and *S. aureus* [7] might have been confounded by underlying health problems or prior antibiotic treatment in the hospitalized patients included in this group. To assess the relation between *S. lugdunensis* and *S. aureus* in non-healthcare-associated humans a cohort of 270 healthy human volunteers was analyzed for nasal carriage of one or both bacterial species. The average age was 26.7 years and 63.7% of the participants were women. Nasal swabs were plated on selective media that allowed the specific detection of either *S. aureus* or *S. lugdunensis*. The identity of representative colonies from each donor was also verified by matrix-assisted laser desorption/ionization time-of-flight mass spectroscopy (MALDI-TOF).

Table 1. *S. aureus* and *S. lugdunensis* distribution in study participants.

	S. lugdunensis-positive (female/male)	*S. lugdunensis*-negative (female/male)	Total (female/male)
S. aureus-positive	1 (0/1)	78 (49/29)	79 (49/30)
S. aureus-negative	16 (5/10)	175 (118/58)	191 (123/68)
Total	17 (5/11)	253 (167/87)	270 (172/98)
Risk of *S. aureus* carriage (%)	5.9* (0.0/9.1)	30.8* (29.3/33.3)	29.3 (28.5/30.6)

Significant differences between *S. lugdunensis*-positive and *S. lugdunensis*-negative patients were analyzed by the Chi-squared test. *P = 0.033

The *S. aureus* carriage rate was 29.3%, which is very close to that of the hospitalized patient cohort and other previous studies. 6.3% of the participants were colonized by *S. lugdunensis* (Table 1), which is slightly lower than for the hospitalized patient cohort (9.1%). Nasal carriage of *S. lugdunensis* was much higher in male (12.3%) compared to female participants (2.9%). Notably, only one of the 270 participants was colonized by both, *S. aureus* and *S. lugdunensis*, which corresponds to a 5.2-fold lower propensity of *S. lugdunensis*-positive humans to carry *S. aureus* compared to *S. lugdunensis*-negative humans. This ratio corresponds well to the 5.9-fold reduced risk of *S. lugdunensis* carriers to be colonized by *S. aureus*, reported for the hospitalized patients cohort [7]. All *S. lugdunensis* isolates from healthy volunteers contained

the lugdunin gene cluster and all *S. aureus* isolates were highly susceptible to lugdunin. Thus, the negative correlation between *S. lugdunensis* and *S. aureus* is the same in healthy and hospitalized human populations.

2. *S. lugdunensis* colonization is more frequent than estimated by nasal swab cultivation and remains largely stable over time

To analyze the dynamics of nasal *S. lugdunensis* persistence or loss the colonization status of eight carriers were monitored at four time points for a period of 23 months (probands A-H; Fig. 1a). In addition, four non-*S. lugdunensis* carriers were included as controls (probands I-L). One of the latter was a *S. aureus* carrier (proband I). In four participants (A-C, F) *S. lugdunensis* was detected at all four time points by cultivation on agar plates. In one carrier (G) *S. lugdunensis* was not detected after seven months but it reemerged after 18 and 23 months. In two (D, E) or one (H) carrier(s), *S. lugdunensis* could not be cultivated at two or three subsequent time points, respectively. Interestingly, *S. lugdunensis* could also be cultivated from the noses of all four initially negative control participants after seven months and, additionally, in the nose of one control participant (K) after 23 months (Fig. 1a). These data suggested that *S. lugdunensis* may have a moderate capacity to persist in the noses of some humans while it temporarily emerges and disappears in others.

The nasal swabs were also analyzed for viable *S. aureus* cells. One of the *S. lugdunensis* carriers (F) became a *S. lugdunensis*-*S. aureus* co-carrier at months 18 and 23 (Fig. 1a). The initial *S. aureus* carrier from the control group (I) lost its *S. aureus* carrier status at months 18 and 23 while one of the initial non-carriers (K) became and remained positive after seven months. Co-carriage of *S. aureus* and *S. lugdunensis* was observed at individual time points in two participants (I, K) of the control group.

At two time points (18 and 23 months), the colonization status was also assessed by metagenome analysis of nasal swabs. To this end, bacteria isolates from nasal swabs were disintegrated, contaminating host DNA was degraded, and the remaining DNA was amplified and shotgun sequenced on an Illumina system. An average of 30 million read pairs was obtained per sample, which were mapped to the NCBI nr protein database by DIAMOND and analyzed with the MEGAN6 algorithm. *S. lugdunensis* genome DNA was indeed found in most of the culture-positive and some additional samples (Fig. 1a) with a median relative abundance of 0.33% ranging from 0.03% to 3.37% (Suppl. Table 1). In only one of eleven culture-positive samples no *S. lugdunensis* DNA was found (Fig. 1a).
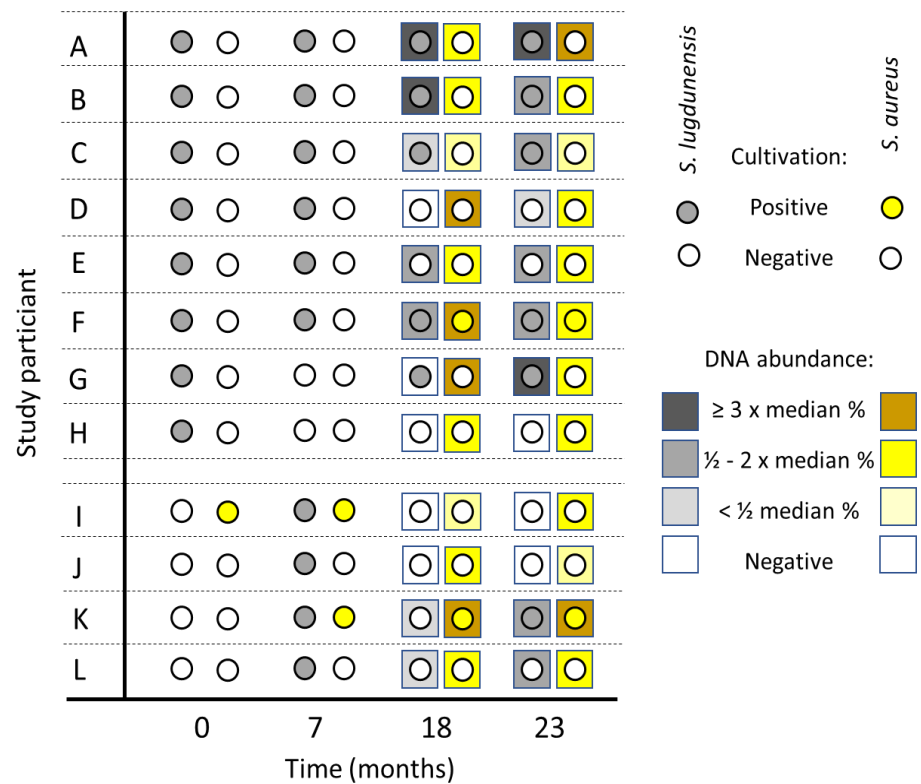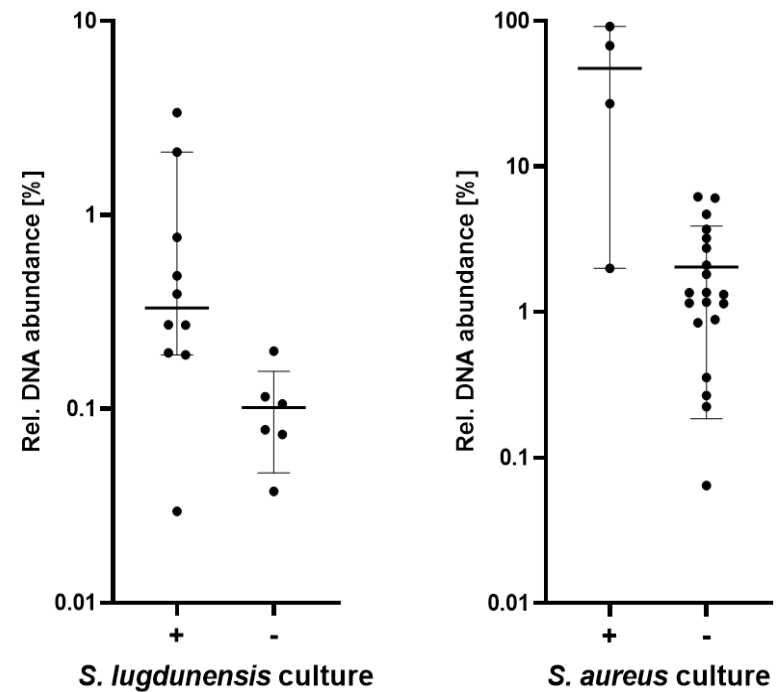
Fig. 1. Detection of *S. lugdunensis* and *S. aureus* in the nose of study participants by cultivation or metagenome analysis.

a, Culture outcomes for *S. lugdunensis* and *S. aureus* in the nasal samples that revealed corresponding reads. For each time point and each proband the culture results for *S. lugdunensis* (circles filled in grey) and *S. aureus* (circles filled in yellow) are shown (control group, samples I – J, is separated by two dashed lines). Negative culture outcome is indicated by non-coloured circles. For time points 18 and 23 months also the relative DNA abundances (= rel. proportions of reads specific for *S. lugdunensis* and *S. aureus*) in the metagenomes are indicated by colour-coded squares. The intensity of the colour shading indicates the relative DNA abundance compared to the corresponding median value of DNA abundance (see legend on the right). **b,** Relative proportions (in percent) of *S. lugdunensis* or *S. aureus* reads in microbiomes with positive or negative culture outcome. Left: relative proportions of *S. lugdunensis* reads versus culture outcome. Median of percentage for culture-positive samples: 0.33%; median of percentage for culture-negative samples: 0.09% (Mann-Whitney test, p = 0.0159). Right: relative proportions *S. aureus* reads versus culture outcome. Median of percentage for culture-positive samples: 47.27%; median of percentage for culture-negative samples: 1.34% (Mann-Whitney test, p = 0.0072). Relative read proportions are shown on the x-axes in log scale. Medians are indicated by horizontal lines with 95% confidence intervals*.

Surprisingly, *S. lugdunensis* DNA was also detected in several of the culture-negative samples, at a low median relative abundance of 0.09% (range between 0.04% and 0.20%) indicating that *S. lugdunensis* may have remained present in most of the original carriers but, occasionally, at very low numbers, which did not reach the cultivation-specific detection limit. Of the four original *S. lugdunensis* carriers who were culture-negative at one or more of the subsequent time points, three contained *S. lugdunensis* DNA even at culture-negative time points. Conversely, *S. lugdunensis* DNA was absent in the noses of two of the *S. lugdunensis* culture-negative control participants while two others contained some *S. lugdunensis* DNA with a relative abundance between 0.04% and 0.27% (the latter revealing a *S. lugdunensis*/*S.aureus* co-culture-positive state) (Fig. 1, Suppl. Table 1). Thus, *S. lugdunensis* is more frequent and colonizes human noses more consistently than estimated by swab cultivation. Samples with a positive culture outcome for *S. lugdunensis* revealed a significantly higher relative abundance of *S. lugdunensis* reads than those that were culture-negative (0.33% versus 0.09% median relative abundance, Mann-Whitney test, p=0.0159, Fig. 1b). Thus, the capacity to cultivate *S. lugdunensis* from carriers appears to depend on a threshold relative abundance in metagenomes, which probably lies somewhere between the median abundances observed for the cultivation-positive and cultivation-negative groups.

The metagenome analysis revealed similar findings for *S. aureus* as for *S. lugdunensis* - cultivation-positive samples had also high percentages of nasal *S. aureus* DNA with a median relative abundance of 47.3% (ranging from 2.0% to 91.4%) but even all culture-negative samples contained traces of *S. aureus* DNA (median relative abundance of 1.3%, ranging from 0.06% to 6.2%, Fig. 1a, Suppl. Table 1). These data suggest that *S. aureus* carriage is much higher in the human population than estimated via subcultivation of nasal swabs and that culture positivity depends on a threshold DNA abundance in metagenomes of above 2.0%. It is interesting to note that the threshold abundance for successful cultivation obviously was much higher for *S. aureus* than for *S. lugdunensis* (Fig. 1b).

The *S. lugdunensis* contigs from each consistently colonized proband (A, B, C, F and K) matched with specific S*. lugdunensis* genomes from databases of only one or two clonal complexes (CC1, CC3, CC6, CC7, or a currently undefined CC) per proband (Fig. 2) suggesting that a given human is usually colonized by one or only a few *S. lugdunensis* clones. This association remained largely the same at the two sampling times, pointing to a stable clonal distribution (samples G-2, K; see Fig. 2).
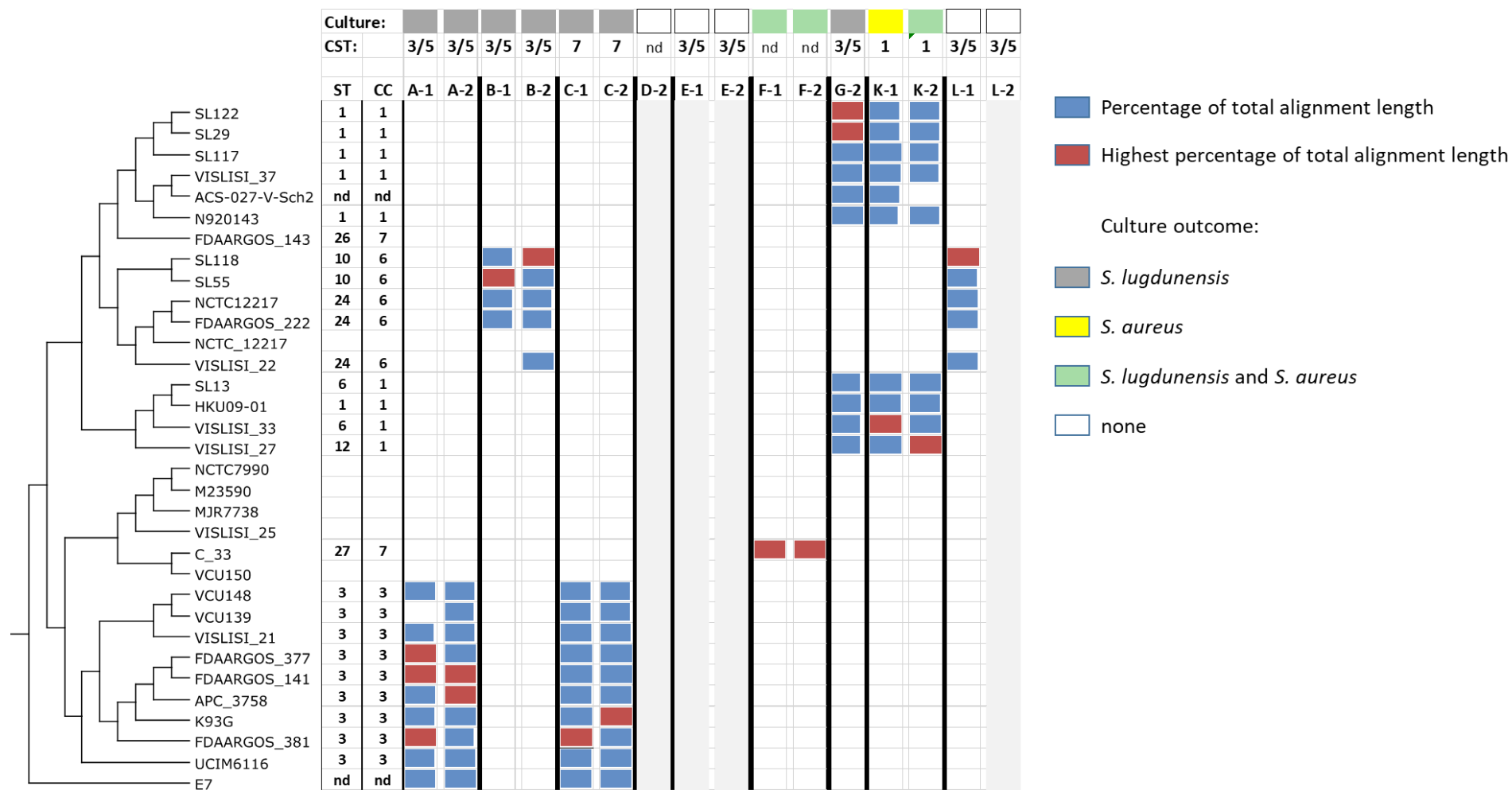
Fig. 2. *S. lugdunensis*-containing metagenomes include only one or a few *S. lugdunensis* clones.

S. lugdunensis strain profiles based on BLASTN comparisons of contigs from assembled metagenome reads with *S. lugdunensis* genome sequences. Sample numbers (1 or 2) indicate the corresponding metagenome analysis after 18 or 23 months, respectively. Blue bars represent the percentages (top 10%) of total hit alignment lengths between sample contigs and the corresponding *S. lugdunensis* strain (thresholds: 99.9% identity, 99.9% contig length in each hit alignment, only those contigs with a length of at least 250 nucleotides were considered). Red bars indicate highest percentage of total alignment length in the corresponding sample (see legend on top of right side). The phylogenetic tree of *S. lugdunensis* strains was downloaded from the NCBI database as Nexus-file and edited with Dendroscope [31]. Please note that genome data for *S. lugdunensis* NCTC12217 are presented twice in the NCBI tree as complete and as draft genome sequence. The strain profiling presented here is based on the complete genome sequence (NCTC12217). Volunteers who were tested positive as *S. lugdunensis* carriers in the accompanying culture assays are indicated by grey rectangles, co-carriers by green rectangles, *S. aureus* carriers by yellow rectangles and non-carriers by non-filled rectangles (see legend on right side). Microbiomes of the CST3/5, CST1 and CST7 types are labelled accordingly. Samples labeled with areas shaded in light grey yielded no analyzable assemblies of the *S. lugdunensis* reads. Sequence types (ST) and corresponding clonal complexes (CC) of the profiled *S. lugdunensis* strains were obtained from https://bigsdb.web.pasteur.fr/staphlugdunensis. nd, no CST or ST/CC assignment possible.

3. *S. lugdunensis* is associated with CSTs three, five, and seven

Based on the metagenome data the nasal microbiome composition of the two samples from twelve participants was elucidated and compared with the previously reported CST classification [8]. Notably, most of the metagenomes could be allocated to one of the seven CSTs (Fig. 3a, Suppl. Table 1). Most S. *lugdunensis* carriers could be assigned to CST3 or CST5 at both (participants A, B, E) or at least one time point (F, G, H), which are dominated by *S. epidermidis* or *Corynebacterium sp.*, respectively. Several of these samples changed over time from CST5 to CST3 or vice versa. The two CSTs had very similar composition and clustered in principal component analysis (Fig. 3b). The dominance by either *S. epidermidis* or *Corynebacterium sp.* appears to vary over time, suggesting that CST3 and CST5 represent dynamic states of the same CST, which we refer to as CST3/5 from now on. Participant D had undergone systemic antibiotic therapy before the first microbiome sampling time point, which was probably the reason for the unusual metagenome composition, which changed from a non-CST-classifiable microbiome composition dominated by *Streptococcus* and *Staphylococcus* to an unprecedented nasal community dominated by *Haemophilus influenceae*. The nasal microbiome of participant F was dominated by *Moraxella*, *Streptococcus*, and *Peptinophilus* and could also not be assigned to one of the known CSTs (Fig. 3a). *S. lugdunensis* associated most consistently with CST3/5 and all CST3/5 samples (except H-1) were found to contain *S. lugdunensis* genomic DNA at above-average abundances between 0.1% and 3.4% (median 0.3%) (Suppl. Table 1). The four control participants had CST7, CST1, or CST3/5, which were largely the same at the two different time points. Genomic DNA amounts in CST1, which is defined by *S. aureus* dominance, revealed very high *S. aureus* DNA abundances of 91.4 and 67.5%.

b
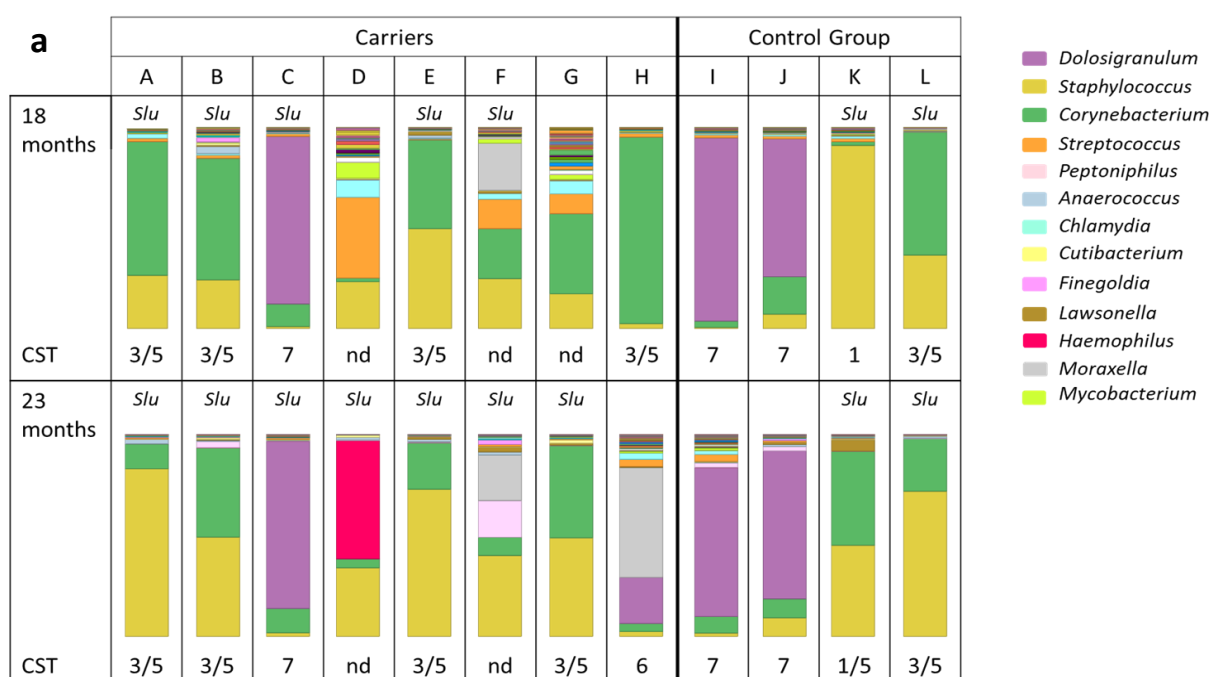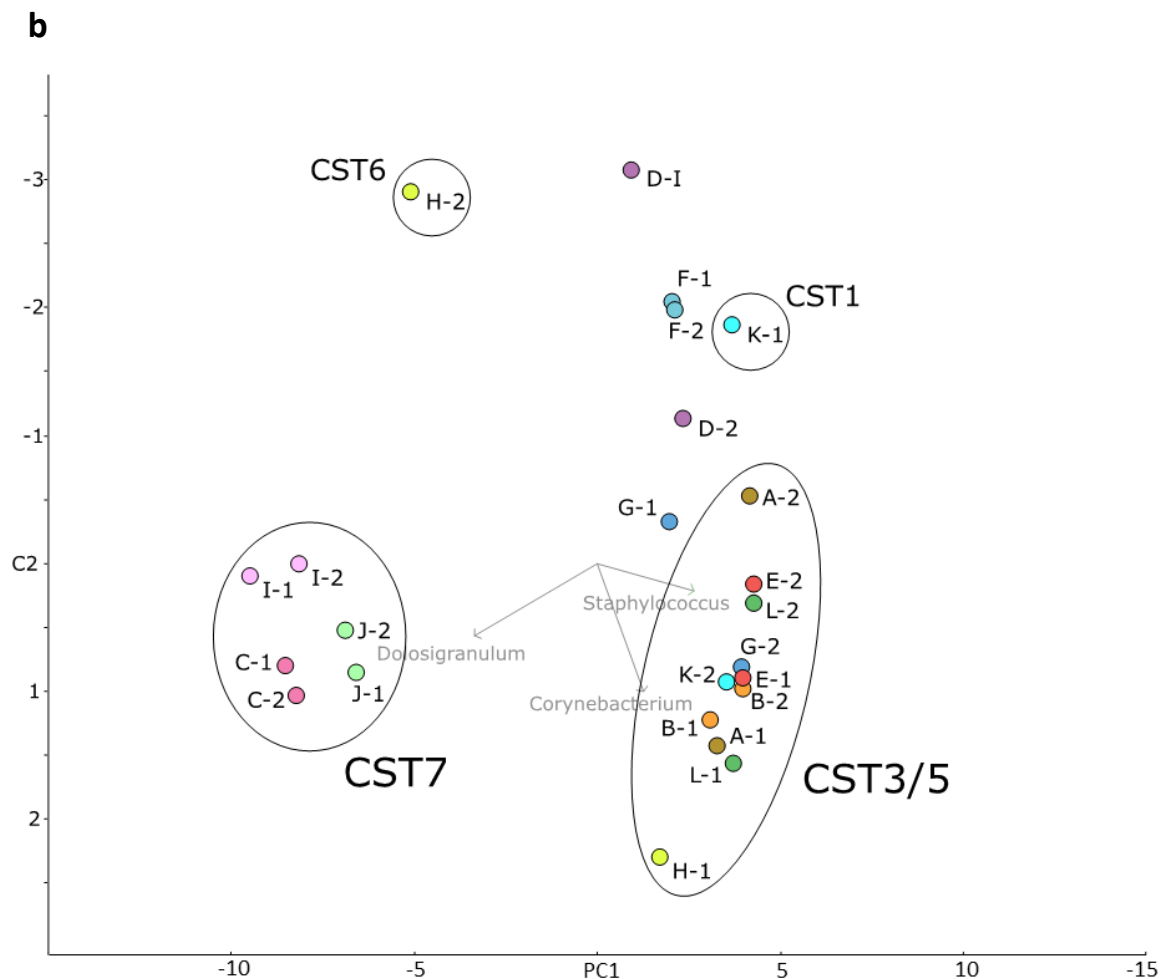
Fig. 3. Most of *the S. lugdunensis*-colonized study participants can be assigned to CST3/5 and CST7. a, Microbiome profiles at the genus level. Relative proportions of bacterial genera present in the nasal microbiomes at time points 18 months and 23 months are presented by stacked bar charts. The different bacterial genera are indicated by colours as shown in the legend on the right. The presence of *S. lugdunensis* reads in the metagenomes is indicated (*Slu*). The microbiome profiles that could be assigned to the community state types (CST) published by *Liu et al* [8] are labelled accordingly. Profiles not fitting to one of these types are designated "nd". **b,** Clustering of the microbiome genus profiles by principal coordinates analysis. Comparison of the microbiome profiles at genus level by principal coordinates analysis based on evolutionary distances according to Hellinger [22]. The data showed the highest variation along principal component 1 (PC1, 52.6%). Principal component 2 (PC2) represents a variation of 15.0%. The microbiomes are represented by coloured circles and numbers correlating with the corresponding metagenome analysis time point (-1, 18 months or -2, 23 months). Clusters representing the two main microbiome types CST3/5 and CST7 are labeled correspondingly. Vectors drawn and labeled in light grey point towards the prevalent genera in the clusters/subclusters. Note that sample K-2 clusters with the CST3/5 microbiomes but *de facto* is a CST1 due to the *Staphylococcus* proportion being mainly composed of *S. aureus*.

In addition to *S. epidermidis*, *S. lugdunensis*, and *S. aureus*, more than 50% of the metagenomes contained *Staphylococcus sciuri*, albeit at low numbers, and at least one third also traces of other CoNS such as *S. capitis* and *S. caprae* (Suppl. Fig. 1). The microbiomes contained a remarkable diversity of *Corynebacterium* species but the abundance of specific species was similar for a specific CST (Suppl. Fig. 2). CST3/5 was dominated by *Corynebacterium accolens* with lower representation by *Corynebacterium tuberculosteraricum*, *Corynebacterium diphteriae* and others (Tab. 2, Suppl. Fig. 2). In contrast, CST7 contained major amounts of genomic DNA from *Corynebacterium propinquum* and *Corynebacterium pseudodiphtheriticum* (Tab. 2, Suppl. Fig. 2). In conclusion, nasal *S. lugdunensis* carriage was associated with a high abundance of *S. epidermidis*, *C. accolens*, *C. tuberculostearicum* and, in one study participant, *D. pigrum*, *C. propinquum*, *C. pseudodiphteriticum*.

Quantitative metagenomic analysis permitted the assignment of bacterial species, which were negatively or positively correlated with the presence of *S. lugdunensis*. Based on a centered log-ratio-transformed abundance table of species reads we performed correlation network analyses with the Namap/Pearson correlation inference option of MetagenoNets [9] with tresh-

Table 2. Bacterial species dominating CST3/5- and CST7-type microbiomes.

CST3/5	%	CST7	%
Staphylococcus epidermidis	46.74	*Dolosigranulum pigrum*	89.69
Corynebacterium accolens	23.12	*Corynebacterium propinquum*	0.88
Staphylococcus aureus	2.09	*Staphylococcus epidermidis*	0.28
Corynebacterium tuberculostearicum	1.96	*Streptococcus pneumoniae*	0.62
Cutibacterium acnes	0.92	*Corynebacterium pseudodiphteriticum*	0.84
Corynebacterium diphteriae	0.87	*Staphylococcus aureus*	0.31
Corynebacterium striatum	0.78	*Mycobacterium sp.*	0.11
Corynebacterium aurimucosum	0.51	*Cutibacterium acnes*	0.13
Staphylococcus capitis	0.33	*Alloiococcus otitis*	0.15
Corynebacterium efficiens	0.32	*Alkalibacterium gilvum*	0.13
Streptococcus pneumoniae	0.28		
Staphylococcus lugdunensis	0.27		
Corynebacterium simulans	0.18		

Species that occur in all microbiomes of the indicated CST type are listed by decreasing median relative abundances ("**%**"). For the co-occurrence analysis with MEGAN6 a threshold of 0.06% relative abundance was applied.

olds for prevalence (0.1%) and occurrence (20%) (see Materials and Methods). Based on these parameters, we obtained correlation measures for 28 species throughout all 24 samples (Fig. 4, Suppl. Table 2). We observed correlation coefficients for *S. lugdunensis* ranging from -0.34 corresponding to the highest negative association with *Streptococcus pneumoniae* to +0.50, the strongest positive correlation with the *Clostridium*-related Firmicute *Finegoldia magna* (Fig. 4). Most of the species dominating ST3/5 (Table 2) were also positively associated with *S. lugdunensis*. The data also revealed a strong negative association of *S. lugdunensis* with *S. aureus* (correlation coefficient -0.22) confirming our previous studies on the competitive interplay between these species [7] (Fig. 4). Moreover, several species, which are not typical nasal colonizers found only at trace amounts were negatively associated with *S. lugdunensis*.
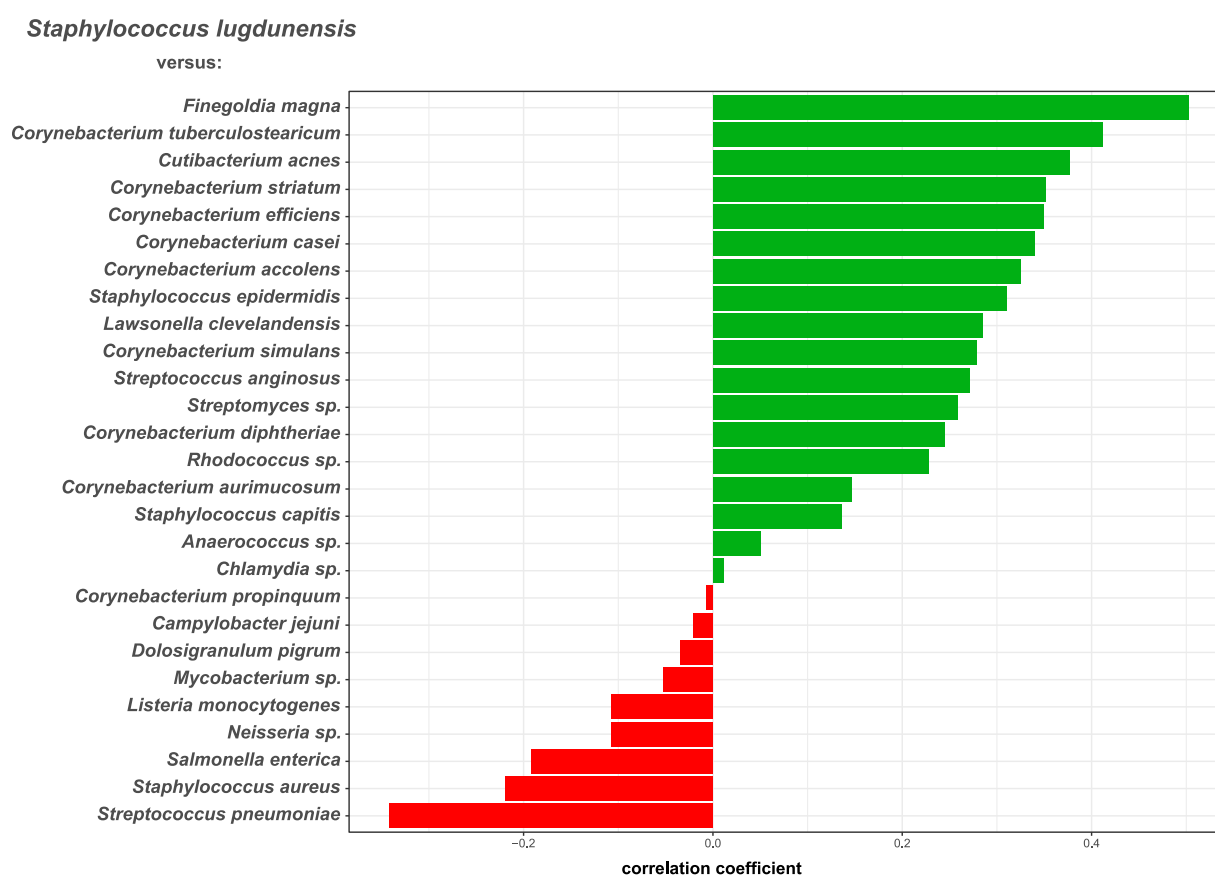
Fig. 4. Specific bacterial species are positively or negatively associated with the abundance of *S. lugdunensis* DNA in nasal metagenomes. Correlation coefficients were inferred based on a centered log-ratio-transformed abundance table of species reads by correlation network analyses using the Namap/Pearson algorithm of MetagenoNets [9] with thresholds for prevalence and occurrence of 0.1% and 20%, respectively. Based on these parameters, we obtained correlation measures for 28 species throughout all 24 samples. Shown are the associations of *S. lugdunensis* with other microbiome species (shown at the x-axis). Positive associations are indicated by green bars, negative associations by red bars. The corresponding Pearson correlation coefficients are indicated at the x-axis.

In addition to the positive association with *Corynebacterium tuberculostearicum*, several other Actinobacteria including *Cutibacterium acnes*, *Corynebacterium striatum, Corynebacterium efficiens*, and the CoNS *S. epidermidis* and *S. capitis,* showed corresponding positive correlations with *S. lugdunensis* (Fig. 4., Suppl. Table 2).

The presence and abundance of *S. aureus* metagenome reads correlated negatively with *S. lugdunensis*, and other species, which have been shown to interfere with *S. aureus* colonization, including *D. pigrum*, *C. propinquum*, *S. pneumoniae*, and *F. magna* (Suppl. Fig. 3). In contrast, positive correlations for *S. aureus* were found for the Actinobacteria *Lawsonella clevelandensis*, *Corynebacterium aurimucosum*, the CoNS *S. epidermidis* and *S. capitis*, and the *Clostridium*-related Firmicute *Anaerococcus sp.*(Suppl. Fig. 3 , Suppl. Table 2).

4. Commensals dominating the *S. lugdunensis*-positive CST3/5 or CST7 support *S. lugdunensis* growth

The positive or negative association of *S. lugdunensis* with specific microbiome members raised the question, which mechanisms might be the basis for the antagonistic or mutualistic interactions. Some of the species among the typical nasal microbiome members, which were strongly negatively associated with *S. lugdunensis*, *S. pneumoniae* and *S. aureus* (Fig. 4), were highly susceptible to lugdunin (Fig. 5), which underscores the potential capacity of lugdunin to exclude specific microbiome members from the human nasal microbiome. However, several species, which were positively associated with *S. lugdunensis*, including several coynebacterial and CoNS species, were also found to be lugdunin-susceptible, indicating that further criteria beyond the mere susceptibility to lugdunin need to be considered to explain the antagonistic interactions of *S. lugdunensis*. These might include the proximity or distance of *S. lugdunensis* to other microbiome members in a specific nasal sub-niche. It should be noted that the bacterial strains tested for susceptibility to lugdunin were representative isolates obtained from available strain collections, which might differ from strains in the nasal microbiomes of the study participants in their properties.

S. lugdunensis was positively associated with a particularly high number of nasal bacterial species (Fig. 4) raising the question how it can interact mutualistically with so many different bacteria. *S. lugdunensis* has been found to be strongly impaired in growth on iron-deprived media reflecting the nasal nutrient availability, which distinguishes *S. lugdunensis* from many other nasal bacteria. Analysis of available genomes indicated that *S. lugdunensis* is probably unable to synthesize iron-sequestering siderophores and may depend on uptake of siderophores produced by other nasal bacteria [10, 11]. This possibility was assessed by moni-
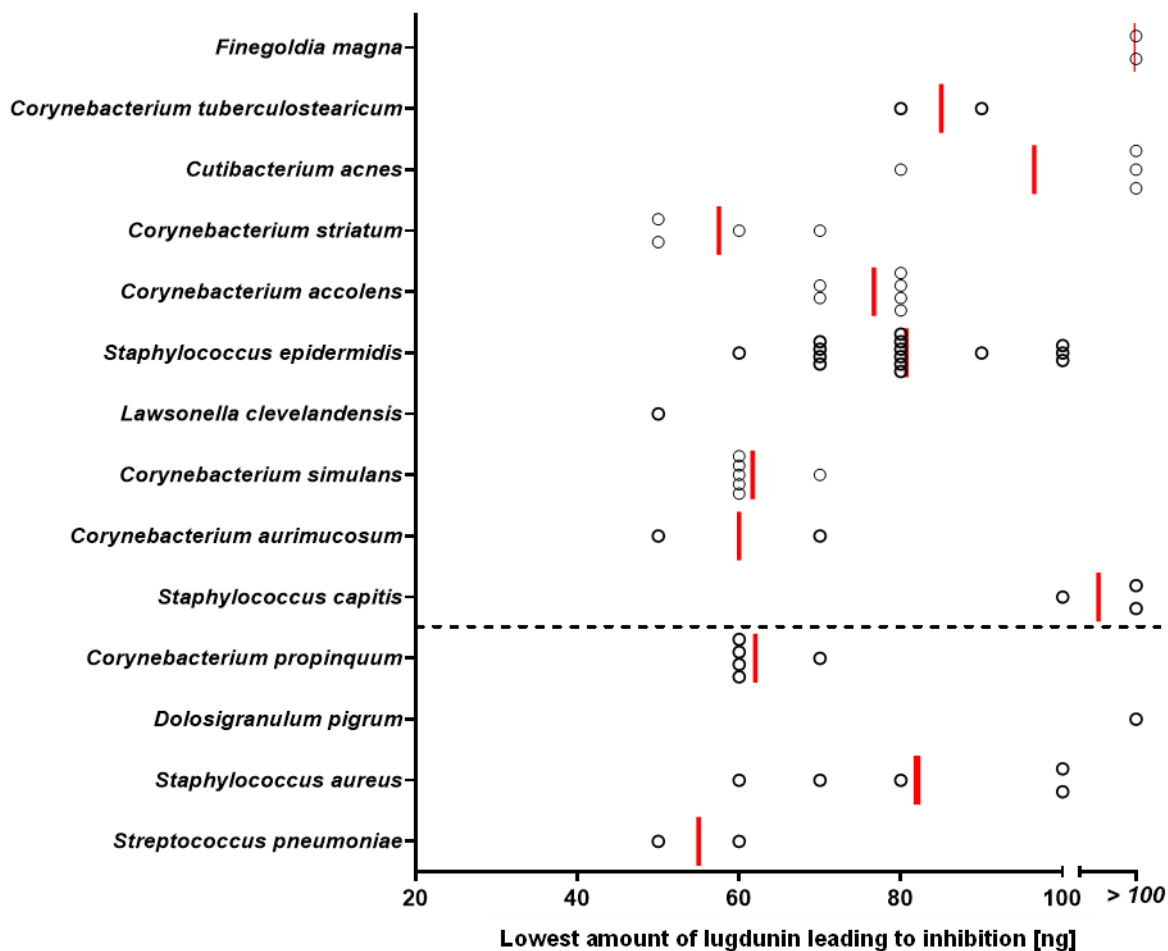
Fig. 5. Lugdunin susceptibility of typical nasal bacterial species. Different amounts of lugdunin (0 to 100 ng in 2 µl) were spotted onto lawns of nasal bacteria, resulting in zones of inhibition after incubation for 24-48 h. Data points represent average values of three independent experiments, and vertical red lines show medians of each group. The dashed line indicates the threshold of positive (above) and negative (below) correlations of nasal bacteria with *S. lugdunensis*.

toring the growth of *S. lugdunensis* on iron-deficient agar plates supplemented with culture filtrates from other nasal bacteria. Culture filtrates of *C. tuberculostearicum*, *S. epidermidis*, and *S. capitis*, which were positively associated with *S. lugdunensis* (Fig. 4), had indeed a strong growth-promoting impact on *S. lugdunensis* (Fig. 6b). However, the tested isolates of a given bacterial species differed profoundly in their impact on *S. lugdunensis* growth indicating that the mutualistic interaction with *S. lugdunensis* is probably strongly strain specific. Several of the tested isolates of other species that showed strong positive associations with *S. lugdunensis* in metagenomes did not promote *S. lugdunensis* growth. In addition, culture filtrates of *Corynebacterium propinquum* and *S. aureus*, which were weakly and strongly negatively associated with *S. lugdunensis*, respectively, also promoted *S. lugdunensis* growth (Fig. 6b).
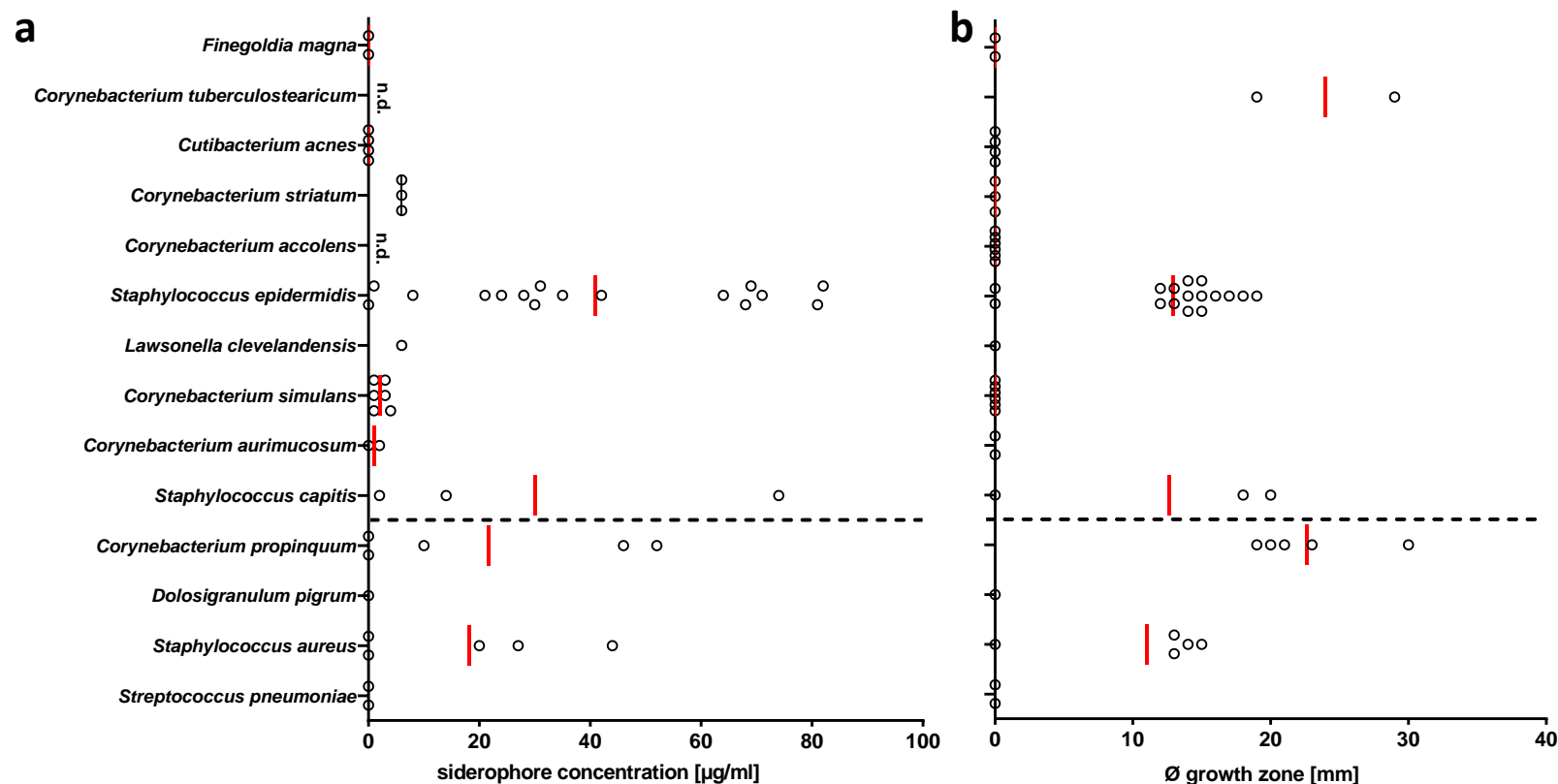
Fig. 6. Nasal bacterial species producing siderophores have the capacity to support growth of *S. lugdunensis*. a, Siderophore concentration in spent media from nasal bacteria after three days of incubation detected via SideroTec Assay™ kit. High concentrations of siderophores could be detected in spent media from staphylococcal species and *C. propinquum*; siderophore detection was not assessable for *C. accolens*, *C. aurimucosum*, and *C. tuberculostearicum* due to presence of Tween 80 in growth medium that interacts with the reaction solutions provided by the SideroTec Assay™ kit. **b,** Occurrence and sizes (diameter in mm) of growth zones of *S. lugdunensis* promoted by siderophore-containing spent media from nasal bacteria. Staphylococcal species, *C. propinquum* and *C. tuberculostearicum* support *S. lugdunensis* growth under iron-restricted conditions. Data points represent average values of three independent biological replicates, and vertical red lines show means of each species. The dashed line indicates the threshold of positive (above) and negative (below) correlations of nasal bacteria with *S. lugdunensis*. n.d. = not detectable.

To assess if the growth-promoting bacterial microbiome members may release siderophores that *S. lugdunensis* can utilize, supernatants of cultures of the test bacteria grown under iron restricted conditions were analyzed for the presence of siderophores, by a colorimetric assay. Siderophore production was found, again, to be strongly strain-dependent, with some isolates of a given species showing no or very strong siderophore release (Fig. 6a). Strongly siderophore-producing isolates were found for *C. propinquum* and *S. epidermidis* but not for most of the nasal commensals that did not support growth of *S. lugdunensis*. *C. tuberculostearicum* could not be tested in this assay because essential components in its growth medium interfered with the colorimetric siderophore detection assay.
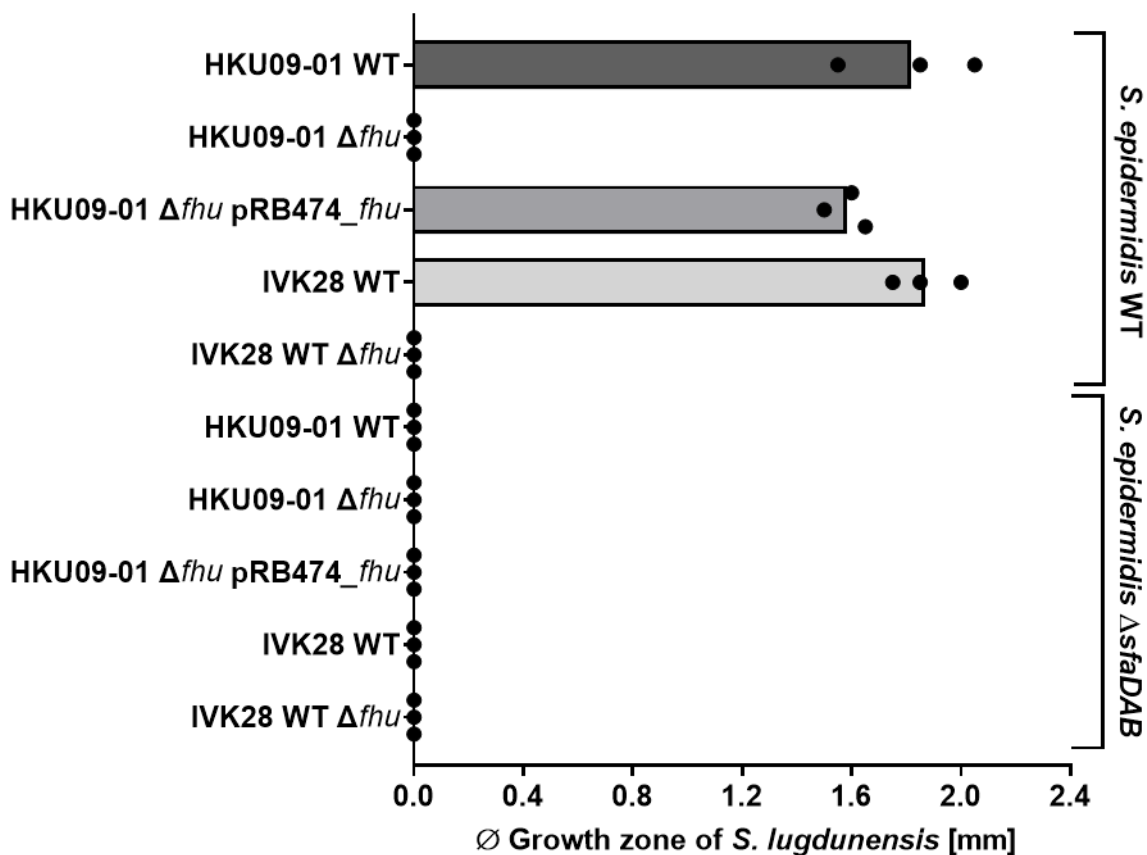
Fig. 7. *S. lugdunensis* growth promotion is *fhu*-dependent. *S. lugdunensis* HKU09-01 and IVK28 wild-type (WT), isogenic Δ*fhu* mutants and complemented strains were grown on iron-restricted agar. Growth promotion was observed only for the wild-type and the complemented strains when spent media were spotted that contained staphyloferrin A produced by *S. epidermidis* WT. Bars represent the mean of three independent experiments and black dots values of single experiments.

While *S. lugdunensis* lacks genes for siderophore synthesis, it encodes the siderophore uptake systems Hts and Sir allowing the acquisition of staphyloferrin A and B [10]. Additionally, it encodes the Fhu system recognizing hydroxamates and the Sst-system for acquisition of catechol/catecholamine type siderophores [12]. In *S. aureus* the FhuA ATPases energizes the Fhu, Hts and Sir systems [13] and the lack of additional ATPases suggest that the same is true in *S. lugdunensis*. The *fhu* operon including *fhuA* was deleted in *S. lugdunensis* HKU-09 and IVK28 and compared to the wild type for its capacity to grow in the presence of siderophore-containing culture filtrates. The *fhu* mutant was unable to grow in the presence of culture filtrates from *S. epidermidis* while the mutant complemented with plasmid-encoded copy of *fhu* grew equally well as the wild type (Fig. 7), which confirms the critical role of siderophore provision by other nasal bacteria for the capacity of *S. lugdunensis* to grow under conditions resembling the human nasal habitat.

Discussion

The human nasal microbiome is less complex but more diverse in composition than the intestinal microbiome. Why the various human CSTs are dominated by specific bacterial species and why other species are found only in certain CSTs but absent from others has remained largely unclear. Nevertheless, a recent twin-cohort study has revealed that host genetics play only a minor role [8] while the interaction among established microbiome residents appear to play key roles. Our study demonstrates that even bacterial species that can be cultivated only from a minority of human nasal microbiomes are more prevalent than previously thought when analyses are based on metagenome data. Both, *S. lugdunensis* and *S. aureus* were identified in several nasal metagenomes from noses, which were culture-negative for these species. These data corroborate previous reports on the frequent presence of *S. aureus* DNA in nasal samples that did not yield positive *S. aureus* cultures [8, 14]. They also shed new light on the human *S. aureus* carrier status, which is obviously much higher than the 30-40% previously estimated in culture-based studies. We found that the probability to cultivate *S. aureus* increased with the numbers of *S. aureus* reads in metagenomes indicating that a certain threshold number of *S. aureus* cells is necessary to achieve a positive culture. Bacterial numbers may change over time, which might explain the volatile *S. aureus* intermediate carrier state, characterized by a repeated change between culture-negative and culture-positive conditions with only low *S. aureus* counts per nare. Very low numbers of *S. aureus* may not increase the risk of an at-risk patient to develop an invasive *S. aureus* infection. Even very low *S. aureus* numbers may be of high relevance though if it is an MRSA strain that might spread to other patients on a hospital ward and may elicit MRSA outbreaks. Future pathogen monitoring approaches should therefore not only rely on bacterial cultures but also

on the analysis of metagenome data to identify even low numbers of notorious pathogens and their antibiotic resistance genes.

Several studies have been published with a focus on the bacterial competition in the human anterior nares [15-17]. Besides the lugdunin-dependent antagonism between *S. lugdunensis* and *S. aureus*, a wealth of information has been gathered describing the interplay with nasal microbiome members that mainly belong to the phyla *Actinobacteria* and *Firmicutes*. The results of our correlation analyses confirm previously described associations between *Corynebacterium*, *Staphylococcus*, *Cutibacterium, Dolosigranulum,* and *Streptococcus* species in the anterior nares [17]. We observed a negative association of *C. accolens* with *S. pneumoniae* (correlation coefficient -0.28) corresponding to their described antagonism [15]. Furthermore, we saw also the recently described correlations of *D. pigrum* with nasal microbiome species [16] reflected in our data: *D. pigrum* revealed strong positive correlations with *C. pseudodiphteriticum* (correlation coefficient +0.69, not shown in Suppl. Table 2 since correlation calculation was done with a deviating prevalence threshold of 0.001%) and *C. propinquum* (correlation coefficient +0.66) and was inversely correlated with *S. aureus* (correlation coefficient -0.41) (Suppl. Table 2).

With microbiome precision editing approaches it could become possible to eliminate *S. aureus* from the noses of at-risk patients or at least to reduce its numbers strongly enough to keep infection risks to a minimum. Finding a way to establish colonization by sufficiently high numbers of *S. lugdunensis* could become a sustainable way of preventing *S. aureus* infections. We provide evidence that *S. lugdunensis* is auxotrophic for iron-scavenging siderophores and may need other microbiome members that release siderophores, which act as common goods to support not only the producer but also other bacteria that have cognate siderophore uptake systems. The available *S. lugdunensis* genomes all lack siderophore-biosynthetic genes but they encode ABC transporters with clear homology to uptake systems for carboxylate, hydroxamate and catechol/catecholamine siderophores [10, 12]. Interestingly, *C. propinquum*, which supported *S. lugdunensis* growth under iron-limiting conditions bear genes for synthesis of a dehydroxynocardamine siderophore [18]. The capacities of different isolates of *S. epidermidis*, *S. hominis*, *S. capitis*, *S. aureus* to support *S. lugdunensis* growth was highly strain-dependent, which may point to either substantial differences in the presence of such genes or in their expression levels.

Several of the positively with *S. lugdunensis*-correlated bacterial species did not support growth of *S. lugdunensis*. It is possible that the strains in the corresponding nasal microbiomes differed from our test strains in the presence of siderophore genes. On the other hand, some of the positive associations may result from higher-order interactions in larger bacterial networks with network members supporting other bacteria that were able to secrete

siderophores. Understanding and harnessing such mechanism will allow innovative strategies for pathogen exclusion form human microbiomes in particular in at-risk patients. *S. lugdunensis* could be engineered to produce its own siderophores or other nasal 'probiotics' strains producing siderophores for *S. lugdunensis* could become valuable for prevention of *S. aureus* infections.

Materials and Methods

Bacterial strains and media. Bacterial strains used in this study are summarized in Suppl. Table 3. All bacteria were grown on basic medium (BM; 1% soy peptone, 0.5% yeast extract, 0.5% NaCl, 0.1% glucose and 0.1% K_2HPO_4, pH 7.2) which was supplemented with 5% sheep blood (Oxoid) and 1.5% agar (BD European Agar) if needed. *C. acnes* and *L. clevelandensis* were incubated under anerobic conditions using an anaerobic jar and AnaeroGen™ (Thermo). For the phenotypic identification of *Staphylococcus lugdunensis*, *S. aureus* and other staphylococcal species in nasal swabs, basic medium (BM), blood agar and selective agar SSL [19] were used. For the siderophore experiments, bacteria were grown in E-BHI, composed of brain heart infusion medium (BHI; Roth) supplemented with 10 µM of the iron chelator ethylenediamine-di(o-hydroxyphenylacetic acid) (EDDHA; LGC Standards GmbH), for 72 h at 37°C and constant shaking at 160 rpm. For transformation experiments with *E. coli* DC10B and *S. lugdunensis*, tryptic soy broth (TSB; Oxoid) or tryptic soy agar (TSA) were used and, when necessary, supplemented with antibiotics at concentrations of 10 µg/ml chloramphenicol (Sigma-Aldrich), 100 µg/ml ampicillin (Roth) and 1 µg/ml anhydrotetracycline (Fluka).

Human volunteer selection, nasal swabbing, and detection of *S. lugdunensis* and *S. aureus*. Samples from 270 healthy volunteers of the University of Tübingen were collected by swabbing both nares with cotton swabs and suspending them in 1ml phosphate buffered saline (PBS). Various dilutions of each sample were plated on complex medium agar (basic medium, BM), blood agar and selective *S. lugdunensis* medium agar (SSL) [19] for phenotypic identification of *S. lugdunensis*, *S. aureus* and other staphylococcal species. The plates were incubated for 24 to 48 h at 37°C under aerobic and anaerobic conditions, respectively. The bacterial identity was evaluated by matrix-assisted laser desorption/ionization-time-of-flight mass spectrometry (mass spectrometer: AXIMA Assurance, Shimadzu Europa GmbH, Duisburg, database: SARAMIS with 23.980 spectra and 3.380 superspectra, BioMérieux, Nürtingen).

Metagenome sequencing of nasal microbiome samples. Nasal microbiome samples were taken from individuals by swabbing both nares successively with one nylon-flocked E-Swab

(ThermoFisher Scientific) and suspending them in 1 ml Amies transport medium. Two replicate swabs were consecutively taken per volunteer. For degradation of contaminating host DNA and subsequent preparation of bacterial DNA, the suspended samples were mixed with AHL-buffer and treated with the QIAamp DNA Microbiome Kit (Qiagen) according to the manufacturer's instructions. Finally, DNA was eluted from the spin columns in 50 µl AVE-buffer. DNA concentration was determined with Qubit 3.0 (Thermo Fisher Scientific) using High Sensitivity (HS) reagents for low DNA concentrations. 2.5 µl of the preparation was used for whole genome amplification with REPLI-g Single Cell Kit (Qiagen). Subsequently, the amplified DNA was purified with Genomic DNA Clean & Concentrator (Zymo Research) and the final DNA concentration was determined with Qubit 3.0.

About 10 µg of the purified DNA was used for next generation sequencing by GATC (Konstanz, Germany). In brief, libraries of fragments of ca. 400 bases were prepared and submitted to Illumina paired-end sequencing with read lengths of 150 bases. After quality-filtering, an average of 30 million read pairs was obtained per sample and provided as compressed fastq.gz file (separate files for each end of the sequenced inserts).

In the first metagenome analysis (after 18 months) we obtained a median of 70.13 million quality-filtered, paired-end reads per sample. In the second metagenome analysis (after 23 months), a median of 52.71 million reads per sample were obtained. Despite taking measures to reduce the proportion of human DNA in the samples we found varying percentages of metagenomic reads mapping to the human DNA reference database: at the first time point (18 months), human-derived reads ranged from 14.4% to 94.3% (median: 74.75%) per sample while at time point 2 (23 months) between 0.5% and 90.9% (median: 28.15%) of the reads mapped to sequences from the hg19 database. At time point 1, a median of 11.45 million bacterial reads per sample (sample D had exceptionally low read numbers due to antibiotic treatment and was left out as an outlier) were obtained, while at the second time point the median of bacterial reads was 21.81 million.

Bioinformatics. The sequence reads from each file were mapped against the NCBI non-redundant (nr) protein database by using the optimized BLASTX algorithm of DIAMOND [20]. For the subsequent functional and taxonomic analysis with MEGAN6 [21], the DIAMOND alignment files were "meganized" by combining the paired-end sequences for each sample and providing them with functional annotations. Taxonomic binning, functional analysis and statistical analyses were performed by using the corresponding functions of MEGAN6. For the comparison of the metagenomes on the genus level, pairwise distances were calculated based on ecological distance according to Hellinger [22].

To exploit the genetic information obtained with the metagenome sequence reads we attempted to be assembled the species-specific reads into larger contiguous sequences. To this end, we used the MetaSpades tool, which is implemented in the SPADES assembler [23]. For species-specific read-assemblies, we first used MEGAN6 to extract the reads assigned to the species of interest as a Fasta file. Then we used MetaSpades to assemble these reads into contigs

In order to determine the *S. lugdunensis* strains that reside in the anterior nares of the carriers we selectively extracted the *S. lugdunensis* reads where possible and assembled them into contigs. The contigs were compared with a database composed of *S. lugdunensis* genome sequences by BlastN and the genomes getting the highest number of hits were regarded as the closest relative(s) to the strains present in the *S. lugdunensis* carriers. Thus, we obtained strain profiles based on the total alignment lengths of hits mapped to a phylogenetic tree of *S. lugdunensis* strains (Fig. 2).

Correlation assays were performed by network analysis with the web-based tool MetagenoNets, (https://web.rniapps.net/metanets/; [9]). For that, an abundance table with read numbers of the bacterial species in the samples was uploaded to MetagenoNets. The abundance data were transformed to centered log-ratios, filtered for a prevalence (minimum proportion of reads in samples) of 0.1 % and an occurrence (minimum percentage of samples showing the species) of 20%. Network inference was calculated by NAMAP (a modified ReBoot method; [24, 25]) based on Pearson correlation coefficients. The results were downloaded as correlation matrix, imported into R [26] using the package corrr [27] and visualized with the R package ggplot2 [28].

Siderophore production and detection. Bacterial strains were incubated on BM blood agar plates for 24 h to 48 h at 37°C. Subsequently, bacterial material was scratched from the plates, washed once with E-BHI medium, adjusted to an optical density at 600 nm (OD_{600}) of 0.05 and incubated in 1 ml E-BHI for 72 h at 37°C and constant shaking at 160 rpm in 24 well plates. In case of *C. accolens, C. tuberculostearicum, C. aurimucosum* and *C. kroppenstedtii*, the medium was additionally supplemented with 0.4% Tween80 (Sigma-Aldrich); *C. acnes and L. clevelandensis* were incubated in 1.5 ml Eppendorf tubes to minimize gas exchange with atmospheric oxygen; *D. pigrum* was incubated with 10% sterile-filtered spent medium of *C. accolens* to enhance growth [29] After 72 h of incubation, the OD_{600} was determined, the bacterial cultures were centrifuged and the supernatants were sterile filtered using 0.22 μm filter (Millex) to obtain the spent media. In order to quantify siderophore concentrations in the spent media, a siderophore detection kit (SideroTec Assay™ from Emergen Bio) was used according to the manufacturer's instructions with small alterations; instead of 100 μl samples,

50 µl samples were used and mixed with 50 µl Chelex treated MilliQ-purified H_2O in order to reduce background signals of the medium.

Analysis of growth support for S. *lugdunensis* under iron-restriction by xenosiderophores produced by nasal bacteria. In order to generate iron-restricted BHI agar plates, 2x BHI was treated with Chelex 100 resin (Sigma-Aldrich) for 24 h at 4°C and supplemented with 40 µM EDDHA. After sterile filtration, the medium was heated to 50°C and mixed 50:50 with 2x agar (50°C) containing 20% complement-inactivated horse serum (10% final concentration) (Sigma-Aldrich) to provide an iron source with complexed iron. Freshly grown *S. lugdunensis* was picked from blood agar plates, washed once with 1x phosphate buffered saline (PBS, Gibco), adjusted to an OD_{600} of 0.5 and streaked evenly onto the BHI agar plates. To evaluate the growth support for *S. lugdunensis* by the siderophore-containing spent media, 10 µl aliquots were spotted on previously plated *S. lugdunensis* cells as follows: Dependent on the endpoint OD_{600} of each culture, different volumes of spent medium were taken and mixed, if necessary, with fresh E-BHI to a final volume of 10 µl (for instance, from a culture with an endpoint OD_{600} of 0.2, 10 µl spent medium was taken whereas from a culture with an endpoint OD_{600} of 2.0, 1 µl spent medium was taken and mixed with 9 µl E-BHI medium). After spotting 10 µl of each spent medium, the plates were incubated for 20 h at 37°C. If the spent media contained siderophores that could promote growth of *S. lugdunensis*, zones of enhanced growth appeared that were characterized according to their diameters.

Generation and complementation of *S. lugdunensis* and *S. epidermidis* mutants. For the construction of *S. lugdunensis* and *S. epidermidis* mutants the thermosensitive plasmid pIMAY [30] and the primers listed in Suppl. Table 4 were used. Targeted mutagenesis was performed as described in [30]. In brief, 500 bp DNA fragments up- and downstream of the ferric hydroxamate uptake (*fhu*) gene locus for *S. lugdunensis* and of the staphyloferrin A biosynthetic genes (*sfaDAB*) for *S. epidermidis* were amplified by PCR using the corresponding primers ((1)/(2) and (3)/(4) for *fhu* knockout, (9)/(10) and (11)/(12) for *sfaDAB* knockout). The resulting PCR products contained overlapping sequences which facilitated hybridization in order to construct the gene deletion sequence. This DNA sequence was inserted into pIMAY, digested via *SacI*/*KpnI* (Thermo) for *fhu* knockout and via *SalI/SacI* (Thermo) for *sfaDAB* knockout, using Gibson assembly (New England BioLabs) according to the manufacturer's instructions. After transformation of *E. coli* DC10B and isolation of the plasmid construct, *S. lugdunensis* or *S. epidermidis* were transformed via electroporation and incubated at 30°C in TSB with 10 µg/ml chloramphenicol. Selection for plasmid integration into the chromosome was performed at 37°C in TSB with 10 µg/ml chloramphenicol, and positive integration clones were subsequently grown at 30°C without chloramphenicol to promote excision of the plasmid. The loss of plasmid was selected on TSA containing 1 µg/ml

anhydrotetracycline and correct *S. lugdunensis* Δ*fhu* or *S. epidermidis* Δ*sfaDAB* knock out clones were confirmed by chloramphenicol susceptibility testing and PCR (primers (5)/(6) for Δ*fhu*, (13)/(14) for Δ*sfaDAB)*.

For complementation in *S. lugdunensis*, primers (7)/(8) were used to amplify the wild type *fhu* gene. The DNA was inserted into *Sal*I/*Xba*I digested pRB474 using Gibson assembly and transformed into *E. coli* DC10B. Subsequently, the complementation plasmid pRB474_*fhu* was transformed into *S. lugdunensis* Δ*fhu*. Chloramphenicol resistant transformants were sub-cultured and correct complementation constructs were confirmed via PCR using primers (15)/(16).

References

1.   Figueiredo ART, Kramer J. Cooperation and Conflict Within the Microbiota and Their Effects On Animal Hosts. Frontiers in Ecology and Evolution. 2020;8(132). doi: 10.3389/fevo.2020.00132.

2.   Otto M. Staphylococci in the human microbiome: the role of host and interbacterial interactions. Current Opinion in Microbiology. 2020;53:71-7. doi: https://doi.org/10.1016/j.mib.2020.03.003.

3.   Heilbronner S, Krismer B, Brötz-Oesterhelt H, Peschel A. The microbiome-shaping roles of bacteriocins. Nat Rev Microbiol. 2021. Epub 2021/06/03. doi: 10.1038/s41579-021-00569-w. PubMed PMID: 34075213.

4.   Tacconelli E, Sifakis F, Harbarth S, Schrijver R, van Mourik M, Voss A, et al. Surveillance for control of antimicrobial resistance. Lancet Infect Dis. 2018;18(3):e99-e106. Epub 2017/11/06. doi: 10.1016/s1473-3099(17)30485-1. PubMed PMID: 29102325.

5.   Tacconelli E, Autenrieth IB, Peschel A. Fighting the enemy within. Science. 2017;355(6326):689-90. Epub 2017/02/18. doi: 10.1126/science.aam6372. PubMed PMID: 28209857.

6.   Janek D, Zipperer A, Kulik A, Krismer B, Peschel A. High Frequency and Diversity of Antimicrobial Activities Produced by Nasal Staphylococcus Strains against Bacterial Competitors. PLoS Pathog. 2016;12(8):e1005812. doi: 10.1371/journal.ppat.1005812. PubMed PMID: 27490492; PubMed Central PMCID: PMCPMC4973975.

7.   Zipperer A, Konnerth MC, Laux C, Berscheid A, Janek D, Weidenmaier C, et al. Human commensals producing a novel antibiotic impair pathogen colonization. Nature. 2016;535(7613):511-6. doi: 10.1038/nature18634. PubMed PMID: 27466123.

8.   Liu CM, Price LB, Hungate BA, Abraham AG, Larsen LA, Christensen K, et al. Staphylococcus aureus and the ecology of the nasal microbiome. Sci Adv. 2015;1(5):e1400216. Epub 2015/11/26. doi: 10.1126/sciadv.1400216. PubMed PMID: 26601194; PubMed Central PMCID: PMCPMC4640600.

9.   Nagpal S, Singh R, Yadav D, Mande SS. MetagenoNets: comprehensive inference and meta-insights for microbial correlation networks. Nucleic Acids Res. 2020;48(W1):W572-W9. doi: 10.1093/nar/gkaa254. PubMed PMID: 32338757; PubMed Central PMCID: PMCPMC7319469.

10.   Brozyna JR, Sheldon JR, Heinrichs DE. Growth promotion of the opportunistic human pathogen, Staphylococcus lugdunensis, by heme, hemoglobin, and coculture with Staphylococcus aureus. Microbiologyopen. 2014;3(2):182-95. doi: 10.1002/mbo3.162. PubMed PMID: 24515974; PubMed Central PMCID: PMCPMC3996567.

11.   Sheldon JR, Heinrichs DE. The iron-regulated staphylococcal lipoproteins. Front Cell Infect Microbiol. 2012;2:41. doi: 10.3389/fcimb.2012.00041. PubMed PMID: 22919632; PubMed Central PMCID: PMCPMC3417571.

12.   Lebeurre J, Dahyot S, Diene S, Paulay A, Aubourg M, Argemi X, et al. Comparative Genome Analysis of Staphylococcus lugdunensis Shows Clonal Complex-Dependent Diversity of the Putative Virulence Factor, ess/Type VII Locus. Front Microbiol. 2019;10:2479. doi: 10.3389/fmicb.2019.02479. PubMed PMID: 31736914; PubMed Central PMCID: PMCPMC6834553.

13.   Sheldon JR, Heinrichs DE. Recent developments in understanding the iron acquisition strategies of gram positive pathogens. FEMS Microbiol Rev. 2015;39(4):592-630. doi: 10.1093/femsre/fuv009. PubMed PMID: 25862688.

14.   Cole AL, Sundar M, Lopez A, Forsman A, Yooseph S, Cole AM. Identification of Nasal Gammaproteobacteria with Potent Activity against Staphylococcus aureus: Novel Insights into the "Noncarrier" State. mSphere. 2021;6(1). doi: 10.1128/mSphere.01015-20. PubMed PMID: 33408227; PubMed Central PMCID: PMCPMC7802429.

15.   Bomar L, Brugger SD, Yost BH, Davies SS, Lemon KP. Corynebacterium accolens Releases Antipneumococcal Free Fatty Acids from Human Nostril and Skin Surface Triacylglycerols. mBio. 2016;7(1):e01725-15. doi: 10.1128/mBio.01725-15. PubMed PMID: 26733066; PubMed Central PMCID: PMCPMC4725001.

16.   Brugger SD, Eslami SM, Pettigrew MM, Escapa IF, Henke MT, Kong Y, et al. Dolosigranulum pigrum Cooperation and Competition in Human Nasal Microbiota. mSphere. 2020;5(5). doi: 10.1128/mSphere.00852-20. PubMed PMID: 32907957; PubMed Central PMCID: PMCPMC7485692.

17.   Hardy BL, Merrell DS. Friend or Foe: Interbacterial Competition in the Nasal Cavity. J Bacteriol. 2021;203(5). doi: 10.1128/JB.00480-20. PubMed PMID: 33077632; PubMed Central PMCID: PMCPMC7890553.

18.   Stubbendieck RM, May DS, Chevrette MG, Temkin MI, Wendt-Pienkowski E, Cagnazzo J, et al. Competition among Nasal Bacteria Suggests a Role for Siderophore-Mediated Interactions in Shaping the Human Nasal Microbiota. Appl Environ Microbiol. 2019;85(10). doi: 10.1128/AEM.02406-18. PubMed PMID: 30578265; PubMed Central PMCID: PMCPMC6498180.

19.   Ho PL, Leung SM, Tse H, Chow KH, Cheng VC, Que TL. Novel selective medium for isolation of Staphylococcus lugdunensis from wound specimens. J Clin Microbiol. 2014;52(7):2633-6. doi: 10.1128/JCM.00706-14. PubMed PMID: 24759715; PubMed Central PMCID: PMCPMC4097709.

20.   Buchfink B, Xie C, Huson DH. Fast and sensitive protein alignment using DIAMOND. Nat Methods. 2015;12(1):59-60. Epub 2014/11/18. doi: 10.1038/nmeth.3176. PubMed PMID: 25402007.

21.   Huson DH, Beier S, Flade I, Gorska A, El-Hadidi M, Mitra S, et al. MEGAN Community Edition - Interactive Exploration and Analysis of Large-Scale Microbiome Sequencing Data. PLoS Comput Biol. 2016;12(6):e1004957. Epub 2016/06/22. doi: 10.1371/journal.pcbi.1004957. PubMed PMID: 27327495; PubMed Central PMCID: PMCPMC4915700.

22.   Mitra S, Gilbert JA, Field D, Huson DH. Comparison of multiple metagenomes using phylogenetic networks based on ecological indices. ISME J. 2010;4(10):1236-42. Epub 2010/04/30. doi: 10.1038/ismej.2010.51. PubMed PMID: 20428222.

23.   Nurk S, Meleshko D, Korobeynikov A, Pevzner PA. metaSPAdes: a new versatile metagenomic assembler. Genome Res. 2017;27(5):824-34. Epub 2017/03/17. doi: 10.1101/gr.213959.116. PubMed PMID: 28298430; PubMed Central PMCID: PMCPMC5411777.

24.   Faust K, Sathirapongsasuti JF, Izard J, Segata N, Gevers D, Raes J, et al. Microbial co-occurrence relationships in the human microbiome. PLoS Comput Biol.

2012;8(7):e1002606. doi: 10.1371/journal.pcbi.1002606. PubMed PMID: 22807668; PubMed Central PMCID: PMCPMC3395616.

25.   Yadav D, Ghosh TS, Mande SS. Global investigation of composition and interaction networks in gut microbiomes of individuals belonging to diverse geographies and age-groups. Gut Pathog. 2016;8:17. doi: 10.1186/s13099-016-0099-z. PubMed PMID: 27158266; PubMed Central PMCID: PMCPMC4858888.

26.   Team RC. R: A Language and Environment for Statistical Computing. R Foundation for Statistical Computing; 2020.

27.   Cimentada MKaSJaJ. corrr: Correlations in R. R package version 0.4.2 ed2020.

28.   Wickham H. ggplot2: Elegant Graphics for Data Analysis. Springer-Verlag New York; 2016.

29.   Brugger SD, Eslami SM, Pettigrew MM, Escapa IF, Henke MT, Kong Y, et al. Dolosigranulum pigrum cooperation and competition in human nasal microbiota. bioRxiv. 2020:678698. doi: 10.1101/678698.

30.   Monk IR, Shah IM, Xu M, Tan MW, Foster TJ. Transforming the untransformable: application of direct transformation to manipulate genetically Staphylococcus aureus and Staphylococcus epidermidis. mBio. 2012;3(2). doi: 10.1128/mBio.00277-11. PubMed PMID: 22434850; PubMed Central PMCID: PMCPMC3312211.

31.   Huson DH, Scornavacca C. Dendroscope 3: an interactive tool for rooted phylogenetic trees and networks. Syst Biol. 2012;61(6):1061-7. doi: 10.1093/sysbio/sys062. PubMed PMID: 22780991.

32.   Kaspar U, Kriegeskorte A, Schubert T, Peters G, Rudack C, Pieper DH, et al. The culturome of the human nose habitats reveals individual bacterial fingerprint patterns. Environ Microbiol. 2016;18(7):2130-42. doi: 10.1111/1462-2920.12891. PubMed PMID: 25923378.

33.   Lemon KP. Personal communication. 2018.

34.   Diep BA, Otto M. The role of virulence determinants in community-associated MRSA pathogenesis. Trends Microbiol. 2008;16(8):361-9. doi: 10.1016/j.tim.2008.05.002. PubMed PMID: 18585915; PubMed Central PMCID: PMCPMC2778837.

35.   Tse H, Tsoi HW, Leung SP, Lau SK, Woo PC, Yuen KY. Complete genome sequence of Staphylococcus lugdunensis strain HKU09-01. J Bacteriol. 2010;192(5):1471-2. doi: 10.1128/JB.01627-09. PubMed PMID: 20047907; PubMed Central PMCID: PMCPMC2820864.

36.   Bruckner R. A series of shuttle vectors for Bacillus subtilis and Escherichia coli. Gene. 1992;122(1):187-92. doi: 10.1016/0378-1119(92)90048-t. PubMed PMID: 1452028.

Supplemental Data

Supplemental Tables

Suppl. Table. 1. Comparison of metagenome data with community state types (CST). Relative proportions (in percent) of selected taxa that had been described as indicators for community state types (CST) as described in [8]. Most abundant taxa are highlighted in bold. Round (1 or 2) indicates the corresponding time of metagenome analysis after 18 months or 23 months, respectively. CST: classification into designated CST types as indicated according to the prevalence of indicator taxa in the microbiomes or none if not determinable (nd). CST6 for sample H-2 was based on a relative proportion of 54.4 % *Moraxella* (not listed). For *S. lugdunensis* the corresponding relative DNA abundances are also shown (in percent). The culture-based carrier states determined in parallel to the metagenome sequencing are indicated under "Culture": Slu, *S. lugdunensis* carrier; Sau, *S. aureus* carrier; co, co-carrier; non, non-carrier.

Sample	Round	*Corynebacterium*	*S. epidermidis*	*S. aureus*	*Dolosigranulum*	CST	*S. lugdunensis*	Culture
A	1	**67.2**	21.6	3.7	0.0	**3/5**	2.11	Slu
	2	12.4	**69.3**	4.7	0.0	**3/5**	0.77	Slu
B	1	**60.4**	14.3	0.9	0.0	**3/5**	0.49	Slu
	2	**44.3**	37.7	1.4	0.0	**3/5**	0.27	Slu
C	1	11.2	0.2	0.2	**83.3**	**7**	0.03	Slu
	2	12.0	0.3	0.1	**82.9**	**7**	0.19	Slu
D	1	3.6	7.3	6.2	0.0	nd	0.00	non
	2	4.4	32.0	1.4	0.0	nd	0.07	non
E	1	44.1	**51.3**	2.1	0.0	**3/5**	0.12	non
	2	23.1	**71.5**	3.2	0.0	**3/5**	0.20	non
F	1	24.8	1.6	27.0	0.0	nd	0.19	co
	2	9.1	26.5	2.0	0.1	nd	0.39	co
G	1	39.8	7.3	6.1	0.0	nd	0.00	Slu
	2	**45.6**	**46.7**	1.3	0.0	**3/5**	3.37	Slu
H	1	**92.9**	2.0	1.2	0.0	**3/5**	0.00	non
	2	3.9	0.2	1.8	23.0	**6**	0.00	non
I	1	3.0	0.1	0.3	**91.2**	**7**	0.00	non
	2	8.2	0.1	1.2	**73.7**	**7**	0.00	non
J	1	18.6	2.2	0.8	**68.6**	**7**	0.00	non
	2	9.3	3.1	0.4	**73.3**	**7**	0.00	non
K	1	1.8	0.5	**91.4**	0.0	**1**	0.04	Sau
	2	**46.5**	1.3	**67.5**	0.1	**1**	0.27	co
L	1	**61.2**	44.6	1.2	0.0	**3/5**	0.08	non
	2	26.0	**73.2**	2.8	0.0	**3/5**	0.11	non

Suppl. Table 2. Correlation coefficients of species present in the nasal microbiomes. Correlation coefficients were inferred based on a centered log-ratio-transformed abundance table of species reads by correlation network analyses using the Namap/Pearson algorithm of MetagenoNets [9] with thresholds for prevalence and occurrence of 0.1% and 20%, respectively. The table shows the resulting correlation measures for 28 species throughout all 24 samples. Positive correlations are emphasized by green shading (with intensity corresponding to amount of the values) while negative correlations are correspondingly shaded in red.

.

	Anaerococcus sp.	Campylobacter jejuni	Chlamydia sp.	Corynebacterium accolens	Corynebacterium aurimucosum	Corynebacterium casei	Corynebacterium diphtheriae	Corynebacterium efficiens	Corynebacterium propinquum	Corynebacterium simulans	Corynebacterium striatum	Corynebacterium tuberculostearicum	Cutibacterium acnes	Dolosigranulum pigrum	Finegoldia magna	Lawsonella clevelandensis	Listeria monocytogenes	Mycobacterium sp.	Neisseria sp.	Rhodococcus sp.	Salmonella enterica	Staphylococcus aureus	Staphylococcus capitis	Staphylococcus epidermidis	Staphylococcus lugdunensis	Streptococcus anginosus	Streptococcus pneumoniae	Streptomyces sp.
Anaerococcus sp.	1.00	0.26	-0.14	0.14	0.47	0.08	0.19	0.24	-0.26	0.07	0.18	0.56	0.62	-0.16	0.27	0.24	0.23	-0.08	0.20	0.28	0.20	0.41	0.27	0.66	0.05	0.19	-0.54	0.25
Campylobacter jejuni	0.26	1.00	0.43	-0.02	0.42	0.09	0.27	-0.09	0.14	0.08	0.18	0.46	0.29	0.15	0.08	0.05	0.67	0.23	0.96	0.15	0.93	0.26	-0.09	0.15	-0.02	0.17	-0.03	0.14
Chlamydia sp.	-0.14	0.43	1.00	-0.34	-0.21	-0.36	-0.23	-0.19	0.13	0.12	-0.15	-0.05	-0.21	-0.01	-0.05	0.09	0.32	0.43	0.42	0.01	0.42	0.06	-0.27	-0.28	0.01	0.00	0.36	0.13
Corynebacterium accolens	0.14	-0.02	-0.34	1.00	0.60	0.32	0.66	0.27	-0.36	0.43	0.74	0.54	0.56	-0.04	0.15	0.51	0.15	0.02	-0.16	0.50	-0.12	0.07	0.20	0.59	0.32	0.52	-0.28	0.40
Corynebacterium aurimucosum	0.47	0.42	-0.21	0.60	1.00	0.52	0.83	0.21	-0.25	0.59	0.79	0.85	0.76	-0.14	0.19	0.52	0.40	0.17	0.34	0.57	0.37	0.46	0.37	0.59	0.15	0.56	-0.30	0.46
Corynebacterium casei	0.08	0.09	-0.36	0.32	0.52	1.00	0.49	0.18	0.19	0.40	0.42	0.36	0.27	0.15	0.28	0.15	-0.07	-0.14	0.16	0.08	0.15	0.16	0.56	0.38	0.34	0.05	-0.38	-0.03
Corynebacterium diphtheriae	0.19	0.27	-0.23	0.66	0.83	0.49	1.00	0.28	-0.22	0.67	0.90	0.64	0.72	-0.06	0.23	0.63	0.44	0.13	0.16	0.77	0.14	0.32	0.33	0.58	0.24	0.73	-0.24	0.64
Corynebacterium efficiens	0.24	-0.09	-0.19	0.27	0.21	0.18	0.28	1.00	-0.27	0.26	0.42	0.19	0.33	0.01	0.34	0.06	0.05	-0.06	-0.14	0.64	-0.22	-0.06	0.46	0.32	0.35	0.59	-0.37	0.51
Corynebacterium propinquum	-0.26	0.14	0.13	-0.36	-0.25	0.19	-0.22	-0.27	1.00	0.05	-0.45	-0.20	-0.22	0.66	-0.13	-0.30	0.11	-0.01	0.23	-0.32	0.28	-0.16	-0.07	-0.20	-0.01	-0.31	0.28	-0.30
Corynebacterium simulans	0.07	0.08	0.12	0.43	0.59	0.40	0.67	0.26	0.05	1.00	0.66	0.46	0.50	0.13	0.04	0.45	0.35	0.53	0.00	0.67	0.08	0.31	0.41	0.31	0.28	0.65	-0.01	0.65
Corynebacterium striatum	0.18	0.18	-0.15	0.74	0.79	0.42	0.90	0.42	-0.45	0.66	1.00	0.62	0.66	-0.24	0.32	0.60	0.34	0.22	0.06	0.76	0.05	0.27	0.33	0.49	0.35	0.78	-0.23	0.67
Corynebacterium tuberculostearicum	0.56	0.46	-0.05	0.54	0.85	0.36	0.64	0.19	-0.20	0.46	0.62	1.00	0.86	-0.17	0.28	0.50	0.33	0.11	0.36	0.49	0.35	0.26	0.25	0.65	0.41	0.50	-0.49	0.46
Cutibacterium acnes	0.62	0.29	-0.21	0.56	0.76	0.27	0.72	0.33	-0.22	0.50	0.66	0.86	1.00	-0.11	0.27	0.52	0.35	0.07	0.14	0.66	0.13	0.27	0.28	0.74	0.38	0.62	-0.54	0.59
Dolosigranulum pigrum	-0.16	0.15	-0.01	-0.04	-0.14	0.15	-0.06	0.01	0.66	0.13	-0.24	-0.17	-0.11	1.00	-0.16	-0.41	0.19	-0.01	0.13	-0.07	0.19	-0.41	-0.07	-0.08	-0.03	-0.17	0.15	-0.01
Finegoldia magna	0.27	0.08	-0.05	0.15	0.19	0.28	0.23	0.34	-0.13	0.04	0.32	0.28	0.27	-0.16	1.00	0.33	-0.18	-0.38	0.07	0.22	-0.08	-0.10	-0.10	0.28	0.50	0.20	-0.41	0.30
Lawsonella clevelandensis	0.24	0.05	0.09	0.51	0.52	0.15	0.63	0.06	-0.30	0.45	0.60	0.50	0.52	-0.41	0.33	1.00	0.17	-0.05	-0.04	0.56	-0.10	0.46	0.07	0.49	0.28	0.55	-0.18	0.50
Listeria monocytogenes	0.23	0.67	0.32	0.15	0.40	-0.07	0.44	0.05	0.11	0.35	0.34	0.33	0.35	0.19	-0.18	0.17	1.00	0.54	0.55	0.47	0.58	0.32	0.13	0.21	-0.11	0.44	0.25	0.42
Mycobacterium sp.	-0.08	0.23	0.43	0.02	0.17	-0.14	0.13	-0.06	-0.01	0.53	0.22	0.11	0.07	-0.01	-0.38	-0.05	0.54	1.00	0.15	0.21	0.26	0.30	0.16	-0.07	-0.05	0.25	0.39	0.31
Neisseria sp.	0.20	0.96	0.42	-0.16	0.34	0.16	0.16	-0.14	0.23	0.00	0.06	0.36	0.14	0.13	0.07	-0.04	0.55	0.15	1.00	0.01	0.97	0.27	-0.02	0.02	-0.11	0.02	-0.04	-0.04
Rhodococcus sp.	0.28	0.15	0.01	0.50	0.57	0.08	0.77	0.64	-0.32	0.67	0.76	0.49	0.66	-0.07	0.22	0.56	0.47	0.21	0.01	1.00	-0.03	0.23	0.34	0.49	0.23	0.93	-0.22	0.90
Salmonella enterica	0.20	0.93	0.42	-0.12	0.37	0.15	0.14	-0.22	0.28	0.08	0.05	0.35	0.13	0.19	-0.08	-0.10	0.58	0.26	0.97	-0.03	1.00	0.30	0.00	-0.01	-0.19	-0.01	0.05	-0.09
Staphylococcus aureus	0.41	0.26	0.06	0.07	0.46	0.16	0.32	-0.06	-0.16	0.31	0.27	0.26	0.27	-0.41	-0.10	0.46	0.32	0.30	0.27	0.23	0.30	1.00	0.40	0.34	-0.22	0.29	-0.10	0.11
Staphylococcus capitis	0.27	-0.09	-0.27	0.20	0.37	0.56	0.33	0.46	-0.07	0.41	0.33	0.25	0.28	-0.07	-0.10	0.07	0.13	0.16	-0.02	0.34	0.00	0.40	1.00	0.33	0.14	0.25	-0.36	0.10
Staphylococcus epidermidis	0.66	0.15	-0.28	0.59	0.59	0.38	0.58	0.32	-0.20	0.31	0.49	0.65	0.74	-0.08	0.28	0.49	0.21	-0.07	0.02	0.49	-0.01	0.34	0.33	1.00	0.31	0.40	-0.64	0.43
Staphylococcus lugdunensis	0.05	-0.02	0.01	0.32	0.15	0.34	0.24	0.35	-0.01	0.28	0.35	0.41	0.38	-0.03	0.50	0.28	-0.11	-0.05	-0.11	0.23	-0.19	-0.22	0.14	0.31	1.00	0.27	-0.34	0.26
Streptococcus anginosus	0.19	0.17	0.00	0.52	0.56	0.05	0.73	0.59	-0.31	0.65	0.78	0.50	0.62	-0.17	0.20	0.55	0.44	0.25	0.02	0.93	-0.01	0.29	0.25	0.40	0.27	1.00	-0.16	0.85
Streptococcus pneumoniae	-0.54	-0.03	0.36	-0.28	-0.30	-0.38	-0.24	-0.37	0.28	-0.01	-0.23	-0.49	-0.54	0.15	-0.41	-0.18	0.25	0.39	-0.04	-0.22	0.05	-0.10	-0.36	-0.64	-0.34	-0.16	1.00	-0.19
Streptomyces sp.	0.25	0.14	0.13	0.40	0.46	-0.03	0.64	0.51	-0.30	0.65	0.67	0.46	0.59	-0.01	0.30	0.50	0.42	0.31	-0.04	0.90	-0.09	0.11	0.10	0.43	0.26	0.85	-0.19	1.00

Suppl. Table. 3. Bacterial strains plasmids and oligonucleotides used in this study

Bacterial strain	Description	Source or reference
Corynebacterium accolens		
DSM 44279	origin unknown	DSMZ
63VAs_B8	human nasal isolate	[32]
83VAs_B5	human nasal isolate	[32]
KPL 1824	human nasal isolate	[33]
KPL 1855	human nasal isolate	[33]
KPL 1996	human nasal isolate	[33]
Corynebacterium aurimucosum		
10VPs_Sm8	human nasal isolate	[32]
48/2	lesional site isolate	AG Peschel strain collection
Corynebacterium kroppenstedtii		
82VAs_B6	human nasal isolate	[32]
Corynebacterium propinquum		
8VAs_B3	human nasal isolate	[32]
63VAs_B4	human nasal isolate	[32]
P7-31	human nasal isolate	this study
56/2	human nasal isolate	AG Peschel strain collection
57/2	human nasal isolate	AG Peschel strain collection
Corynebacterium pseudodiphteriticum		
87VAs_B4	human nasal isolate	[32]
90VAs_B3	human nasal isolate	[32]
P1-29	human nasal isolate	this study
P2-34	human nasal isolate	this study
P6-3	human nasal isolate	this study
Corynebacterium simulans		
81MNs_B1	human nasal isolate	[32]
50MNs_Sm2	human nasal isolate	[32]
50VAs_B5	human nasal isolate	[32]
79/2	groin isolate	AG Peschel strain collection
73/2	groin isolate	AG Peschel strain collection
77/2	groin isolate	AG Peschel strain collection
Corynebacterium striatum		
24/2	human nasal isolate	AG Peschel strain collection
46/2	lesion site isolate	AG Peschel strain collection
38/2	groin isolate	AG Peschel strain collection
Corynebacterium tuberculostearicum		
87VAs_B5	human nasal isolate	[32]
12VAs_B4	human nasal isolate	[32]
Cutibacterium acnes		
44VAs_Sa4	human nasal isolate	[32]

50VAs_Sa1	human nasal isolate	[32]
83VAs_Sa3	human nasal isolate	[32]
87VAs_SaT9	human nasal isolate	[32]
Cutibacterium avidum		
Clone#11	human nasal isolate	AG Peschel strain collection
Dolosigranulum pigrum		
9VAs_B4	human nasal isolate	[32]
Escherichia coli		
DH5α	K-12 derivative	New England BioLabs
DC10B	Δ*dcm* in the DH10B background	[30]
CMFI_AI 1	axilla isolate	AG Peschel strain collection
CMFI_AI 2	groin isolate	AG Peschel strain collection
CMFI_AI 3	axilla isolate	AG Peschel strain collection
Finegoldia magna		
63 Vas_Sa4	human nasal isolate	[32]
83 Vas_Sa6	human nasal isolate	[32]
Klebsiella pneumoniae		
ATCC700603	human urine isolate	ATCC
Lawsonella clevelandensis		
DSM 45743	human nasal isolate	DSMZ
Moraxella catarrhalis		
44VAs_Sm4	human nasal isolate	[32]
80VAs_B4	human nasal isolate	[32]
Staphylococcus aureus		
USA300 LAC	CA-MRSA isolate	[34]
IVK41	human nasal isolate	[6]
IVK55	human nasal isolate	[6]
IVK56	human nasal isolate	[6]
IVK58	human nasal isolate	[6]
Staphylococcus capitis		
10VAs_KB2	human nasal isolate	[32]
44UNs_B2	human nasal isolate	[32]
50VAs_KB6	human nasal isolate	[32]
Staphylococcus caprae		
VA18305/14	human clinical isolate	Eppendorfklinikum, Hamburg
BK3880/14	human clinical isolate	Eppendorfklinikum, Hamburg
Staphylococcus epidermidis		
B1-1	human nasal isolate	this study
B1-5	human nasal isolate	this study
B1-10	human nasal isolate	this study
B5-7	human nasal isolate	this study
B5-7 Δ*sfaDAB*	deletion of *sfa* gene locus	this study
B5-26	human nasal isolate	this study
S1-2	human nasal isolate	this study

S1-15	human nasal isolate	this study
S1-27	human nasal isolate	this study
S2-2	human nasal isolate	this study
M14-19	human nasal isolate	this study
M15-6	human nasal isolate	this study
M16-32	human nasal isolate	this study
W1-7	human nasal isolate	this study
W1-7Δ*sfaDAB*	deletion of *sfa* gene locus	this study
W3-6	human nasal isolate	this study
W5-7	human nasal isolate	this study
W8-6	human nasal isolate	this study
Staphylococcus hominis		
50MNs_Sa6	human nasal isolate	[32]
89VPs_B7	human nasal isolate	[32]
9VPs_KB1	human nasal isolate	[32]
Staphylococcus lugdunensis		
HKU09-01	human skin infection isolate	[35]
HKU09-01 Δ*fhu*	deletion of fhu gene locus	this study
HKU09-01 Δ*fhu* pRB474_fhu	complementation of fhu gene locus; fhu genes encoded on pRB474	this study
IVK28	human nasal isolate	[6]
IVK28 Δ*fhu*	deletion of fhu gene locus	this study
Staphylococcus pettenkofferi		
210-70229632	human clinical isolate	AG Peschel strain collection
Staphylococcus sciuri		
DSM 16827	Norway rat isolate	DSMZ
DSM 15613	sliced veal leg isolate	DSMZ
9VPs_Sm2	human nasal isolate	[32]
Staphylococcus warneri		
VA16066/14	human clinical isolate	Eppendorfklinikum, Hamburg
BK6091/14	human clinical isolate	Eppendorfklinikum, Hamburg
Streptococcus pneumoniae		
ATCC 6301		ATCC
ATCC 49619	sputum isolate	ATCC

Plasmid	Description	Reference
pIMAY	thermosensitive vector for allelic exchange	[30]
pRB474	*E. coli/S. aureus* shuttle vector; constitutive active expression vector	[36]

| Oligonucleotides	Sequence (5'-3')	Purpose
(1) Fhu up for	TATAGGGCGAATTG<u>GAGCTC</u>TTTAGTATTT TTACCTTCTGCC	Generating upstream recombinant region for *fhu* deletion
(2) Fhu up rev	TAGAAAGTTGGGGAATTATGTAATAAAATT CGTGTTGGAA	generating upstream recombinant region for *fhu* deletion
(3) Fhu dw for	CATAATTCCCCAACTTTCTA	generating downstream recombinant region for *fhu* deletion
(4) Fhu dw rev	GGGAACAAAAGCTG<u>GGTACC</u>ATTATTAAGC GTATTGATGATC	generating downstream recombinant region for *fhu* deletion
(5) fhu chrom. Up for	CTTTCACAGATGGACTCATT	Screening for chromosomal *fhu* deletion
(6) fhu chrom. Dw Rev	TATTAATCTCTGTATTTTTAGG	Screening for chromosomal *fhu* deletion
(7) fhu comp for	TTGCATGCCTGCAG<u>GTCGAC</u>AAATAGAAAG TTGGGGAATT	generating *fhu* genes for complementation with pRB474
(8) fhu comp rev	GTACCCGGGGATCC<u>TCTAGA</u>TTAAATAGAT TTAGCTTTATACAT	generating *fhu* genes for complementation with pRB474
(9) sfaDAB ko up for	CGAG<u>GTCGAC</u>AATAGAGAGGGATAACTAAG	Generating upstream recombinant region for *sfaDAB* deletion
(10) sfaDAB ko up rev	TTCTAAATGATGGTCTATCATTTAGAACGT	generating upstream recombinant region for *sfaDAB* deletion
(11) sfaDAB ko dw for	TGATAGACCATCATTTAGAACAATGGATTT	generating downstream recombinant region for *sfaDAB* deletion
(12) sfaDAB ko dw rev	ATTG<u>GAGCTC</u>TTATAATTAGGTCCAAGATT	generating downstream recombinant region for *sfaDAB* deletion
(13) Chrom sfaDAB up for	TTATAAATCATTCTTTCTATGAA	Screening for chromosomal *sfaDAB* deletion
(14) Chrom sfaDAB dw rev	TTACTGGTGTGAAATGAATT	Screening for chromosomal *sfaDAB* deletion
(15) 473 Eco	CCTCAAGCTAGAGAGTCATTACCCC	Screening for pRB474_*fhu* positive transformants
(16) 473 Hind	CTGGATTTGTTCAGAACGCTCGG	Screening for pRB474_*fhu* positive transformants

Supplemental Figures
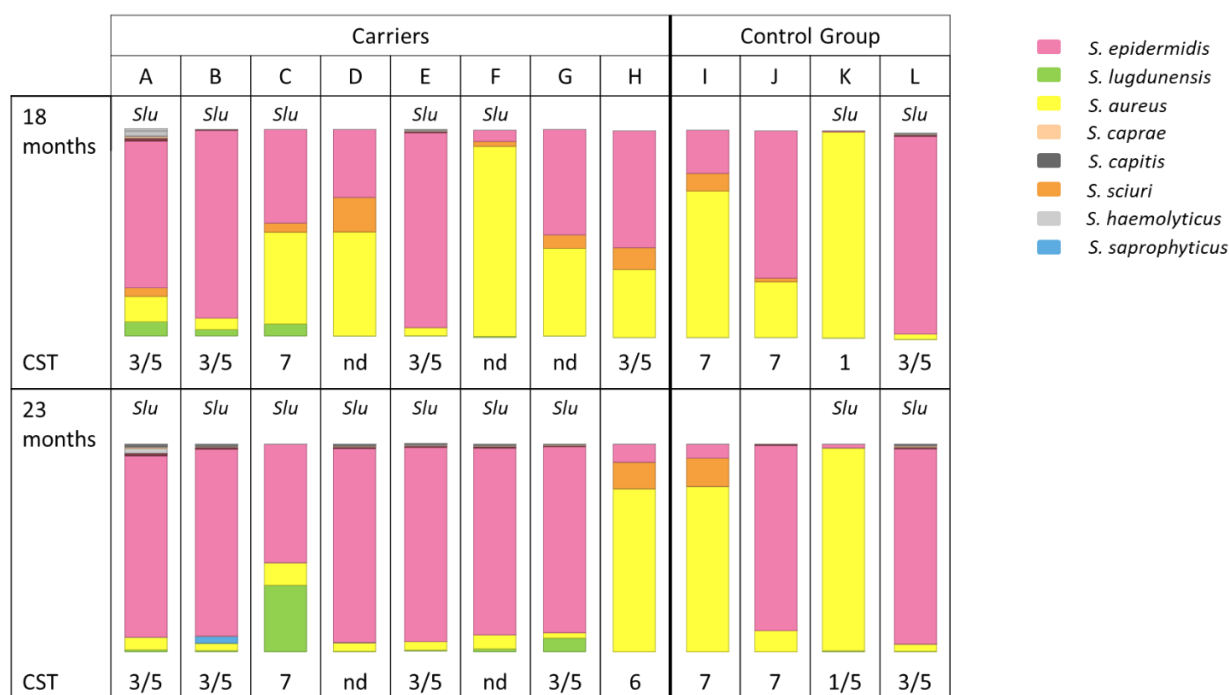
Suppl. Fig. 1. Microbiome profiles within the genus *Staphylococcus* at the species level. Relative proportions of staphylococcal species present in the nasal microbiomes at time points 18 months and 23 months are presented by stacked bar charts. The different bacterial genera are indicated by colours as shown in the legend on the right. The presence of *S. lugdunensis* reads in the metagenomes is indicated (*Slu*). The microbiome profiles that could be assigned to the community state types (CST) published by *Liu et al* [8] are labelled accordingly. Profiles not fitting to one of these types are designated "nd".
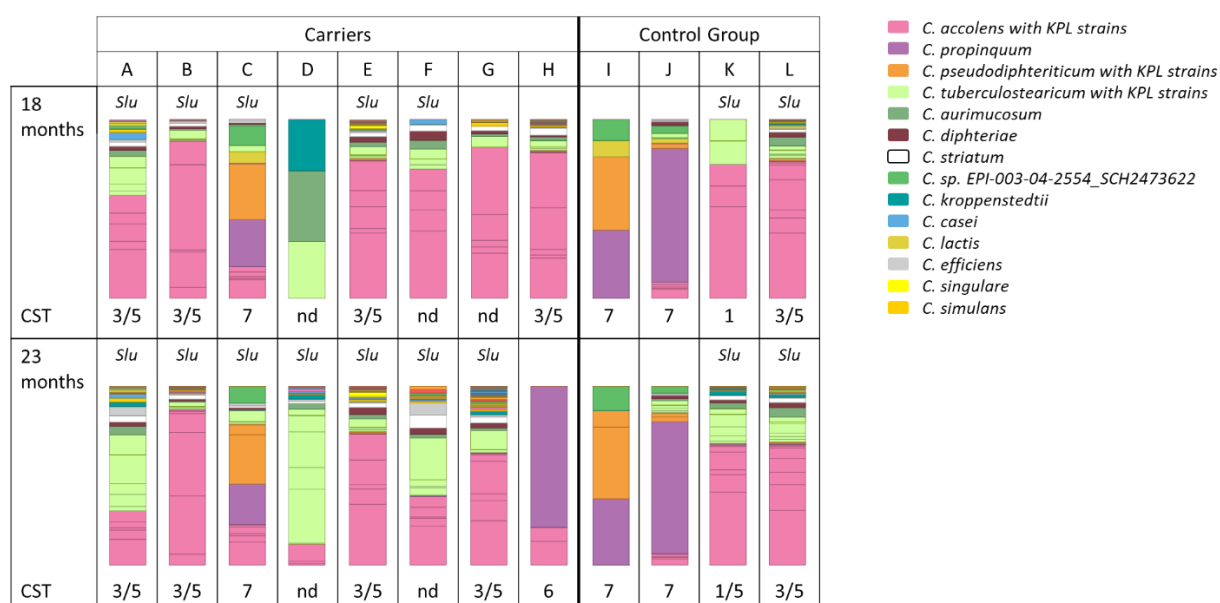
Suppl. Fig. 2. Microbiome profiles within the genus *Corynebacterium* at the species level. *Corynebacterium* species profiles determined in metagenome analyses at time points 18 and 23 months. Relative proportions of *Corynebacterium* species present in the nasal microbiomes are presented by stacked bar charts. The different *Corynebacterium* species are indicated by colours as listed in the legend on the right. For *C. accolens*, *C. pseudodiphteriticum* and *C. tuberculostearicum*, different strains ("KPL strains") were determined but labeled with the same colours according to a strain assignment by Kathrin P. Lemon [33]. The presence of *S. lugdunensis* reads in the metagenomes is indicated (*Slu*). The microbiome profiles that could be assigned to the community state types (CST) published by [8] are labelled accordingly. Profiles not fitting to one of these types are designated "nd".
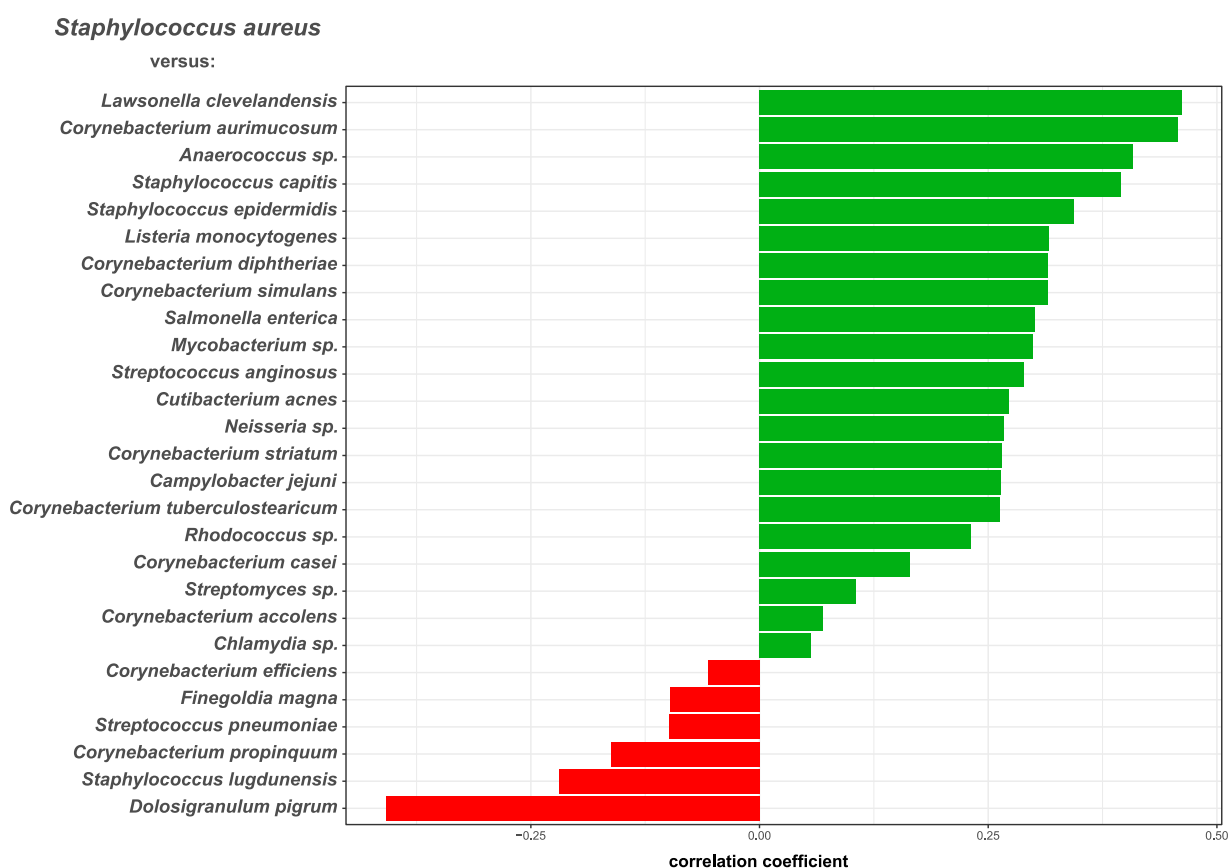

Suppl. Fig. 3. Correlation of *S. aureus* with other microbiome species. Correlation coefficients were inferred based on a centered log-ratio-transformed abundance table of species reads by correlation network analyses using the Namap/Pearson algorithm of MetagenoNets [9] with thresholds for prevalence and occurrence of 0.1% and 20%, respectively. Based on these parameters, we obtained correlation measures for 28 species throughout all 24 samples. Shown are the associations of *S. aureus* with other microbiome species (shown at the x-axis). Positive associations are indicated by green bars, negative associations by red bars. The corresponding Pearson correlation coefficients are indicated at the x-axis.
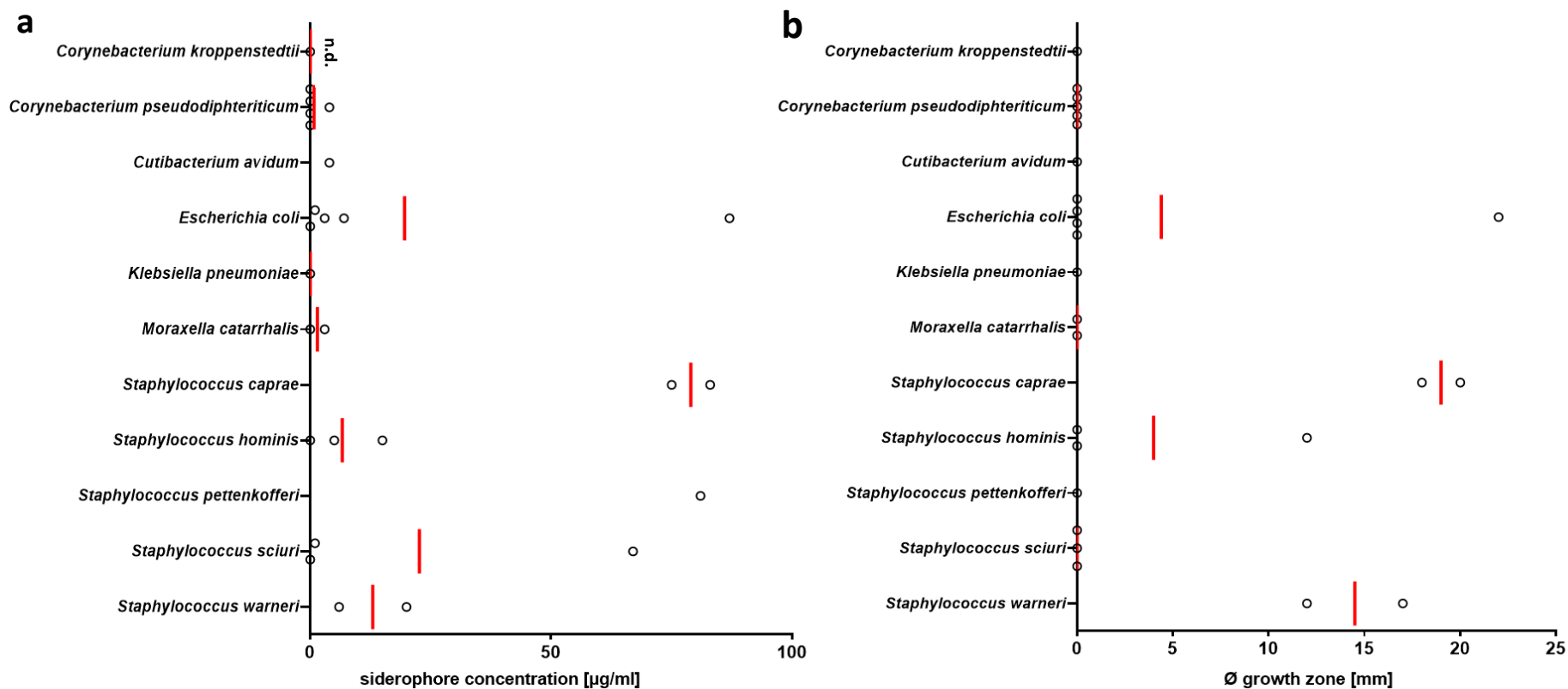
Suppl. Fig. 4. Nasal bacterial species producing siderophores have the capacity to support growth of *S. lugdunensis*. a, Siderophore concentration in spent media from nasal bacteria after three days of incubation detected via SideroTec Assay™ kit. Siderophores could be detected in spent media from staphylococcal species and *E. coli*; siderophore detection was not assessable for *C. kroppenstedtii* due to presence of Tween 80 in growth medium that interacts with the reaction solutions provided by the SideroTec Assay™ kit. **b,** Occurrence and sizes (diameter in mm) of growth zones of *S. lugdunensis* promoted by siderophore-containing spent media from nasal bacteria. Staphylococcal species and *E. coli* support *S. lugdunensis* growth under iron-restricted conditions. Data points represent average values of three independent biological replicates, and vertical red lines show means of each species. n.d. = not detectable.
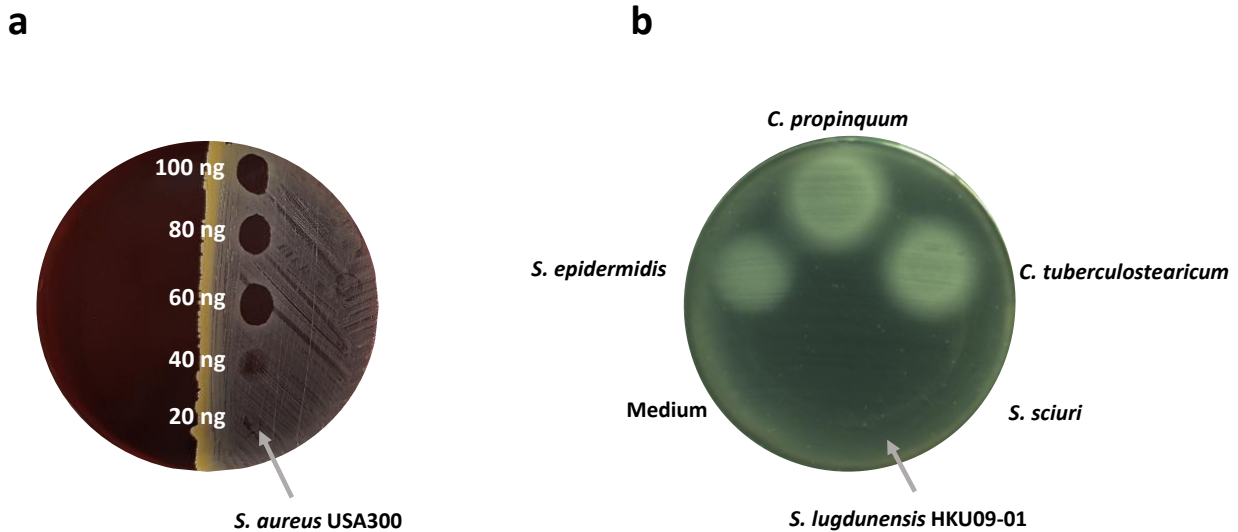
Suppl. Fig. 5. Representative pictures of lugdunin susceptibility determination of nasal bacteria and *S. lugdunensis* growth promotion by siderophore-containing spent media from nasal bacteria. a, Lugdunin susceptibility determination by the example of *S. aureus* USA300. 2 µl containing different amounts of lugdunin (0 to100 ng) were spotted onto a lawn of bacteria on sheep blood agar plates, resulting in zones of inhibition for lugdunin susceptible bacteria after incubation for 24-48 h at 37°C. The spot with the lowest amount of lugdunin showing a clear inhibition was used to determine lugdunin susceptibility. **b,** Growth promotion of *S. lugdunensis* HKU09-01 by siderophore-containing spent media of nasal bacteria. Iron-restricted BHI agar supplemented with 10% horse serum (transferrin source) were inoculated with a lawn of *S. lugdunensis*. Prior to incubation for 20 h at 37°C spent media of different bacteria were spotted on *S. lugdunensis* that resulted in zones of enhanced growth when siderophores were present. Diameters were measured and noted.
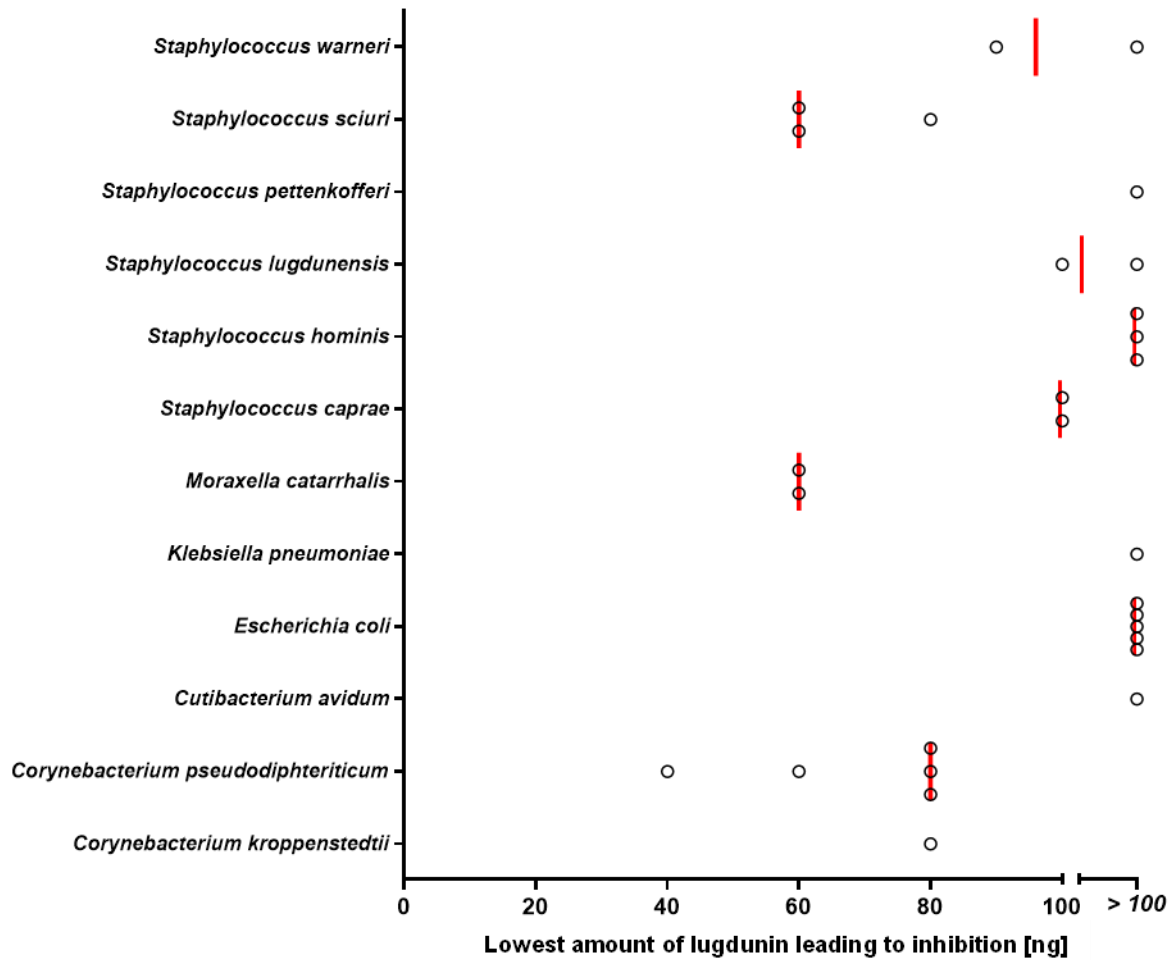
Suppl. Fig. 6. Lugdunin susceptibility of nasal bacterial species. Different amounts of lugdunin (0 to 100 ng in 2 µl) were spotted onto lawns of nasal bacteria, resulting in zones of inhibition after incubation for 24-48 h. Data points represent average values of three independent experiments, and vertical red lines show medians of each group.

Chapter 4

Secretion of and self-resistance to the novel fibupeptide antimicrobial lugdunin by distinct ABC transporters in *Staphylococcus lugdunensis*

Sophia Krauss[1,2,3,§], Alexander Zipperer[1,2,§,*], Sebastian Wirtz[3,4], Julian Saur[3,4], Martin C. Konnerth[3,4,*], Simon Heilbronner[1,2,3], Benjamin O. Torres Salazar[1,2,3], Stephanie Grond[3,4], Bernhard Krismer[1,2,3,#], Andreas Peschel[1,2,3]

1. Interfaculty Institute of Microbiology and Infection Medicine, Infection Biology, University of Tübingen, Germany.

2. German Center for Infection Research (DZIF), partner site Tübingen, Germany.

3. Cluster of Excellence EXC 2124 Controlling Microbes to Fight Infection.

4. Organic Chemistry, University of Tübingen, Germany.

§ Sophia Krauss and Alexander Zipperer contributed equally to this manuscript

Running Title: Lugdunin secretion and self-resistance

Address correspondence to Bernhard Krismer (b.krismer@uni-tuebingen.de)

Abstract

Lugdunin is the first reported non-ribosomally synthesized antibiotic from human microbiomes. Its production by the commensal *Staphyloccocus lugdunensis* eliminates the pathogen *Staphylococcus aureus* from human nasal microbiomes. The cycloheptapeptide lugdunin is the founding member of the new class of fibupeptide antibiotics, which have a novel mode of action and represent promising new antimicrobial agents. How *S. lugdunensis* releases and achieves producer self-resistance to lugdunin has remained unknown. We report that two ABC transporters encoded upstream of the lugdunin-biosynthetic operon have distinct, yet overlapping roles in lugdunin secretion and self-resistance. While deletion of the *lugEF* transporter genes abrogated most of the lugdunin secretion, the *lugGH* transporter genes had a dominant role in resistance. Yet, all four genes were required for full-level lugdunin resistance. The small accessory putative membrane protein LugI further contributed to lugdunin release and resistance levels conferred by the ABC transporters. Whereas LugIEFGH also conferred resistance to lugdunin congeners with inverse structure or with amino acid exchange at position six, they neither affected the susceptibility to a lugdunin variant with an exchange at position two nor to other cyclic peptide antimicrobials such as daptomycin or gramicidin S. The obvious selectivity of the resistance mechanism raises hopes that it will not confer cross-resistance to other antimicrobials or to optimized lugdunin derivatives to be used for the prevention and treatment of *S. aureus* infections.

Introduction

The dynamic changes in microbiome composition are governed by multiple antagonistic or mutualistic microbial interactions [1]. Several microbiome members achieve fitness benefits in competition with other bacteria through the production of bacteriocins or related antimicrobials [2, 3]. The biosynthetic genes for the production of antimicrobials are located in highly variable and often mobile clusters, which usually also include genes conferring self-resistance to the producer strain [4, 5]. Such mechanisms can confer resistance to a more or less narrow range of antimicrobials thus defining the capacity of antimicrobials-producing bacterial strains to tolerate their own compound plus, potentially, those from competitors. The capacity to produce bacteriocins and related molecules has been found to be particularly abundant in microbiome members from nutrient-poor habitats such as the human nose [6]. We are only beginning to understand the diversity and relevance of such molecules [7].

We have recently reported that most isolates of *Staphylococcus lugdunensis*, a colonizer of the human skin and nasal mucosa, produce lugdunin, the founding member of a new class of circular antimicrobial peptides named fibupeptides [8, 9]. Lugdunin is synthesized by non-

ribosomal peptide synthetases and inhibits target bacteria by dissipating their membrane potential, probably in a protonophore-like fashion [9]. In addition to its direct antimicrobial activity, lugdunin stimulates human skin cells to produce antibacterial host defense peptides that synergize with lugdunin in the elimination of susceptible microbes [10]. Lugdunin-producing *S. lugdunensis* can eradicate the major human pathogen *Staphylococcus aureus* and nasal carriage of *S. lugdunensis* strongly reduces the rate of nasal colonization by *S. aureus* [8]. The suitability of lugdunin as a potential new drug for *S. aureus* decolonization and therapy depends also on the risk of resistance development. We found that *S. aureus* cannot develop spontaneous resistance to lugdunin even after several passages in cultures with increasing subinhibitory concentrations of lugdunin [8]. It has remained unclear though how *S. lugdunensis* achieves self-resistance to its product and if potential resistance genes could be mobilized and transferred to *S. aureus* or other pathogens.

Here we analyzed the *lugEFGH* genes encoded next to the lugdunin biosynthesis genes and show that the four ABC-transporter encoding genes are necessary and sufficient to confer lugdunin resistance. LugEFGH and the accessory small putative membrane protein LugI were required for both, optimal secretion of endogenous lugdunin and resistance to exogenous lugdunin and even slight changes in lugdunin structure abrogated the capacity of the ABC exporters to protect against these compounds.

Results

The lugdunin gene cluster includes 13 genes, many of which encode proteins of unknown functions

The recent identification of the lugdunin gene cluster comprising the biosynthetic *lugABCD* genes and the putative regulator *lugR* [8] prompted us to elucidate the boundaries of the cluster and identify additional genes potentially involved in lugdunin synthesis, export, regulation, and self-resistance. The cluster plus some of the adjacent genes has a significantly lower G+C content than the rest of the chromosome (26.7 vs. 33.8%, respectively), and the region spanning *lugH* and *lugR* has even less than 24% G+C (Fig. 1a) suggesting that *lugRABCD* plus nine additional genes form the full gene cluster (Fig. 1b). *lugD*, coding for the starter unit in lugdunin biosynthesis, is flanked by the genes encoding LugT, a putative type-II thioesterase that may repair stalled peptidyl carrier protein (PCP) domains [11], and LugZ, which is homologous to 4'-phosphopantetheinyl transferases and probably converts apo-PCP to the active holo-form by attachment of the 4-phosphopantetheine cofactor [11]. Further downstream, probably forming a separate transcriptional unit, *lugM* encodes a putative monooxygenase the role of which in the biosynthesis process remains unclear.
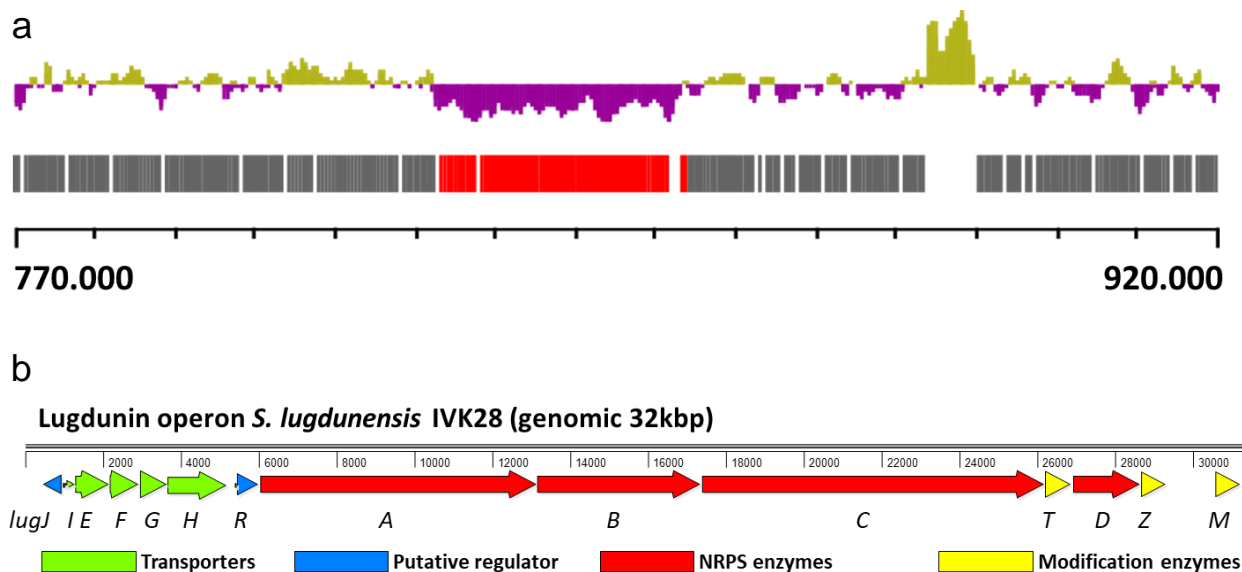
Figure 1. Decreased G+C content (a) and genetic organization (b) of the lugdunin gene cluster. The *S. lugdunensis* IVK28 chromosomal section between nucleotides 770,000 and 920,000 (NCBI accession number PRJNA669000) along with the encoded open reading frames in red (lugdunin gene cluster *lugJ* to *lugM*) and gray (other genes) and the corresponding G+C content in purple (below average; 26.7% for the lugdunin operon) and green (above average; 33.82% for the entire genome) is shown in (a). Organization of the lugdunin gene cluster with functional assignment in different colors is shown in (b). Protein accession numbers are listed in supplementary Table S1.

Upstream of *lugR* five genes (*lugIEFGH*) form another operon (Fig. 1b). LugI is predicted to encode a 79-amino acids long integral membrane protein with two transmembrane helices and no similarity to proteins of known function (Suppl. Fig.S1). LugE and LugG contain conserved 'Walker' motives probably representing the ATP-binding components of ABC transporter complexes [12]. LugF and LugH are related to the integral membrane parts of putative ABC transporters of other Firmicutes, with LugF containing six and LugH twelve putative transmembrane segments (Suppl. Fig.S1). According to the canonical architecture of ABC transporter complexes, the four proteins could form two distinct transporters, one as a LugEF homodimer and a second with a LugG homodimer linked to one LugH copy. Upstream of *lugI*, the gene *lugJ* is encoded in opposite direction, which may constitute a second regulator gene in addition to *lugR*. LugJ most likely belongs to the winged-helix type HTH-containing transcriptional regulators. Most antibiotic biosynthetic gene clusters encode proteins conferring self-resistance to the producing strain. Usually, these are either antibiotic-insensitive variants of target proteins, enzymes for the modification of target structures (e.g. rRNAs), or antibiotic exporters [13]. None of the genes in the lugdunin cluster seemed to reflect the first two types of self-resistance genes while the putative ABC transporter genes were regarded as

130

candidates for accomplishing lugdunin secretion and self-resistance and were analyzed further.

ABC transporters encoded in the *lug* gene cluster mediate lugdunin release and confer resistance to lugdunin

To analyze a potential role of the ABC transporters in lugdunin export and self-resistance, different combinations of *lugEFGH* and the co-transcribed gene *lugI* were deleted in the lugdunin-producing strain *S. lugdunensis* IVK28. To avoid polar effects on downstream transcripts an allelic replacement strategy with no insertion of foreign DNA fragments was used. When inhibition zones around spotted bacterial suspensions with identical diameters of the wild type and mutants on agar containing lugdunin-susceptible *S. aureus* cells were compared (Fig. 2a), the *lugIEFGH* mutant (Δ*lugIEFGH*) showed no inhibition, indicating that some or all of the five genes are required for lugdunin export. Deletion of only *lugEFGH* strongly reduced but did not abolish lugdunin release. The inhibitory distance was about 25% compared to the wild type (Fig. 2a), suggesting that LugI has a very modest but LugEFGH-independent role in lugdunin release. However, the sole inactivation of *lugI* caused no reduction in lugdunin release. Deletion of *lugEF* had a significant impact on the level of lugdunin export, which was almost as strong as in the Δ*lugEFGH* mutant, indicating that LugEF have a dominant role in lugdunin export. In contrast, the Δ*lugGH* mutant released even slightly higher amounts of lugdunin (about 38%) and exhibited a growth defect in liquid culture compared to the wild type (Fig. 2b), suggesting a role in resistance to lugdunin rather than export. Accordingly, the other *lugGH*-deficient mutant strains Δ*lugEFGH* and Δ*lugIEFGH* displayed similar growth defects (Fig. 2b).

To investigate the role of LugIEFGH in lugdunin self-resistance, several combinations of the genes were deleted in *S. lugdunensis* Δ*lugD*, which does not produce lugdunin [8], and the susceptibility of the resulting mutants to lugdunin was analyzed. Deletion of the entire gene set (*lugIEFGH*) strongly decreased the minimal inhibitory concentration (MIC) to exogenous lugdunin from 10.5 µg/ml to 2.0 µg/ml, indicating that the genes are involved in producer self-resistance to lugdunin (Fig. 3). Deletion of either *lugEF* or *lugGH* also led to reduced lugdunin MIC values indicating that both ABC transporters play a role in lugdunin self-resistance. Deletion of *lugI* led to a decrease of the MIC to the identical level as the *lugGH* deletion. Deletion of *lugEF*, *lugIEF*, or *lugIEFGH* led to a stepwise MIC decrease to the lowest observed level. Δ*lugEFGH*, still expressing *lugI*, showed the same MIC level as the *lugIEFGH* mutant, indicating that although *lugI* deletion has an effect on the overall MIC level, LugI seems to rely on the presence of one of the transporters to modulate lugdunin self-resistance (Fig. 3a). The

lugdunin MIC of the *S. lugdunensis lugEFGH* deletion mutant was at the same level as those of a representative panel of nasal *S. aureus* and *S. epidermidis* strains (2.7 µg/ml on average; Suppl. Fig. S2) suggesting that there is probably no additional self-resistance system involved.
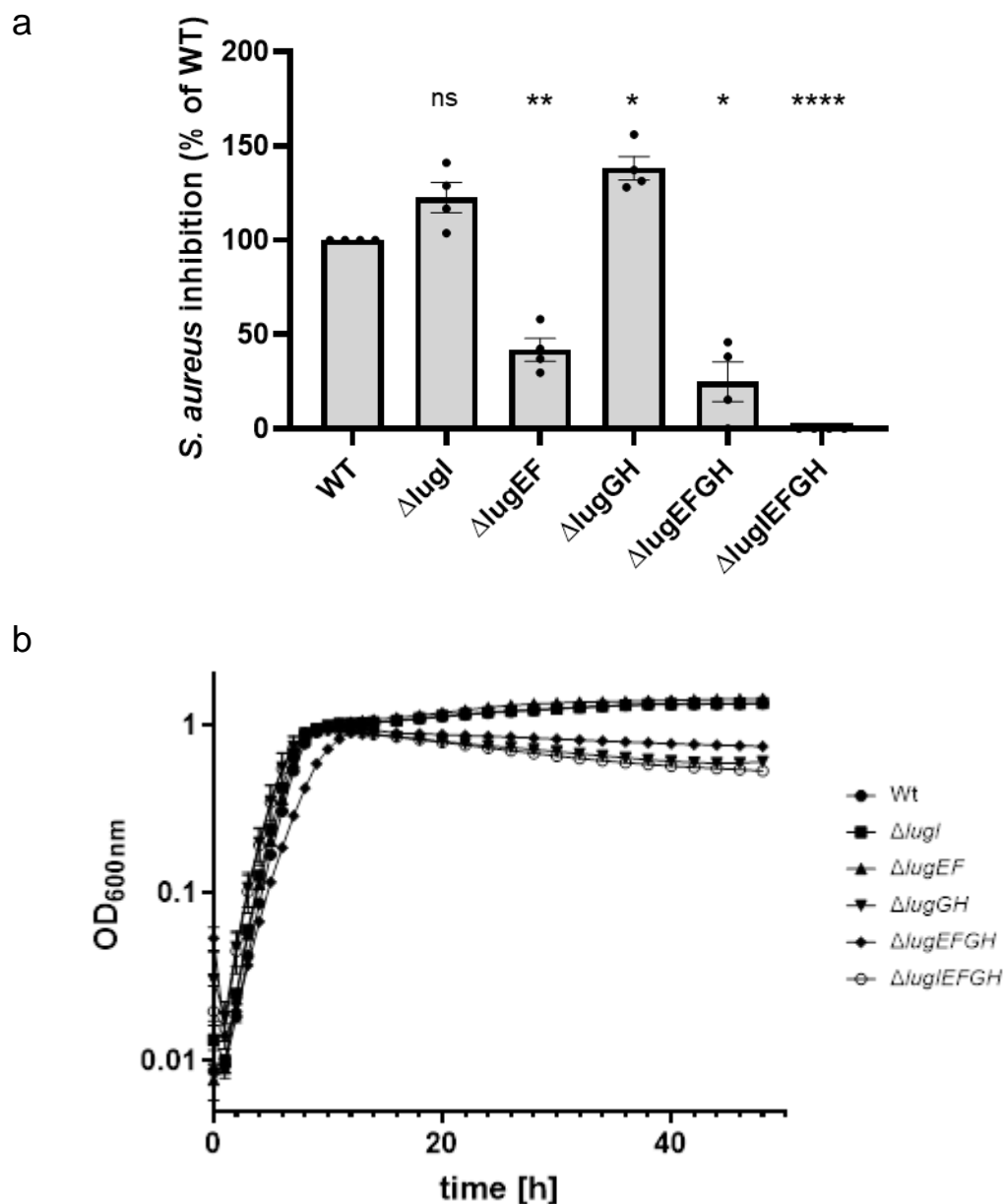

Figure 2. Impact of combinations of deletions of the lugIEFGH genes on S. lugdunensis lugdunin secretion (a) and growth (b). (a) Differences in inhibition zone distances around colonies of S. lugdunensis wild type (WT), set to 100%, or mutants with the indicated deletions on agar containing lugdunin-susceptible S. aureus. (b) Growth in broth culture of the strains shown in (a). Means and SEM of at least 4 (a) or 3 (b) independent experiments are shown. Significant differences were calculated by one-way ANOVA (Dunnett's multiple comparisons test) (*, P ≤ 0.05; **, P ≤ 0.01; ***, P ≤ 0.005).

To confirm the capacity of *lugIEFGH* to confer lugdunin resistance, the genes were cloned in different combinations in the pRB474 vector downstream of a constitutive promoter and introduced into *S. aureus* N315. *lugGH* expression led to a significantly increased lugdunin MIC (Fig. 3b), which confirms the important contribution of this subset of genes to lugdunin resistance. The additional expression of *lugEF* further raised the resistance of *S. aureus* to lugdunin, which supports the notion that full lugdunin resistance depends on the presence of all four ABC transporter genes. However, expression of *lugEF* alone did not cause a notable level of resistance. The presence of the entire operon *lugIEFGH* increased the lugdunin MIC to the highest observed level of 15.9 µg/ml indicating that the small *lugI* also contributes to resistance. When *lugI* was expressed in combination with *lugEF* (pRB474-lugIEF) no increased MIC compared to lugEF expression alone was observed. In contrast, *lugI* expression with *lugGH* (pRB474-lugIGH) enhanced the MIC to the same level as *lugEFGH* expression indicating that LugI might have a supporting effect with LugGH rather than with LugEF. Accordingly, the exclusive expression of *lugI* did not alter the susceptibility to lugdunin. The lugdunin MIC reached in *S. aureus* pRB474-lugIEFGH was identical to or even higher than that of *S. lugdunensis* IVK28, probably as a consequence of the high plasmid copy number (Fig. 3b).

The resistance conferred by the ABC transporters LugIEFGH is largely specific for native lugdunin

While some ABC drug exporters have broad substrate specificities, others are highly selective for only certain compounds [14]. The *lugIEFGH* genes were assessed for their capacity to protect *S. aureus* against lugdunin derivatives (see chemical structures 1-4 in Suppl. Fig. S3) and other antimicrobial compounds to elucidate the transporters' substrate range. The three derivatives enantio-lugdunin, 6-Trp-lugdunin and 2-Ala-lugdunin were selected, because they had similar activities as native lugdunin. 6-Trp-lugdunin was even slightly more active than native lugdunin. Since most other lugdunin derivatives showed no or only residual activity, we could include only the two active versions (9). The constitutive expression of LugIEFGH did not affect the susceptibility of *S. aureus* to the membrane-active cyclic peptide antibiotics daptomycin, and gramicidin S, or to the small non-peptide protonophors CCCP and nigericin, indicating that the resistance mechanism has a strict preference for the structure of lugdunin (Fig. 4a). LugIEFGH also conferred some degree of resistance to the lugdunin enantiomer (enantio-lugdunin), which has the same structure as regular lugdunin but an inverse D-/L-amino acid configuration [8, 9], albeit with a much lower efficacy as to native lugdunin. Similar though even less pronounced findings were obtained with 6-Trp-lugdunin, which contains a D-tryptophan at position six instead of a D-valine [9].
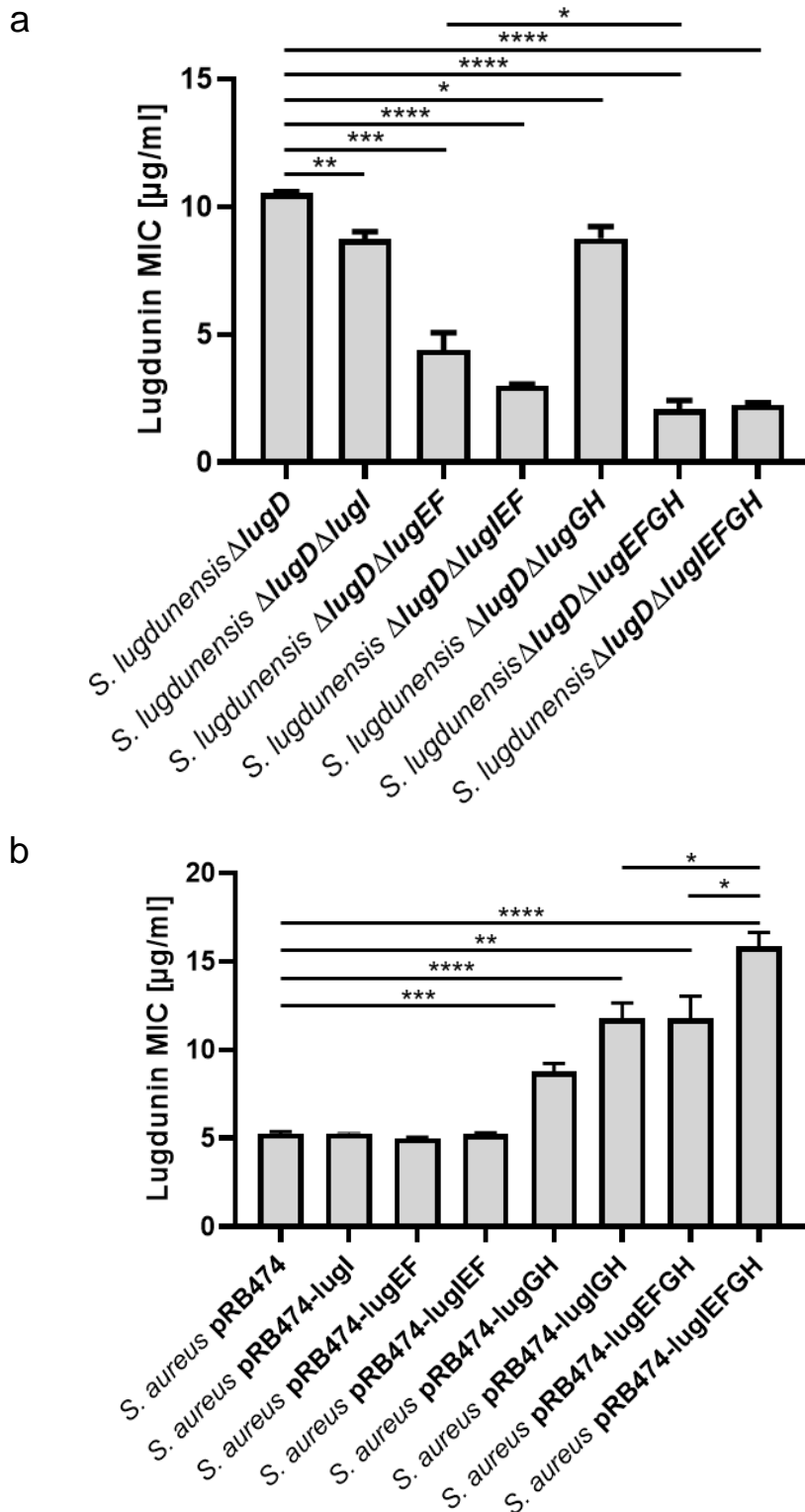
Figure 3. Impact of *lugIEFGH* deletion in the *S. lugdunensis* Δ*lugD* strain (a) or constitutive expression in *S. aureus* (b) on lugdunin susceptibility. Means and SEM of at least five independent experiments are shown. Significant differences were calculated by one-way ANOVA (Brown-Forsythe and Welsh) (*, P ≤ 0.05; **, P ≤ 0.01; ***, P ≤ 0.005).

In contrast, 2-Ala-lugdunin (D-alanine instead of D-valine at position two) [9] had equal antimicrobial activity against *S. aureus* with or without LugIEFGH, implying that no resistance against the 2-Ala congener was conferred. Thus, LugIEFGH are largely specific for lugdunin in its native structure, and lugdunin alterations at position two are less well tolerated by the transporter than alterations at position six.
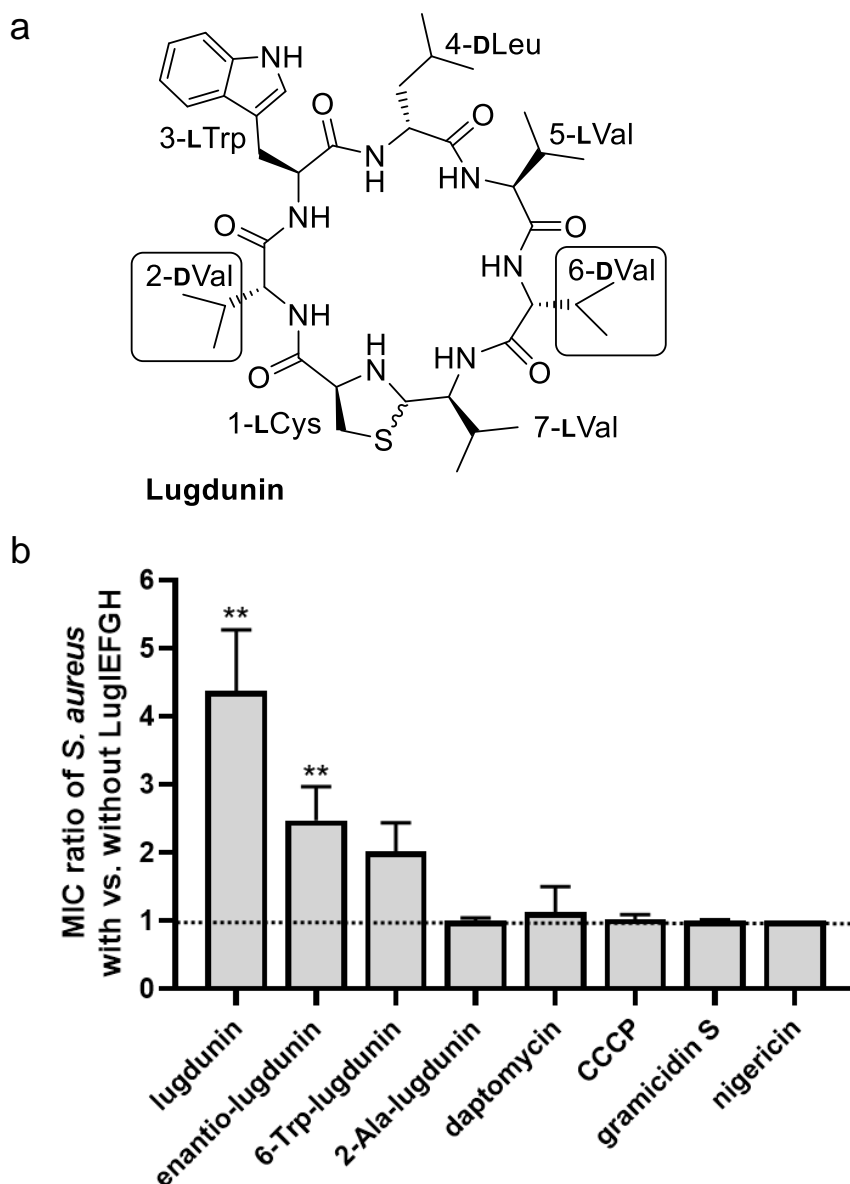

Figure 4. Impact of *lugIEFGH* on *S. aureus* susceptibility to lugdunin variants and other cyclic peptide antimicrobials. Chemical structure of lugdunin and positions of alterations in derivatives used in (b) are shown in (a). The ratios of MICs elucidated for *S. aureus* pRB474-lugIEFGH vs. *S. aureus* pRB474 is shown in (b). Means +/- SEM from at least three independent experiments and significant differences between MICs for the two strains, calculated by Student's multiple unpaired t-test (with Holm-Sidak correction) are shown (**, P ≤ 0.01). Mean MIC values for all compounds and both strains are listed in supplementary Table S2.

Discussion

Lugdunin, the first non-ribosomally synthesized antibiotic from human microbiomes, has a novel structure and an unusual protonophore-like mode of action, which distinguishes it from most of the antibiotics in clinical use [9]. Lugdunin causes proton leakage in synthetic, protein-free membrane vesicles, suggesting that it does not need to target a proteinaceous molecule to exert its antibacterial activity [9]. The atypical mode of action raised the question whether the bacterial producer strains would also use an unusual mechanism to achieve self-resistance to lugdunin. As shown for other cyclic peptides, lugdunin may be able to oligomerize in membranes [15-17], which might also have an influence on its recognition by the lugdunin transporters. We demonstrate that *S. lugdunensis* uses the four ABC transporter proteins LugEFGH for lugdunin secretion and self-resistance (Fig. 5), which is reminiscent of several other antimicrobial molecule producers [2, 18]. The use of two separate ABC transporters for antimicrobial secretion and self-resistance has previously been documented for instance for several lantibiotics and other bacteriocins [18]. Moreover, the phenol-soluble modulin (PSM) peptides produced by most *Staphylococcus* species are secreted by an ABC transporter complex, which is encoded by four genes most probably forming two separate transporters, PmtAB and PmtCD [19]. They confer self-resistance to PSMs and several other membrane-damaging cationic antimicrobial peptides (CAMPs) [20].
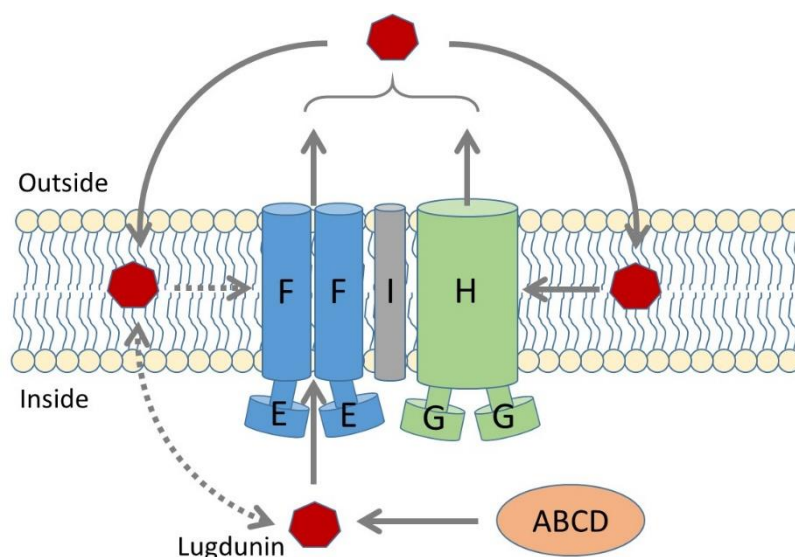
Figure 5. Model for the roles of LugIEFGH in lugdunin secretion and self-resistance. LugEF has a dominant role in lugdunin secretion and a minor role in lugdunin resistance. In contrast, LugGH is mostly responsible for self-resistance, presumably by taking lugdunin up from the membrane bilayer. LugI contributes to secretion and resistance by collaborating with the ABC transporters in a currently unclear fashion. Putative minor lugdunin passage ways are shown as dashed arrows. ABCD depicts the intracellular lugdunin-biosynthetic enzymes.

The roles of LugEF and LugGH in lugdunin export and self-resistance overlapped to some degree, which is also reminiscent of some bacteriocin-synthetic systems with two separate ABC transporters [21, 22]. LugGH had a dominant role in lugdunin resistance in *S. aureus*, which was even enhanced by the presence of LugI. Accordingly, LugGH had only a weak effect on lugdunin release in *S. lugdunensis.* Although deletion of *lugGH* in *S. lugdunensis* had only a minor effect on the MIC compared to *lugEF* deletion, it had a strong impact on the growth and fitness of lugdunin-producing *S. lugdunensis,* which is in agreement with its capacity to protect the producer against its product. The *S. lugdunensis lugGH* mutant released even slightly more lugdunin than the wild type for unclear reasons, maybe as a consequence of dysregulation of the lugdunin-biosynthetic process in these highly stressed mutant bacteria. This might also be the explanation for the unexpected strong impact of *lugEF* deletion in *S. lugdunensis* on the MIC, although LugEF does not change the MIC level in *S. aureus*. As for several other ABC exporters conferring resistance to membrane-active compounds, it can be assumed that LugH takes up its cargo from the membrane bilayer by opening the channel laterally (Fig. 5). In contrast to LugGH, LugEF did not seem to affect the producer's fitness but had a dominant impact on lugdunin release, probably by acquiring lugdunin from the biosynthetic machinery (LugABCD) in the cytoplasm. Nevertheless, LugEF also contributed to lugdunin resistance, maybe by exporting excess cytoplasmic or membrane-embedded lugdunin (Fig. 5). It is currently not clear if the two transporter systems form indeed a complex together with LugI. It is possible that LugEF may be associated with the biosynthesis machinery formed by LugABCD to directly export newly synthesized lugdunin, which, in addition to the stoichiometry of the LugIEFGH products, remains to be explored.

It remains unclear how LugI may contribute to lugdunin secretion and self-resistance, but it is obvious that its role in resistance depends on the presence of both ABC transporters. Accessory membrane proteins have been described for other ABC transporters, for instance the *S. aureus* VraDEH system, which confers resistance to CAMPs. In addition to the ATPase VraD and the integral membrane component VraE the system includes the small VraH protein, which is required for high-level resistance to gallidermin and daptomycin and has been denoted a "peptide resistance ABC transporter activity modulator" [23], a term also appropriate for LugI. VraH has a similar size and predicted membrane topology as LugI, but no obvious sequence similarity. Accessory integral membrane proteins are also known to complement ABC transporters secreting and conferring producer self-resistance to the lantibiotics epidermin and gallidermin [21, 22].

Only inversion of the lugdunin structure in enantio-lugdunin or a minor change at amino acid position six of lugdunin were tolerated by the resistance mechanism although resistance to these congeners was much less pronounced than for native lugdunin. In contrast, changes at

position two abrogated the capacity of LugIEFGH to confer resistance completely. The high selectivity distinguishes the lugdunin resistance mechanism from those to other antimicrobial molecules such as PSMs or from multi-drug ABC exporters such as Sav1866 [24] or AbcA [25, 26]. Slight modifications of lugdunin that maintain or even increase its antimicrobial activity will therefore make it difficult for LugIEFGH to neutralize such variants if they would be developed for clinical use, even if *lugIEFGH* could spread horizontally between different bacterial species. More detailed studies will be necessary to elucidate the molecular basis for the selectivity and elucidate if and which mutations in the self-resistance proteins might alter or broaden its preferences for peptide cargo.

LugIEFGH have never been found outside the *lug* operon of *S. lugdunensis*, neither in *S. aureus* nor other nasal microbiome members. Only a few members of the Bacillales order, mainly from the environmental or intestinal bacterial genera *Salinicoccus*, Planococcus, *Exiguobacterium,* or *Gracilibacillus*, respectively, harbor homologs of the *lugIEFGH* cluster, albeit without the lugdunin biosynthesis genes. Additionally, *Streptococcus mutans* genomes encode an ABC transporter with homology to LugGH, but lack LugI or LugEF homologs. Despite its lower G+C content, the *lug* gene cluster does not seem to constitute a promiscuous genetic element, which may restrict its mobility among species other than *S. lugdunensis.*

Materials and Methods

Strains and growth conditions. The *Staphylococcus* strains used in this study were *S. aureus* N315, *S. aureus* USA300 LAC, and *S. lugdunensis* IVK28. Further strains used for MIC determination were *S. aureus* N315 with plasmids pRB474, pRB474-lugI, pRB474-lugEF, pRB474-lugIEF, pRB474-lugGH, pRB474-lugIGH, pRB474-lugEFGH, and pRB474-lugIEFGH. The construction of the plasmids is described below. *E. coli* DC10B was used as the cloning host for further transformation in *S. aureus* N315 (expression of transporter genes) or *S. aureus* PS187 for subsequent phage transduction into *S. lugdunensis* IVK28 [27].

Basic medium (BM: 1% soy peptone A3 (Organotechnie SAS, France), 0.5% OHLY KAT yeast extract (Deutsche Hefewerke GmbH, Germany), 0.5% NaCl, 0.1% glucose and 0.1% K_2HPO_4, pH 7.2) was used as the standard growth medium and for MIC determinations. If necessary, antibiotic was used at a concentration of 10 µg ml^{-1} for chloramphenicol. *E. coli* transformants were grown in lysogeny broth (LB; Lennox)-medium (1% tryptone, 0.5% yeast extract, 0.5% NaCl; Carl Roth GmbH, Germany) supplemented with 100 µg ml^{-1} ampicillin or corresponding LB agar.

To analyze growth curves strains were grown overnight in BM with suitable antibiotics under continuous shaking at 37°C. Each strain was adjusted to OD_{600} =1 in MHB and 2.5 µl of the

bacterial stock solutions were pipetted to 500 µl MHB in a 48-well microtiter plate. The plates were incubated for 48 h under continuous shaking in a microplate reader and OD_{600} was measured every 15 minutes.

Synthetic lugdunin congeners and control compounds. All synthetic lugdunin derivatives were synthesized as described elsewhere [9]. Daptomycin (Cubicin) was purchased from MSD Sharp & Dohme GmbH (Haar, Germany), CCCP, gramicidin S and nigericin were obtained from SigmaAldrich (now Merck, Germany).

Generation of *S. lugdunensis* IVK28 knockout mutants. DNA manipulation, isolation of plasmid DNA, and transformation of *E. coli* were performed by use of standard procedures. Enzymes for molecular cloning were obtained from Thermo Fisher Scientific and New England Biolabs. For the generation of knock-out mutants the temperature-sensitive shuttle-vector pBASE6 was used and mutants were generated by allelic replacement as described previously [28]. Flanking regions of the genes to be deleted were amplified by PCR (Table 1), and ligated to shuttle vector pBASE6 after digestion with suitable restriction enzymes. Cloning was performed in *E. coli* DC10B from where sequence-verified plasmids were transferred to *S. aureus* PS187 by electroporation. Phage ϕ187 was used for transduction of *S. lugdunensis* IVK28 as described elsewhere [27]. Mutations in *S. lugdunensis* were confirmed by PCR amplification of the entire *lugJIEFGH* region with control primers and analysis of the fragment sizes in comparison to the wild type. For the construction of the *lugIGH* mutant the confirmed *lugGH* mutant was transduced with the plasmid for *lugI* deletion and the second deletion was performed in the Δ*lugGH* background.

Expression of ABC transporter genes in *S. aureus* N315. The transporters of *S. lugdunensis* IVK28 were cloned in pRB474 as follows. For the *lugEF* construct, the primers ABC1-down and ABC2-up (Table 2) were used to amplify *lugEF*, and the primers ABC regulator forw and ABC2-up were used to amplify *lugIEF.* To express only *lugI* the gene was amplified with primers ABC regulator forw and lugI rev. *lugGH* was generated with the primers ABC3-down and ABC4-up. For the generation of the *lugIGH* construct the plasmid pRB474-lugGH was digested with PstI and treated with alkaline phosphatase. Here, *lugI* was amplified with the primers ABC regulator forw and lugI rev Pst, digested with PstI and ligated into the PstI digested pRB474-lugGH. The correct orientation of *lugI* in front of *lugGH* was confirmed by sequencing. *lugEFGH* was generated with the primers ABC1-down and ABC4-up. The PCR fragment for *lugIEFGH* was amplified with the primers ABC regulator forw and ABC4-up. All PCR products and plasmid pRB474 were digested with PstI and SacI, to ligate the PCR fragments into pRB474. The resulting constructs pRB474-lugI, pRB474-lugEF, pRB474-

lugIEF, pRB474-lugGH, pRB474-lugIGH, pRB474-lugEFGH, and pRB474-lugIEFGH were transferred into *E. coli* DC10B [29] and, subsequently into *S. aureus* N315.

Analysis of lugdunin secretion. To analyze the capacity of *S. lugdunensis* IVK28 and its isogenic mutants to export lugdunin, an *S. aureus* inhibition assay was performed. *S. aureus* USA300 LAC was grown overnight in BM, and BM agar, cooled down to 50°C after autoclaving, was inoculated to a final OD of 0.00125 with this overnight culture. From this suspension defined 15 ml agar plates with 8.4 cm diameter were poured. *S. lugdunensis* strains were grown overnight in BM, centrifuged, and washed in 1/10 volume phosphate buffered saline (PBS) to remove residual cell-associated lugdunin. After a second centrifugation step, cultures were adjusted to an optical density (600 nm) of 20, and 10 µl of the suspensions were spotted on the solidified BM agar plates containing *S. aureus*. After drying of the spots, the plates were incubated at 37°C for 24 h and inhibition zones were photographed and analyzed with ImageJ software (version 1.8.0_112). For each experiment all strains to be analyzed were spotted on the same agar plate and the inhibition zone, defined as the distance between the *S. lugdunensis* IVK28 colony and the growing *S. aureus* cells, was defined as 100%.

MIC determination. Strains used for MIC determinations were grown overnight in BM, with chloramphenicol for plasmid containing strains, under continuous shaking at 37°C. Each strain was adjusted to $OD_{600}=0.0625$ in BM. The antimicrobial molecule stock solutions were serially diluted in BM in 96-well microtiter plates. Each well with 100 µl medium, and chloramphenicol if required, was inoculated with 2 µl of the $OD_{600}=0.0625$ bacterial stock solution. The plates were incubated at 37 °C for 24 hours under continuous shaking (160 rpm). OD_{600} of each well was measured with a microplate reader and the concentration leading to a 75%-growth reduction was calculated and defined as MIC value.

Statistics. Statistical analyses were performed using Graph Pad Prism 8.01. One-way ANOVA was used to compare MIC levels of individual strains against the reference strain, and t-tests were used for the comparison of MIC levels against various compounds with or without transporter genes.

References

1.   Krismer B, Weidenmaier C, Zipperer A, Peschel A. The commensal lifestyle of Staphylococcus aureus and its interactions with the nasal microbiota. Nat Rev Microbiol. 2017;15(11):675-87. Epub 2017/10/13. doi: 10.1038/nrmicro.2017.104. PubMed PMID: 29021598.

2.   Cotter PD, Hill C, Ross RP. Bacteriocins: developing innate immunity for food. Nat Rev Microbiol. 2005;3(10):777-88. Epub 2005/10/06. doi: 10.1038/nrmicro1273. PubMed PMID: 16205711.

3.   Otto M. Staphylococci in the human microbiome: the role of host and interbacterial interactions. Curr Opin Microbiol. 2020;53:71-7. Epub 2020/04/17. doi: 10.1016/j.mib.2020.03.003. PubMed PMID: 32298967.

4.   Arnison PG, Bibb MJ, Bierbaum G, Bowers AA, Bugni TS, Bulaj G, et al. Ribosomally synthesized and post-translationally modified peptide natural products: overview and recommendations for a universal nomenclature. Nat Prod Rep. 2013;30(1):108-60. Epub 2012/11/21. doi: 10.1039/c2np20085f. PubMed PMID: 23165928; PubMed Central PMCID: PMCPMC3954855.

5.   Medema MH, Kottmann R, Yilmaz P, Cummings M, Biggins JB, Blin K, et al. Minimum Information about a Biosynthetic Gene cluster. Nat Chem Biol. 2015;11(9):625-31. Epub 2015/08/19. doi: 10.1038/nchembio.1890. PubMed PMID: 26284661; PubMed Central PMCID: PMCPMC5714517.

6.   Janek D, Zipperer A, Kulik A, Krismer B, Peschel A. High Frequency and Diversity of Antimicrobial Activities Produced by Nasal Staphylococcus Strains against Bacterial Competitors. PLoS Pathog. 2016;12(8):e1005812. doi: 10.1371/journal.ppat.1005812. PubMed PMID: 27490492; PubMed Central PMCID: PMCPMC4973975.

7.   Sugimoto Y, Camacho FR, Wang S, Chankhamjon P, Odabas A, Biswas A, et al. A metagenomic strategy for harnessing the chemical repertoire of the human microbiome. Science. 2019;366(6471). Epub 2019/10/05. doi: 10.1126/science.aax9176. PubMed PMID: 31582523.

8.   Zipperer A, Konnerth MC, Laux C, Berscheid A, Janek D, Weidenmaier C, et al. Human commensals producing a novel antibiotic impair pathogen colonization. Nature. 2016;535(7613):511-6. doi: 10.1038/nature18634. PubMed PMID: 27466123.

9.   Schilling NA, Berscheid A, Schumacher J, Saur JS, Konnerth MC, Wirtz SN, et al. Synthetic Lugdunin Analogues Reveal Essential Structural Motifs for Antimicrobial Action and Proton Translocation Capability. Angew Chem Int Ed Engl. 2019;58(27):9234-8. Epub 2019/05/07. doi: 10.1002/anie.201901589. PubMed PMID: 31059155; PubMed Central PMCID: PMCPMC6618241.

10.   Bitschar K, Sauer B, Focken J, Dehmer H, Moos S, Konnerth M, et al. Lugdunin amplifies innate immune responses in the skin in synergy with host- and microbiota-derived factors. Nat Commun. 2019;10(1):2730. Epub 2019/06/23. doi: 10.1038/s41467-019-10646-7. PubMed PMID: 31227691; PubMed Central PMCID: PMCPMC6588697.

11.   Kotowska M, Pawlik K. Roles of type II thioesterases and their application for secondary metabolite yield improvement. Appl Microbiol Biotechnol. 2014;98(18):7735-46. Epub 2014/08/02. doi: 10.1007/s00253-014-5952-8. PubMed PMID: 25081554; PubMed Central PMCID: PMCPMC4147253.

12.   Locher KP. Mechanistic diversity in ATP-binding cassette (ABC) transporters. Nat Struct Mol Biol. 2016;23(6):487-93. Epub 2016/06/09. doi: 10.1038/nsmb.3216. PubMed PMID: 27273632.

13.   Mungan MD, Alanjary M, Blin K, Weber T, Medema MH, Ziemert N. ARTS 2.0: feature updates and expansion of the Antibiotic Resistant Target Seeker for comparative genome mining. Nucleic Acids Res. 2020. Epub 2020/05/20. doi: 10.1093/nar/gkaa374. PubMed PMID: 32427317.

14.   Orelle C, Mathieu K, Jault JM. Multidrug ABC transporters in bacteria. Res Microbiol. 2019;170(8):381-91. Epub 2019/06/30. doi: 10.1016/j.resmic.2019.06.001. PubMed PMID: 31251973.

15.   De Riccardis F, Izzo I, Montesarchio D, Tecilla P. Ion transport through lipid bilayers by synthetic ionophores: modulation of activity and selectivity. Acc Chem Res. 2013;46(12):2781-90. doi: 10.1021/ar4000136. PubMed PMID: 23534613.

16.   Duax WL, Griffin JF, Langs DA, Smith GD, Grochulski P, Pletnev V, et al. Molecular structure and mechanisms of action of cyclic and linear ion transport antibiotics. Biopolymers. 1996;40(1):141-55.   doi: 10.1002/(SICI)1097-0282(1996)40:1%3C141::AID-BIP6%3E3.0.CO;2-W. PubMed PMID: 8541445.

17.   Ghadiri MR, Granja JR, Buehler LK. Artificial transmembrane ion channels from self-assembling peptide nanotubes. Nature. 1994;369(6478):301-4. doi: 10.1038/369301a0. PubMed PMID: 7514275.

18.   Bierbaum G, Sahl HG. Lantibiotics: mode of action, biosynthesis and bioengineering. Curr   Pharm   Biotechnol.   2009;10(1):2-18.   Epub   2009/01/20.   doi: 10.2174/138920109787048616. PubMed PMID: 19149587.

19.   Chatterjee SS, Joo HS, Duong AC, Dieringer TD, Tan VY, Song Y, et al. Essential Staphylococcus aureus toxin export system. Nature medicine. 2013;19(3):364-7. Epub 2013/02/12. doi: 10.1038/nm.3047. PubMed PMID: 23396209; PubMed Central PMCID: PMCPMC3594369.

20.   Cheung GYC, Fisher EL, McCausland JW, Choi J, Collins JWM, Dickey SW, et al. Antimicrobial Peptide Resistance Mechanism Contributes to Staphylococcus aureus Infection. J Infect Dis. 2018;217(7):1153-9. Epub 2018/01/20. doi: 10.1093/infdis/jiy024. PubMed PMID: 29351622; PubMed Central PMCID: PMCPMC5939666.

21.   Peschel A, Schnell N, Hille M, Entian KD, Gotz F. Secretion of the lantibiotics epidermin and gallidermin: sequence analysis of the genes gdmT and gdmH, their influence on epidermin production and their regulation by EpiQ. Mol Gen Genet. 1997;254(3):312-8. Epub 1997/04/16. doi: 10.1007/s004380050421. PubMed PMID: 9150266.

22.   Hille M, Kies S, Gotz F, Peschel A. Dual role of GdmH in producer immunity and secretion of the Staphylococcal lantibiotics gallidermin and epidermin. Appl Environ Microbiol. 2001;67(3):1380-3. Epub 2001/03/07. doi: 10.1128/aem.67.3.1380-1383.2001. PubMed PMID: 11229936; PubMed Central PMCID: PMCPMC92739.

23.   Popella P, Krauss S, Ebner P, Nega M, Deibert J, Gotz F. VraH Is the Third Component of the Staphylococcus aureus VraDEH System Involved in Gallidermin and Daptomycin Resistance and Pathogenicity. Antimicrob Agents Chemother. 2016;60(4):2391-401. doi: 10.1128/AAC.02865-15.   PubMed   PMID: 26856834;   PubMed   Central   PMCID: PMCPMC4808217.

24.   Velamakanni S, Yao Y, Gutmann DA, van Veen HW. Multidrug transport by the ABC transporter Sav1866 from Staphylococcus aureus. Biochemistry. 2008;47(35):9300-8. doi: 10.1021/bi8006737. PubMed PMID: 18690712.

25.   Costa SS, Viveiros M, Amaral L, Couto I. Multidrug Efflux Pumps in Staphylococcus aureus: an Update. Open Microbiol J. 2013;7:59-71. Epub 2013/04/10. doi: 10.2174/1874285801307010059. PubMed PMID: 23569469; PubMed Central PMCID: PMCPMC3617543.

26.   Yoshikai H, Kizaki H, Saito Y, Omae Y, Sekimizu K, Kaito C. Multidrug-Resistance Transporter AbcA Secretes Staphylococcus aureus Cytolytic Toxins. J Infect Dis. 2016;213(2):295-304. Epub 2015/07/15. doi: 10.1093/infdis/jiv376. PubMed PMID: 26160745.

27.   Winstel V, Kuhner P, Rohde H, Peschel A. Genetic engineering of untransformable coagulase-negative staphylococcal pathogens. Nat Protoc. 2016;11(5):949-59. Epub 2016/04/23. doi: 10.1038/nprot.2016.058. PubMed PMID: 27101516.

28.   Geiger T, Francois P, Liebeke M, Fraunholz M, Goerke C, Krismer B, et al. The stringent response of Staphylococcus aureus and its impact on survival after phagocytosis through the induction of intracellular PSMs expression. PLoS pathogens. 2012;8(11):e1003016. doi: 10.1371/journal.ppat.1003016. PubMed PMID: 23209405; PubMed Central PMCID: PMCPMC3510239.

29.   Monk IR, Shah IM, Xu M, Tan MW, Foster TJ. Transforming the untransformable: application of direct transformation to manipulate genetically Staphylococcus aureus and Staphylococcus epidermidis. mBio. 2012;3(2). doi: 10.1128/mBio.00277-11. PubMed PMID: 22434850; PubMed Central PMCID: PMCPMC3312211.

30.   Omasits U, Ahrens CH, Muller S, Wollscheid B. Protter: interactive protein feature visualization and integration with experimental proteomic data. Bioinformatics. 2014;30(6):884-6. doi: 10.1093/bioinformatics/btt607. PubMed PMID: 24162465.

Supplemental Information

Table S1: Accession numbers of the proteins involved in lugdunin biosynthesis, transport and putative regulation

Protein	Accession number
LugJ	WP_002460039.1
LugI	WP_002460038.1
LugE	WP_002478838.1
LugF	WP_002478839.1
LugG	WP_002460034.1
LugH	WP_002460033.1
LugR	WP_002460032.1
LugA	WP_002492248.1
LugB	WP_081094477.1
LugC	WP_037540567.1
LugT	WP_002460022.1
LugD	WP_002478846.1
LugZ	WP_002478847.1
LugM	WP_002492211.1

Table S2: Mean MIC values in BM-medium of all tested compounds for *S. aureus* pRB474 and pRB474-lugIEFGH

Compound	MIC *S. aureus* pRB474	MIC *S. aureus* pRB474-lugIEFGH	Ratio
lugdunin	8.15	33.68	4.13
Enantio-lugdunin	31.3	69.75	2.23
6-Trp-lugdunin	16.43	31.05	1.89
2-Ala-lugdunin	40.17	39.93	0.99
daptomycin	2.17	2.17	1
CCCP	0.63	0.64	1.02
gramicidin S	2.75	2.74	1.00
nigericin	0.25	0.25	1.00
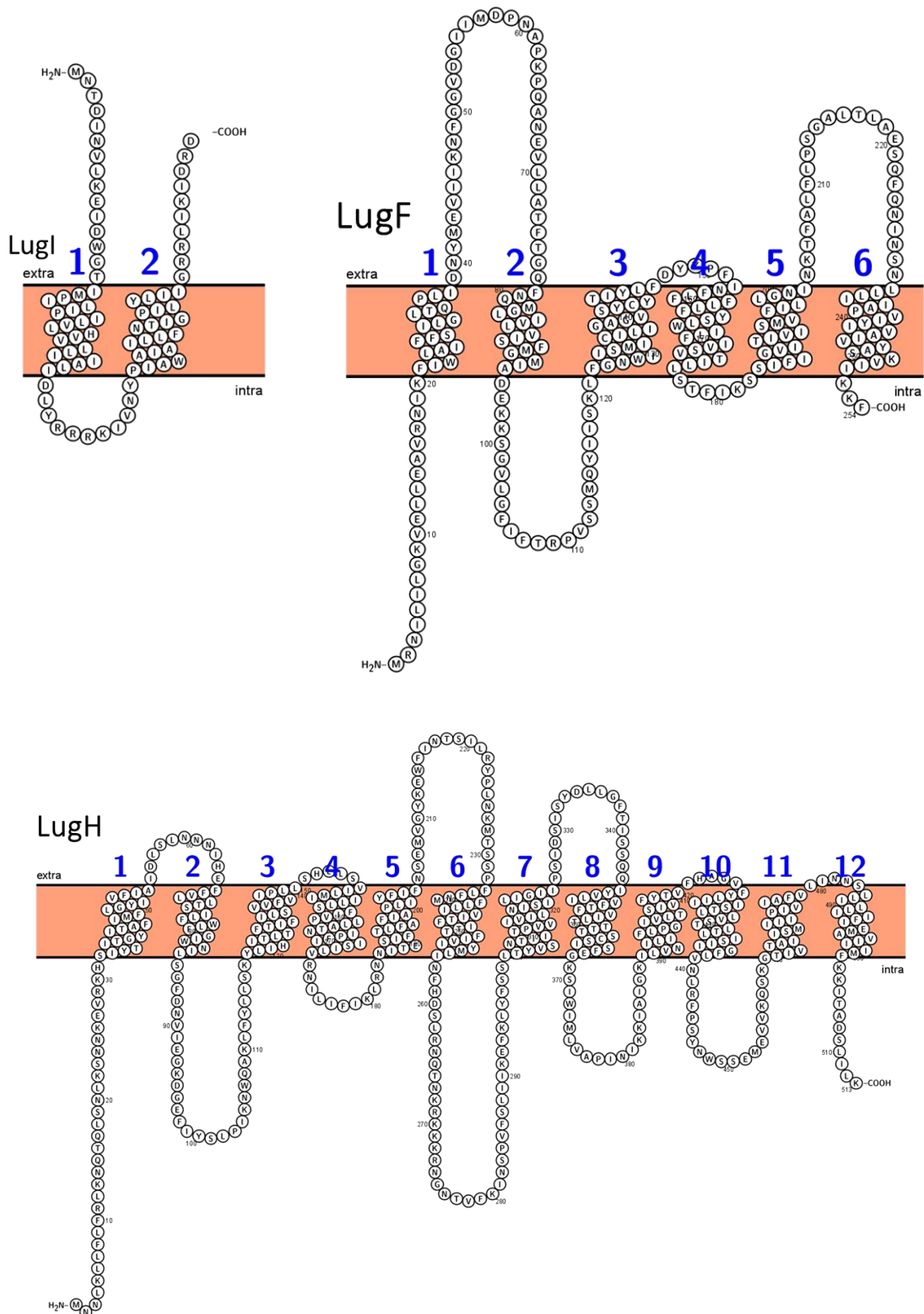
Fig. S1: Predicted transmembrane topologies of LugI, LugF, and LugH. The transmembrane topology for LugI, LugF, and LugH was predicted with the help of PROTTER (version 1.0; http://wlab.ethz.ch/protter/start/) [30].

Fig. S2: Comparison of lugdunin susceptibility of individual nasal *S. aureus* and *S. epidermidis* isolates. The MIC of lugdunin was tested against representative nasal *S. aureus* and *S. epidermidis* isolates. Shown are the medians with interquartile range for the two groups.

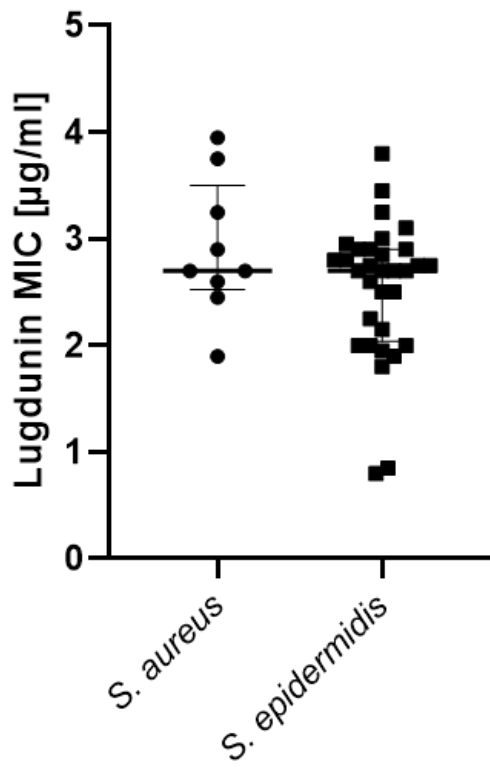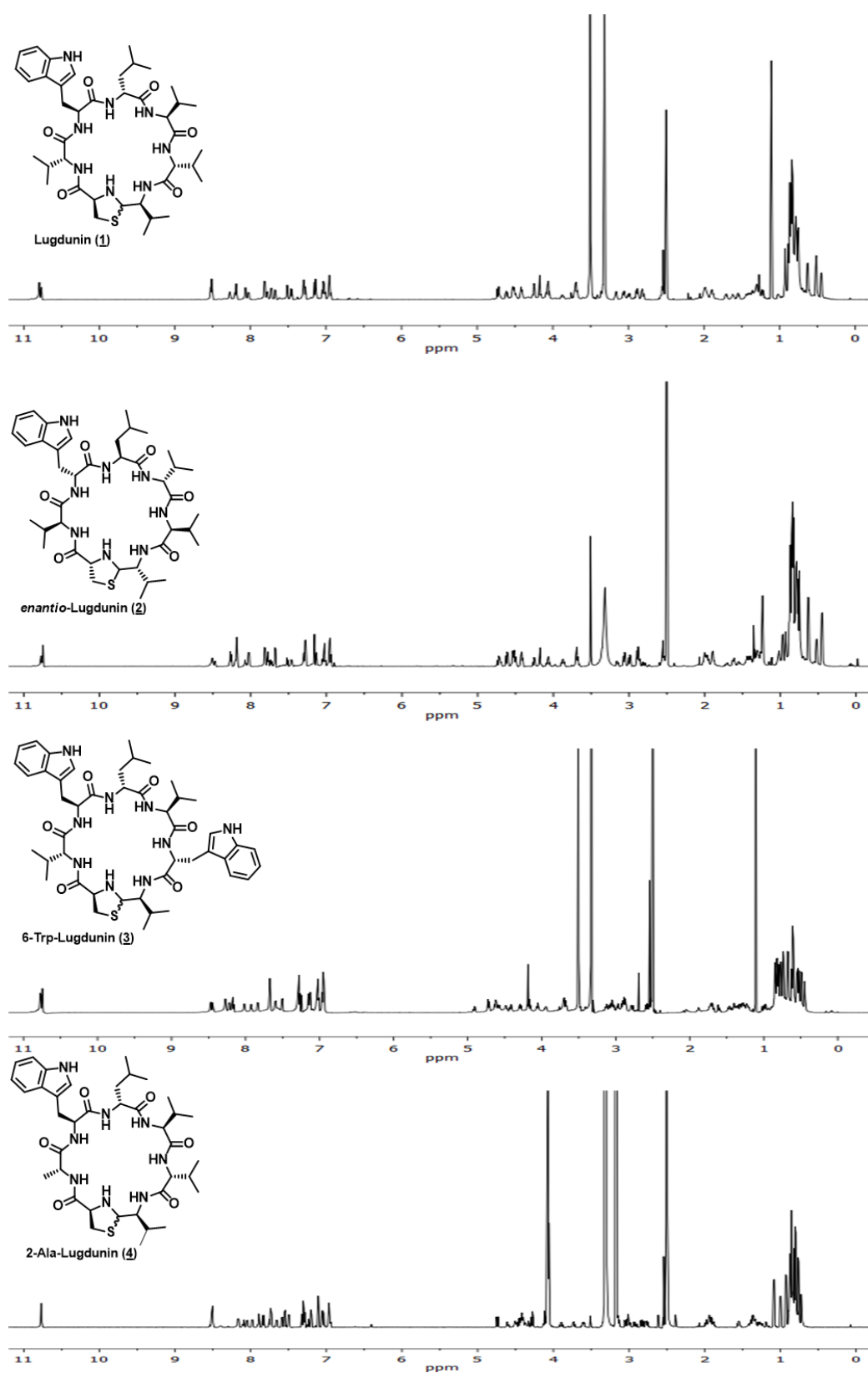**Fig. S3:** Chemical structural formula of synthetic lugdunin analogues **1** – **4** and ^{1}H NMR spectra thereof (d$_6$-dmso, 700 MHz, 303K).

Chapter 5 – General discussion

The human microbiome as a reservoir of secondary metabolites

The human body is home to a variety of microorganisms, including bacterial as well as fungal species, and viruses, which as a whole constitute the human microbiome [1]. The microbiome has been found to govern the human host's wellbeing, as perturbations in its composition (dysbiosis) are linked to the emergence of diseases and medical conditions such as obesity, diabetes, or inflammatory bowel disease [2-4]. In addition, commensal members of the microbiome contribute to the host defense against (exogenous) pathogenic species, e.g., by occupying pathogens´ potential colonization sites and thereby preventing infections [5-7]. Interestingly, the human body also hosts facultative pathogenic bacterial species (or pathobionts) such as *S. aureus*, which can switch between a commensal and a pathogenic state and cause a variety of infections. As commensal, *S. aureus* colonizes the nasal cavity of ~30% of the human population and nasal carriage elevates the risk of infection with the endogenous *S. aureus* strain [8, 9]. The reasons, however, why only a subset of individuals is colonized by *S. aureus* are still largely unknown. Thus, a better understanding of the mechanisms shaping microbiome composition and dynamics is required. That would not only help identify the factors facilitating/promoting pathogen colonization but also develop strategies to prevent pathogen colonization events and reduce the risk of infections.

The composition of bacterial communities is generally governed by host-bacteria and interbacterial interactions [10, 11]. The latter are largely mediated by secondary metabolites, which are diverse small molecules with a wide range of bioactivities and include antimicrobial bacteriocins, signal-interfering molecules and metal-scavenging metallophores. In particular, the release of bacteriocins is thought to impact bacterial communities tremendously, as close-by microbes are directly inhibited in their growth [12].

Bacteriocins are typically encoded by complex and diverse biosynthetic gene clusters (BGCs) and many of them are located on mobile genetic elements (MGE) such as transposons or plasmids. This makes bacteriocin production a strain-specific more than a species-specific trait. It also promotes recombination and distribution of BGCs via horizontal gene transfer, as indicated by the frequent acquisition and loss events of bacteriocin-related genes [13, 14].

A systematic metagenome analysis revealed that the human microbiome harbors a huge reservoir of BGCs for a broad range of secondary metabolites, which are widely distributed across different bacterial taxa [15]. Interestingly, most of these BGCs have never been studied or even described. This illustrates, on the one hand, how little is known about the human microbiome and the ecological role of secondary metabolites and, on the other hand, that the human microbiome represents a rich source of novel compounds that awaits to be explored.

The human skin and nose represent habitats with a variety of stressors bacteria have to cope with in order to survive or persist, such as limited nutrient availability, acidity, or high salt concentrations. This suggests a fierce competition amongst bacteria which also involves the release of bacteriocins. Indeed, studies on skin and nose microbiomes revealed that staphylococci are frequent producers of bacteriocins, such as lantibiotics, sactibiotics, thiopeptides to name a few. [16, 17]. Recently, a first-in-human phase 1 study demonstrated that topic administration of *Staphylococcus hominis* A9, a human skin isolate producing the lantibiotic ShA9, significantly reduced the abundance of *S. aureus* at atopic dermatitis (AD) sites, which often causes AD exacerbations by promoting inflammation [18]. This human trial underlines the potential of human microbiome-derived bacteriocins and/or their producers to influence microbiome compositions and as putative bacteriotherapy strategy against pathobionts.

In a screening of nasal bacteria from healthy volunteers, Janek et al. investigated 89 staphylococcal strains of which the vast majority (84%) was found to produce antimicrobial compounds [16]. Interestingly, many isolates displayed narrow but different antimicrobial activity patterns, indicating a huge pool of diverse bacteriocins. Two of these nasal isolates were of particular interest as they displayed antimicrobial activities against MRSA: The first one is *S. lugdunensis* IVK28, producing lugdunin, the first human microbiome derived non-ribosomal peptide (NRP) with antimicrobial activity and the founding member of the antibiotic class of fibupeptides [19]. The second one is *S. epidermidis* IVK83, producing epifadin, the first staphylococcal bacteriocin synthesized by NRP synthetases (NRPS) and polyketide synthases (PKS).

Epifadin, an unusual antimicrobial molecule derived from the human microbiome

Firmicutes and Actinobacteria are amongst the most frequent phyla of the human nasal microbiome and include genera such as *Staphylococcus*, *Streptococcus*, *Corynebacterium* and *Cutibacterium* [20, 21]. Interestingly, several studies based on the nasal microbiome demonstrated that the presence of *S. epidermidis* negatively correlates with some of these

nasal microbiome members, suggesting that they may be major competitors of *S. epidermidis*. For instance, both, *S. epidermidis* and *C. acnes* produce various antimicrobials that are capable of inhibiting each other [22]. Similarly, the majority of nasal *S. epidermidis* isolates inhibits *C. pseudodiphteriticum* and *D. pigrum* [16]. Furthermore, phenol soluble modulins (PSMγ and PSMδ) produced by *S. epidermidis* synergize with host derived antimicrobial peptides, resulting in an enhanced killing of *S. pyogenes* [23]. Within the genus *Staphylococcus* nasal *S. aureus* carriage is negatively correlated with *S. epidermidis* [24], probably due to multifactorial reasons. Production of the serine protease ESP by *S. epidermidis* strains displays potent antibiofilm and anti-colonization activity against *S. aureus* and an epidemiological analysis could correlate the presence of ESP-producing *S. epidermidis* with a decreased abundance of *S. aureus* in the human nose [25]. Further, PSMs, in particular PSMδ [26], or bacteriocins such as epidermin [27, 28], epilancin 15x [29] or Pep5 [30], all antimicrobial molecules produced by *S. epidermidis,* have been shown to impair *S. aureus* growth. Intriguingly, the human nasal isolate *S. epidermidis* IVK83 inhibits a broad spectrum of bacteria, including most of the above-mentioned nasal inhabitants. This could be attributed to the production of epifadin, a novel effective weapon in the arsenal of *S. epidermidis* that enables epifadin producing strains to outcompete major competitors.

Besides its broad spectrum of inhibition, another special feature of epifadin is its extraordinarily short lifetime. We could demonstrate that light-exclusion and acidity (pH 5) are prerequisites for epifadin stability. Interestingly, the nostrils represent a habitat with reduced light exposure, while the skin represents an acidic environment with an average pH around 5 and varying light exposure depending on the body site [31]. Since *S. epidermidis* is a frequent colonizer of the skin and nose it can be assumed that epifadin is particularly effective in these environments. However, even under favorable conditions epifadin is unstable, which may be the reason why epifadin is constitutively produced in order to display its full antimicrobial potential. Albeit described for some bacteriocins such as enterocin B and lacticin 3147 [32, 33], constitutive production of bacteriocins is rather uncommon. In fact, bacteriocin biosynthesis can be highly cost-intensive and can have a huge impact on physiological fitness, which is why it is usually strictly regulated. Thus, it is tempting to speculate that the overall benefit of epifadin release overweighs the cost of its production.

When considering possible collateral damage on mutualistic bacteria or the host, the low stability of epifadin may not necessarily be disadvantageous since it can probably not reach concentrations toxic for these off-targets. Thus, the production of broad-spectrum bacteriocins with a short lifetime such as epifadin may represent a well-directed strategy for bacteria to outcompete a broad range of close-by competitors and simultaneously reduce negative side effects on mutualistic bacteria or the host.

As mentioned above, *S. epidermidis* IVK83 inhibits microbiome-associated pathobionts, suggesting that epifadin producing bacteria may contribute to the exclusion of pathobionts such as *S. aureus* in some individuals. This assumption is supported by our findings that the production of epifadin completely eradicated *S. aureus in vitro* and significantly reduced *S. aureus* nasal carriage *in vivo*. The link between bacteriocin production and pathogen exclusion is also exemplified by lugdunin-producing *S. lugdunensis*, whose presence within the nasal microbiome was shown to correlate with a 6-fold reduced risk of *S. aureus* nasal carriage in humans [19]. However, the lugdunin BGC appears to be present in virtually all *S. lugdunensis* genomes, whereas the epifadin BGC is encoded on a plasmid in a strain-specific manner. A total of five *S. epidermidis* strains harboring the epifadin BGC could be isolated in three different countries from different body sites of the skin and nose, which indicates a widespread ecological relevance of epifadin. However, the actual frequency of epifadin production and its role and impact on the human microbiome remain to be elucidated. Nevertheless, the application of epifadin-producing *S. epidermidis* as probiotic for the prevention of *S. aureus* nasal carriage may be considered in the future, analogous to *S. hominis* ShA9 or *S. lugdunensis* [18, 19].

Another option for the decolonization or treatment of pathobionts would be the application of purified antimicrobial compounds. The antibiotic mupirocin is currently used for decolonization of nasal MRSA; however, mupirocin resistance is steadily increasing [34, 35]. Thus, it demands novel compounds such as epifadin, which has shown to be highly potent against *S. aureus* even at low concentrations. The application of putative therapeutics generally requires extensive knowledge about the structure, physicochemical properties, and safety of the compound in order to generate appropriate formulations. However, due to its instability and a concomitant low yield of the purified active compound, structure elucidation and further characterization of epifadin turned out to be difficult. Nonetheless, partial structure elucidation was possible, and MS/MS (tandem-mass spectrometry) as well as NMR (nuclear magnetic resonance) confirmed that the N-terminal part of epifadin is composed of L-Phe, D-Phe, L-Asp, D-Asn and L-Ala, as predicted by the online tool antiSMASH. The N-terminal peptide moiety is most likely linked via a discontinuous polyene chain (tetraene - six single bonds - diene) to a C-terminal L-Asp, which may be further modified to a tetramic acid. The presence of the latter, albeit not yet confirmed by NMR analysis, is supported by the genetic architecture of the epifadin BGC. Here, the domain organization of the NRPS/PKS encoded by *efiE* resembles that of *mloJ* of the antibiotic malonomycin BGC, which catalyzes the formation of the tetramic acid via a Dieckmann cyclization [36].

Interestingly, the UV spectrum of purified epifadin displayed three characteristic absorbance maxima around 220 nm (~215 nm for peptide bonds), 280 nm (aromatic amino acids) and 383

nm. As for the latter, similar absorptions could be observed for amphotericin B, a polyketide antimycotic produced by *Streptomyces nodosum* [37], or militarinone C, a pyridine alkaloid with a tetramic acid moiety produced by *Paecilomyces militaris* [38]. Here, the characteristic absorptions are attributed to the polyene parts of these molecules, which corroborates that epifadin also contains polyene parts.

Polyenes have been shown to be susceptible to isomerization events caused by light, which can result in a more stable form, e.g., in case of candicidin D, or to a loss of activity in case of marinomycins A–C [39-41]. Thus, a polyene structure may explain the observed light susceptibility of epifadin. In addition, polyenes seem to be a common trait among antimycotics as they are present in nystatin, natamycin, amphotericin A/B, and candicidin D [39, 42]. Interestingly, epifadin-producing *S. epidermidis* IVK83 also displays antifungal activities against *Saccharomyces cerevisiae* and *Candida albicans*, the latter being a pathobiont that can be frequently found in the gastrointestinal (GI) tract of humans [43]. The human skin microbiome inhabits several fungal species, such as *Malassezia*, *Aspergillus*, *Cryptococcus*, *Penicillium* and others, of which some are also associated with infections [44]. Whether epifadin is capable of inhibiting skin fungal species is unknown. However, although structure elucidation is still ongoing, which would allow further characterization of epifadin and chemical synthesis of more stable derivatives, epifadin or its derivatives may be considered not only for antibacterial but also for antifungal therapy in the future.

We could demonstrate that an unknown gene cluster consisting of an unusual set of NRPS, PKS, one hybrid NRPS/PKS and genes for NRPS biosynthesis is responsible for the production of epifadin. Only a few examples of NRPS have been described in *Staphylococcus*: in *S. lugdunensis* an NRPS system has been linked to the production of the bacteriocin lugdunin [19] while a hybrid NRPS/PKS with some similarity to enzymes of yersiniabactin biosynthesis has been involved in the synthesis of an unknown putative metallophore (lugdubactin) (still ongoing unpublished work). The other NRPS systems have been described in *S. aureus* and other staphylococci and linked to the production of pyrazinone-containing aureusimines [45, 46]. Remarkably, neither PKS nor hybrid NRPS/PKS systems have ever been described before in *Staphylococcus*. Thus, the epifadin operon is not only the first staphylococcal gene cluster encoding such systems, but also the first that links PKS and hybrid NRPS/PKS to bacteriocin production in *Staphylococcus*.

S. epidermidis and *S. saccharolyticus* [47] appear to be the only staphylococcal species to harbor the epifadin gene cluster, although clusters with similar gene organization can be found across several plant-associated *Lactococcus lactis* strains (e.g., KF147) [48, 49] and oral *Streptococcus mutans* strains (e.g., UA140) [50]. Whether the molecule(s) produced by the

streptococcal and/or lactococcal gene cluster are identical to epifadin or their biosynthesis only resembles that of epifadin is uncertain because of the lack of structural information about these molecule(s). Although their amino acid composition is similar to that of epifadin based on the antiSMASH prediction, it appears that these molecules have functions different from those of epifadin or that these bacteria use their compounds for different purposes. The lactococcal and streptococcal molecules have been shown to protect these bacteria from oxygen and oxidative stress [48, 50], but differences in H_2O_2 protection between epifadin-producing and non-producing *S. epidermidis* IVK83 could not be observed. However, in contrast to *S. epidermidis*, both *Lactococcus* and *Streptococcus* lack catalase-encoding genes, making them more susceptible towards oxidative stress. Thus, these bacteria may require epifadin-like molecules in order to cope with oxidative stress. In addition, *S. epidermidis* IVK83-derived epifadin is susceptible to oxidation since supplementation of the DMSO extracts with 6-O-palmitoylascorbic acid, an antioxidant, could strongly reduce its instability. Thus, it can neither be confirmed nor excluded that the observed protective activity in *Lactococcus* and *Streptococcus* is due to epifadin-like molecules that "snatch away" the atmospheric oxygen or ROS, or rather to different but similar compounds. Epifadin produced by *S. epidermidis* displays an antimicrobial activity against several nasal inhabitants, whereas antimicrobial activities of the lactococcal and streptococcal molecules have not been described so far. Thus, the question whether these molecules are identical remains to be answered. If it should turn out that those molecules are indeed identical to epifadin, it would be an outstanding example of how different bacteria can use the same secondary metabolite class to cope with distinct stressors possibly to adapt to different environments.

The two NRPS systems of the epifadin gene cluster are predicted to incorporate the above-mentioned amino acids, whereas the three PKS and the PKS part of the hybrid system are most likely responsible for the incorporation of the polyene part. However, structure prediction, in particular of the PKS part, turned out to be difficult. Of the four PKS-encoding genes, only *efiB* encodes for an acyltransferase (AT), which is important for building block selection and loading, and hence for the elongation process [51]. Thus, this system most likely represents a noncanonical modular type-I PKS system with EfiB as a free-standing trans-AT that is probably used by each of the PKS modules EfiC, EfiD and the hybrid EfiE [52, 53]. AntiSMASH predicts EfiB to utilize malonyl-CoA as substrate. However, the number of C-atoms incorporated would not be sufficient to generate the polyene part of epifadin, if each module were to be used only once. There are other examples of PKSs where modules are iteratively used in order to generate the whole molecule: borrelidin in *Streptomyces parvulus* Tü4055, is synthesized by six PKS modules, although eight modules have been predicted to be required for the nonaketide product [54, 55]; and the undecaketide stigmatellin produced by *Stigmatella*

aurantiaca using only nine PKS modules, although ten extension cycles were thought to be required [56]. Thus, one may assume that EfiC-E are also used more than once to generate the polyene.

The three PKS genes and the hybrid NRPS/PKS gene are interspaced by *efiO*, which encodes a putative phytoene dehydrogenase/NAD(P)/FAD-dependent oxidoreductase. Phytoene dehydrogenases (desaturases) have been shown to play an important role in carotenoid biosynthesis, as they introduce double bonds into phytoenes (mostly tetraterpenes) via a multi-step process, resulting in intermediates that eventually become carotenoids [57]. In *S. aureus*, the dehydrosqualene (4,4′-diapophytoene) desaturase CrtN converts dehydrosqualene via double bond formation into 4,4'-diaponeurosporene, an intermediate that is further enzymatically modified to staphyloxanthin, a yellow pigment responsible for *S. aureus* characteristic color and a virulence factor [58, 59]. Whether EfiO exhibits a similar function to CrtN, and to what extent EfiO is involved in double bond formation of the polyene remains unknown. Furthermore, the possibility that EfiO has even the opposite function of phytoene dehydrogenases cannot be excluded: since both EfiC and EfiD contain dehydratase and ketoreductase domains, which usually catalyze double bond formation in polyketides, EfiO may be responsible for the reintroduction of single bonds, resulting in the discontinuous polyene chain of epifadin. Although the exact function of EfiO remains to be elucidated, its modification must be important, since an *efiO* knockout resulted in a complete lack of epifadin production in *S. epidermidis* IVK83.

Aside from biosynthetic genes, the *efi* cluster also harbors the two genes *efiG/H* encoding putative ATP-binding cassette (ABC) transporters. In general, bacteriocin BGCs contain their cognate transporter(s) in order to specifically export the bacteriocin or its precursors, which in some cases are processed to the mature form during transport, e.g., some lantibiotics [60, 61]. In addition, transporters can provide (cross) immunity against the cognate or related bacteriocins. In an attempt to generate an inducible epifadin overexpression strain of IVK83, we exchanged the native promoter of the epifadin gene cluster with a xylose-inducible promoter, thus generating a mutant strain that did not express cluster-related genes, including *efiG/H*, unless xylose was added to the culture medium. However, no visible inhibition was observed when the epifadin-producing wild type *S. epidermidis* IVK83 was spotted on a lawn of the mutant strain in absence of induction (data not shown), indicating that *efiG/H* may not confer resistance towards epifadin. Interestingly, of the 16 *S. epidermidis* strains tested for their susceptibility to epifadin, nine (56%) were not inhibited by *S. epidermidis* IVK83 and the remaining strains displayed only minor (19%) or moderate (25%) inhibition. Thus, it may be assumed that the majority of the *S. epidermidis* strains are intrinsically resistant by an unknown mechanism. Attempts to knockout *efiG/H* even in a non-producing IVK83 mutant have not been

successful so far, which would be necessary for further characterization of the two extremely similar transporters. Thus, further work is required in order to elucidate the actual role of EfiG/H in epifadin resistance and/or its export.

Secretion of and immunity to the antimicrobial lugdunin in *S. lugdunensis*

In contrast to EfiG/H, the roles of the two transporters LugEF and LugGH encoded within the lugdunin BGC in *S. lugdunensis* have recently been elucidated. We could demonstrate that the two ABC transporters exhibit different but overlapping roles in lugdunin export (LugEF) and resistance (LugGH), with the small accessory putative membrane protein LugI contributing to both. Remarkably, the two transporters and LugI are needed to generate full level resistance [62].

Distinct functions of the transporters encoded within bacteriocin BGCs seem to be common in bacteria and have been described before, e.g., for lantibiotic BGCs that harbor *lanT,* coding for lantibiotic export proteins, and *lanFEG* coding for lantibiotic immunity/resistance proteins [61]. Although these transporters are often assigned a specific role, they may also display overlapping and ancillary functions. For instance, the knockout of *nisFEG* in *L. lactis* resulted in a decrease not only in nisin immunity but also in nisin production, despite the presence of a functional *nisT* [63]. Similar observations could also be made for the lantibiotic epidermin/gallidermin [64, 65]. In contrast to the nisin BGC, epidermin/gallidermin BGCs also harbor *lanH*, which encodes an accessory membrane protein involved in immunity and production of the respective bacteriocin, probably in an analogous way to LugI for lugdunin production. Accessory membrane proteins can occasionally be found among different bacteriocin BGCs, particularly in lantibiotics, where they often contribute to immunity and production of its cognate bacteriocin [66-68]. However, how accessory proteins contribute to resistance and bacteriocin production is still largely unknown.

ABC transporters usually consist of nucleotide-binding domains, responsible for energy supply, and transmembrane domains, responsible for substrate recognition [69]. Although ABC multi-drug resistance (MDR) transporters exist that facilitate export of various molecules, most ABC transporters appear to be highly substrate specific, which is partially reflected by the low sequence conservation of their recognition sites. This appears also true for the lugdunin ABC transporters LugIEFGH, which confer only partial protection, if any, against lugdunin derivatives. Structure elucidation of the transporter system is planned for the future, which will not only help identify the binding sites of lugdunin but also extend our knowledge on the mode

of interactions of lugdunin, the two transporters LugEF/GH and the accessory membrane protein LugI.

A comparative analysis of nasal microbiomes suggests siderophores contribute to *S. lugdunensis* nasal colonization

The lugdunin BGC appears to be present in virtually all *S. lugdunensis* genomes, and our previous study has shown that *S. lugdunensis* nasal carriage is correlated to a 6-fold reduced risk of *S. aureus* nasal carriage in hospitalized individuals, probably due to the production of lugdunin [19]. In our study, we investigated *S. lugdunensis* - *S. aureus* correlation in a cohort of 270 healthy individuals. Again, in *S. lugdunensis* carriers we could observe a 5-fold reduced risk of being colonized by *S. aureus*, in agreement with the previous observation [19]. The observed rate of *S. lugdunensis* nasal colonization was 6.3%, which is lower than the 9.1% and 9.3%, respectively, described in other studies [19, 70]. By monitoring a cohort of eight *S. lugdunensis* carriers and a control group of four non-carriers over 23 months with culture-based methods, we ascertained *S. lugdunensis* carriage to be partially dynamic, with four individuals being persistent carriers and eight being intermittent carriers. Dynamics in nasal microbiome compositions are influenced by many factors. Aside from interbacterial interactions between microbiome members, they include environmental factors like transitions between seasons and the concomitant changes in temperature, humidity, pollen dispersion and hours of sunlight. Also smoking or infections and subsequent antibiotic treatment have shown to affect the microbiome over time [71, 72].

At two time points of our study, metagenome analyses were performed in order to elucidate nasal microbiome compositions associated with *S. lugdunensis* carriage. Several groups have investigated nasal microbiome compositions for various reasons, e.g., in order to identify a nasal core microbiome, to look for differences in microbiome compositions between various nasal sites, between healthy and diseased individuals with different ages or sex, or to elucidate correlations between bacteria and their ecological environment that could explain their absence or presence in the host [1, 73-78]. While many of those approaches used 16S rRNA amplicon sequencing, which provides only limited information as it often fails to resolve taxonomies beyond genus level, our metagenome analysis is based on the more precise whole-genome shotgun sequencing. Thus, our study is one of the first that allows microbiome description on a species level.

Nasal bacterial density and composition can be considerably diverse among human individuals. Using 16S rRNA sequencing in a representative cohort of 178 volunteers, Liu et

al. could identify seven so called "community state types" (CSTs), which are defined by the prevalence and abundance of specific bacterial species [74]. We found *S. lugdunensis* to be associated with CST3, CST5 and CST7, which are dominated by coagulase negative *Staphylococcus* species, *Corynebacterium* spp. and *Dolosigranulum*, respectively. Interestingly, while CST7 appeared to be stable over time, a consistent transition from CST5 to CST3 could be observed. Since CST3 and CST5 displayed similar compositions in our cohort and varied primarily in the abundances of the dominating bacteria, both CSTs probably represent dynamic variants of the same CST. Among the most abundant species within the different CSTs were *S. epidermidis*, *C. accolens* and *Dolosigranulum pigrum*, which is in agreement with previous studies [74, 79].

With around 15 different species, the genus *Corynebacterium* was the most diverse taxon in our cohort, similar to observations by others [79]. Corynebacteria are frequent colonizers of moist body sites, such as the nose, and interestingly, several interactions between corynebacterial and staphylococcal species have been described. For instance, *C. accolens* is positively correlated with *S. aureus* as it occurs relatively often in *S. aureus* carriers, and both, *S. aureus* and *C. accolens* have been shown to support each other's growth *in vitro* [20]. A positive correlation could also be observed in our study. In contrast, *C. pseudodiphtheriticum* is mainly found in *S. aureus* non-carriers and only partially profits from co-culture with *S. aureus* at the expenses of the latter [20]. Nasal *S. aureus* interference upon *Corynebacterium* exposure has also been reported by others, although the underlying mechanisms yet remain to be elucidated [80, 81]. Nevertheless, the findings of Hardy et al. [82] and Ramsey et al. [83] may provide some evidence of these antagonistic relationships. They showed that *C. pseudodiphtheriticum* and *C. striatum* interfere with *S. aureus* by targeting the *agr* (*agrBDCA*) quorum sensing system and *agr*-regulated virulence factors (PSMs). Interestingly, while inactivation of *agrBDCA* or deletion of *psm* genes confers *S. aureus* resistance to the unknown corynebacterial factor(s), reintroduction of *psmα* was sufficient to observe *C. pseudodiphtheriticum*-mediated killing [82]. This indicates that some *Corynebacterium* species force *S. aureus* towards commensalism because they would otherwise be killed. Furthermore, corynebacteria also target CoNS. The species *C. propinquum* produces the siderophore dehydroxynocardamine, which displays strong inhibitory activity against CoNS under iron-limited conditions [84]. Since the nasal cavities possess only scarce iron deposits and dehydroxynocardamine has been shown to be produced *in vivo*, *C. propinquum* may impact CoNS nasal colonization.

Interestingly, *Corynebacterium* species such as *C. propinquum* and *C. pseudodiphtheriticum* have been reported to commonly co-occur with *D. pigrum* [85-87], which is in agreement with our observations. On the one hand, *D. pigrum* is a lactic acid bacterium capable of producing

lactic acid via fermentation, and it is speculated that it reduces the local pH, which is favorable for lipophilic and non-fermenting *Corynebacterium* spp. [88]. On the other hand, *Dolosigranulum pigrum* exhibits several auxotrophies (e.g., for the amino acids methionine, arginine and glutamine, and the vitamins biotin and nicotinate) and relies on the human host and close-by co-colonizing bacteria for the provision of nutrients [85, 89]. Thus, *Dolosigranulum* and Corynebacteria may be co-dependent bacteria, which may explain their often-observed co-occurrence [88]. Furthermore, nasal carriage of *D.pigrum* and *Corynebacterium* spp. has been associated with a healthy microbiome development and was reported to negatively correlate with pathobionts such as *S. aureus* or *S. pneumoniae* [85, 90]. Since *D. pigrum* and *C. propinquum* are also highly negatively correlated with *S. aureus* in our cohort, it may be assumed that the absence of *S. aureus* in CST7 is in part due to the presence of those two species.

S. lugdunensis nasal carriage has been shown to be negatively correlated with that of *S. aureus*. Thus, it could be assumed that bacteria co-existing with *S. lugdunensis* within the nasal microbiome may be more resistant towards lugdunin than negatively correlated bacteria. Although this is partially true, e.g., for *D. pigrum or Finegoldia magna*, most positively correlated bacteria show similar or even higher susceptibility to lugdunin than *S. aureus*. One possible explanation might be that these bacteria are not in close spatial proximity to *S. lugdunensis*, thereby being protected from the hydrophobic, and hence weakly diffusing lugdunin. In contrast, *S. aureus* and *S. lugdunensis* may be in closer contact and directly compete for adhesion sites, which may be required for lugdunin-mediated killing. Nasal attachment of *S. aureus* is known to be multifactorial and is mediated by wall teichoic acids (WTA) [91], cell wall-anchored proteins such as serine-aspartic acid repeat proteins (SdrC and SdrD) [92, 93], clumping factor B (ClfB) [94] or iron-regulated surface determinant A (IsdA) [93, 95]. However, nothing is known about *S. lugdunensis* factors mediating adherence/colonization in the human nose, and hence, this topic requires further investigation [96].

Since the human nose represents an environment with limited access to nutrients or metals, *S. lugdunensis* may depend on co-colonizing bacteria providing such essential factors. Indeed, *S. lugdunensis* exhibits auxotrophies for pantothenate (vitamin B5), nicotinate (vitamin B3) and thiamine (vitamin B1), as previously also described for *S. aureus* [97]. Vitamins are essential micronutrients for all organisms and are often co-factors for enzymes. Although vitamin secretion by probiotic bacteria has been described [98-100], it is arguable whether nasal bacteria also "willingly" secrete vitamins in such a nutrient-poor environment, since they are required for their own survival. However, lugdunin-mediated killing and subsequent lysis of co-

colonizing bacteria may enable *S. lugdunensis* to access valuable vitamins (or other essential metabolites), which this bacterium is not capable of producing on its own.

Unlike some other *Staphylococcus* species, *S. lugdunensis* is incapable of producing any of the two carboxylate siderophores staphyloferrin A and B. However, the uptake machineries for carboxylate, hydroxamate and catechol/catecholamine siderophores appear to be intact, indicating that *S. lugdunensis* may snatch siderophores secreted by other bacteria in order to cope with the limited iron availability in the nose [101, 102]. Indeed, several positively correlated siderophore-producing bacteria such as *C. propinquum*, *S. capitis* or *S. epidermidis* promote growth of *S. lugdunensis* under iron-limited conditions. Interestingly, though dehydroxynocardamine produced by *C. propinquum* has been reported to inhibit CoNS [84], *S. lugdunensis* seems to be capable of using even this siderophore for iron acquisition. Whether dehydroxynocardamine or another siderophore produced by *C. propinquum* is in fact responsible for the observed enhanced growth remains to be elucidated. Although siderophore-mediated interbacterial and (human) host-bacteria interactions have been described [103, 104], only little is known about the ecological importance of siderophores in influencing nasal bacterial community compositions. Thus, our study is one of the first providing insights into how nasal bacteria such as *S. lugdunensis* putatively benefit from xenosiderophores produced by other nasal bacteria.

Final conclusions

Interbacterial interactions are complex and versatile, and we are only beginning to understand the underlying mechanisms shaping microbial communities. *S. epidermidis* IVK83 and *S. lugdunensis* IVK28 exemplify how bacteria antagonize putative competitors like *S. aureus* via the production of antimicrobials, thereby interfering with *S. aureus* nasal colonization in cotton rats and potentially also in humans. Furthermore, *S. lugdunensis* (and other bacteria) can also benefit from (secondary) metabolites produced by other bacteria, such as siderophores, indicating that also mutualistic or commensal relationships govern microbial community compositions. Donia et al. [15], among others, have shown that the human microbiome is a rich source of still unknown BGCs. This clearly indicates that there is yet more to explore and that challenging, but interesting discoveries can be expected in the field of microbiome research.

References

1.   Human Microbiome Project C. Structure, function and diversity of the healthy human microbiome. Nature. 2012;486(7402):207-14. doi: 10.1038/nature11234. PubMed PMID: 22699609.

2.   Turnbaugh PJ, Hamady M, Yatsunenko T, Cantarel BL, Duncan A, Ley RE, et al. A core gut microbiome in obese and lean twins. Nature. 2009;457(7228):480-4. Epub 2008/12/02. doi: 10.1038/nature07540. PubMed PMID: 19043404; PubMed Central PMCID: PMCPMC2677729.

3.   Qin J, Li Y, Cai Z, Li S, Zhu J, Zhang F, et al. A metagenome-wide association study of gut microbiota in type 2 diabetes. Nature. 2012;490(7418):55-60. doi: 10.1038/nature11450.

4.   Nishino K, Nishida A, Inoue R, Kawada Y, Ohno M, Sakai S, et al. Analysis of endoscopic brush samples identified mucosa-associated dysbiosis in inflammatory bowel disease. J Gastroenterol. 2018;53(1):95-106. Epub 2017/08/31. doi: 10.1007/s00535-017-1384-4. PubMed PMID: 28852861.

5.   Coates R, Moran J, Horsburgh MJ. Staphylococci: colonizers and pathogens of human skin. Future Microbiol. 2014;9(1):75-91. Epub 2013/12/18. doi: 10.2217/fmb.13.145. PubMed PMID: 24328382.

6.   Nakatsuji T, Chen TH, Narala S, Chun KA, Two AM, Yun T, et al. Antimicrobials from human skin commensal bacteria protect against Staphylococcus aureus and are deficient in atopic dermatitis. Sci Transl Med. 2017;9(378):eaah4680. doi: 10.1126/scitranslmed.aah4680. PubMed PMID: 28228596.

7.   Yoon MY, Lee K, Yoon SS. Protective role of gut commensal microbes against intestinal infections. Journal of Microbiology. 2014;52(12):983-9. doi: 10.1007/s12275-014-4655-2.

8.   Lee AS, de Lencastre H, Garau J, Kluytmans J, Malhotra-Kumar S, Peschel A, et al. Methicillin-resistant Staphylococcus aureus. Nat Rev Dis Primers. 2018;4:18033. Epub 2018/06/01. doi: 10.1038/nrdp.2018.33. PubMed PMID: 29849094.

9.   von Eiff C, Becker K, Machka K, Stammer H, Peters G. Nasal carriage as a source of Staphylococcus aureus bacteremia. Study Group. N Engl J Med. 2001;344(1):11-6. Epub 2001/01/04. doi: 10.1056/nejm200101043440102. PubMed PMID: 11136954.

10.   Flowers L, Grice EA. The Skin Microbiota: Balancing Risk and Reward. Cell Host & Microbe. 2020;28(2):190-200. doi: https://doi.org/10.1016/j.chom.2020.06.017.

11.   Otto M. Staphylococci in the human microbiome: the role of host and interbacterial interactions. Current Opinion in Microbiology. 2020;53:71-7. doi: https://doi.org/10.1016/j.mib.2020.03.003.

12.   Krismer B, Weidenmaier C, Zipperer A, Peschel A. The commensal lifestyle of Staphylococcus aureus and its interactions with the nasal microbiota. Nature Reviews Microbiology. 2017;15(11):675-87. doi: 10.1038/nrmicro.2017.104.

13.   Cotter PD, Ross RP, Hill C. Bacteriocins — a viable alternative to antibiotics? Nature Reviews Microbiology. 2013;11(2):95-105. doi: 10.1038/nrmicro2937.

14.   Smillie CS, Smith MB, Friedman J, Cordero OX, David LA, Alm EJ. Ecology drives a global network of gene exchange connecting the human microbiome. Nature. 2011;480(7376):241-4. doi: 10.1038/nature10571.

15.   Donia MS, Cimermancic P, Schulze CJ, Wieland Brown LC, Martin J, Mitreva M, et al. A systematic analysis of biosynthetic gene clusters in the human microbiome reveals a common family of antibiotics. Cell. 2014;158(6):1402-14. doi: 10.1016/j.cell.2014.08.032. PubMed PMID: 25215495.

16.   Janek D, Zipperer A, Kulik A, Krismer B, Peschel A. High Frequency and Diversity of Antimicrobial Activities Produced by Nasal Staphylococcus Strains against Bacterial Competitors. PLoS Pathog. 2016;12(8):e1005812. doi: 10.1371/journal.ppat.1005812. PubMed PMID: 27490492; PubMed Central PMCID: PMCPMC4973975.

17.   O'Sullivan JN, Rea MC, O'Connor PM, Hill C, Ross RP. Human skin microbiota is a rich source of bacteriocin-producing staphylococci that kill human pathogens. FEMS Microbiology Ecology. 2018;95(2). doi: 10.1093/femsec/fiy241.

18.   Nakatsuji T, Hata TR, Tong Y, Cheng JY, Shafiq F, Butcher AM, et al. Development of a human skin commensal microbe for bacteriotherapy of atopic dermatitis and use in a phase 1 randomized clinical trial. Nat Med. 2021. Epub 2021/02/24. doi: 10.1038/s41591-021-01256-2. PubMed PMID: 33619370.

19.   Zipperer A, Konnerth MC, Laux C, Berscheid A, Janek D, Weidenmaier C, et al. Human commensals producing a novel antibiotic impair pathogen colonization. Nature. 2016;535(7613):511-6. doi: 10.1038/nature18634.

20.   Yan M, Pamp SJ, Fukuyama J, Hwang PH, Cho D-Y, Holmes S, et al. Nasal microenvironments and interspecific interactions influence nasal microbiota complexity and S. aureus carriage. Cell host & microbe. 2013;14(6):631-40. doi: 10.1016/j.chom.2013.11.005. PubMed PMID: 24331461.

21.   Lemon KP, Klepac-Ceraj V, Schiffer HK, Brodie EL, Lynch SV, Kolter R. Comparative analyses of the bacterial microbiota of the human nostril and oropharynx. mBio. 2010;1(3):e00129-10. doi: 10.1128/mBio.00129-10. PubMed PMID: 20802827.

22.   Christensen GJ, Scholz CF, Enghild J, Rohde H, Kilian M, Thürmer A, et al. Antagonism between Staphylococcus epidermidis and Propionibacterium acnes and its genomic basis. BMC Genomics. 2016;17:152. Epub 2016/03/01. doi: 10.1186/s12864-016-2489-5. PubMed PMID: 26924200; PubMed Central PMCID: PMCPMC4770681.

23.   Cogen AL, Yamasaki K, Muto J, Sanchez KM, Crotty Alexander L, Tanios J, et al. Staphylococcus epidermidis antimicrobial delta-toxin (phenol-soluble modulin-gamma) cooperates with host antimicrobial peptides to kill group A Streptococcus. PLoS One. 2010;5(1):e8557. Epub 2010/01/07. doi: 10.1371/journal.pone.0008557. PubMed PMID: 20052280; PubMed Central PMCID: PMCPMC2796718.

24.   Frank DN, Feazel LM, Bessesen MT, Price CS, Janoff EN, Pace NR. The human nasal microbiota and Staphylococcus aureus carriage. PLoS One. 2010;5(5):e10598. Epub 2010/05/26. doi: 10.1371/journal.pone.0010598. PubMed PMID: 20498722; PubMed Central PMCID: PMCPMC2871794.

25.   Iwase T, Uehara Y, Shinji H, Tajima A, Seo H, Takada K, et al. Staphylococcus epidermidis Esp inhibits Staphylococcus aureus biofilm formation and nasal colonization. Nature. 2010;465(7296):346-9. doi: 10.1038/nature09074.

26.   Cogen AL, Yamasaki K, Sanchez KM, Dorschner RA, Lai Y, MacLeod DT, et al. Selective Antimicrobial Action Is Provided by Phenol-Soluble Modulins Derived from Staphylococcus epidermidis, a Normal Resident of the Skin. Journal of Investigative Dermatology. 2010;130(1):192-200. doi: https://doi.org/10.1038/jid.2009.243.

27.   Kellner R, Jung G, Hörner T, Zähner H, Schnell N, Entian KD, et al. Gallidermin: a new lanthionine-containing polypeptide antibiotic. Eur J Biochem. 1988;177(1):53-9. Epub 1988/10/15. doi: 10.1111/j.1432-1033.1988.tb14344.x. PubMed PMID: 3181159.

28.   Götz F, Perconti S, Popella P, Werner R, Schlag M. Epidermin and gallidermin: Staphylococcal lantibiotics. International Journal of Medical Microbiology. 2014;304(1):63-71. doi: https://doi.org/10.1016/j.ijmm.2013.08.012.

29.   Ekkelenkamp MB, Hanssen M, Danny Hsu S-T, de Jong A, Milatovic D, Verhoef J, et al. Isolation and structural characterization of epilancin 15X, a novel lantibiotic from a clinical strain of Staphylococcus epidermidis. FEBS Letters. 2005;579(9):1917-22. doi: 10.1016/j.febslet.2005.01.083.

30.   Sahl HG, Brandis H. Production, purification and chemical properties of an antistaphylococcal agent produced by Staphylococcus epidermidis. J Gen Microbiol. 1981;127(2):377-84. Epub 1981/12/01. doi: 10.1099/00221287-127-2-377. PubMed PMID: 7343644.

31.   Lambers H, Piessens S, Bloem A, Pronk H, Finkel P. Natural skin surface pH is on average below 5, which is beneficial for its resident flora. International Journal of Cosmetic Science. 2006;28(5):359-70. doi: https://doi.org/10.1111/j.1467-2494.2006.00344.x.

32.   McAuliffe O, O'Keeffe T, Hill C, Ross RP. Regulation of immunity to the two-component lantibiotic, lacticin 3147, by the transcriptional repressor LtnR. Molecular Microbiology. 2001;39(4):982-93. doi: https://doi.org/10.1046/j.1365-2958.2001.02290.x.

33.   Franz CM, Worobo RW, Quadri LE, Schillinger U, Holzapfel WH, Vederas JC, et al. Atypical genetic locus associated with constitutive production of enterocin B by Enterococcus faecium BFE 900. Appl Environ Microbiol. 1999;65(5):2170-8. Epub 1999/05/01. doi: 10.1128/aem.65.5.2170-2178.1999. PubMed PMID: 10224016; PubMed Central PMCID: PMCPMC91313.

34.   Septimus EJ, Schweizer ML. Decolonization in Prevention of Health Care-Associated Infections. Clin Microbiol Rev. 2016;29(2):201-22. Epub 2016/01/29. doi: 10.1128/cmr.00049-15. PubMed PMID: 26817630; PubMed Central PMCID: PMCPMC4786886.

35.   Antonov NK, Garzon MC, Morel KD, Whittier S, Planet PJ, Lauren CT. High prevalence of mupirocin resistance in Staphylococcus aureus isolates from a pediatric population. Antimicrob Agents Chemother. 2015;59(6):3350-6. Epub 2015/04/01. doi: 10.1128/aac.00079-15. PubMed PMID: 25824213; PubMed Central PMCID: PMCPMC4432188.

36.   Law BJC, Zhuo Y, Winn M, Francis D, Zhang Y, Samborskyy M, et al. A vitamin K-dependent carboxylase orthologue is involved in antibiotic biosynthesis. Nature Catalysis. 2018;1(12):977-84. doi: 10.1038/s41929-018-0178-2.

37.   Chang Y, Wang Y-H, Hu C-Q. Simultaneous determination of purity and potency of amphotericin B by HPLC. The Journal of Antibiotics. 2011;64(11):735-9. doi: 10.1038/ja.2011.83.

38.   Schmidt K, Riese U, Li Z, Hamburger M. Novel Tetramic Acids and Pyridone Alkaloids, Militarinones B, C, and D, from the Insect Pathogenic Fungus Paecilomyces militaris. Journal of Natural Products. 2003;66(3):378-83. doi: 10.1021/np020430y.

39.   Bailey CS, Zarins-Tutt JS, Agbo M, Gao H, Diego-Taboada A, Gan M, et al. A natural solution to photoprotection and isolation of the potent polyene antibiotic, marinomycin A. Chemical Science. 2019;10(32):7549-53. doi: 10.1039/C9SC01375J.

40.   Szczeblewski P, Laskowski T, Bałka A, Borowski E, Milewski S. Light-Induced Transformation of the Aromatic Heptaene Antifungal Antibiotic Candicidin D into Its All-Trans Isomer. Journal of Natural Products. 2018;81(7):1540-5. doi: 10.1021/acs.jnatprod.7b00821.

41.   Kwon HC, Kauffman CA, Jensen PR, Fenical W. Marinomycins A−D, Antitumor-Antibiotics of a New Structure Class from a Marine Actinomycete of the Recently Discovered Genus "Marinispora". Journal of the American Chemical Society. 2006;128(5):1622-32. doi: 10.1021/ja0558948.

42.   Caffrey P, De Poire E, Sheehan J, Sweeney P. Polyene macrolide biosynthesis in streptomycetes and related bacteria: recent advances from genome sequencing and experimental studies. Appl Microbiol Biotechnol. 2016;100(9):3893-908. doi: 10.1007/s00253-016-7474-z.

43.   Neville BA, d'Enfert C, Bougnoux M-E. Candida albicans commensalism in the gastrointestinal tract. FEMS Yeast Research. 2015;15(7). doi: 10.1093/femsyr/fov081.

44.   Findley K, Oh J, Yang J, Conlan S, Deming C, Meyer JA, et al. Topographic diversity of fungal and bacterial communities in human skin. Nature. 2013;498(7454):367-70. doi: 10.1038/nature12171.

45.   Zimmermann M, Fischbach MA. A Family of Pyrazinone Natural Products from a Conserved Nonribosomal Peptide Synthetase in Staphylococcus aureus. Chem Biol. 2010;17(9):925-30. doi: https://doi.org/10.1016/j.chembiol.2010.08.006.

46.   Wyatt MA, Wang W, Roux CM, Beasley FC, Heinrichs DE, Dunman PM, et al. Staphylococcus aureus nonribosomal peptide secondary metabolites regulate virulence. Science. 2010;329(5989):294-6. Epub 2010/06/05. doi: 10.1126/science.1188888. PubMed PMID: 20522739.

47.   Brüggemann H, Poehlein A, Brzuszkiewicz E, Scavenius C, Enghild JJ, Al-Zeer MA, et al. Staphylococcus saccharolyticus Isolated From Blood Cultures and Prosthetic Joint Infections Exhibits Excessive Genome Decay. Front Microbiol. 2019;10(478). doi: 10.3389/fmicb.2019.00478.

48.   Golomb BL, Yu AO, Coates LC, Marco ML. The Lactococcus lactis KF147 nonribosomal peptide synthetase/polyketide synthase system confers resistance to oxidative stress during growth on plant leaf tissue lysate. Microbiologyopen. 2018;7(1):e00531. Epub 2017/09/18. doi: 10.1002/mbo3.531. PubMed PMID: 28921941.

49.   Khayatt BI, van Noort V, Siezen RJ. The Genome of the Plant-Associated Lactic Acid Bacterium Lactococcus lactis KF147 Harbors a Hybrid NRPS-PKS System Conserved in Strains of the Dental Cariogenic Streptococcus mutans. Curr Microbiol. 2020;77(1):136-45. Epub 2019/11/11. doi: 10.1007/s00284-019-01799-1. PubMed PMID: 31705391.

50.   Wu C, Cichewicz R, Li Y, Liu J, Roe B, Ferretti J, et al. Genomic island TnSmu2 of Streptococcus mutans harbors a nonribosomal peptide synthetase-polyketide synthase gene cluster responsible for the biosynthesis of pigments involved in oxygen and H2O2 tolerance.

Appl Environ Microbiol. 2010;76(17):5815-26. Epub 2010/07/20. doi: 10.1128/aem.03079-09. PubMed PMID: 20639370; PubMed Central PMCID: PMCPMC2935078.

51.   Zhang W, Liu J. Recent Advances in Understanding and Engineering Polyketide Synthesis. F1000Res. 2016;5:F1000 Faculty Rev-208. doi: 10.12688/f1000research.7326.1. PubMed PMID: 26962443.

52.   Shelest E, Heimerl N, Fichtner M, Sasso S. Multimodular type I polyketide synthases in algae evolve by module duplications and displacement of AT domains in trans. BMC Genomics. 2015;16(1):1015. doi: 10.1186/s12864-015-2222-9.

53.   Chen H, Du L. Iterative polyketide biosynthesis by modular polyketide synthases in bacteria. Appl Microbiol Biotechnol. 2016;100(2):541-57. Epub 2015/11/09. doi: 10.1007/s00253-015-7093-0. PubMed PMID: 26549236.

54.   Olano C, Wilkinson B, Sánchez C, Moss SJ, Sheridan R, Math V, et al. Biosynthesis of the Angiogenesis Inhibitor Borrelidin by Streptomyces parvulus Tü4055: Cluster Analysis and Assignment of Functions. Chem Biol. 2004;11(1):87-97. doi: https://doi.org/10.1016/j.chembiol.2003.12.018.

55.   Olano C, Wilkinson B, Moss SJ, Braña AF, Méndez C, Leadlay PF, et al. Evidence from engineered gene fusions for the repeated use of a module in a modular polyketide synthase. Chem Commun (Camb). 2003;(22):2780-2. Epub 2003/12/04. doi: 10.1039/b310648a. PubMed PMID: 14651102.

56.   Gaitatzis N, Silakowski B, Kunze B, Nordsiek G, Blöcker H, Höfle G, et al. The Biosynthesis of the Aromatic Myxobacterial Electron Transport Inhibitor Stigmatellin Is Directed by a Novel Type of Modular Polyketide Synthase∗. Journal of Biological Chemistry. 2002;277(15):13082-90. doi: https://doi.org/10.1074/jbc.M111738200.

57.   Sandmann G. Evolution of carotene desaturation: The complication of a simple pathway. Archives of Biochemistry and Biophysics. 2009;483(2):169-74. doi: https://doi.org/10.1016/j.abb.2008.10.004.

58.   Wieland B, Feil C, Gloria-Maercker E, Thumm G, Lechner M, Bravo JM, et al. Genetic and biochemical analyses of the biosynthesis of the yellow carotenoid 4,4'-diaponeurosporene of Staphylococcus aureus. J Bacteriol. 1994;176(24):7719-26. Epub 1994/12/01. doi: 10.1128/jb.176.24.7719-7726.1994. PubMed PMID: 8002598; PubMed Central PMCID: PMCPMC197231.

59.   Pelz A, Wieland K-P, Putzbach K, Hentschel P, Albert K, Götz F. Structure and Biosynthesis of Staphyloxanthin from Staphylococcus aureus*. Journal of Biological Chemistry. 2005;280(37):32493-8. doi: https://doi.org/10.1074/jbc.M505070200.

60.   Nishie M, Shioya K, Nagao J-i, Jikuya H, Sonomoto K. ATP-dependent leader peptide cleavage by NukT, a bifunctional ABC transporter, during lantibiotic biosynthesis. Journal of Bioscience and Bioengineering. 2009;108(6):460-4. doi: https://doi.org/10.1016/j.jbiosc.2009.06.002.

61.   Bierbaum G, Sahl HG. Lantibiotics: Mode of Action, Biosynthesis and Bioengineering. Current Pharmaceutical Biotechnology. 2009;10(1):2-18. doi: http://dx.doi.org/10.2174/138920109787048616.

62.   Krauss S, Zipperer A, Wirtz S, Saur J, Konnerth MC, Heilbronner S, et al. Secretion of and self-resistance to the novel fibupeptide antimicrobial lugdunin by distinct ABC transporters

in Staphylococcus lugdunensis. Antimicrob Agents Chemother. 2020. Epub 2020/10/28. doi: 10.1128/aac.01734-20. PubMed PMID: 33106269.

63.   Siegers K, Entian KD. Genes involved in immunity to the lantibiotic nisin produced by Lactococcus lactis 6F3. Appl Environ Microbiol. 1995;61(3):1082-9. Epub 1995/03/01. doi: 10.1128/aem.61.3.1082-1089.1995. PubMed PMID: 7793910; PubMed Central PMCID: PMCPMC167363.

64.   Hille M, Kies S, Götz F, Peschel A. Dual Role of GdmH in Producer Immunity and Secretion of the Staphylococcal Lantibiotics Gallidermin and Epidermin. Applied and Environmental Microbiology. 2001;67(3):1380. doi: 10.1128/AEM.67.3.1380-1383.2001.

65.   Peschel A, Schnell N, Hille M, Entian KD, Götz F. Secretion of the lantibiotics epidermin and gallidermin: sequence analysis of the genes gdmT and gdmH, their influence on epidermin production and their regulation by EpiQ. Molecular and General Genetics MGG. 1997;254(3):312-8. doi: 10.1007/s004380050421.

66.   Aso Y, Okuda K, Nagao J, Kanemasa Y, Thi Bich Phuong N, Koga H, et al. A novel type of immunity protein, NukH, for the lantibiotic nukacin ISK-1 produced by Staphylococcus warneri ISK-1. Biosci Biotechnol Biochem. 2005;69(7):1403-10. Epub 2005/07/26. doi: 10.1271/bbb.69.1403. PubMed PMID: 16041148.

67.   Okuda K, Aso Y, Nakayama J, Sonomoto K. Cooperative transport between NukFEG and NukH in immunity against the lantibiotic nukacin ISK-1 produced by Staphylococcus warneri ISK-1. J Bacteriol. 2008;190(1):356-62. Epub 2007/10/24. doi: 10.1128/jb.01300-07. PubMed PMID: 17951378; PubMed Central PMCID: PMCPMC2223764.

68.   Pozzi R, Coles M, Linke D, Kulik A, Nega M, Wohlleben W, et al. Distinct mechanisms contribute to immunity in the lantibiotic NAI-107 producer strain Microbispora ATCC PTA-5024. Environ Microbiol. 2016;18(1):118-32. Epub 2015/04/30. doi: 10.1111/1462-2920.12892. PubMed PMID: 25923468.

69.   Smits SHJ, Schmitt L, Beis K. Self-immunity to antibacterial peptides by ABC transporters. FEBS Lett. 2020;594(23):3920-42. Epub 2020/10/12. doi: 10.1002/1873-3468.13953. PubMed PMID: 33040342.

70.   Bieber L, Kahlmeter G. Staphylococcus lugdunensis in several niches of the normal skin flora. Clin Microbiol Infect. 2010;16(4):385-8. Epub 2009/06/13. doi: 10.1111/j.1469-0691.2009.02813.x. PubMed PMID: 19519842.

71.   Camarinha-Silva A, Jáuregui R, Pieper DH, Wos-Oxley ML. The temporal dynamics of bacterial communities across human anterior nares. Environ Microbiol Rep. 2012;4(1):126-32. Epub 2012/02/01. doi: 10.1111/j.1758-2229.2011.00313.x. PubMed PMID: 23757239.

72.   Olsen K, Falch BM, Danielsen K, Johannessen M, Ericson Sollid JU, Thune I, et al. Staphylococcus aureus nasal carriage is associated with serum 25-hydroxyvitamin D levels, gender and smoking status. The Tromsø Staph and Skin Study. European Journal of Clinical Microbiology & Infectious Diseases. 2012;31(4):465-73. doi: 10.1007/s10096-011-1331-x.

73.   Dimitri-Pinheiro S, Soares R, Barata P. The Microbiome of the Nose-Friend or Foe? Allergy Rhinol (Providence). 2020;11:2152656720911605-. doi: 10.1177/2152656720911605. PubMed PMID: 32206384.

74.   Liu CM, Price LB, Hungate BA, Abraham AG, Larsen LA, Christensen K, et al. Staphylococcus aureus and the ecology of the nasal microbiome. Sci Adv.

2015;1(5):e1400216. Epub 2015/11/26. doi: 10.1126/sciadv.1400216. PubMed PMID: 26601194; PubMed Central PMCID: PMCPMC4640600.

75.   Wos-Oxley ML, Plumeier I, von Eiff C, Taudien S, Platzer M, Vilchez-Vargas R, et al. A poke into the diversity and associations within human anterior nare microbial communities. Isme j. 2010;4(7):839-51. Epub 2010/02/26. doi: 10.1038/ismej.2010.15. PubMed PMID: 20182526.

76.   Liu Q, Liu Q, Meng H, Lv H, Liu Y, Liu J, et al. Staphylococcus epidermidis Contributes to Healthy Maturation of the Nasal Microbiome by Stimulating Antimicrobial Peptide Production. Cell Host & Microbe. 2020;27(1):68-78.e5. doi: https://doi.org/10.1016/j.chom.2019.11.003.

77.   Cole AM, Tahk S, Oren A, Yoshioka D, Kim YH, Park A, et al. Determinants of Staphylococcus aureus nasal carriage. Clin Diagn Lab Immunol. 2001;8(6):1064-9. Epub 2001/11/01. doi: 10.1128/cdli.8.6.1064-1069.2001. PubMed PMID: 11687441; PubMed Central PMCID: PMCPMC96227.

78.   Bomar L, Brugger SD, Lemon KP. Bacterial microbiota of the nasal passages across the span of human life. Current opinion in microbiology. 2018;41:8-14. Epub 2017/11/20. doi: 10.1016/j.mib.2017.10.023. PubMed PMID: 29156371.

79.   Kaspar U, Kriegeskorte A, Schubert T, Peters G, Rudack C, Pieper DH, et al. The culturome of the human nose habitats reveals individual bacterial fingerprint patterns. Environ Microbiol. 2016;18(7):2130-42. doi: 10.1111/1462-2920.12891. PubMed PMID: 25923378.

80.   Kiryukhina NV, Melnikov VG, Suvorov AV, Morozova YA, Ilyin VK. Use of Corynebacterium pseudodiphtheriticum for elimination of Staphylococcus aureus from the nasal cavity in volunteers exposed to abnormal microclimate and altered gaseous environment. Probiotics Antimicrob Proteins. 2013;5(4):233-8. Epub 2013/12/01. doi: 10.1007/s12602-013-9147-x. PubMed PMID: 26783069.

81.   Uehara Y, Nakama H, Agematsu K, Uchida M, Kawakami Y, Abdul Fattah AS, et al. Bacterial interference among nasal inhabitants: eradication of Staphylococcus aureus from nasal cavities by artificial implantation of Corynebacterium sp. J Hosp Infect. 2000;44(2):127-33. Epub 2000/02/09. doi: 10.1053/jhin.1999.0680. PubMed PMID: 10662563.

82.   Hardy BL, Dickey SW, Plaut RD, Riggins DP, Stibitz S, Otto M, et al. Corynebacterium pseudodiphtheriticum Exploits Staphylococcus aureus Virulence Components in a Novel Polymicrobial Defense Strategy. mBio. 2019;10(1). Epub 2019/01/10. doi: 10.1128/mBio.02491-18. PubMed PMID: 30622190; PubMed Central PMCID: PMCPMC6325251.

83.   Ramsey MM, Freire MO, Gabrilska RA, Rumbaugh KP, Lemon KP. Staphylococcus aureus Shifts toward Commensalism in Response to Corynebacterium Species. Front Microbiol. 2016;7:1230. Epub 2016/09/02. doi: 10.3389/fmicb.2016.01230. PubMed PMID: 27582729; PubMed Central PMCID: PMCPMC4988121.

84.   Stubbendieck RM, May DS, Chevrette MG, Temkin MI, Wendt-Pienkowski E, Cagnazzo J, et al. Competition among Nasal Bacteria Suggests a Role for Siderophore-Mediated Interactions in Shaping the Human Nasal Microbiota. Appl Environ Microbiol. 2019;85(10). doi: 10.1128/AEM.02406-18. PubMed PMID: 30578265; PubMed Central PMCID: PMCPMC6498180.

85.   Brugger SD, Eslami SM, Pettigrew MM, Escapa IF, Henke MT, Kong Y, et al. Dolosigranulum pigrum Cooperation and Competition in Human Nasal Microbiota. mSphere.

2020;5(5). doi: 10.1128/mSphere.00852-20. PubMed PMID: 32907957; PubMed Central PMCID: PMCPMC7485692.

86. Lappan R, Imbrogno K, Sikazwe C, Anderson D, Mok D, Coates H, et al. A microbiome case-control study of recurrent acute otitis media identified potentially protective bacterial genera. BMC microbiology. 2018;18(1):13-. doi: 10.1186/s12866-018-1154-3. PubMed PMID: 29458340.

87. Hasegawa K, Linnemann RW, Mansbach JM, Ajami NJ, Espinola JA, Petrosino JF, et al. Nasal Airway Microbiota Profile and Severe Bronchiolitis in Infants: A Case-control Study. Pediatr Infect Dis J. 2017;36(11):1044-51. doi: 10.1097/INF.0000000000001500. PubMed PMID: 28005692.

88. de Steenhuijsen Piters WA, Sanders EA, Bogaert D. The role of the local microbial ecosystem in respiratory health and disease. Philos Trans R Soc Lond B Biol Sci. 2015;370(1675). Epub 2015/07/08. doi: 10.1098/rstb.2014.0294. PubMed PMID: 26150660; PubMed Central PMCID: PMCPMC4528492.

89. Renz A, Widerspick L, Dräger A. First Genome-Scale Metabolic Model of Dolosigranulum pigrum Confirms Multiple Auxotrophies. Metabolites. 2021;11(4):232. doi: 10.3390/metabo11040232. PubMed PMID: 33918864.

90. Bosch A, de Steenhuijsen Piters WAA, van Houten MA, Chu M, Biesbroek G, Kool J, et al. Maturation of the Infant Respiratory Microbiota, Environmental Drivers, and Health Consequences. A Prospective Cohort Study. Am J Respir Crit Care Med. 2017;196(12):1582-90. Epub 2017/07/01. doi: 10.1164/rccm.201703-0554OC. PubMed PMID: 28665684.

91. Weidenmaier C, Peschel A. Teichoic acids and related cell-wall glycopolymers in Gram-positive physiology and host interactions. Nat Rev Microbiol. 2008;6(4):276-87. Epub 2008/03/11. doi: 10.1038/nrmicro1861. PubMed PMID: 18327271.

92. Askarian F, Ajayi C, Hanssen A-M, van Sorge NM, Pettersen I, Diep DB, et al. The interaction between Staphylococcus aureus SdrD and desmoglein 1 is important for adhesion to host cells. Sci Rep. 2016;6:22134-. doi: 10.1038/srep22134. PubMed PMID: 26924733.

93. Corrigan RM, Miajlovic H, Foster TJ. Surface proteins that promote adherence of Staphylococcus aureusto human desquamated nasal epithelial cells. BMC Microbiology. 2009;9(1):22. doi: 10.1186/1471-2180-9-22.

94. O'Brien LM, Walsh EJ, Massey RC, Peacock SJ, Foster TJ. Staphylococcus aureus clumping factor B (ClfB) promotes adherence to human type I cytokeratin 10: implications for nasal colonization. Cell Microbiol. 2002;4(11):759-70. Epub 2002/11/13. doi: 10.1046/j.1462-5822.2002.00231.x. PubMed PMID: 12427098.

95. Clarke SR, Wiltshire MD, Foster SJ. IsdA of Staphylococcus aureus is a broad spectrum, iron-regulated adhesin. Molecular Microbiology. 2004;51(5):1509-19. doi: https://doi.org/10.1111/j.1365-2958.2003.03938.x.

96. Heilbronner S, Foster TJ. Staphylococcus lugdunensis: a Skin Commensal with Invasive Pathogenic Potential. Clin Microbiol Rev. 2021;34(2). Epub 2020/12/29. doi: 10.1128/cmr.00205-20. PubMed PMID: 33361142; PubMed Central PMCID: PMCPMC7950365.

97. Bosi E, Monk JM, Aziz RK, Fondi M, Nizet V, Palsson B. Comparative genome-scale modelling of Staphylococcus aureus strains identifies strain-specific metabolic capabilities linked to pathogenicity. Proc Natl Acad Sci U S A. 2016;113(26):E3801-9. Epub 2016/06/12.

doi: 10.1073/pnas.1523199113. PubMed PMID: 27286824; PubMed Central PMCID: PMCPMC4932939.

98.   Salvetti S, Celandroni F, Ghelardi E, Baggiani A, Senesi S. Rapid determination of vitamin B2 secretion by bacteria growing on solid media. J Appl Microbiol. 2003;95(6):1255-60. doi: https://doi.org/10.1046/j.1365-2672.2003.02095.x.

99.   Chen J, Vestergaard M, Jensen TG, Shen J, Dufva M, Solem C, et al. Finding the Needle in the Haystack-the Use of Microfluidic Droplet Technology to Identify Vitamin-Secreting Lactic Acid Bacteria. mBio. 2017;8(3). Epub 2017/06/01. doi: 10.1128/mBio.00526-17. PubMed PMID: 28559484; PubMed Central PMCID: PMCPMC5449655.

100.   García-Angulo VA. Overlapping riboflavin supply pathways in bacteria. Crit Rev Microbiol. 2017;43(2):196-209. Epub 2016/11/09. doi: 10.1080/1040841x.2016.1192578. PubMed PMID: 27822970.

101.   Brozyna JR, Sheldon JR, Heinrichs DE. Growth promotion of the opportunistic human pathogen, Staphylococcus lugdunensis, by heme, hemoglobin, and coculture with Staphylococcus aureus. Microbiologyopen. 2014;3(2):182-95. Epub 2014/02/07. doi: 10.1002/mbo3.162. PubMed PMID: 24515974.

102.   Conroy BS, Grigg JC, Kolesnikov M, Morales LD, Murphy MEP. Staphylococcus aureus heme and siderophore-iron acquisition pathways. BioMetals. 2019;32(3):409-24. doi: 10.1007/s10534-019-00188-2.

103.   Kramer J, Özkaya Ö, Kümmerli R. Bacterial siderophores in community and host interactions. Nature Reviews Microbiology. 2020;18(3):152-63. doi: 10.1038/s41579-019-0284-4.

104.   Ellermann M, Arthur JC. Siderophore-mediated iron acquisition and modulation of host-bacterial interactions. Free Radic Biol Med. 2017;105:68-78. Epub 2016/10/22. doi: 10.1016/j.freeradbiomed.2016.10.489. PubMed PMID: 27780750.

Contributions to publications

Chapter 1 - Secondary Metabolites Governing Microbiome Interaction of Staphylococcal Pathogens and Commensals

I wrote the review under guidance/supervision of Andreas Peschel, Bernhard Krismer and Simon Heilbronner. Furthermore, I generated all the figures (Fig. 1-5) and tables (Table 1-2).

Simon Heilbronner made substantial contributions to the conception and design of the work and revising the work critically for important intellectual content.

Andreas Peschel made substantial contributions to the conception and design of the work and revising the work critically for important intellectual content.

Bernhard Krismer made substantial contributions to the conception and design of the work and revising the work critically for important intellectual content.

Chapter 2 - Staphylococcus epidermidis uses a fugacious mixed polypeptide/polyketide antimicrobial to outcompete Staphylococcus aureus - (unpublished)

I established the epifadin purification protocol from cultivation of *S. epidermidis* IVK83 to the DMSO extraction. I performed all biological assays related to the testing of the antimicrobial activity of *S. epidermidis* IVK83 strains, epifadin containing DMSO extracts and purified epifadin, which includes Table 1, Fig. 1c, Fig. 2, Fig. 3c, Fig. 9 and Fig. 10a. Further I performed competition assays *in vitro* (Fig. 11 a, Fig. S6) and *in vivo* (Fig. 11b) with technical support from Darya Belikova. Also, I analyzed DNA sequencing data to elucidate pIVK83 (Fig. 1a/b), utilized antiSMASH to predict the composition of epifadin (Fig 5), and generated Δ*efiO* mutant (data not included in this manuscript).

Nadine A. Schilling identified the responsible bioactive compound and elucidated the peptide structure **2** of the degradation product by coupled HPLC (Fig. 3a/b) and high-resolution mass spectrometry (Fig. 6). Her chemical synthesis of **2** and chemical derivatization of the natural product 1 (Fig. S2) supported structure elucidation. J. M. Beltran purified epifadin for activity tests and NMR studies.

Taulant Dema established the optimized purification of epifadin (**1**) under exclusion of light and oxygen. Taulant Dema performed structure elucidation of **1** from the detailed 2-dimensional NMR analyses under exclusion of oxygen (Fig. S7, Fig. S8). Taulant Dema's mechanistic studies from mass spectrometry data resulted in the given assignment of the peptide-polyene-tetramic acid structure of epifadin (**1**), supported by his proposed six membered transition state for the key fragmentation to tetrapeptide (**2**) and PKS moiety (Fig. 4, Fig. 7, Fig. 8, Fig. S3, Fig. S4). Taulant Dema synthesized and purified the peptide amide 2 and thus enabled MS and NMR analyses (Fig. S1, Fig. S5, Table S2).

Daniela Janek performed the transposon mutagenesis of *S. epidermidis* IVK83, generated the Δ*efiTP* mutant and complemented mutant and did initial antimicrobial activity testing of IVK83 against some nasal bacteria.

Anne Berscheid analyzed mode of action of epifadin using epifadin-containing precipitate and IVK83 strains via reporter strains of *Bacillus subtilis* (data not included in this manuscript)

Sophia Krauss provided us two other *S. epidermidis* strains harboring the plasmid highly similar to pIVK83 and analyzed DNA sequencing data of these plasmids.

Min Li provided us another *S. epidermidis* strain harboring a plasmid highly similar to pIVK83

Mal Horsburgh identified another *S. epidermidis* strain harboring a plasmid highly similar to pIVK83.

Heike Brötz-Oesterhelt supervised Jan Straetner who performed the toxicity assay of epifadin against human cells (Fig. 10b).

Stephanie Grond contributed to the design of chemical experiments for this study, supported chemical analyses and critical discussed data.

Andreas Peschel supervised my work with substantial contributions to the conception and design of the experiments, the manuscript and revising the work critically for important intellectual content.

Bernhard Krismer supervised my work with substantial contributions to the conception and design of the experiments, the manuscript and revising the work critically for important intellectual content.

Matthias Hamburger provided us with authentic sample of militarinone C.

Chapter 3 - Siderophore-producing commensals facilitate nasal colonization by the lugdunin-producing Staphylococcus lugdunensis to exclude the pathogen Staphylococcus aureus - (unpublished)

I performed all siderophore-related experiments, including cultivation of and siderophore production from nasal bacteria, determination of siderophore concentrations (Fig. 6A, Suppl. Fig. 4A), growth promotion experiments of *Staphylococcus lugdunensis* (Fig. 6B, Suppl. Fig. 4B, Fig. 7, Suppl. Fig. 5B), generation *of S. lugdunensis* Δ*fhu* and *S. epidermidis* Δ*sfaDAB* and their respective complemented mutants with technical support from Darya Belikova and Vera Augsburger. Further, I performed lugdunin susceptibility assays against the tested nasal bacteria (Fig. 5, Suppl. Fig. 5A, Suppl. Fig. 6).

Ralf Rosenstein performed all metagenome-related experiments, including CST determination (Table 2, Fig. 3B, Suppl. Table 1) detection of *S. aureus/S. lugdunensis* carriers (Fig. 1A/B), detection of *S. lugdunensis*-containing metagenomes (Fig. 2), generation of microbiome profiles (Fig. 3A, Suppl. Fig. 1, Suppl. Fig. 2), and correlational analyses (Fig. 4, Suppl. Fig. 3, Suppl. Table 2).

Claudia Sauer analyzed *S. aureus/S. lugdunensis* distribution in study participants (Table 1) and isolated nasal bacterial strains with technical support from Cosima Hirt.

Simon Heilbronner made substantial contributions to the conception and design of the work and revising the work critically for important intellectual content.

Bernhard Krismer supervised my work with substantial contributions to the conception and design of the experiments, the manuscript and revising the work critically for important intellectual content.

Andreas Peschel supervised my work with substantial contributions to the conception and design of the experiments, the manuscript and revising the work critically for important intellectual content.

Chapter 4 - Secretion of and Self-Resistance to the Novel Fibupeptide Antimicrobial Lugdunin by Distinct ABC Transporters in Staphylococcus lugdunensis

I performed the minimal inhibitory concentration assays for the comparison of lugdunin susceptibility of nasal *Staphylococcus aureus* and *Staphylococcus epidermidis* isolates (Fig. S2).

Sophia Krauss performed MIC assays (Fig. 4b, Table S2) constructed plasmids and strains.

Alexander Zipperer constructed plasmids and strains and extracted lugdunin from culture broth.

Martin C. Konnerth, Sebastian N. Wirtz and Julian S. Saur performed chemical synthesis of lugdunin and lugdunin congeners (Fig. 4a, Table S2, Fig. S3), accomplished chromatographic purification of compounds, and accompanied the project with detailed chemical analyses with coupled HPLC-UV-MS. M. C. Konnerth, S. N. Wirtz, J. S. Saur and N. A. Schilling were involved in fruitful discussions for the biological and chemical experiments for analysis of lugdunin secretion.

Simon Heilbronner performed GC analysis of lugdunin operon (Fig. 1a) and ImageJ analysis of lugdunin (Fig. 2a).

Stephanie Grond contributed to the design of chemical experiments for this study, supported chemical analyses and critical discussed data.

Bernhard Krismer performed MIC assays, did the analysis (Fig. 2a/b, 3a/b), the calculations and made substantial contributions to the conception and design of the experiments, the manuscript and revising the work critically for important intellectual content.

Andreas Peschel designed the model for the roles of LugIEFGH (Fig. 5) and made substantial contributions to the conception and design of the experiments, the manuscript and revising the work critically for important intellectual content.

Luise Ruda, Vera Augsburger, Gabriele Hornig, Timm Schäfle, and Manuel Beltran gave excellent technical support.

Curriculum vitae

Removed